# Biogeography of crop progenitors and wild plant resources in the terminal Pleistocene and Early Holocene of West Asia, 14.7–8.3 ka

Joe Roe[a,b,*], Amaia Arranz-Otaegui[c]

[a] *University of Bern, Switzerland,*

[b] *University of Copenhagen, Denmark,*

[c] *University of the Basque Country, Spain,*

**Abstract**

This paper presents the first continuous, spatially-explicit reconstructions of the palaeodistributions of 65 plant species found regularly in association with early agricultural archaeological sites in West Asia, including the progenitors of the first crops. We used machine learning to train an ecological niche model of each species based on its present-day distribution in relation to climate and environmental variables. Predictions of the potential niches of these species at key stages of the Pleistocene–Holocene transition could then be derived from these models using downsampled data from palaeoclimate simulations. Our models performed well against independent contemporary test data, but their ability to predict the occurrence of specific species at archaeological sites was much more variable, probably reflecting a tendency of the method to underestimate the species' fundamental niche. Nevertheless, the majority of species are predicted to have had more restricted geographic distributions under past climate conditions compared to today. Crop progenitors and several wild food species modelled are modelled to have been concentrated in the Levant and, to a lesser extent, Cyprus and Western Anatolia, suggesting these regions may have served as glacial *refugia*. The average size of species' niche shrunk by an average of c. 25% from the terminal Pleistocene to the Early Holocene, indicating that economically significant plants were adapted to cryo-arid conditions and did not, as often assumed, initially respond positively to the 'ameliorated' climate of the Holocene.

*Corresponding author

*Email address:* jar@hum.ku.dk (Joe Roe)

## 1. Introduction

The Pleistocene–Holocene transition in West Asia marked a turning point in global environmental history, as humans brought the first plants under cultivation and began modifying surrounding ecosystems to support their own subsistence. West Asia is part of the native range of a remarkable number of domesticable plant species, including wild relatives of wheat, barley, peas, lentils, and other crops of global importance (Harlan and Zohary, 1966; Diamond, 2002; Zohary et al., 2012). These species supported uniquely dense and complex Late Epipalaeolithic (15–11.7 ka) societies (Bar-Yosef, 1998; Maher et al., 2012) based on foraging (Harris and Hillman, 1989; Colledge, 2001; Weiss et al., 2004) and eventually plant management and pre-domestication cultivation (Colledge, 2001; Weiss et al., 2006; Harris, 2007; Willcox et al., 2008). The first agro-ecosystems emerged as these plants were domesticated in the Pre-Pottery Neolithic period (11.7–8.5 ka) and were shaped by the broader ecosystem in which it was embedded.

Decades of research in archaeobotany and zooarchaeology have reconstructed the subsistence economies of Late Epipalaeolithic and Neolithic sites in great detail. Together with studies of other environmental archaeological records and a variety of palaeoclimate archives (Jones et al., 2019), they also tell us much about the environments surrounding these settlements. However, each of these sources of evidence is subject to the wide variety of taphonomic and recovery biases that are inherent in any direct record of the past. They are also, by definition, records of the (human) environment at particular times and places. Interpolating these snapshots to give a holistic picture of the regional ecologies is not straightforward – to date, it has tended to rely on non-explicit, inductive modelling. The majority are also filtered through human action, producing a mixed single that makes it difficult to disentangle anthropic effects from the background of environmental change in this period of rapid climatic alteration.

In this paper we present a complementary, deductive approach based on ecological niche modelling. Rather than inferring environmental conditions from preserved physical evidence, we predict the potential niche of individual species relevant to human subsistence based on a model of their current environmental niche and simulations of past palaeoclimate. Though hypothetical, this gives us an independent line of evidence on past ecologies that is independent of the environmental archaeological and palaeoclimatic records. This means that the ancient data can be reserved for assessing the model's ability to 'hindcast' past conditions. In this sense, discrepencies between the two records are perhaps the most interesting result, as they indicate processes affecting one or both records that are not fully accounted for and therefore generate new questions. Our computational approach is also readily scaled up, allowing us to model spatially-explicit palaeodistributions for a large number of species, for the whole region, under multiple reconstructed climate scenarios.

## 2. Background

The transition to agriculture represents one of the most fundamental changes in human history. West Asia is one of the regions where this process has been studied in the most detail: decades of research have traced the gradual development of a Neolithic way of life and the changes that occurred in the plant species and their geographical distribution as a result. Although archaeobotanical assemblages can be biased due to issues of preservation, sampling, recovery techniques, and lab procedures (Dennell, 1976; Hastorf and Popper, 1988)—and although they include not just food remains but plant resources that were used for other purposes or arrived at the site accidentally (Hastorf and Popper, 1988)—large-scale studies have still revealed coherent patterns in the exploitation of plants over time (Colledge et al., 2004; Arranz-Otaegui et al., 2016).

The possibility of an abrupt, geographically-constrained process of plant domestication was proposed in the 1990s (Hillman and Davies, 1990, 1992; Heun et al., 1997; Özkan et al., 2002) and developed as an explanatory model in the 2000s (Lev-Yadun et al., 2000a; Gopher et al., 2001; Abbo et al., 2005). As part of this model, some authors (Lev-Yadun et al., 2000a; Gopher et al., 2001; Abbo et al., 2010, 2012) argued that eight plant species, collectively referred to as 'founder crops' or the 'Neolithic crop package' (Zohary and Hopf, 1988) were selected and domesticated once, without any phase of pre-domestication cultivation (Abbo et al., 2011, p. 177). This process could have been rapid under strong artificial selection (Hillman and Davies, 1990, 1992) and may have occurred in a single region or 'core area' – generally located in southeast Turkey (Ladizinsky and Adler, 1976; Heun et al., 1997; Özkan et al., 2002; Ozkan et al., 2005; Mori, 2003; Luo et al., 2007). From this single point of origin, it was supposed that domesticated or semi-domesticated plants radiated outwards to other regions (Abbo et al., 2006; Kilian et al., 2007; Özkan et al., 2011).

The 'short gestation' paradigm was challenged by others (Helbæk, 1969; Harris, 1989; Kislev, 1989; Colledge, 2001; Weiss et al., 2004; Willcox et al., 2008; Fuller et al., 2018). Helbæk (in Kirkbride, 1966) argued that before the appearance of domesticated plants, a phase of cultivation of wild seeds must have taken place. The existence of a phase of cultivation of morphologically wild cereals or 'pre-domestication cultivation' was identified in the archaeological record through the study of plant domestication traits such as grain size, shattering v. non-shattering rachises. The archaeobotanical evidence shows that during the Pre-Pottery Neolithic A (PPNA) cereals exhibited sizes similar to those recorded in domestic species, but their dispersal mechanism was still the same as the one present in morphologically-wild species (i.e. shattering, see Kirkbride, 1966; Kislev, 1989; Hillman et al., 2001; Colledge, 2001; Willcox et al., 2008). This evidence suggested that wild cereal stands could have been cultivated for as much as a thousand years before non-shattering domestic forms became prevalent in the archaeological record (Tanno and Willcox, 2006, 2012; Arranz-Otaegui et al., 2016). Additional archaeobotanical (Colledge, 2001; Willcox et al., 2008, 2009; Riehl et al., 2013; Arranz-Otaegui et al., 2016; Weide et al., 2018; Douché and

Willcox, 2018; Whitlam et al., 2018) and genetic data (Badr et al., 2000; Molina-Cano et al., 2005; Kilian et al., 2007; Özkan et al., 2011; Iob and Botigué, 2023) in recent years has further challenged the short-gestation model to explain the origins of plant domestication and agriculture in West Asia.

Similarly, the concept of a limited set of eight 'founder crops' (Zohary and Hopf, 1988) that were the first species cultivated, domesticated and then spread as the basis of Neolithic agricultural systems, is not supported by the latest evidence. Our previous analyses of the composition of available archaeobotanical datasets shows that these crops were of marginal importance during the Epipalaeolithic period (Arranz-Otaegui et al., 2018) and that Neolithic subsistence did not rely either solely or primarily on the exploitation of these species (Arranz-Otaegui and Roe, 2023). Instead, multiple species of grasses, legumes, fruits, nuts, and other plants were exploited over the Late Pleistocene-Early Holocene transition in southwest Asia.

### *2.1. Biogeography and agricultural origins*

The study of the natural distribution of the progenitors of domesticated crops has been a central part of discussions on the origins of agriculture and plant domestication from the beginning. von Humboldt (1807) acknowledged the importance of the natural distribution of wild species to explain the origin and domestication of crops like spelt and rye. de Candolle (1886) integrated the study of plant ecology and biogeography and influenced Darwin (1859), who later reflected in detail about the geographical distribution of plants and species diversity. At that time, there was intense debate about whether there were single or multiple "centres of creation" of species. Researchers aimed to evaluate whether plant and animal species emerged in the same locations where they were currently distributed.

After Darwin, this early interest in crop origins evolved into more specific discussions about the "centres of plant domestication". Vavilov (1926) was among the first to seek to determine the number of regions in which plants had been independently domesticated (Harris, 1990). His main method was 'differential phytogeography': he classified the variation within a crop and established the regions of maximum diversity, to locate the geographic regions in which crops originated. Using this method, Vavilov suggested that there were at least eight centres of origin. His work was later criticised by Harlan (1971), who argued that 'centres of origin' and 'centres of diversity' had to be separated. For Harlan, a 'centre' was as an "area in which things originate and out of which things are dispersed" (Harlan, 1971, p. 468), and he suggested that three main centres of origin of domesticated crops existed. He further indicated that Vavilov's approach to the question was simplistic and that more data proxies had to be considered (e.g. archaeology, history, geology), an approach more in the tradition of de Candolle (1886). Indeed, the inclusion of archaeobotany and genetics in the last decades, together with the study of wild relative distributions has been fundamental in characterising the origins of agriculture (Fuller and Colledge, 2008). As a result of modern interdisciplinary studies, the number of

recognised centres of plant domestication has increased considerably, from the three centres suggested by Harlan in 1971 to the six to eight centres argued for in the 1990s (Smith, 1995) and up to as much as 24 potential centres reported in 2009 (Purugganan and Fuller, 2009; see also Fuller, 2010).

Biogeographic research into the centres of origin and/or domestication of crops has also long informed broader understanding of the process of agricultural origins. In *Man Makes Himself*, Childe (1936) correctly located the centre of origin of European agriculture in the 'Fertile Crescent' of West Asia (unlike for example Pumpelly (1908) before him). This was not based on the region's prehistoric archaeological record, which at the time had only been cursorily explored. Instead he was guided to the region by biogeographic work by Vavilov and Peake and Fleure (1927); only later was this prediction validated by archaeological work on the Epipalaeolithic and Neolithic of Palestine (Boyd, 2018). In subsequent decades, the search for more precise origin zones of specific domestic plants relied on the assumption that "the locus of domestication of a wild plant would presumably be within its area of original distribution in the wild state" (Butzer, 1971; paraphrasing Helbæk, 1959) – and that this "natural habitat" has not changed significantly over the last 12,000 years (Butzer, 1971).

Contemporary research on crop origins was pioneered by Harlan and Zohary, who compared the current distribution of the wild progenitors of domesticated plants in southwest Asia (Harlan and Zohary, 1966; Zohary, 1969, 1973; Zohary and Hopf, 1973) to the rapidly-expanding archaeobotanical record (Harlan, 1971; Harlan, 1977; see also Zohary and Hopf, 1988; Harlan and Zohary, 1966). They both were interested in evaluating which were the wild ancestors of domesticated crops and studying their natural distribution to understand their domestication process (Zohary, 1969, 1973; Zohary and Spiegel-Roy, 1975). Indeed, the natural distribution of the wild relatives of domestic plant species was later used as a criterion to infer 'pre-domestic cultivation' in the archaeological record. For example, the presence of seeds of chickpea at Jericho led Hopf (1986) to interpret the remains as cultivars, as the natural distribution of the wild form of chickpea was located further to the north. The same rationale was applied to the einkorn remains found at several Pre-Pottery Neolithic sites in the southern Levant (Hopf, 1969; Colledge, 2001), as the wild progenitors of this species was thought to be restricted to the northern Levantine area (Heun et al., 1997; Zohary et al., 2012). The same idea—presence of plants outside their natural range—has been repeated in the literature more recently by several other authors (Tanno and Willcox, 2006; Willcox et al., 2008; Hillman et al., 2001).

Despite the importance of biogeography in the development and validation of hypotheses regarding the origins of agriculture, there have been few studies of the wild range of specific crop progenitors or other relevant plant species (cf. for domestic animals, e.g. Yeomans et al., 2017). Observations regarding translocation or range expansion must therefore rely on a relatively rough and ahistoric notion of a species' 'natural distribution' – that is, one based primarily on contemporary or recent-historic occurrences. Yet we know there has been

considerable climatic and environmental change in West Asia since the terminal Pleistocene (Jones et al., 2019), so it is very unlikely that these ranges were in fact static. Reconstructions of broader environments have attempted to trace their fluctuations through time, either for the entire region (e.g. van Zeist and Bottema, 1991; Hillman in Moore et al., 2000) or parts of it (e.g. Cordova, 2007), but these are at the level of the vegetation zone rather than individual species. They also invariably rely on what might be called 'expert interpolation' (where the author composes a map based on his or her own knowledge of the relevant data) rather than an explicit modelling process. This makes it difficult, if not impossible, for users of such reconstructions to understand exactly how they were derived or what could explain, for example, the significant discrepencies between the predictions of different experts.

### *2.2. Ecological niche modelling in archaeology*

Ecological niche modelling or species distribution modelling is widely used by ecologists to mathematically predict the geographic distribution of a species from a sample of occurrences (Franklin and Miller, 2009; Sillero et al., 2021). Essentially, it involves combining records of where an organism has been observed with environmental data (climate, topography, etc.) for those locations to model the range of environmental values at which that species – its environmental niche. This model can then be used to predict the potential niche of the organism in question either in the same or a different environment. Townsend Peterson and Soberón (2012) suggests reserving the term 'species distribution modelling' for when the method is used to recover the verifiable range of a species in a real and existing environment, and using 'ecological niche modelling' as the broader term covering hypothetical or predictive applications – a convention we follow here when referring to predictive or 'hindcast' models of past niches. Within this overarching framework, ecological niche modelling encompasses a wide range of applications and a variety of potential environmental predictors, modelling approaches, and methodologies, which we will not attempt to review here.

Ecological niche modelling has long been of interest to archaeologists as both a means of exploring the biological niche of humans and for reconstructing the past environments they inhabited (David Polly and Eronen, 2011; Franklin et al., 2015). In the first sense, it has been used most extensively to model the niche of humans and other hominin species (e.g. Benito et al., 2017; Yousefi et al., 2020; Banks et al., 2021; Yaworsky et al., 2024a,b; Guran et al., 2024), especially in the Palaeolithic. This overlaps with what archaeologists usually call generically 'predictive modelling' (Verhagen and Whitley, 2020)—or more precisely 'site distribution modelling'—which is essentially the same approach as (and often borrows methodologies from) ecological niche modelling but applied to the occurrence of archaeological sites. Here what is modelled is not strictly a biological niche alone, but also aspects of human geography, taphonomy, and archaeological visibility. These applications can be distinguished from 'palaeoecological niche modelling', where the object of model remains, as in ecology, a

non-human biological niche.

Franklin et al. (2015) review palaeoecological niche modelling and advocate for its greater adoption in environmental archaeology. In an early application to West Asia, Conolly et al. (2012) used the occurrence of wild and domestic *Bos* remains at prehistoric archaeological sites to map the evolving niche of cattle over the Pleistocene–Holocene transition. It has been used to model the availability of fauna exploited by humans at wider scales (e.g. de Andrés-Herrero et al., 2018; Yaworsky et al., 2023) and, in a West Asian context, of foraged plant resources in the landscape around the Neolithic sites on the Konya Plain (Collins et al., 2018). Modelling the spread of crops has been another significant archaeological application (e.g. Krzyzanska et al., 2022; Krzyzanska, 2023), though not as yet applied to West Asia.

In the majority of studies to date (palaeo)ecological niche modelling has been applied to archaeological data in an 'inductive' fashion, i.e. faunal and botanical remains from ancient sites are used as the occurrence dataset for training a model using either past or present environmental data. However, both the zooarchaeological and archaeobotanical records are sparse and subject to a complex array of depositional, taphonomic and recovery biases factors that , many of which are not fully understood and/or cannot be corrected for. This means that while the archaeological attestation of the presence of a species might generally be relied upon, it is highly unlikely that its absence is representative of true past distributions.

The alternative approach is to train the model using contemporary occurrence and environmental data and then use palaeoenvironmental data to 'hindcast' its predictions backwards in time. Like Franklin et al. (2015), we view the hindcasting approach as more promising, because training datasets for both occurrences and environment are far more readily available, complete and reliable for the present than the past. There is some scepticism in the ecological niche modelling literature about the ability of such models to make accurate predictions in unknown environments (like the past, Franklin et al., 2015), but here the hindcasting approach also presents an opportunity: it reserves archaeological occurrence data as an independent dataset that can be used to assess the retrodictive performance of the model. This possibily was suggested by Franklin et al. (2015) but to our knowledge our study represents the first attempt to actually do so.

The major practical limitation of the hindcasting approach is that it relies on spatially explicit, high resolution palaeoenvironmental surfaces with continuous coverage of the region and periods of interest. Until recently, this has not been widely available for most applications, which is perhaps why only a minority of studies use it (cf. Krzyzanska et al., 2022; Yaworsky et al., 2023). In this study, we are able to take advantage of the increasing availability of high resolution, global palaeoclimate data derived from simulation experiments with general circulation models of climate (Brown et al., 2018, 2020; Karger et al., 2023).

## 3. Data and model

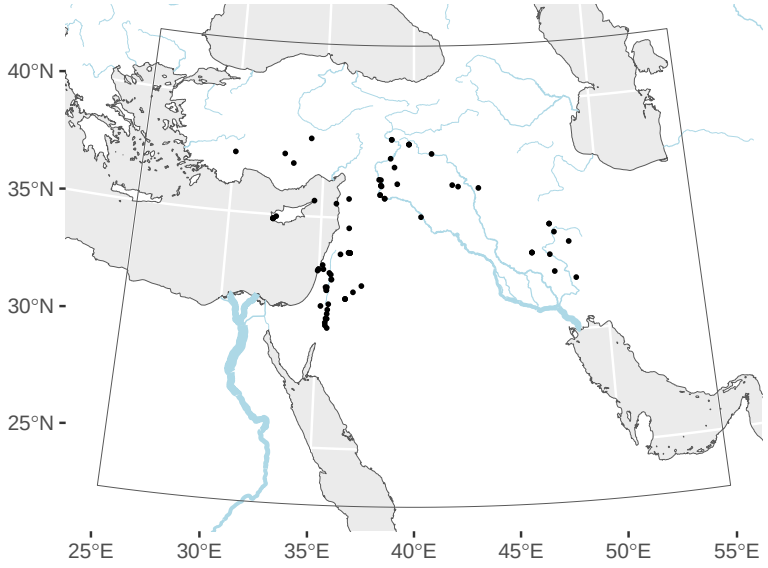


Figure 1: Map of the study region (West Asia, grey box) with locations of Late Epipalaeolithic and Pre-Pottery Neolithic archaeobotanical assemblages.

The aim of our study was to model the biogeography of species relevant to human subsistence economies in West Asia (excluding the Southern Arabian peninsula, see Figure 1) during the archaeological Late Epipalaeolithic (15–11.7 ka) and Pre-Pottery Neolithic (11.7–8.3 ka) periods. Based on current understandings, we assume that plant-based subsistence during this period was broad, geographically- and temporally-varied, and reflects a gradual, geographically decentred, and nonlinear tranistion to greater reliance on cultivars (i.e. agriculture, see Section 2). Our starting point was a list of 68 taxa (Table 1) comprising the identified species observed at at least 3 Late Epipalaeolithic/Pre-Pottery Neolithic sites, according to our previous study of the regional archaeobotanical data (Arranz-Otaegui and Roe, 2023). This was based on dataset collated from three previously published regional archaeobotanical databases: ADEMNES (Riehl and Kümmel, 2005), ORIGINS (Wallace et al., 2018b), and COMPAG (Lucas and Fuller, 2018; Fuller et al., 2018; based on Colledge et al., 2004; Shennan and Conolly, 2007). We did not attempt to distinguish between the source of the remains (cf. Wallace et al., 2018a); archaeobotanical assemblages are subject to a variety of preservational and recovery biases, so by no means were all the species on our list consumed or even deliberately collected by people. However, we assume that there presence at a site of human settlement at least implies that they were part of the wider ecosystem that supported habitation there.

The taxonomic identifications of archaeobotanical material given in our source

databases were previously controlled to ensure consistency between sources and to remove taxa that cannot be reliably distinguished (for details see Arranz-Otaegui and Roe, 2023). Taxonomic names were then matched to the canonical form specified in the GBIF Backbone Taxonomy (GBIF Secretariat, 2023) so they could be related to modern occurrences. Archaeologically-attested domestic species meeting our inclusion criteria were substituted for their wild progenitors (where different) when gathering occurrence data, since the domestic forms are now widespread and presumably uninformative of the species original niche.

### *3.1. Occurrence data*

Georeferenced occurrence data for West Eurasia between 0 and 60° of latitude was obtained from the Global Biodiversity Information Facility (GBIF) using via and the R package 'rgbif' (Chamberlain and Boettiger, 2017; Chamberlain et al., 2024). The GBIF dataset (GBIF, 2025a) excluded fossil occurrences, recorded absences, and records with missing or dubious coordinates. Although niche models have reasonable predictive power even with small training samples (Stockwell and Peterson, 2002; Hernandez et al., 2006; Wisz et al., 2008), we did not attempt to model 3 taxa with less than 40 usable occurrences, following recommendations for niche models generally and Random Forest-based models specifically (Stockwell and Peterson, 2002; Luan et al., 2020). Multiple records of the same taxon at the same coordinate were discarded because they do not impart information to the model. The resulting cleaned dataset used to train our niche models comprises 3392920 occurrences from 4769 constituent datasets.

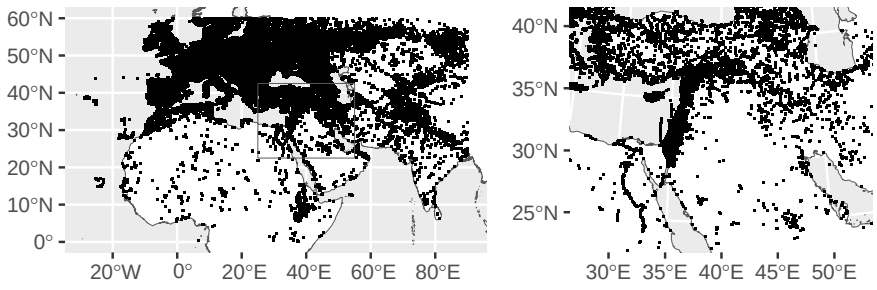


Figure 2: Georeferenced occurrence records from West Eurasia used to train models (N=1412083). Inset, right: prediction region (West Asia).

GBIF is currently the best available general-purpose occurrence dataset for the West Asia region, its coverage is uneven both geographically and from species to species. The Southern Levant, and Israel specifically, is significantly more densely sampled than other parts of West Asia (Figure 2).

Random Forest is a presence–absence approach to niche modelling and therefore requires not just data on where a species is present, but where it is definitely not present. However 'absence' data is rarely available because it requires exhaustive survey. In practice, most applications of niche modelling are 'presence-only' and, where absence data is required (as for Random Forest), it is supplied as a random background sample of points.[1] The purpose of this sample is to inform the model about the nature of the underlying environment. The stochastic generation process means that some of these points will overlap or fall close to presences, so ensuring the model is not overly influenced by background samples is critical to its predictive importance (Valavi et al., 2022). Here we follow the advice of Barbet-Massin et al. (2012) for regression-based species distribution models and use a large ( 10000) uniform sample of points from across the land area of the study region. These points are then weighted equally against the presences in the regression to produce a 'balanced Random Forest' (Valavi et al., 2022).

### *3.2. Predictor data*

We modelled the occurrence of species as a function of 24 geospatial predictor variables. These included:

- Sixteen 'bioclimatic' variables derived from monthly temperature and precipitation values, following standard practice for species distribution models (Hijmans et al., 2005). Contemporary bioclimatic predictor data for West Asia was extracted from the global CHELSA dataset (Karger et al., 2017), which predicts temperature and precipitation from downscaled general circulation model output at 1 km resolution.
- Terrain aspect and slope, which at high resolution perform well as proxies for solar radiation when modelling plant occurrence (Austin and Van Niel, 2011; Leempoel et al., 2015); and the topographic wetness index (TWI), which serves as a proxy for soil moisture and is particularly important in modelling arid environments (Kopecký and ˇCí ˇzková, 2010; Campos et al., 2016; Di Virgilio et al., 2018). All three were derived from the SRTM30+ digital elevation model using algorithms from WhiteboxTools (Lindsay, 2016).
- Edaphic data from SoilGrids (Hengl et al., 2014, 2017), which improves model performance for plants (Dubuis et al., 2013; Mod et al., 2016; Velazco et al., 2017). Based on a recent assessment of the reliability of

[1] We use a background sample that is representative of the entire study area, as opposed to attempting to construct a 'pseudo-absence' sample. See Sillero et al. (2021) for the distinction.

SoilGrids data for species distribution modelling (Miller et al., 2024), we used a subset of four variables relating to soil texture (clay, silt, sand) and pH at the surface (0-5 cm depth).

For hindcasting, we used reconstructed bioclimatic data for three key climatologies generated from downscaled paleoclimate simulations from the HadCM3 general circulation model (Fordham et al., 2017; Brown et al., 2018): the Bølling–Allerød (c. 14.7–12.9 ka), the Younger Dryas (c. 12.9–11.7 ka), and the Early Holocene (11.7–8.3 ka). Terrain and soil predictors were held constant, since reconstructions of these variables in the past are not available at sufficient scale. It is unlikely that either macroscale topography or soil characteristics have altered significantly over the period of time considered here, so we assume that this does not degrade model performance, and may in fact benefit it by providing 'anchoring' predictors that are independent of climate change.

For training, test predictions, and archaeological predictions predictor data was left in its native projection and resolution. For hindcast palaeodistributions, it was transformed to common equal-area projection and resolution of 5 km.

### *3.3. Random Forest*

Ecological niche modelling is a classification problem that can be approached with a wide range of statistical methods. A substantial literature exists on the relatively performance of these approaches and their respective parameterisations (reviewed in Valavi et al., 2022). Random Forest, a widely-used machine learning algorithm, is amongst the best performing methods for presence-only species distribution models, providing it is appropriately parameterised to account for the class imbalance between presence and background samples (Valavi et al., 2021, 2022). For our application, it also has the advantage of requiring little to no manual parameter tuning to achieve good predictive results, which makes it easier to model a larger numbers of taxa.

For each taxon we trained a classification model to predict occurrence (presence or absence/background) based on up to 24 predictor variables (Section 3.2). Highly correlated (Pearson's $r$>0.7) predictors were removed on a taxon-by-taxon basis, to mitigate issues of overfitting due to colinearity (Dormann et al., 2013), as were redundant predictors with zero variance. We used the Random Forest algorithm implemented in the R package 'ranger' (Wright and Ziegler, 2017) and the 'tidymodels' (Kuhn and Silge, 2022) framework for data preprocessing and model selection. To avoid overfitting, we follow Valavi et al. (2021) in their recommended hyperparameters and use of down-sampling to balance presence and background samples. Models for each taxon were fit independently, with redundant zero-variance predictors excluded, and assessed based on balanced training (¾) and test (¼) partitions.

## 4. Model assessment

We trained Random Forest models for 65 taxa using contemporary occurrence data from GBIF, a random sample of background points, and the predictor vari-

ables described in Section 3.2. Substituting the "current" climate predictors for those derived from palaeoclimatic simulations (Brown et al., 2018), we could then generate hindcast predictions for reconstructed past environments in 4 key climate periods – a total of 260 modelled palaeodistributions. Predicted distributions for individual taxa are presented in the appendix and accompanying material.

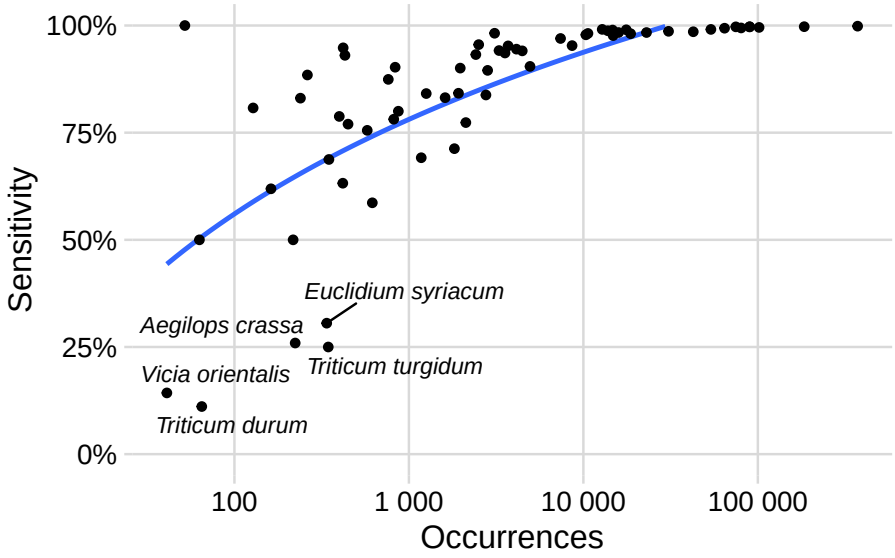


Figure 3: Model sensitivity by number of training occurrences

We assessed the predictive performance of the fitted niche models in the contemporary environment based on the reserved test partition (Table 1). Model accuracy (proportion of correctly classified presence and background samples) ranged between 93% and 100%, with an average of 98%. Sensitivity (proportion of correctly classified presence samples) ranged between 11% and 100%, with an average of 83%. The area under the models' receiver operating characteristic curves (ROC-AUC) was on average 0.986±0.017. Model sensitivity is loosely correlated with the number of occurrences available for training (Figure 3), with the worst-performing models all having less than 1000 recorded occurrences: *Triticum durum*, *Euclidium syriacum*, *Triticum turgidum*, *Aegilops crassa*, and *Vicia orientalis*. Test metrics and ROC curves for the individual models are included in the appendix.

The ability of the hindcast models to predict the occurrence of specific species at archaeological sites is worse, with just 8% of presences in archaeobotanical assemblages successfully predicted at a threshold of 0.5. Model sensitivity (proportion of corrected predicted presenses) in relation to the archaeological data is on average 0.06±0.12 (Table 1). A full assessment of the hindcasting perfor-

mance of the individual models can be found in the appendix.

In summary, the majority of our models perform poorly as simple binary classifiers with a threshold of `P(present)>0.5`. However, this is an arbitrary threshold; lowering it can improve sensitivity (proportion of occurrences correctly predicted) at the cost of specificity (proportion of non-occurrences incorrectly predicted). There are several approaches to selecting informative thresholds for binary classification in the ENM literature (Liu et al., 2005, 2013, 2016), with most aiming for an optimum compromise between sensitivity and specificity. We were unable to find a thresholding technique that significantly improved the hindcast models' performance as binary classifiers. By definition, binarizing model output also discards information from the underlying probabilistic prediction, so we have opted to present results probabilistically as far as possible. In principle the archaeological occurrences themselves could be used to 'calibrate' the hindcast models and select an optimum threshold, but there aren't enough archaeological attestations of most of the modelled species for this to be practicable at this time.

Table 1: Summary of species modelled

| | Occurrences | | Model | | | |
|---|---|---|---|---|---|---|
| Taxon | Arch. | Cur. | Acc. | ROC-AUC | Sens. cur. | Sens. arch. |
| *Aegilops crassa* | 4 | 223 | 0.98 | 0.98 | 0.26 | 0.00 |
| *Aegilops speltoides* | 0 | 448 | 0.99 | 0.99 | 0.77 | — |
| *Aegilops tauschii* | 0 | 1257 | 0.97 | 0.99 | 0.84 | — |
| *Aizoanthemopsis hispanica*[1] | 4 | 762 | 0.99 | 1.00 | 0.87 | 0.50 |
| *Ammi majus* | 4 | 10337 | 0.97 | 0.99 | 0.98 | 0.00 |
| *Androsace maxima* | 17 | 4946 | 0.94 | 0.98 | 0.90 | 0.00 |
| *Arenaria serpyllifolia* | 3 | 101617 | 0.98 | 0.99 | 1.00 | 0.00 |
| *Arnebia decumbens* | 21 | 617 | 0.97 | 0.97 | 0.59 | 0.05 |
| *Arnebia linearifolia* | 13 | 239 | 1.00 | 1.00 | 0.83 | 0.00 |
| *Atriplex prostrata* | 4 | 80186 | 0.99 | 0.99 | 0.99 | 0.00 |
| *Avena sterilis* | 5 | 15906 | 0.96 | 0.99 | 0.98 | 0.40 |
| *Bassia arabica* | 4 | 262 | 1.00 | 0.99 | 0.88 | 0.00 |
| *Bolboschoenus glaucus* | 5 | 418 | 0.98 | 0.97 | 0.63 | 0.00 |
| *Bolboschoenus maritimus*[2] | 31 | 53813 | 0.98 | 1.00 | 0.99 | 0.00 |
| *Brachypodium distachyon* | 5 | 13800 | 0.98 | 0.99 | 0.99 | 0.20 |
| *Bromus sterilis* | 3 | 89764 | 0.99 | 0.99 | 1.00 | 0.00 |
| *Buglossoides arvensis* | 23 | 23004 | 0.95 | 0.98 | 0.98 | 0.09 |
| *Buglossoides tenuiflora* | 26 | 399 | 0.99 | 0.98 | 0.79 | 0.04 |
| *Capparis spinosa* | 4 | 8617 | 0.96 | 0.99 | 0.95 | 0.00 |
| *Carex divisa* | 9 | 7400 | 0.96 | 0.99 | 0.97 | 0.00 |
| *Chenopodium album* | 5 | 184412 | 0.99 | 0.99 | 1.00 | 0.00 |
| *Cicer reticulatum*[3] | 3 | 52 | 1.00 | 1.00 | 1.00 | 0.00 |
| *Citrullus colocynthis* | 4 | 1823 | 0.94 | 0.96 | 0.71 | 0.00 |
| *Crithopsis delileana* | 3 | 430 | 1.00 | 1.00 | 0.93 | 0.00 |
| *Euclidium syriacum* | 3 | 338 | 0.98 | 0.96 | 0.31 | 0.00 |
| *Ficus carica* | 8 | 64440 | 0.98 | 0.99 | 0.99 | 0.38 |
| *Fumaria densiflora* | 4 | 3704 | 0.96 | 0.99 | 0.95 | 0.00 |
| *Gypsophila elegans* | 3 | 1613 | 0.96 | 0.99 | 0.83 | 0.00 |
| *Gypsophila pilosa* | 5 | 348 | 0.99 | 0.99 | 0.69 | 0.00 |

| | | | | | | |
|---|---|---|---|---|---|---|
| *Gypsophila vaccaria*[4] | 8 | 1177 | 0.95 | 0.96 | 0.69 | 0.00 |
| *Henrardia pubescens* | 3 | 1[5] | — | — | — | — |
| *Hordeum bulbosum* | 4 | 4134 | 0.97 | 0.99 | 0.94 | 0.00 |
| *Hordeum murinum* | 5 | 74770 | 0.98 | 0.99 | 1.00 | 0.00 |
| *Hordeum spontaneum*[6] | 76 | 3098 | 0.99 | 1.00 | 0.98 | 0.21 |
| *Lathyrus aphaca* | 4 | 18652 | 0.96 | 0.99 | 0.98 | 0.00 |
| *Lathyrus oleraceus*[7] | 8 | 819 | 0.98 | 0.99 | 0.78 | 0.00 |
| *Lathyrus sativus* | 4 | 2120 | 0.93 | 0.97 | 0.77 | 0.00 |
| *Lepidium perfoliatum* | 3 | 2764 | 0.94 | 0.98 | 0.84 | 0.00 |
| *Linum bienne*[8] | 14 | 12824 | 0.98 | 0.99 | 0.99 | 0.07 |
| *Lolium rigidum* | 5 | 10620 | 0.97 | 0.99 | 0.98 | 0.00 |
| *Lolium temulentum* | 3 | 4463 | 0.94 | 0.98 | 0.94 | 0.00 |
| *Medicago radiata* | 20 | 834 | 0.98 | 1.00 | 0.90 | 0.30 |
| *Phalaris paradoxa* | 3 | 3287 | 0.96 | 0.99 | 0.94 | 0.00 |
| *Phragmites australis* | 4 | 373066 | 0.99 | 0.99 | 1.00 | 0.00 |
| *Pistacia atlantica* | 6 | 2419 | 0.98 | 1.00 | 0.93 | 0.33 |
| *Poa bulbosa* | 5 | 30769 | 0.96 | 0.98 | 0.99 | 0.20 |
| *Polygonum arenarium*[9] | 7 | 25[5] | — | — | — | — |
| *Polygonum corrigioloides* | 6 | 12[5] | — | — | — | — |
| *Prosopis farcta* | 5 | 2512 | 0.99 | 1.00 | 0.96 | 0.00 |
| *Rumex pulcher* | 6 | 17606 | 0.97 | 0.99 | 0.99 | 0.00 |
| *Salsola kali* | 6 | 14701 | 0.98 | 1.00 | 0.99 | 0.00 |
| *Salvia absconditiflora*[10] | 3 | 128 | 1.00 | 1.00 | 0.81 | 0.00 |
| *Secale cereale* | 4 | 14813 | 0.95 | 0.98 | 0.98 | 0.00 |
| *Secale strictum*[11] | 3 | 162 | 0.99 | 0.98 | 0.62 | 0.00 |
| *Suaeda fruticosa* | 3 | 577 | 0.99 | 0.99 | 0.76 | 0.00 |
| *Taeniatherum caput-medusae* | 4 | 1969 | 0.97 | 0.99 | 0.90 | 0.00 |
| *Triticum aestivum*[12] | 4 | 217 | 0.99 | 0.96 | 0.50 | 0.00 |
| *Triticum durum* | 3 | 65 | 0.99 | 0.95 | 0.11 | 0.00 |
| *Triticum monococcum*[13] | 47 | 870 | 0.97 | 0.99 | 0.80 | 0.04 |
| *Triticum turgidum*[14] | 53 | 345 | 0.98 | 0.91 | 0.25 | 0.00 |
| *Triticum urartu* | 0 | 420 | 1.00 | 1.00 | 0.95 | — |
| *Verbena officinalis* | 3 | 89655 | 0.99 | 0.99 | 1.00 | 0.00 |
| *Vicia ervilia* | 26 | 1924 | 0.95 | 0.98 | 0.84 | 0.27 |
| *Vicia faba* | 7 | 42644 | 0.97 | 0.99 | 0.99 | 0.29 |
| *Vicia narbonensis*[15] | 3 | 2826 | 0.95 | 0.99 | 0.90 | 0.33 |
| *Vicia orientalis*[16] | 16 | 41 | 1.00 | 0.97 | 0.14 | 0.00 |
| *Vitis sylvestris* | 3 | 63 | 1.00 | 1.00 | 0.50 | 0.00 |
| *Zygophyllum fabago* | 3 | 3554 | 0.97 | 0.99 | 0.94 | 0.00 |

[1]Including *Aizoon hispanicum*
[2]Including *Scirpus maritimus*
[3]Including *Cicer arietinum*
[4]Including *Vaccaria pyramidata*
[5]Excluded from modelling due to sample size
[6]Including *Hordeum vulgare*
[7]Including *Pisum sativum* and *Pisum elatius*
[8]Including *Linum usitatissimum*
[9]Including *Polygonum venantianum*
[10]Including *Salvia cryptantha*
[11]Including *Secale montanum*
[12]Including *Triticum spelta* and *Triticum aestivocompactum*
[13]Including *Triticum boeoticum*
[14]Including *Triticum aestivum*, *Triticum dicoccum*, and *Triticum dicoccoides*
[15]Including *Vicia narbonense*
[16]Including *Lens culinaris* and *Lens orientalis*

## 5. Discussion

### *5.1. Reduction in potential niche sizes over the Pleistocene/Holocene boundary*

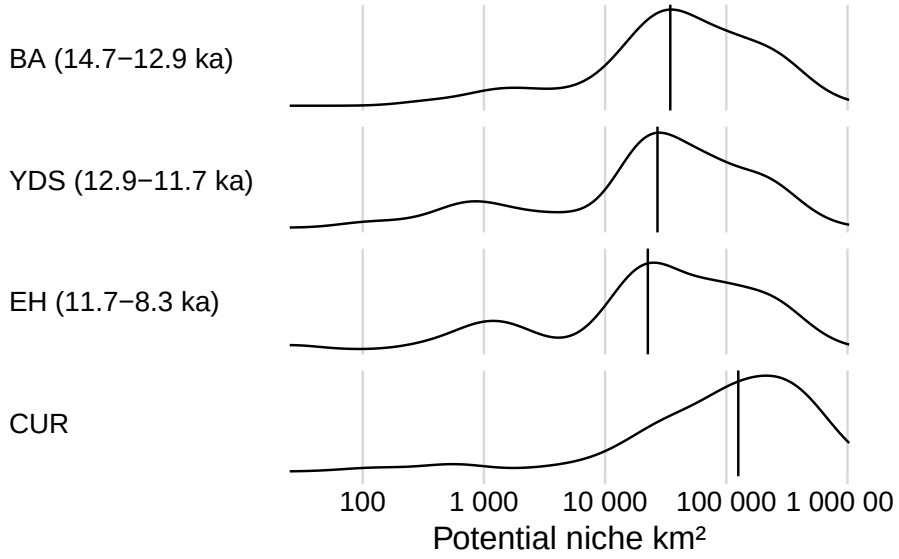


Figure 4: Distribution of predicted species niche size by period (logarithmic scale). Dashed lines indicate the median niche size.

Our reconstructed palaeodistributions (shown in full in the appendix) indicate that the majority of species had significantly different potential geographic niches in the Late Pleistocene/Early Holocene compared today. 55 of 65 species are predicted reduced niches in the past; 52 of more than 10% or more. Though the magnitude of the change in potential niche size from prehistory to the present likely reflects a degree of overfitting in the model (discussed further

in Section 5.3), fluctuations in modelled niche size between the Bølling-Allerød (14.7–12.9 ka), Younger Dryas (12.9–11.7 ka), and Early Holocene (11.7–8.3 ka) are more directly comparable (Figure 4). The average potential niche size of modelled species was 35% smaller in the Early Holocene compared to the Bølling–Allerød, and 22% smaller during the Younger Dryas. This perhaps indicates that although this period is considered one of climatatic amelioration globally (Jones et al., 2019), the colder conditions of the Pleistocene may have supported more extensive plant-based economies in West Asia specifically.

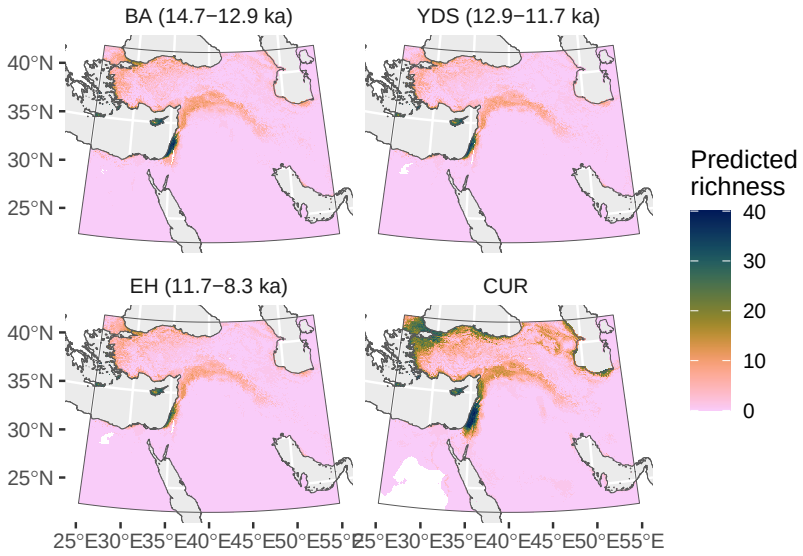


Figure 5: Predicted species richness (sum of predicted ranges) by period

Many taxa that occur (or are predicted to occur) across the 'hilly flanks' today—including most crop progenitors—are reconstructed to have had a significantly more restricted distribution in the terminal Pleistocene/Early Holocene (Figure 5). These include *Ficus carica* (fig); *Hordeum* spp. (wild barleys); *Lathyrus aphaca* and *L. sativus* (both marginally edible legumes); *Triticum aestivum compactum* (in the N. Levant), *T. monococcum aegilopoides*, *T. durum*, and *Triticum urartu* (but not the other wheat progenitor, *T. turgidum dicoccum* – see Section 5.2); *Aegilops speltoides*, but not *Aegilops tauschii* (goatgrasses); and *Vicia* spp. (vetches), including *Vicia faba* (broad beans). Most of Anatolia, Northern Mesopotamia, and the Zagros Mountains in particular disappear from the predicted niches of these species, leaving the Levant and to a lesser extent the Aegean and Cyprus as refugia.

Our results for the Levant are consistent with the current understanding of this region as developing early intensive foraging economies (the Natufian culture, Bar-Yosef, 1998) and as a centre of origin of agriculture (Zeder, 2011). Within

the Levant, many species show moderate reductions in potential niche size over the Pleistocene/Holocene boundary, retreating from the Badia/transjordan region (e.g. barley, fig. Figure 8).

Loss of the Northern Mesopotamia–Anatolia region from the predicted potential niches of crop progenitors is interesting in light of the 'golden triangle' hypothesis (Lev-Yadun et al., 2000b; Kozłowski and Aurenche, 2005; Abbo et al., 2010), which puts this region at the centre of the development of agriculture and plant domestication. Multiple lines of archaeological evidence have emerged that point away from this hypothesis and towards a more geographically diverse origin (Asouti, 2006; Fuller et al., 2011; Arranz-Otaegui et al., 2016), and our reconstructions are also consistent with the late arrival of intensive plant-based foraging economies in this region (cf. the Natufian of the Levant).

The near-absence of the Zagros in any predicted niches is also surprising, given mounting evidence that animal domestication took place just as early in the eastern *Mashriq* as it did in the west (Zeder, 2024). We consider that the most likely explanation for this is that our flora does not include the species that were most important to plant subsistence in the east. Archaeobotanical data on Neolithic sites in the Zagros is limited (compared to the Levant in particular) due to a hiatus in field research there from the 1980s to early 2010s (Zeder, 2024). Recent research (Riehl et al., 2013; Weide et al., 2017, 2018; Whitlam et al., 2018; González Carretero et al., 2023) indicates that plant subsistence in this region was based on a distinct set of species than that of the Levant and Anatolia.

Cyprus and the Aegean are not conventionally considered part of the primary zone of domestication but rather amongst the first regions that acquired agriculture from West Asia. Our analysis complicates this picture, as it indicates that the wild distribution of many crop progenitors included these regions. Early examples of several domesticates are recorded at sites on Cyprus, Western Anatolia and Greece (Arranz-Otaegui and Roe, 2023), and the Aegean region was probably connected to West Asia by a land bridge via Anatolia until the Early Holocene (Aksu and Hiscott, 2022). Were these area part of the same broader 'interaction sphere' that produced Neolithic agriculture in West Asia?

Exceptions to the dominant trend of niche size reduction include *Cicer reticulatum* (wild chickpea), which has a relatively stable potential niche centered on Northern Mesopotamia; and *Triticum turgidum dicoccum* (wild emmer wheat), which is predicted to occur in two limited zones centered around the Black Sea Coast of Anatolia and the Palmyra basin. In the latter case, neither of these areas are part of the predicted (by our model) modern distribution of wild emmer, which is centered around the Caucasus and Northern Mesopotamia. But it would be consistent with archaeological evidence for early cultivation at sites in the Upper Euphrates (Willcox, 2024).

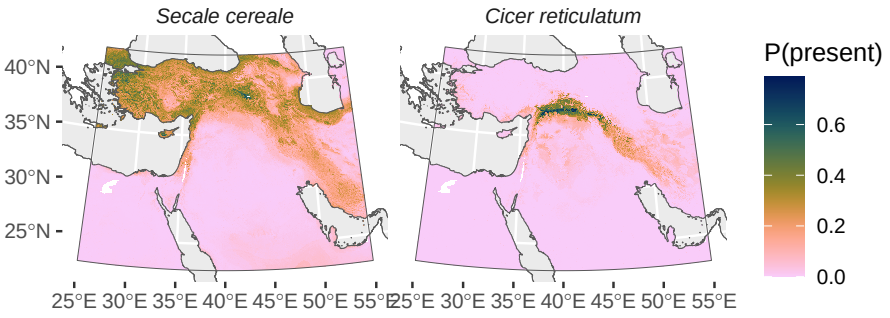


Figure 6: Predicted palaeodistribution of wild chickpea and rye in the Early Holocene (11.7–8.2 ka)

### *5.2. Biogeography of crop progenitors*

Almost all the cereal and legume crop progenitors we modelled are predicted to have only been found in the Levant during the terminal Pleistocene and Early Holocene (see appendix). Part of this may be do with the fact that both our initial flora and training occurrence dataset have a strong bias towards the southern Levant, but the modelled *current* potential niche of these plants do tend to include Anatolia and the Zagros, so this cannot be the only factor. It has previously been proposed that the Southern Levant was an "important glacial refuge area for wild cereals" (Roberts et al., 2018), which accords with these results.

One notable exception is the wild ancestor of chickpea (*Cicer reticulatum*), which is predicted to have a distribution centered on Northern Mesopotamia but encompassing much of the the 'hilly flanks' (except the southern Levant, Figure 6). Another is rye (*Secale cereale*), which is inferred to be primarily Anatolian (Figure 6). This is perhaps relevant to rye's unusual domestication history, as a crop of West Asian origin that was intensively exploited (Hillman et al., 2001; Douché and Willcox, 2018) but apparently not first cultivated until much later than the 'founder crops', in Europe (Schreiber et al., 2021).

Flax (*Linum bienne*) is predicted to have had a highly concentrated distribution in Cyprus and along the Mediterranean coast of the southern Levant. This is consistent with its low ubiquity in archaeobotanical assemblages (Arranz-Otaegui and Roe, 2023), despite conventionally being considered a 'founder

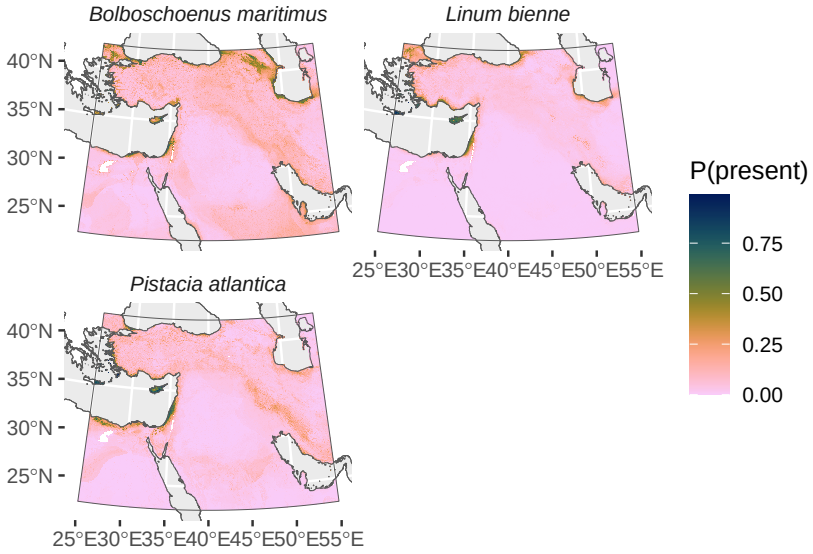


Figure 7: Predicted palaeodistribution of flax, pistachio and clubrush in the Early Holocene (11.7–8.2 ka)

crop', and presumably implies that its domestication was similarly geographically constrained. It is the only unambiguous crop progenitor with such a restricted potential niche, though pistachio (*Pistacia atlantica*) and clubrush (*Bolboschoenus maritimus*) are similarly constrained to the Mediterranean coast (and North Africa, in the case of pistachio). This is despite the fact that they are well-attested in the archaeotanical record from across West Asia.

Wild barley (*Hordeum spontaneum*) its relatives show a contraction of their predicted potential niche from the Pleistocene to the Holocene, concurrent with it being brought into cultivation (Figure 8). It also sees a marked decline in the archaeobotanical record from the Early PPNA/Early PPNB (where it was amongst the most common taxa) to the Late PPNB and Late Neolithic (Arranz-Otaegui and Roe, 2023). Pistachio (*Pistacia atlantica*) shows similar trends, but it is less certain that this species was managed in the Neolithic. Conversely, the various wild wheat species native to West Asia show almost no response to Pleistocene/Holocene climate change, even within the Levant, and in the archaeobotanical record wheat displays the opposite trend to barley and pistachio – becoming gradually more abundant through the course of the Neolithic and dominant by its end (Arranz-Otaegui and Roe, 2023).

Bread wheat (*Triticum aestivum*), the most common wheat cultivar today, has a complex ancestry that involves two recent hybridisation events (Levy and Feldman, 2022): most recently between domestic emmer (*Triticum turgidum dicoccum*) and a goatgrass (*Aegilops tauschii*) c. 9 ka, and before that, in emmer,

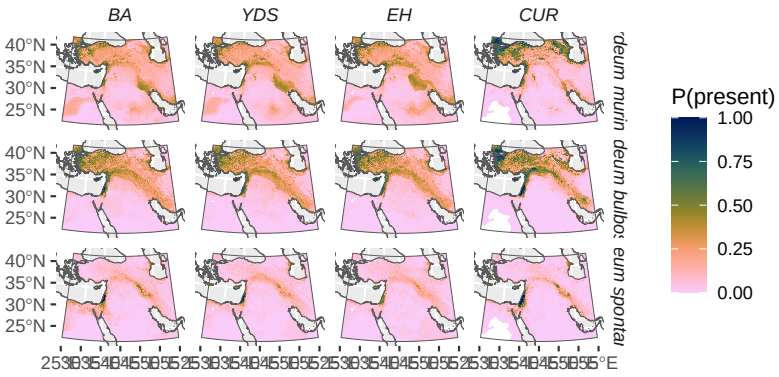


Figure 8: Predicted palaeodistribution of wild barleys

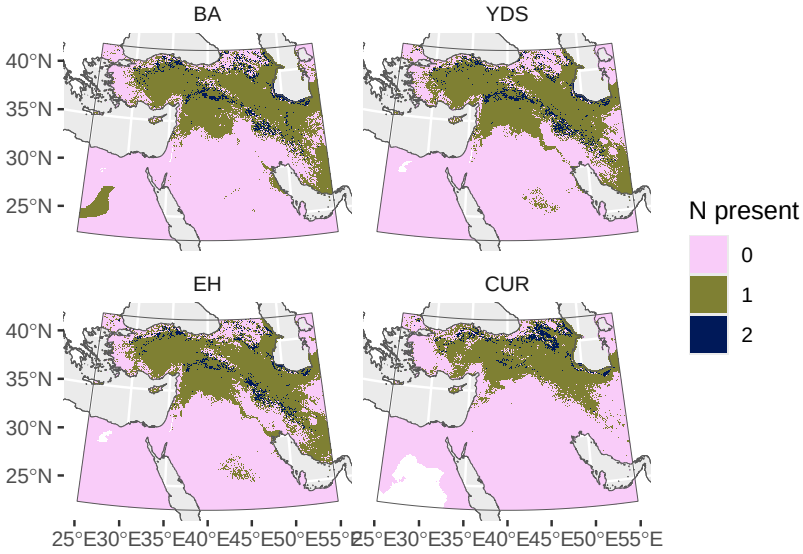


Figure 9: Combined predicted palaeodistributions of bread wheat progenitors

between wild red einkorn (*T. urartu*) and another goatgrass (*Aegilops speltoides*). The predicted potential niches of the two recent progenitors—*T. turgidum dicoccum* and *A. tauschii*—have relateively limited areas of overlap. These include the Syrian Jazira (Figure 9), close to the only two sites in our archaeobotanical database where bread wheat (*T. aestivum*) co-occurs with both of the recent progenitors (*A. tauschii* and *T. turgidum dicoccum*): Tell Abu Hureyra and El Kowm II (Arranz-Otaegui and Roe, 2023).[2] Taken together this suggests an origin of domesticated bread wheat, otherwise only loosely geographically constrained to the Levant–Upper Euphrates corridor (Levy and Feldman, 2022), in this vicinity.

### *5.3. Disagreement between hindcast models and archaeobotanical composition*

In general there is middling to low agreement between our hindcast predictions of species niches and observed archaeological occurrences of the same species (**?**).

The hindcasting performance of models is not strongly correlated with either the number of occurrences in the training dataset, the performance of the model on test data, or the number of attested archaeological occurrences (Figure 10). This indicates against a single, simple explanation for the discrepancy, i.e. that one or the other signal is 'wrong'.

The core issue is that the two sets of evidence discussed here—modelled

[2]We are grateful to Benjamin Nowak for pointing this out to us.

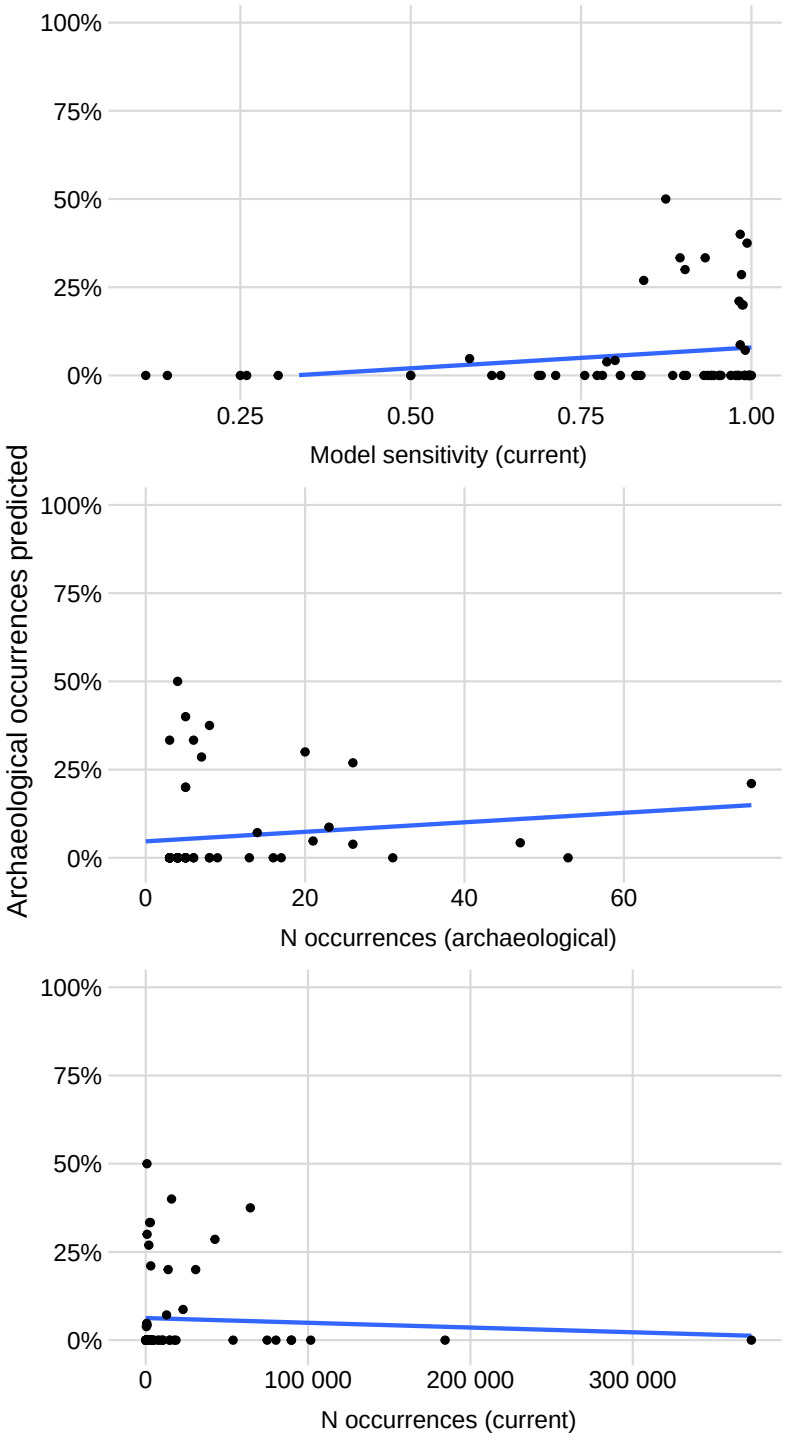


Figure 10: Summary of hindcasting performance of models in relation to model performance and available archaeological test data

palaeodistributions and archaeologically-attested palaeooccurrences—are signals of related but distinct phenomena. The hindcast niche models are projections of the species' present realised niche into a reconstructed past climatology. The archaeobotanical record is an incomplete sample of a past realised niche passed through various anthropic and taphonomic filters. Neither can be assumed to be fully accurate representations of the ultimate aim of this study, which is the *fundamental* niche of the species in relation to reconstructable climate and environmental factors – though both carry information about it.

For each specific species there are a variety of potential explanations for why the signals differ, but without further lines of evidence we are not in a position to distinguish them. In general, our models probably underestimate the fundamental niche or potential distribution of the target taxon for a variety of reasons:

- The inherent tendency of machine learning models to overfit to the training scenario, despite our efforts to mitigate this;
- Uneven spatial sampling intensity of the GBIF occurrence dataset (see Section 3.1), meaning that some parts of the species' niche are probably either over- and under-represented in the training data;
- Use of fairly coarse (2000 year) time-averaged climate slices, which capture a general trend but are probably unrepresentative of the environment around sites at the specific time at which they were occupied.

At the same time, there are several reasons to believe that the archaeobotanical data (at least as it has been compiled for this study) *overestimates* the fundamental niche:

- Archaeological deposits are also time-averaged signals, in some cases over quite large spans of time;
- The chronology attached to our archaeobotanical data is imprecise, e.g. primarily based on point estimates of radiocarbon dates (Michczyński, 2007), producing a further averaging effect;
- Archaeological occurences could be the result of human transplanting, range expansion and/or transport, especially considering this is the period where agriculture began to be practiced;
- Most archaeobotanical samples in our archaeological test dataset were small, so individual errors and misidentifications have a correspondingly large impact on quantification of model performance.

At the same time, we cannot rule out more substantive reasons for the discrepency between predicted and observed archaeological occurrences. The niches of the modelled species could have changed since the Early Holocene, which would not be captured in a model trained purely on modern specimens. Human economic choices—mobility, foraging strategies, cultivation, etc.—could also produce archaeobotanical assemblages whose composition depart significantly from that of the surrounding local flora.

What are the implications of this assessment? In the immediate term, the

modelled palaeodistributions presented here should be taken as conservative estimates – a minimal likely potential niche of the species. Closer inspection of discrepencies between the modelled and attested distributions of particular species in relation to specific environmental, taphonomic and cultural factors could yield further insights. Future applications of hindcast palaeoecological niche models in archaeology could refine the methodology in several ways: using more finely resolved palaeoclimate sequences (e.g. Karger et al., 2023); building more refined archaeological chronologies; performing hyperparameter tuning to further mitigate overfitting;[3] and compiling expanded archaeological datasets that could be use to calibrate binary classification.

## 6. Conclusion

We present the first continuous, spatially explicit models of the palaeodistributions of 65 plant species found regularly in association with Late Epipalaeolithic and Early Neolithic sites in West Asia. This deductive approach—modelling the niche of a species based on its occurrence in relation to environmental factors today, and using this together with palaeoclimate simulations to infer its past distribution—represents a new line of evidence on the archaeoecology of the world's first agricultural societies. It provides a complementary picture to that gleaned from environmental archaeology and climatological archives because it is independent of the taphonomic, anthropic, and recovery-related processes that affect these records.

The modelled palaeodistributions of the species presented here (see appendix) represent plausible minimum potential niche under the average climatic conditions of the Bølling-Allerød, Younger Dryas, and Early Holocene periods. The models' generally high performance as assessed against independent contemporary test datasets lend confidence to these predictions. Their application as a binary predictor of archaeological presence or absence is significantly less promising, which likely reflects a combination of methodological limitations of our modelling approach, the incomplete and coarsely temporally-resolved nature of the archaeobotanical test dataset, and genuine discrepencies between the species' fundamental niche and its occurrence in the archaeological record. Whether on the broad scale (e.g. the restricted geographic range of most species compared to their attestation in the archaeological record), or relating to specific species (i.e. false positives and false negatives), these discrepencies suggest several avenues for future investigation.

Modelling a large number of species using machine learning, the substantial occurrence datasets available for the present day, and a hindcasting approach to past distributions also represents a significant advance in the methodology of palaeoecological niche modelling. This approach is enabled by the availability of high quality, global open datasets in ecology (GBIF, 2025b; GBIF Secretariat,

[3]We did not perform hyperparameter tuning in this study due to computational limitations.

2023), earth science (Farr et al., 2007), and climatology (Karger et al., 2017; Brown et al., 2018). However, several areas of methodological improvement are evident. Notably, the state of open data availability in archaeology lags conspiciously behind the fields mentioned above. Though we have benefited from the relatively long tradition of compiling archaeobotanical data in our region of study (Colledge et al., 2004; Shennan and Conolly, 2007; Riehl and Kümmel, 2005; Lucas and Fuller, 2018; Fuller et al., 2018; Wallace et al., 2018a,b), further development of open, comprehensive and up-to-date 'backbone' datasets on site locations and chronologies is needed to advance archaeoecological modelling to the same level.

## 7. Data availability

The data and R code used to produce this study is archived with Zenodo at https://doi.org/10.5281/zenodo.14629984. Modelled palaeodistributions in raster format (.TIF) can be found in the same repository.

## 8. Acknowledgements

We are grateful to Alex Weide and the second, anonymous reviewer of our manuscript, whose suggestions have greatly improved this study.

This work was partially funded by the European Research Council (ERC-2021-STG project 101039060, *PalaeOrigins: Tracing the Epipalaeolithic origins of plant management in southwest Asia*).

## References

Abbo, S., Gopher, A., Peleg, Z., Saranga, Y., Fahima, T., Salamini, F., Lev-Yadun, S., 2006. The ripples of "The Big (agricultural) Bang": The spread of early wheat cultivation. Genome 49, 861–863. doi:10.1139/g06-049.

Abbo, S., Gopher, A., Rubin, B., Lev-Yadun, S., 2005. On the Origin of Near Eastern Founder Crops and the 'Dump-heap Hypothesis'. Genetic Resources and Crop Evolution 52, 491–495. doi:10.1007/s10722-004-7069-x.

Abbo, S., Lev-Yadun, S., Gopher, A., 2010. Agricultural Origins: Centers and Noncenters; A Near Eastern Reappraisal. Critical Reviews in Plant Sciences 29, 317–328. doi:10.1080/07352689.2010.502823.

Abbo, S., Lev-Yadun, S., Gopher, A., 2011. Origin of Near Eastern plant domestication: Homage to Claude Levi-Strauss and "La Pensée Sauvage". Genetic Resources and Crop Evolution 58, 175–179. doi:10.1007/s10722-010-9630-0.

Abbo, S., Lev-Yadun, S., Gopher, A., 2012. Plant Domestication and Crop Evolution in the Near East: On Events and Processes. Critical Reviews in Plant Sciences 31, 241–257. doi:10.1080/07352689.2011.645428.

Aksu, A.E., Hiscott, R.N., 2022. Persistent Holocene outflow from the Black Sea to the eastern Mediterranean Sea still contradicts the Noah's Flood Hypothesis: A review of 1997–2021 evidence and a regional paleoceanographic synthesis for the latest Pleistocene–Holocene. Earth-Science Reviews 227, 103960. doi:10.1016/j.earscirev.2022.103960.

Arranz-Otaegui, A., Colledge, S., Zapata, L., Teira-Mayolini, L.C., Ibáñez, J.J., 2016. Regional diversity on the timing for the initial appearance of cereal cultivation and domestication in southwest Asia. Proceedings of the National Academy of Sciences 113, 14001–14006. doi:10.1073/pnas.1612797113.

Arranz-Otaegui, A., González Carretero, L., Roe, J., Richter, T., 2018. "Founder crops" v. wild plants: Assessing the plant-based diet of the last hunter-gatherers in southwest Asia. Quat. Sci. Rev. 186, 263–283. doi:10.1016/j.quascirev.2018.02.011.

Arranz-Otaegui, A., Roe, J., 2023. Revisiting the concept of the 'Neolithic Founder Crops' in southwest Asia. Vegetation History and Archaeobotany doi:10.1007/s00334-023-00917-1.

Asouti, E., 2006. Beyond the Pre-Pottery Neolithic B interaction sphere. Journal of World Prehistory 20, 87–126. doi:10.1007/s10963-007-9008-1.

Austin, M.P., Van Niel, K.P., 2011. Improving species distribution models for climate change studies: Variable selection and scale. Journal of Biogeography 38, 1–8. doi:10.1111/j.1365-2699.2010.02416.x.

Badr, A., M, K., Sch, R., Rabey, H.E., Effgen, S., Ibrahim, H.H., Pozzi, C., Rohde, W., Salamini, F., 2000. On the Origin and Domestication History of Barley (Hordeum vulgare). Molecular Biology and Evolution 17, 499–510. doi:10.1093/oxfordjournals.molbev.a026330.

Banks, W.E., Moncel, M.H., Raynal, J.P., Cobos, M.E., Romero-Alvarez, D., Woillez, M.N., Faivre, J.P., Gravina, B., d'Errico, F., Locht, J.L., Santos, F., 2021. An ecological niche shift for Neanderthal populations in Western Europe 70,000 years ago. Scientific Reports 11, 5346. doi:10.1038/s41598-021-84805-6.

Bar-Yosef, O., 1998. The Natufian culture in the Levant, threshold to the origins of agriculture. Evolutionary Anthropology 6, 159–177. doi:10.1002/(SICI)1520-6505(1998)6:5<159::AID-EVAN4>3.0.CO;2-7.

Barbet-Massin, M., Jiguet, F., Albert, C.H., Thuiller, W., 2012. Selecting pseudo-absences for species distribution models: How, where and how many?: How to use pseudo-absences in niche modelling? Methods Ecol. Evol. 3, 327–338. doi:10.1111/j.2041-210X.2011.00172.x.

Benito, B.M., Svenning, J.C., Kellberg-Nielsen, T., Riede, F., Gil-Romera, G., Mailund, T., Kjaergaard, P.C., Sandel, B.S., 2017. The ecological niche and

distribution of Neanderthals during the Last Interglacial. J. Biogeogr. 44, 51–61. doi:10.1111/jbi.12845.

Boyd, B., 2018. Settled? Recent debates in the archaeology of the Epipalaeolithic and Pre-Pottery Neolithic of Southwest Asia. Asian Archaeology 1, 63–73. doi:10.1007/s41826-018-0006-3.

Brown, J.L., Hill, D.J., Dolan, A.M., Carnaval, A.C., Haywood, A.M., 2018. PaleoClim, high spatial resolution paleoclimate surfaces for global land areas. Sci Data 5, 180254. doi:10.1038/sdata.2018.254.

Brown, S.C., Wigley, T.M.L., Otto-Bliesner, B.L., Fordham, D.A., 2020. StableClim, continuous projections of climate stability from 21000 BP to 2100 CE at multiple spatial scales. Scientific Data 7, 335. doi:10.1038/s41597-020-00663-3.

Butzer, K.W., 1971. Agricultural origins in the Near East as a geographical problem, in: Streuver, S. (Ed.), Prehistoric Agriculture. American Museum Sourcebooks in Anthropology.

Campos, V.E., Cappa, F.M., Viviana, F.M., Giannoni, S.M., 2016. Using remotely sensed data to model suitable habitats for tree species in a desert environment. Journal of Vegetation Science 27, 200–210. doi:10.1111/jvs.12328.

de Candolle, A., 1886. The Origin of Cultivated Plants. Cambridge University Press, Cambridge. doi:10.1017/CBO9781139107365.

Chamberlain, S., Barve, V., Mcglinn, D., Oldoni, D., Desmet, P., Geffert, L., Ram, K., 2024. rgbif: Interface to the Global Biodiversity Information Facility API. URL: https://CRAN.R-project.org/package=rgbif. r package version 3.8.1.

Chamberlain, S., Boettiger, C., 2017. R python, and ruby clients for gbif species occurrence data. PeerJ PrePrints URL: https://doi.org/10.7287/peerj.preprints.3304v1.

Childe, V.G., 1936. Man Makes Himself. Watts & Co, London.

Colledge, S., 2001. Plant Exploitation on Epipalaeolithic and Early Neolithic Sites in the Levant. BAR International Series, Oxbow, Oxford.

Colledge, S., Conolly, J., Shennan, S., 2004. Archaeobotanical Evidence for the Spread of Farming in the Eastern Mediterranean. Current Anthropology 45, S35–S58. doi:10.1086/422086.

Collins, C., Asouti, E., Grove, M., Kabukcu, C., Bradley, L., Chiverrell, R., 2018. Understanding resource choice at the transition from foraging to farming: An application of palaeodistribution modelling to the Neolithic of the Konya Plain, south-central Anatolia, Turkey. J. Archaeol. Sci. 96, 57–72. doi:10.1016/j.jas.2018.02.003.

Conolly, J., Manning, K., Colledge, S., Dobney, K., Shennan, S., 2012. Species distribution modelling of ancient cattle from early Neolithic sites in SW Asia and Europe. Holocene 22, 997–1010. doi:10.1177/0959683612437871.

Cordova, C.E., 2007. Millennial Landscape Change in Jordan: Geoarchaeology and Cultural Ecology. University of Arizona Press, Tucson, AZ.

Darwin, C., 1859. On the Origin of Species by Means of Natural Selection, or the Preservation of Favoured Races in the Struggle for Life. John Murray, London.

David Polly, P., Eronen, J.T., 2011. Mammal Associations in the Pleistocene of Britain: Implications of Ecological Niche Modelling and a Method for Reconstructing Palaeoclimate, in: Ashton, N., Lewis, S.G., Stringer, C. (Eds.), Developments in Quaternary Sciences. Elsevier. volume 14, pp. 279–304. doi:10.1016/B978-0-444-53597-9.00015-7.

de Andrés-Herrero, M., Becker, D., Weniger, G.C., 2018. Reconstruction of LGM faunal patterns using Species Distribution Modelling. The archaeological record of the Solutrean in Iberia. Quat. Int. 485, 199–208. doi:10.1016/j.quaint.2017.10.042.

Dennell, R.W., 1976. The economic importance of plant resources represented on archaeological sites. Journal of Archaeological Science 3, 229–247. doi:10.1016/0305-4403(76)90057-1.

Di Virgilio, G., Wardell-Johnson, G.W., Robinson, T.P., Temple-Smith, D., Hesford, J., 2018. Characterising fine-scale variation in plant species richness and endemism across topographically complex, semi-arid landscapes. Journal of Arid Environments 156, 59–68. doi:10.1016/j.jaridenv.2018.04.005.

Diamond, J., 2002. Evolution, consequences and future of plant and animal domestication. Nature 418, 700–707. doi:10.1038/nature01019.

Dormann, C.F., Elith, J., Bacher, S., Buchmann, C., Carl, G., Carré, G., Marquéz, J.R.G., Gruber, B., Lafourcade, B., Leitão, P.J., Münkemüller, T., McClean, C., Osborne, P.E., Reineking, B., Schröder, B., Skidmore, A.K., Zurell, D., Lautenbach, S., 2013. Collinearity: a review of methods to deal with it and a simulation study evaluating their performance. Ecography 36, 27–46. URL: https://onlinelibrary.wiley.com/doi/abs/10.1111/j.1600-0587.2012.07348.x, doi:10.1111/j.1600-0587.2012.07348.x. _eprint: https://nsojournals.onlinelibrary.wiley.com/doi/pdf/10.1111/j.1600-0587.2012.07348.x.

Douché, C., Willcox, G., 2018. New archaeobotanical data from the Early Neolithic sites of Dja'de el-Mughara and Tell Aswad (Syria): A comparison between the Northern and the Southern Levant. Paléorient 44, 45–58. arXiv:26595374.

Dubuis, A., Giovanettina, S., Pellissier, L., Pottier, J., Vittoz, P., Guisan, A., 2013. Improving the prediction of plant species distribution and community composition by adding edaphic to topo-climatic variables. Journal of Vegetation Science 24, 593–606. doi:10.1111/jvs.12002.

Farr, T.G., Rosen, P.A., Caro, E., Crippen, R., Duren, R., Hensley, S., Kobrick, M., Paller, M., Rodriguez, E., Roth, L., Seal, D., Shaffer, S., Shimada, J., Umland, J., Werner, M., Oskin, M., Burbank, D., Alsdorf, D., 2007. The Shuttle Radar Topography Mission. Rev. Geophys. 45, RG2004. doi:10.1029/2005RG000183.

Fordham, D.A., Saltré, F., Haythorne, S., Wigley, T.M.L., Otto-Bliesner, B.L., Chan, K.C., Brook, B.W., 2017. PaleoView: A tool for generating continuous climate projections spanning the last 21 000 years at regional and global scales. Ecography 40, 1348–1358. doi:10.1111/ecog.03031.

Franklin, J., Miller, J.A., 2009. Mapping Species Distributions: Spatial Inference and Prediction. Cambridge University Press.

Franklin, J., Potts, A.J., Fisher, E.C., Cowling, R.M., Marean, C.W., 2015. Paleodistribution modeling in archaeology and paleoanthropology. Quat. Sci. Rev. 110, 1–14. doi:10.1016/j.quascirev.2014.12.015.

Fuller, D.Q., 2010. An emerging paradigm shift in the origins of agriculture. General Anthropology 17, 1–12.

Fuller, D.Q., Colledge, S., 2008. Recent lessons from Near Eastern archaeobotany: Wild cereal use, pre-domestication cultivation and tracing multiple origins and dispersals. Pragdhara 18, 105–134.

Fuller, D.Q., Lucas, L., Carretero, L.G., Stevens, C., 2018. From intermediate economies to agriculture: Trends in wild food use, domestication and cultivation among early villages in Southwest Asia. Paléorient 44, 59–74. arXiv:26595375.

Fuller, D.Q., Willcox, G., Allaby, R.G., 2011. Cultivation and domestication had multiple origins: Arguments against the core area hypothesis for the origins of agriculture in the Near East. World Archaeol. 43, 628–652. doi:10.1080/00438243.2011.624747.

GBIF, 2025a. Gbif Occurrence Download. URL: https://doi.org/10.15468/dl.t8sqqm.

GBIF, 2025b. What is GBIF? https://www.gbif.org/what-is-gbif.

GBIF Secretariat, 2023. GBIF Backbone Taxonomy. doi:10.15468/39OMEI.

González Carretero, L., Lucas, L., Stevens, C., Fuller, D.Q., 2023. Investigating early agriculture, plant use and culinary practices at Neolithic Jarmo (Iraqi Kurdistan). Journal of Archaeological Science: Reports 52, 104264. doi:10.1016/j.jasrep.2023.104264.

Gopher, A., Abbo, S., Yadun, S.L., 2001. The "when", the "where" and the "why" of the Neolithic revolution in the Levant. Documenta Praehistorica 28, 49–62. doi:10.4312/dp.28.3.

Guran, S.H., Yousefi, M., Kafash, A., Ghasidian, E., 2024. Reconstructing contact and a potential interbreeding geographical zone between Neanderthals and anatomically modern humans. Scientific Reports 14, 20475. doi:10.1038/s41598-024-70206-y.

Harlan, J.R., 1971. Agricultural Origins: Centers and Noncenters. Science 174, 468–474. doi:10.1126/science.174.4008.468.

Harlan, J.R., 1977. The Origins of Cereal Agriculture in the Old World, in: Reed, C.A. (Ed.), Origins of Agriculture. De Gruyter Mouton, pp. 357–384. doi:10.1515/9783110813487.357.

Harlan, J.R., Zohary, D., 1966. Distribution of Wild Wheats and Barley. Science 153, 1074–1080. URL: https://www.science.org/doi/abs/10.1126/science.153.3740.1074, doi:10.1126/science.153.3740.1074. publisher: American Association for the Advancement of Science.

Harris, D.R., 1989. An evolutionary continuum of people–plant interaction, in: The Emergence of Agriculture. Routledge.

Harris, D.R., 1990. Vavilov's concept of centres of origin of cultivated plants: Its genesis and its influence on the study of agricultural origins. Biological Journal of the Linnean Society 39, 7–16. doi:10.1111/j.1095-8312.1990.tb01608.x.

Harris, D.R., 2007. Agriculture, Cultivation and Domestication: Exploring the Conceptual Framework of Early Food Production, in: Rethinking Agriculture. Routledge.

Harris, D.R., Hillman, G.C., 1989. Introduction, in: Foraging and Farming: The Evolution of Plant Exploitation. Routledge.

Hastorf, C.A., Popper, V.S., 1988. Current Paleoethnobotany: Analytical Methods and Cultural Interpretations of Archaeological Plant Remains. University of Chicago Press.

Helbæk, H., 1969. Plant Collecting, Dry-Farming and Irrigation Agriculture in Prehistoric Deh Luran. volume 1. University of Michigan Ann Arbor.

Helbæk, H., 1959. How farming began in the Old World. Archaeology 12, 183–189.

Hengl, T., de Jesus, J.M., MacMillan, R.A., Batjes, N.H., Heuvelink, G.B.M., Ribeiro, E., Samuel-Rosa, A., Kempen, B., Leenaars, J.G.B., Walsh, M.G., Gonzalez, M.R., 2014. SoilGrids1km–global soil information based on automated mapping. PLoS One 9, e105992. doi:10.1371/journal.pone.0105992.

Hengl, T., Mendes de Jesus, J., Heuvelink, G.B.M., Ruiperez Gonzalez, M., Kilibarda, M., Blagotić, A., Shangguan, W., Wright, M.N., Geng, X., Bauer-Marschallinger, B., Guevara, M.A., Vargas, R., MacMillan, R.A., Batjes, N.H., Leenaars, J.G.B., Ribeiro, E., Wheeler, I., Mantel, S., Kempen, B., 2017. SoilGrids250m: Global gridded soil information based on machine learning. PLoS One 12, e0169748. doi:10.1371/journal.pone.0169748.

Hernandez, P.A., Graham, C.H., Master, L.L., Albert, D.L., 2006. The effect of sample size and species characteristics on performance of different species distribution modeling methods. Ecography 29, 773–785. URL: https://onlinelibrary.wiley.com/doi/abs/10.1111/j.0906-7590.2006.04700.x, doi:10.1111/j.0906-7590.2006.04700.x.

Heun, M., Schäfer-Pregl, R., Klawan, D., Castagna, R., Accerbi, M., Borghi, B., Salamini, F., 1997. Site of Einkorn Wheat Domestication Identified by DNA Fingerprinting. Science 278, 1312–1314. doi:10.1126/science.278.5341.1312.

Hijmans, R.J., Cameron, S.E., Parra, J.L., Jones, P.G., Jarvis, A., 2005. Very high resolution interpolated climate surfaces for global land areas. Int. J. Climatol. 25, 1965–1978. doi:10.1002/joc.1276.

Hillman, G., Hedges, R., Moore, A., Colledge, S., Pettitt, P., 2001. New evidence of Lateglacial cereal cultivation at Abu Hureyra on the Euphrates. The Holocene 11, 383–393. doi:10.1191/095968301678302823.

Hillman, G.C., Davies, M.S., 1990. Measured domestication rates in wild wheats and barley under primitive cultivation, and their archaeological implications. Journal of World Prehistory 4, 157–222. doi:10.1007/BF00974763.

Hillman, G.C., Davies, M.S., 1992. Domestication Rate in Wild Wheats and Barley under Primitive Cultivation: Premiminary Results and Archaeological Implications of Field Measurements of Selection Coefficient. Monographie du CRA , 113–158.

Hopf, M., 1969. Plant remains and early farming in Jericho 1, in: The Domestication and Exploitation of Plants and Animals. Aldine, Chicago.

Hopf, M., 1986. Archaeological Evidence of the Spread and Use of Some Members of the Leguminosae Family, in: Barigozzi, C. (Ed.), Developments in Agricultural and Managed Forest Ecology. Elsevier. volume 16 of *The Origin and Domestication of Cultivated Plants*, pp. 35–60. doi:10.1016/B978-0-444-42703-8.50008-7.

Iob, A., Botigué, L., 2023. Genomic analysis of emmer wheat shows a complex history with two distinct domestic groups and evidence of differential hybridization with wild emmer from the western Fertile Crescent. Vegetation History and Archaeobotany 32, 545–558. doi:10.1007/s00334-022-00898-7.

Jones, M.D., Abu-Jaber, N., AlShdaifat, A., Baird, D., Cook, B.I., Cuthbert, M.O., Dean, J.R., Djamali, M., Eastwood, W., Fleitmann, D., Haywood, A., Kwiecien, O., Larsen, J., Maher, L.A., Metcalfe, S.E., Parker, A., Petrie, C.A., Primmer, N., Richter, T., Roberts, N., Roe, J., Tindall, J.C., Ünal-İmer, E., Weeks, L., 2019. 20,000 years of societal vulnerability and adaptation to climate change in southwest Asia. WIREs Water 6, e1330. doi:10.1002/wat2.1330.

Karger, D.N., Conrad, O., Böhner, J., Kawohl, T., Kreft, H., Soria-Auza, R.W., Zimmermann, N.E., Linder, H.P., Kessler, M., 2017. Climatologies at high resolution for the earth's land surface areas. Sci Data 4, 170122. doi:10.1038/sdata.2017.122.

Karger, D.N., Nobis, M.P., Normand, S., Graham, C.H., Zimmermann, N.E., 2023. CHELSA-TraCE21k – high-resolution (1 km) downscaled transient temperature and precipitation data since the Last Glacial Maximum. Climate of the Past 19, 439–456. doi:10.5194/cp-19-439-2023.

Kilian, B., Özkan, H., Walther, A., Kohl, J., Dagan, T., Salamini, F., Martin, W., 2007. Molecular Diversity at 18 Loci in 321 Wild and 92 Domesticate Lines Reveal No Reduction of Nucleotide Diversity during Triticum monococcum (Einkorn) Domestication: Implications for the Origin of Agriculture. Molecular Biology and Evolution 24, 2657–2668. doi:10.1093/molbev/msm192.

Kirkbride, D., 1966. Five Seasons at the Pre-Pottery Neolithic Village of Beidha In Jordan. Palestine Exploration Quarterly doi:10.1179/peq.1966.98.1.8.

Kislev, M.E., 1989. Origins of the cultivation oflathyrus sativus andL. cicera (fabaceae). Economic Botany 43, 262–270. doi:10.1007/BF02859868.

Kopecký, M., ˇCíˇzková, v.S.e., 2010. Using topographic wetness index in vegetation ecology: Does the algorithm matter? Appl. Veg. Sci. 13, 450–459. doi:10.1111/j.1654-109X.2010.01083.x.

Kozłowski, S.K., Aurenche, O., 2005. Territories, Boundaries and Cultures in the Neolithic Near East. Archaeopress.

Krzyzanska, M., 2023. Modelling spatio-temporal changes in the ecological niches of major domesticated crops in China: Application of Species Distribution Modelling. Ph.D. thesis. University of Cambridge.

Krzyzanska, M., Hunt, H.V., Crema, E.R., Jones, M.K., 2022. Modelling the potential ecological niche of domesticated buckwheat in China: Archaeological evidence, environmental constraints and climate change. Vegetation History and Archaeobotany 31, 331–345. doi:10.1007/s00334-021-00856-9.

Kuhn, M., Silge, J., 2022. Tidy Modeling with R: A Framework for Modeling in the Tidyverse. O'Reilly.

Ladizinsky, G., Adler, A., 1976. The origin of chickpea Cicer arietinum L. Euphytica 25, 211–217. doi:10.1007/BF00041547.

Leempoel, K., Parisod, C., Geiser, C., Daprà, L., Vittoz, P., Joost, S., 2015. Very high-resolution digital elevation models: Are multi-scale derived variables ecologically relevant? Methods in Ecology and Evolution 6, 1373–1383. doi:10.1111/2041-210X.12427.

Lev-Yadun, S., Gopher, A., Abbo, S., 2000a. The Cradle of Agriculture. Science 288, 1602–1603. doi:10.1126/science.288.5471.1602.

Lev-Yadun, S., Gopher, A., Abbo, S., 2000b. The Cradle of Agriculture. Science 288, 1602–1603. doi:10.1126/science.288.5471.1602.

Levy, A.A., Feldman, M., 2022. Evolution and origin of bread wheat. The Plant Cell 34, 2549–2567. doi:10.1093/plcell/koac130.

Lindsay, J.B., 2016. Whitebox GAT: A case study in geomorphometric analysis. Comput. Geosci. 95, 75–84. doi:10.1016/j.cageo.2016.07.003.

Liu, C., Berry, P.M., Dawson, T.P., Pearson, R.G., 2005. Selecting thresholds of occurrence in the prediction of species distributions. Ecography 28, 385–393. URL: https://onlinelibrary.wiley.com/doi/abs/10.1111/j.0906-7590.2005.03957.x, doi:10.1111/j.0906-7590.2005.03957.x. _eprint: https://nsojournals.onlinelibrary.wiley.com/doi/pdf/10.1111/j.0906-7590.2005.03957.x.

Liu, C., Newell, G., White, M., 2016. On the selection of thresholds for predicting species occurrence with presence-only data. Ecology and Evolution 6, 337–348. URL: https://onlinelibrary.wiley.com/doi/abs/10.1002/ece3.1878, doi:10.1002/ece3.1878. _eprint: https://onlinelibrary.wiley.com/doi/pdf/10.1002/ece3.1878.

Liu, C., White, M., Newell, G., 2013. Selecting thresholds for the prediction of species occurrence with presence-only data. Journal of Biogeography 40, 778–789. URL: https://onlinelibrary.wiley.com/doi/abs/10.1111/jbi.12058, doi:10.1111/jbi.12058. _eprint: https://onlinelibrary.wiley.com/doi/pdf/10.1111/jbi.12058.

Luan, J., Zhang, C., Xu, B., Xue, Y., Ren, Y., 2020. The predictive performances of random forest models with limited sample size and different species traits. Fisheries Research 227, 105534. doi:10.1016/j.fishres.2020.105534.

Lucas, L., Fuller, D., 2018. Dataset: From intermediate economies to agriculture: Trends in wild food use, domestication and cultivation among early villages in southwest Asia.

Luo, M.C., Yang, Z.L., You, F.M., Kawahara, T., Waines, J.G., Dvorak, J., 2007. The structure of wild and domesticated emmer wheat populations, gene flow between them, and the site of emmer domestication. Theoretical and Applied Genetics 114, 947–959. doi:10.1007/s00122-006-0474-0.

Maher, L.A., Richter, T., Stock, J.T., 2012. The Pre-Natufian Epipaleolithic: Long-term Behavioral Trends in the Levant. Evolutionary Anthropology: Issues, News, and Reviews 21, 69–81. doi:10.1002/evan.21307.

Michczyński, A., 2007. Is it Possible to Find a Good Point Estimate of a Calibrated Radiocarbon Date? Radiocarbon 49, 393–401. doi:10.1017/S0033822200042326. publisher: Cambridge University Press.

Miller, T., Blackwood, C.B., Case, A.L., 2024. Assessing the utility of SoilGrids250 for biogeographic inference of plant populations. Ecology and Evolution 14, e10986. doi:10.1002/ece3.10986.

Mod, H.K., Scherrer, D., Luoto, M., Guisan, A., 2016. What we use is not what we know: Environmental predictors in plant distribution models. Journal of Vegetation Science 27, 1308–1322. doi:10.1111/jvs.12444.

Molina-Cano, J.L., Russell, J.R., Moralejo, M.A., Escacena, J.L., Arias, G., Powell, W., 2005. Chloroplast DNA microsatellite analysis supports a polyphyletic origin for barley. Theoretical and Applied Genetics 110, 613–619. doi:10.1007/s00122-004-1878-3.

Moore, A.M.T., Hillman, G.C., Legge, A.J., 2000. Village on the Euphrates: From Foraging to Farming at Abu Hureyra. Oxford University Press, Oxford.

Mori, N., 2003. Origins of domesticated emmer and common wheat inferred from chloroplast DNA fingerprinting, in: Proc. 10th. Int. Wheat Genetics Symp., Paestum, Italy, 2003, pp. 25–28.

Ozkan, H., Brandolini, A., Pozzi, C., Effgen, S., Wunder, J., Salamini, F., 2005. A reconsideration of the domestication geography of tetraploid wheats. Theoretical and Applied Genetics 110, 1052–1060. doi:10.1007/s00122-005-1925-8.

Özkan, H., Brandolini, A., Schäfer-Pregl, R., Salamini, F., 2002. AFLP Analysis of a Collection of Tetraploid Wheats Indicates the Origin of Emmer and Hard Wheat Domestication in Southeast Turkey. Molecular Biology and Evolution 19, 1797–1801. doi:10.1093/oxfordjournals.molbev.a004002.

Özkan, H., Willcox, G., Graner, A., Salamini, F., Kilian, B., 2011. Geographic distribution and domestication of wild emmer wheat (Triticum dicoccoides). Genetic Resources and Crop Evolution 58, 11–53. doi:10.1007/s10722-010-9581-5.

Peake, H., Fleure, H.J., 1927. Corridors of Time III: Peasants and Potters. Clarendon Press, Oxford.

Pumpelly, R., 1908. Explorations in Turkestan. Number 73 in Carnegie Institution Publication, Carnegie Institution, Washington, DC.

Purugganan, M.D., Fuller, D.Q., 2009. The nature of selection during plant domestication. Nature 457, 843–848. doi:10.1038/nature07895.

Riehl, S., Kümmel, C., 2005. Archaeobotanical Database Of Eastern Mediterranean And Near Eastern Sites (ADEMNES).

Riehl, S., Zeidi, M., Conard, N.J., 2013. Emergence of Agriculture in the Foothills of the Zagros Mountains of Iran. Science 341, 65–67. doi:10.1126/science.1236743.

Roberts, N., Woodbridge, J., Bevan, A., Palmisano, A., Shennan, S., Asouti, E., 2018. Human responses and non-responses to climatic variations during the last Glacial-Interglacial transition in the eastern Mediterranean. Quaternary Science Reviews 184, 47–67. URL: https://www.sciencedirect.com/science/article/pii/S0277379117302809, doi:10.1016/j.quascirev.2017.09.011.

Schreiber, M., Özkan, H., Komatsuda, T., Mascher, M., 2021. Evolution and Domestication of Rye, in: Rabanus-Wallace, M.T., Stein, N. (Eds.), The Rye Genome. Springer International Publishing, Cham, pp. 85–100. doi:10.1007/978-3-030-83383-1_6.

Shennan, S.J., Conolly, J., 2007. Dataset: The Origin and Spread of Neolithic Plant Economies in the Near East and Europe.

Sillero, N., Arenas-Castro, S., Enriquez-Urzelai, U., Vale, C.G., Sousa-Guedes, D., Martínez-Freiría, F., Real, R., Barbosa, A.M., 2021. Want to model a species niche? A step-by-step guideline on correlative ecological niche modelling. Ecological Modelling 456, 109671. URL: https://www.sciencedirect.com/science/article/pii/S0304380021002301, doi:10.1016/j.ecolmodel.2021.109671.

Smith, B.D., 1995. The Emergence of Agriculture. Scientific American Library, New York, NY.

Stockwell, D.R.B., Peterson, A.T., 2002. Effects of sample size on accuracy of species distribution models. Ecological Modelling 148, 1–13. URL: https://www.sciencedirect.com/science/article/pii/S030438000100388X, doi:10.1016/S0304-3800(01)00388-X.

Tanno, K.i., Willcox, G., 2006. How Fast Was Wild Wheat Domesticated? Science 311, 1886–1886. doi:10.1126/science.1124635.

Tanno, K.i., Willcox, G., 2012. Distinguishing wild and domestic wheat and barley spikelets from early Holocene sites in the Near East. Vegetation History and Archaeobotany 21, 107–115. doi:10.1007/s00334-011-0316-0.

Townsend Peterson, A., Soberón, J., 2012. Species Distribution Modeling and Ecological Niche Modeling: Getting the Concepts Right. NatCon 10, 102–107. doi:10.4322/natcon.2012.019.

Valavi, R., Elith, J., Lahoz-Monfort, J.J., Guillera-Arroita, G., 2021. Modelling species presence-only data with random forests. Ecography 44, 1731–1742. doi:10.1111/ecog.05615.

Valavi, R., Guillera-Arroita, G., Lahoz-Monfort, J.J., Elith, J., 2022. Predictive performance of presence-only species distribution models: A benchmark study with reproducible code. Ecological Monographs 92, e01486. doi:10.1002/ecm.1486.

van Zeist, W., Bottema, S., 1991. Late Quaternary Vegetation of the Near East. Beihefte Zum Tübinger Atlas Des Vorderen Orients: Naturwissenschaften, Reichert.

Vavilov, N., 1926. Studies on the Origin of Cultivated Plants. Institute of Applied Botany and Plant Breeding, Leningrad.

Velazco, S.J.E., Galvão, F., Villalobos, F., De Marco Júnior, P., 2017. Using worldwide edaphic data to model plant species niches: An assessment at a continental extent. PloS One 12, e0186025. doi:10.1371/journal.pone.0186025, arXiv:29049298.

Verhagen, P., Whitley, T.G., 2020. Predictive Spatial Modelling, in: Archaeological Spatial Analysis. Routledge.

von Humboldt, A., 1807. Essai Sur La Géographie Des Plantes. Paris.

Wallace, M., Jones, G., Charles, M., Forster, E., Stillman, E., Bonhomme, V., Livarda, A., Osborne, C.P., Rees, M., Frenck, G., Preece, C., 2018a. Re-analysis of archaeobotanical remains from pre- and early agricultural sites provides no evidence for a narrowing of the wild plant food spectrum during the origins of agriculture in southwest Asia. Veg. Hist. Archaeobot. doi:10.1007/s00334-018-0702-y.

Wallace, M., Livarda, A., Charles, M., Jones, G., 2018b. Origins of agriculture: Archaeobotanical database. doi:10.5284/1046750.

Weide, A., Riehl, S., Zeidi, M., Conard, N.J., 2017. Reconstructing subsistence practices: Taphonomic constraints and the interpretation of wild plant remains at aceramic Neolithic Chogha Golan, Iran. Vegetation History and Archaeobotany 26, 487–504. doi:10.1007/s00334-017-0607-1.

Weide, A., Riehl, S., Zeidi, M., Conard, N.J., 2018. A systematic review of wild grass exploitation in relation to emerging cereal cultivation throughout the Epipalaeolithic and aceramic Neolithic of the Fertile Crescent. PLOS ONE 13, e0189811. doi:10.1371/journal.pone.0189811.

Weiss, E., Kislev, M.E., Hartmann, A., 2006. Autonomous Cultivation Before Domestication. Science 312, 1608–1610. doi:10.1126/science.1127235.

Weiss, E., Wetterstrom, W., Nadel, D., Bar-Yosef, O., 2004. The broad spectrum revisited: Evidence from plant remains. Proceedings of the National Academy of Sciences 101, 9551–9555. doi:10.1073/pnas.0402362101.

Whitlam, J., Bogaard, A., Matthews, R., Matthews, W., Mohammadifar, Y., Ilkhani, H., Charles, M., 2018. Pre-agricultural plant management in the uplands of the central Zagros: The archaeobotanical evidence from Sheikh-e Abad. Vegetation History and Archaeobotany 27, 817–831. doi:10.1007/s00334-018-0675-x.

Willcox, G., 2024. Sowing, harvesting and tilling at the end of the Pleistocene/beginning of the Holocene in northern Syria: A reassessment of cereal and pulse exploitation. Vegetation History and Archaeobotany doi:10.1007/s00334-023-00984-4.

Willcox, G., Buxo, R., Herveux, L., 2009. Late Pleistocene and early Holocene climate and the beginnings of cultivation in northern Syria. The Holocene 19, 151–158. doi:10.1177/0959683608098961.

Willcox, G., Fornite, S., Herveux, L., 2008. Early Holocene cultivation before domestication in northern Syria. Vegetation History and Archaeobotany 17, 313–325. doi:10.1007/s00334-007-0121-y.

Wisz, M.S., Hijmans, R.J., Li, J., Peterson, A.T., Graham, C.H., Guisan, A., Group, N.P.S.D.W., 2008. Effects of sample size on the performance of species distribution models. Diversity and Distributions 14, 763–773. URL: https://onlinelibrary.wiley.com/doi/abs/10.1111/j.1472-4642.2008.00482.x, doi:10.1111/j.1472-4642.2008.00482.x.

Wright, M.N., Ziegler, A., 2017. Ranger: A Fast Implementation of Random Forests for High Dimensional Data in C++ and R. Journal of Statistical Software 77, 1–17. doi:10.18637/jss.v077.i01.

Yaworsky, P.M., Hussain, S.T., Riede, F., 2023. Climate-driven habitat shifts of high-ranked prey species structure Late Upper Paleolithic hunting. Scientific Reports 13, 4238. doi:10.1038/s41598-023-31085-x.

Yaworsky, P.M., Hussain, S.T., Riede, F., 2024a. The effects of climate and population on human land use patterns in Europe from 22ka to 9ka ago. Quaternary Science Reviews 344, 108956. doi:10.1016/j.quascirev.2024.108956.

Yaworsky, P.M., Nielsen, E.S., Nielsen, T.K., 2024b. The Neanderthal niche space of Western Eurasia 145 ka to 30 ka ago. Scientific Reports 14, 7788. doi:10.1038/s41598-024-57490-4.

Yeomans, L., Martin, L., Richter, T., 2017. Expansion of the known distribution of Asiatic mouflon (Ovis orientalis) in the Late Pleistocene of the Southern Levant. Royal Society Open Science 4, 170409. doi:10.1098/rsos.170409.

Yousefi, M., Heydari-Guran, S., Kafash, A., Ghasidian, E., 2020. Species distribution models advance our knowledge of the Neanderthals' paleoecology on the Iranian Plateau. Scientific Reports 10, 14248. doi:10.1038/s41598-020-71166-9.

Zeder, M.A., 2011. The Origins of Agriculture in the Near East. Curr. Anthropol. 52, S221–S235. doi:10.1086/659307, arXiv:10.1086/659307.

Zeder, M.A., 2024. Out of the Shadows: Reestablishing the Eastern Fertile Crescent as a Center of Agricultural Origins: Part 1. Journal of Archaeological Research doi:10.1007/s10814-024-09195-5.

Zohary, D., 1969. The progenitors of wheat and barley in relation to domestication and agricultural dispersal in the Old World, in: The Domestication and Exploitation of Plants and Animals. Routledge.

Zohary, D., Hopf, M., 1973. Domestication of Pulses in the Old World. Science 182, 887–894. doi:10.1126/science.182.4115.887.

Zohary, D., Hopf, M., 1988. Domestication of Plants in the Old World: The Origin and Spread of Domesticated Plants in Southwest Asia, Europe, and the Mediterranean Basin. 1st ed ed., Oxford University Press, Oxford.

Zohary, D., Spiegel-Roy, P., 1975. Beginnings of Fruit Growing in the Old World. Science 187, 319–327. doi:10.1126/science.187.4174.319.

Zohary, D., Weiss, E., Hopf, M., 2012. Domestication of Plants in the Old World: The Origin and Spread of Domesticated Plants in Southwest Asia, Europe, and the Mediterranean Basin. 4th ed ed., Oxford University Press, Oxford.

Zohary, M., 1973. Geobotanical Foundations of the Middle East. Gustav Eischer, Stuttgart.

# Biogeography of crop progenitors and wild plant resources in the terminal Pleistocene and Early Holocene of West Asia, 14.7–8.3 ka

Fitted model summaries and predicted palaeodistributions

AUTHORS
Joe Roe
Amaia Arranz-Otaegui

AFFILIATIONS
University of Bern
University of Copenhagen
University of the Basque Country

ABSTRACT
This appendix describes ecological niche models of 65 plant species relevant to the subsistence of Late Epipalaeolithic (15–11.7 ka) and Neolithic (11.7–8.2 ka) societies in West Asia. It includes summaries of the training data and performance metrics of the fitted models together with predicted palaeodistributions of each species for three simulated climatologies over the Pleistocene/Holocene boundary (the Bølling–Allerød, 14.7–12.9 ka; Younger Dryas, 12.9–11.7 ka; and Early Holocene, 11.7–8.3 ka) as well as current conditions. For a full description of the methodology, references, and discussion of the results, please see the main text. The data and R code used to produce the models, as well as the full predicted palaeodistributions in raster format, are achived with Zenodo at https://doi.org/10.5281/zenodo.14629984.

## *Aegilops crassa*

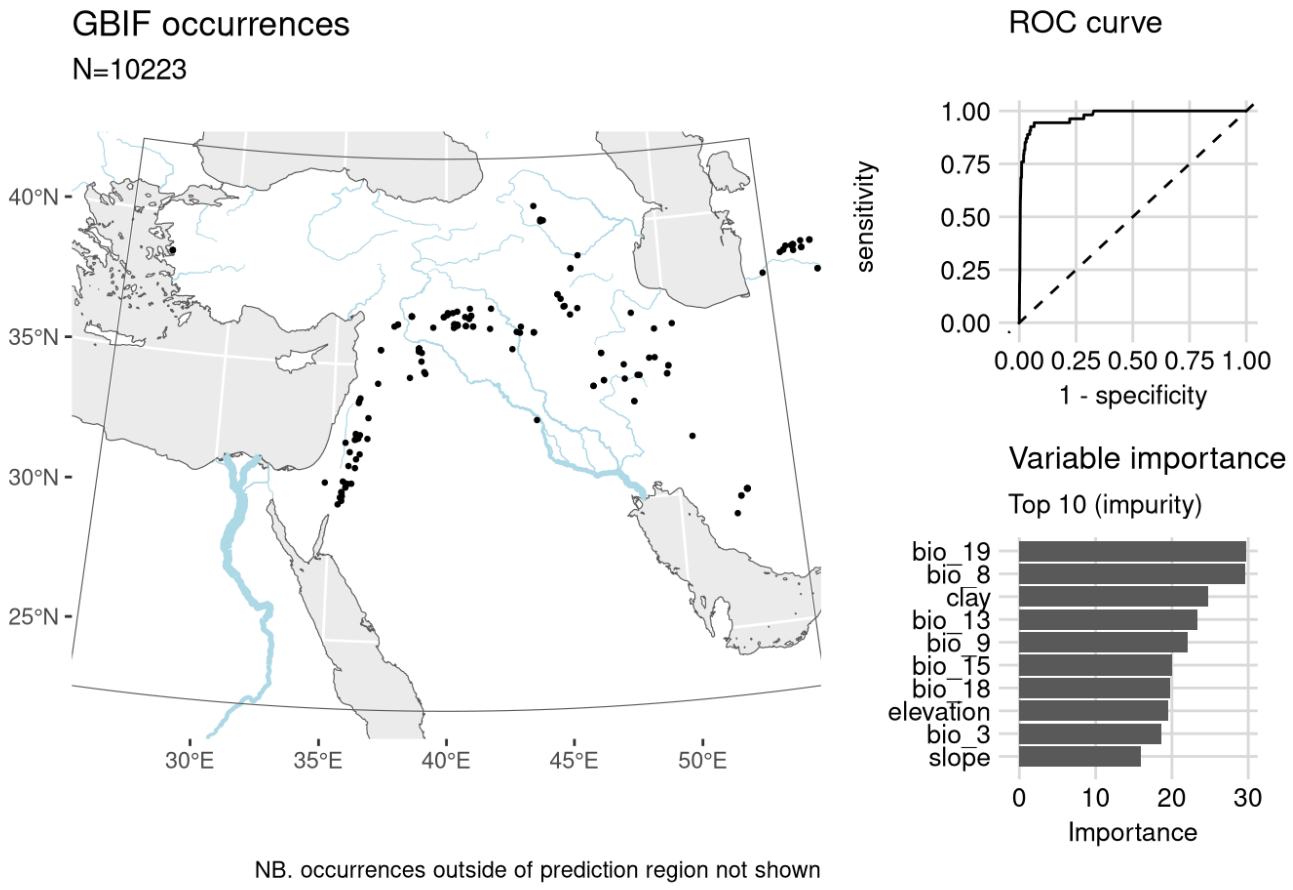


Figure 1: Fitted model summary for *Aegilops crassa*

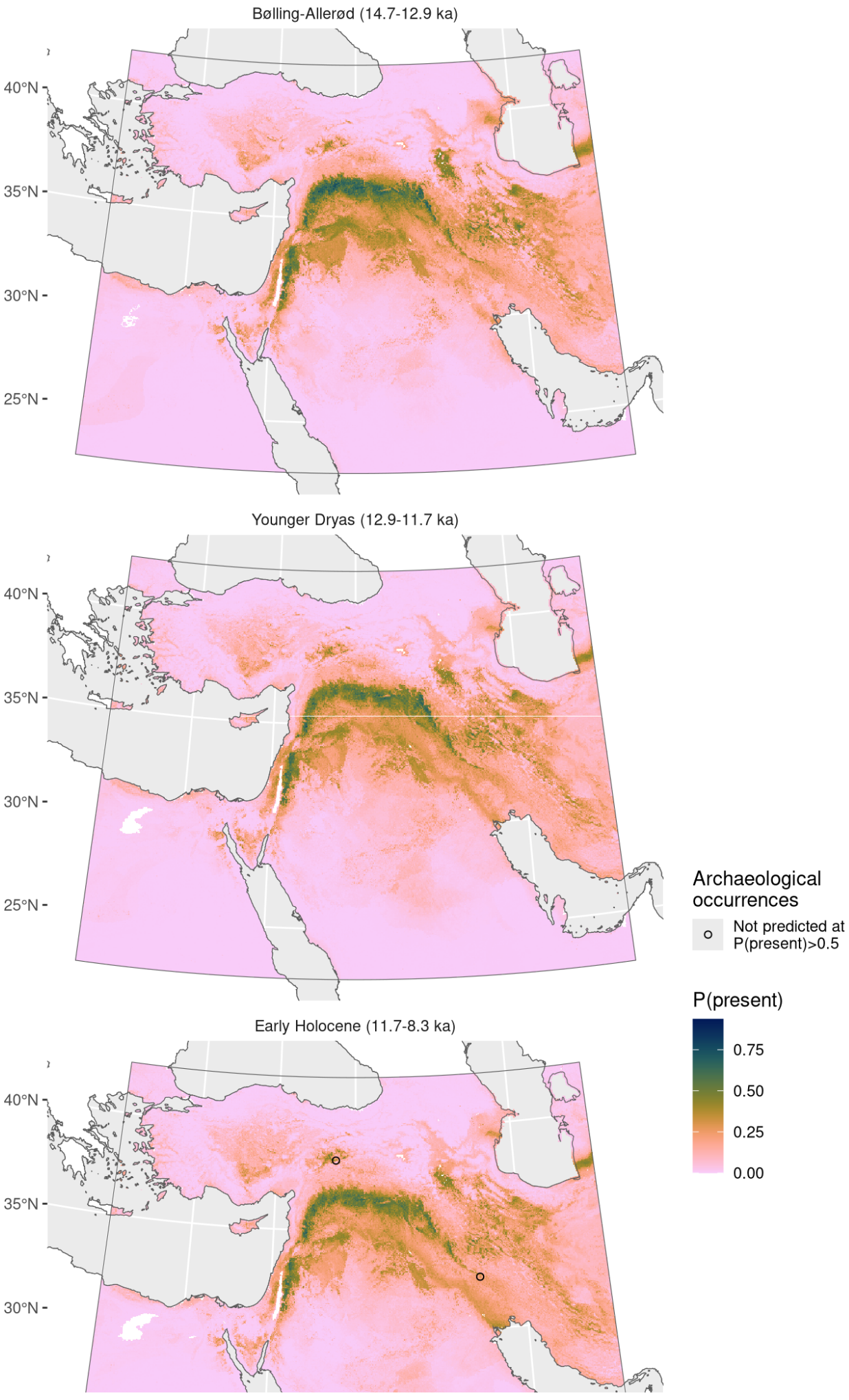
Bølling-Allerød (14.7-12.9 ka)
Younger Dryas (12.9-11.7 ka)
Early Holocene (11.7-8.3 ka)
40°N
35°N
30°N
25°N
Archaeological occurrences
Not predicted at P(present)>0.5
P(present)
0.75
0.50
0.25
0.00

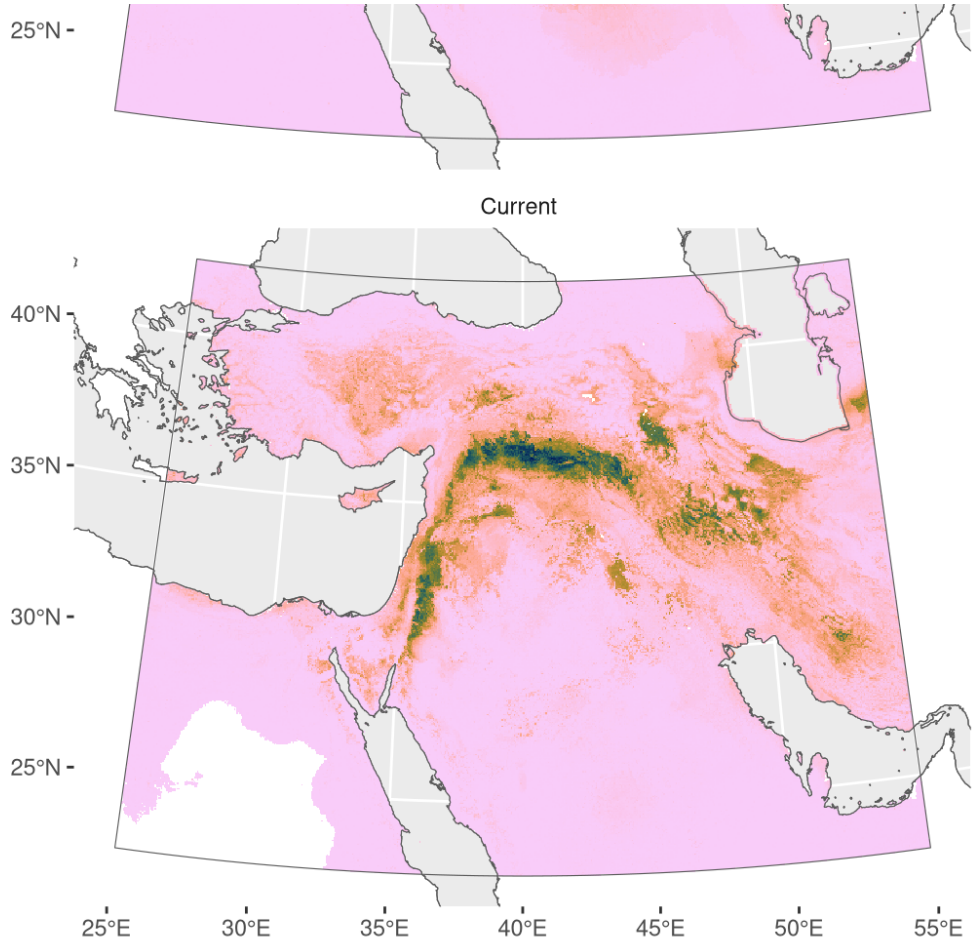


Figure 2: Predicted palaeodistributions of *Aegilops crassa*

Table 1: Archaeological occurrences of *Aegilops crassa*

Archaeological occurrences of *Aegilops crassa*

| Site | Age range | N assemblages | Average prop. | Source | Predicted? |
|---|---|---|---|---|---|
| Early Holocene (11.7-8.3 ka) | | | | | |
| Cafer Höyük | 10.6–9.7 ka | 1 | 0.08% | ORIGINS | no |
| Ali Kosh | 10.1–8.0 ka | 3 | 1.60% | ORIGINS | no |

# *Aegilops speltoides*

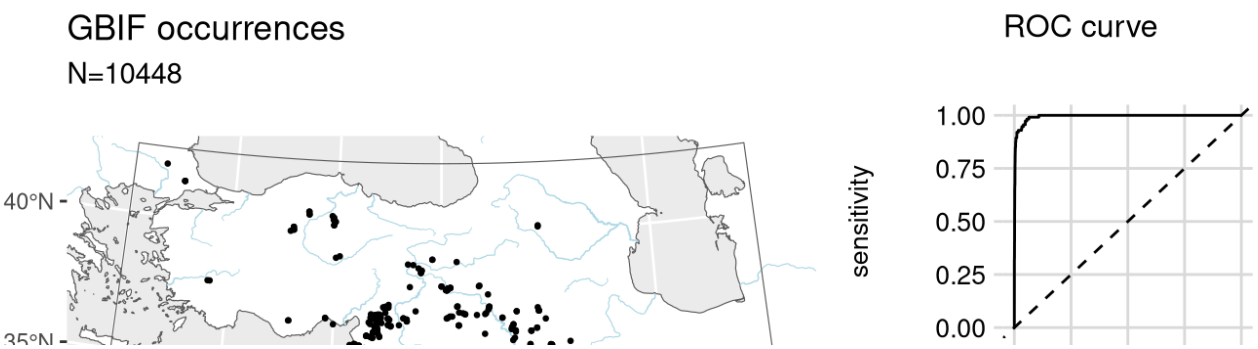

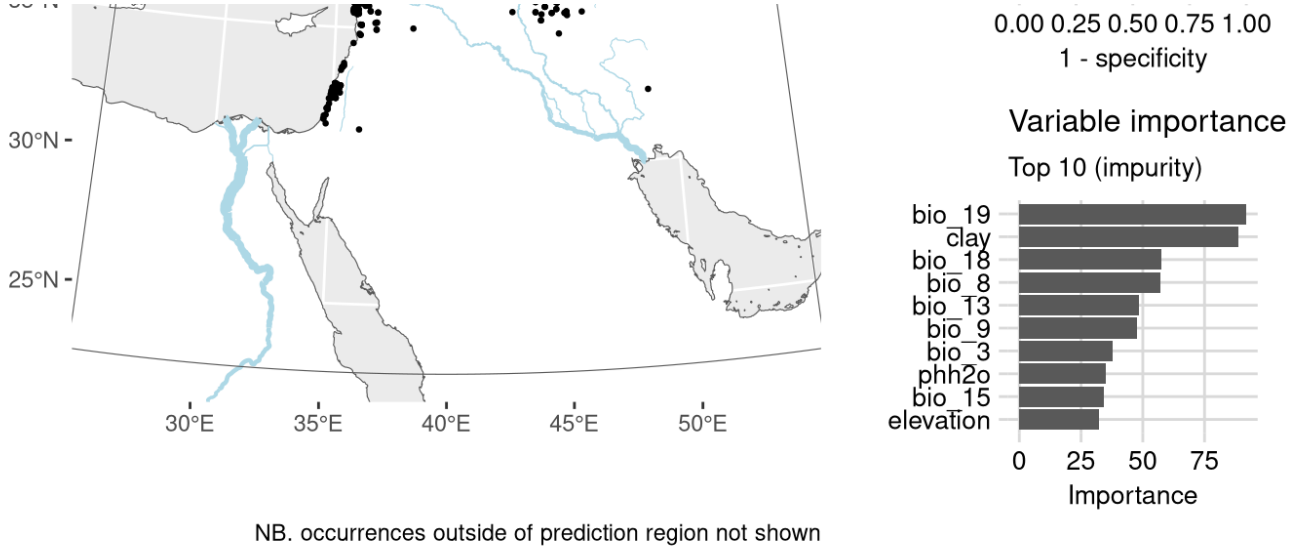


Figure 3: Fitted model summary for *Aegilops speltoides*

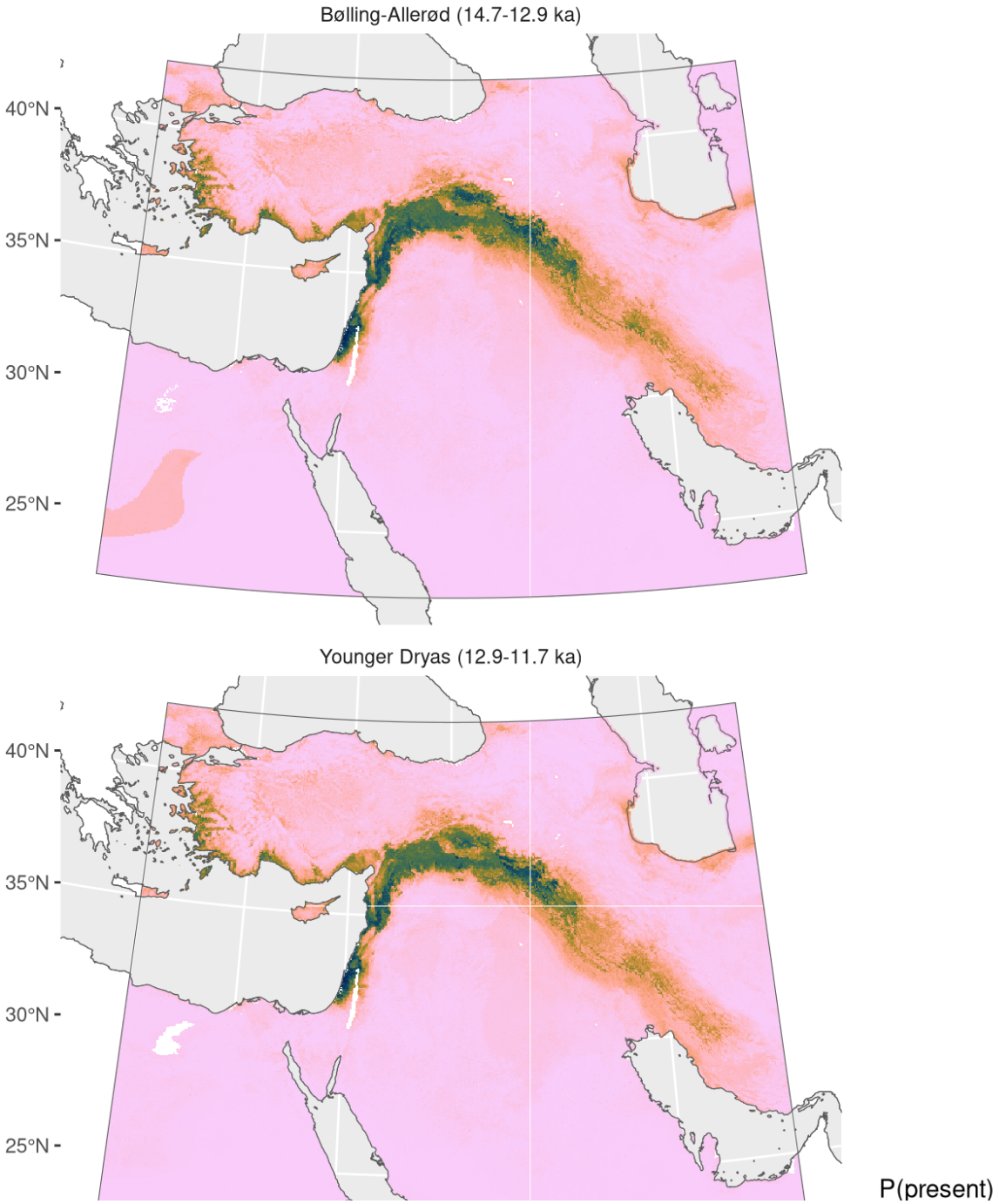

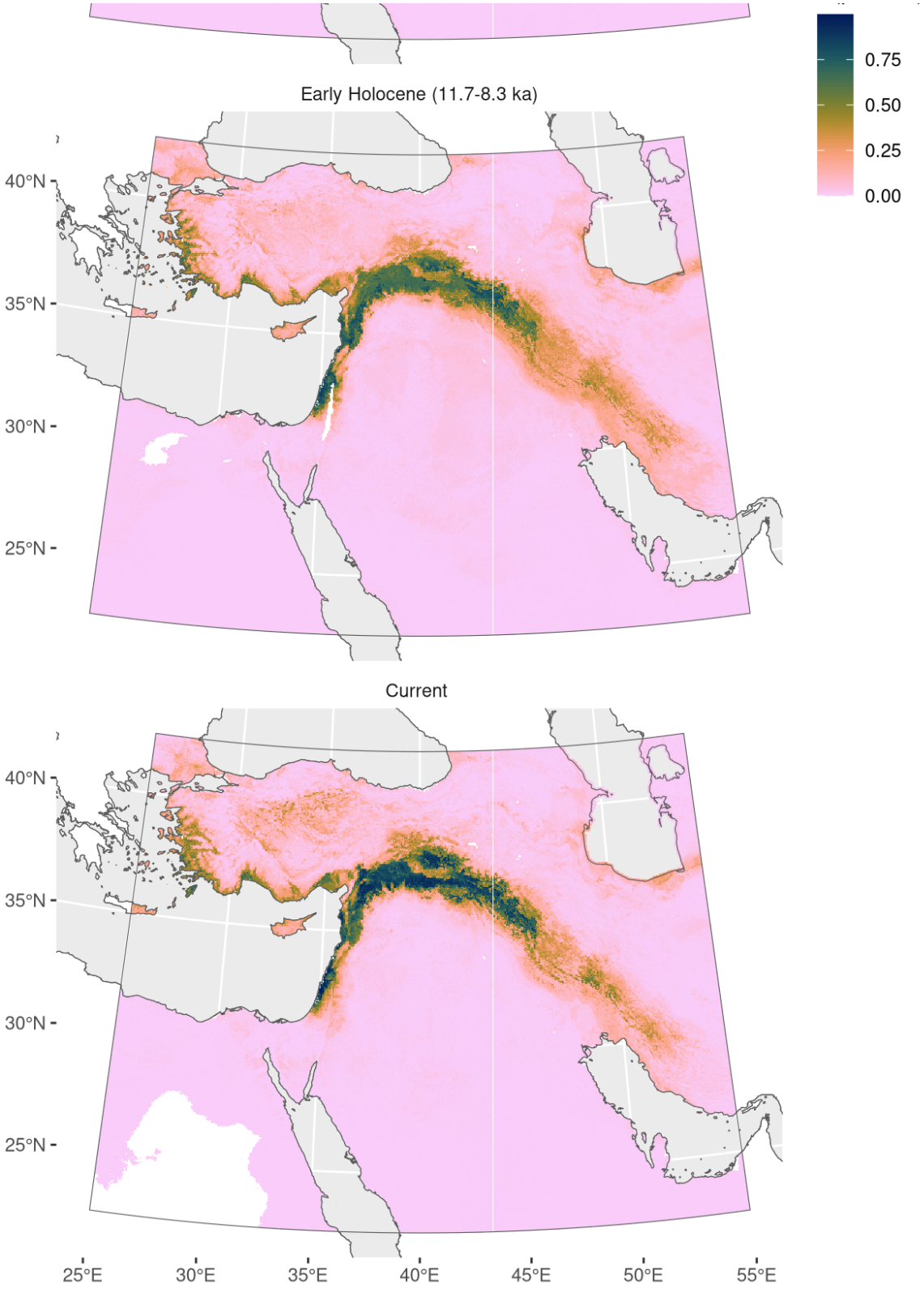


Figure 4: Predicted palaeodistributions of *Aegilops speltoides*

Table 2

# *Aegilops tauschii*

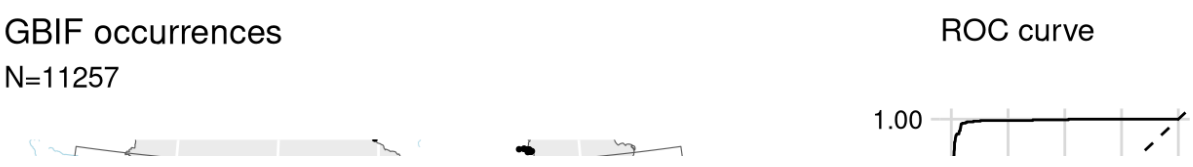

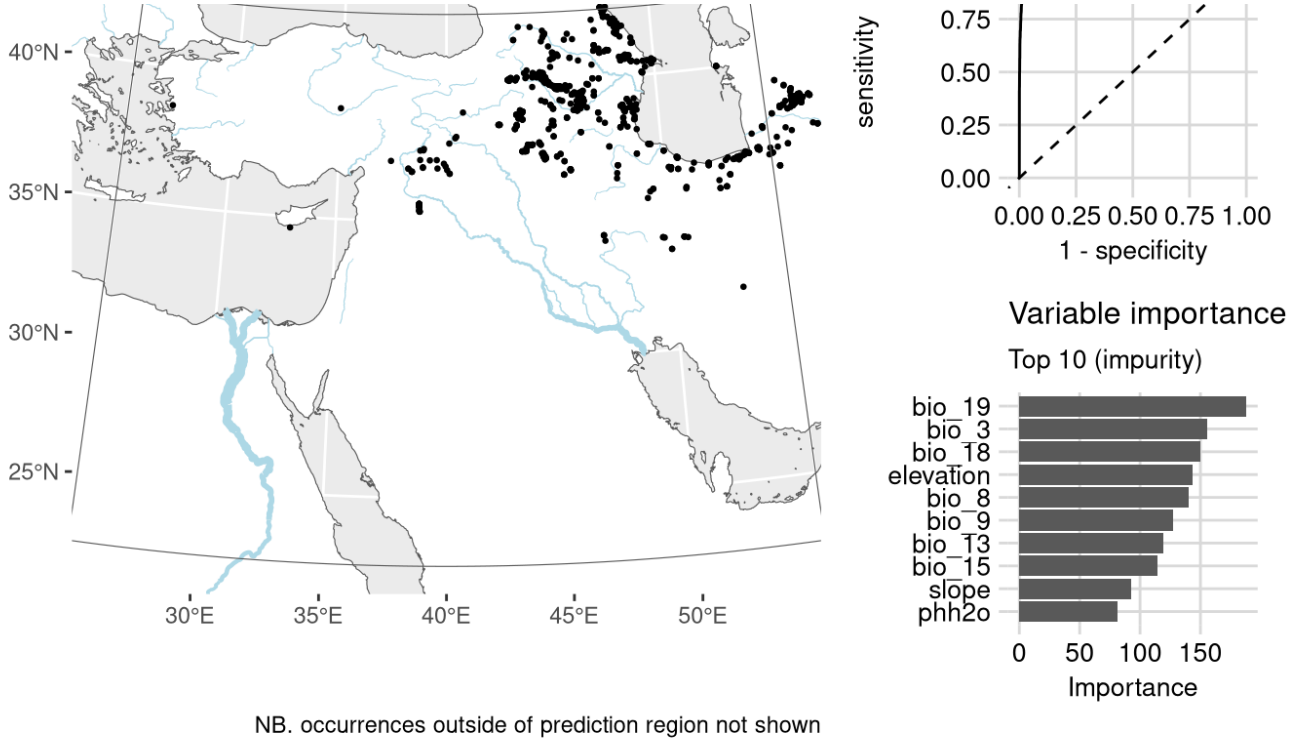


Figure 5: Fitted model summary for *Aegilops tauschii*

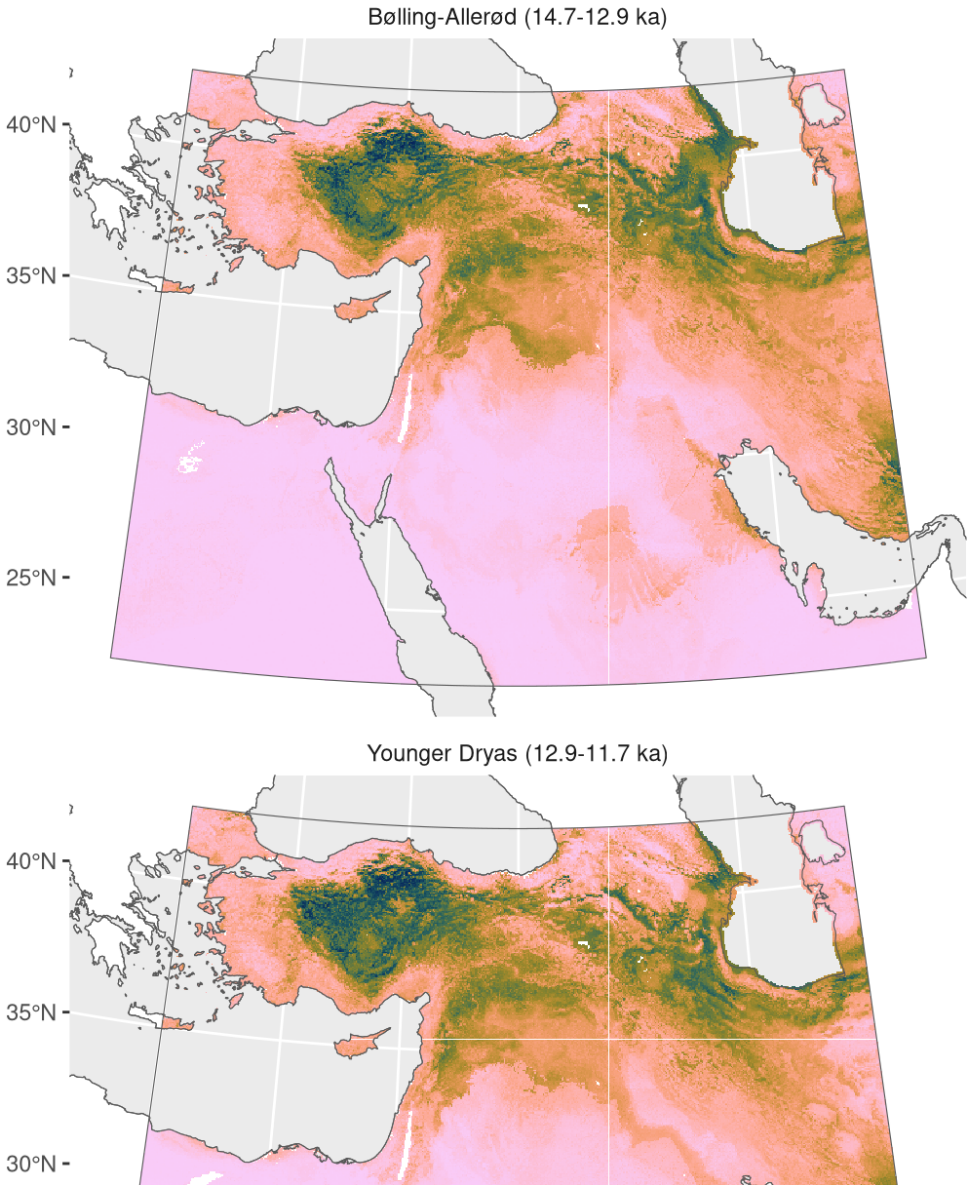

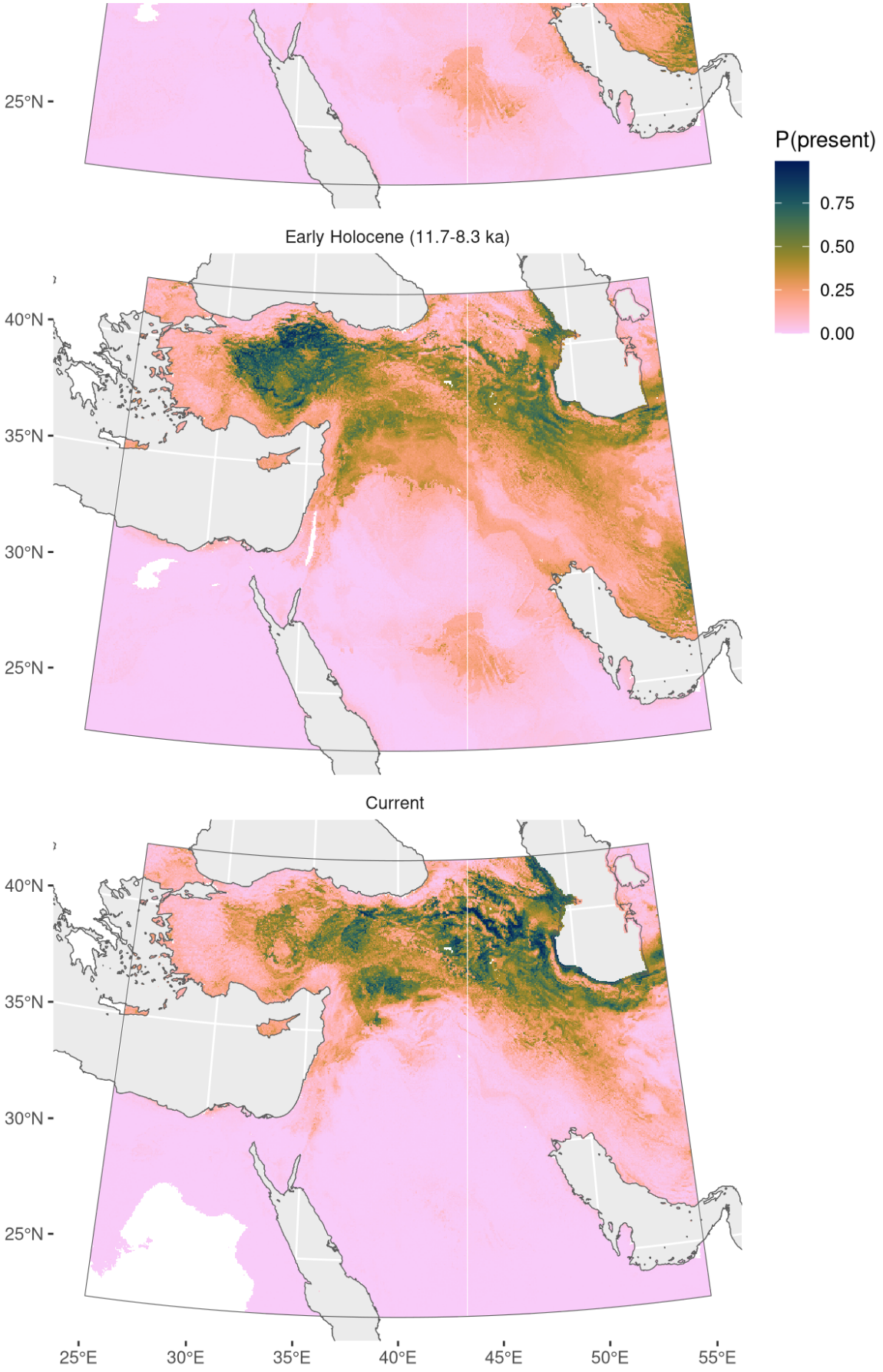


Figure 6: Predicted palaeodistributions of *Aegilops tauschii*

Table 3

# *Aizoanthemopsis hispanica*

Including Aizoon hispanicum.

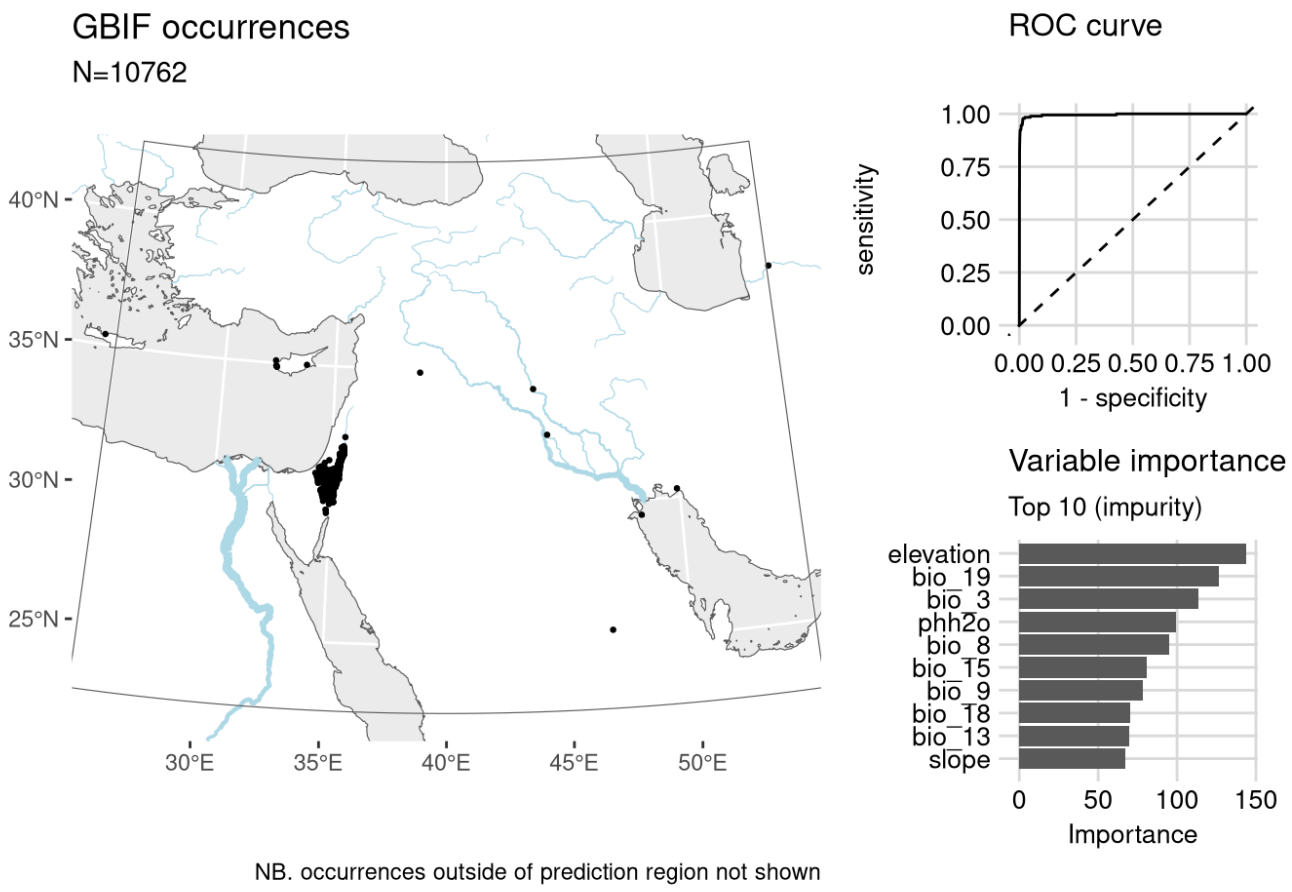


Figure 7: Fitted model summary for *Aizoanthemopsis hispanica*

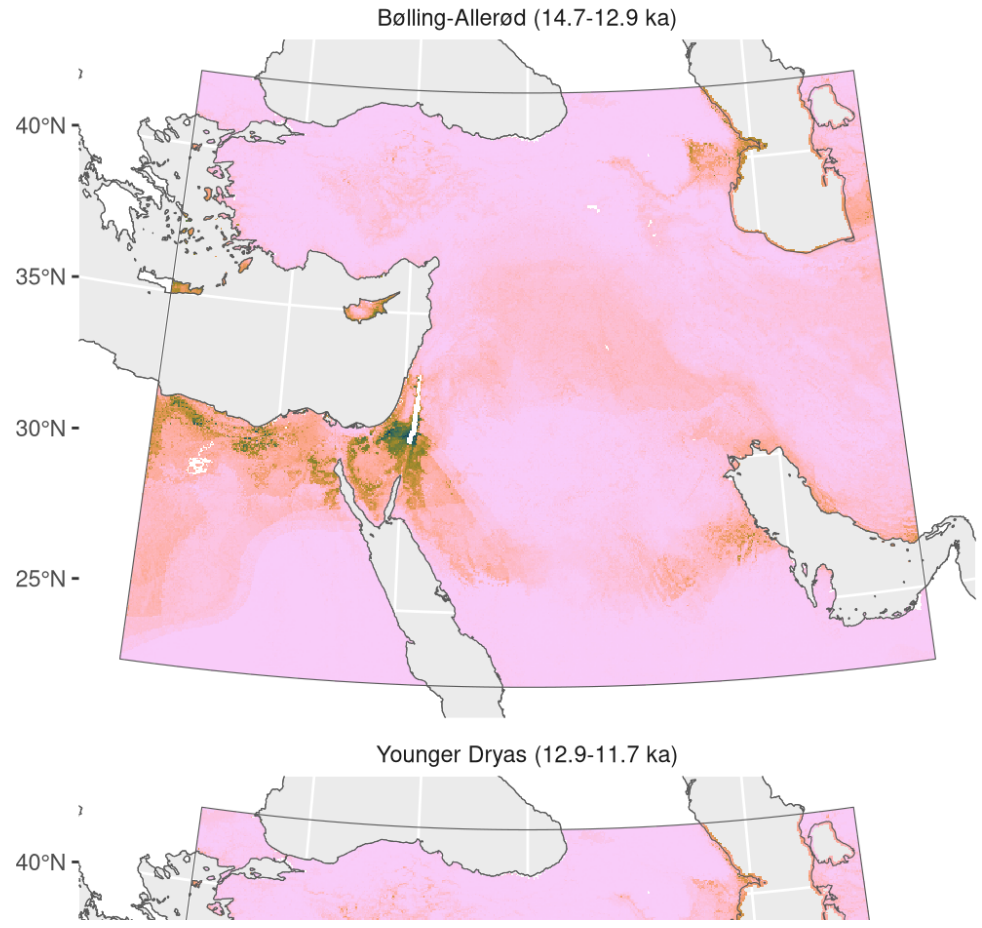

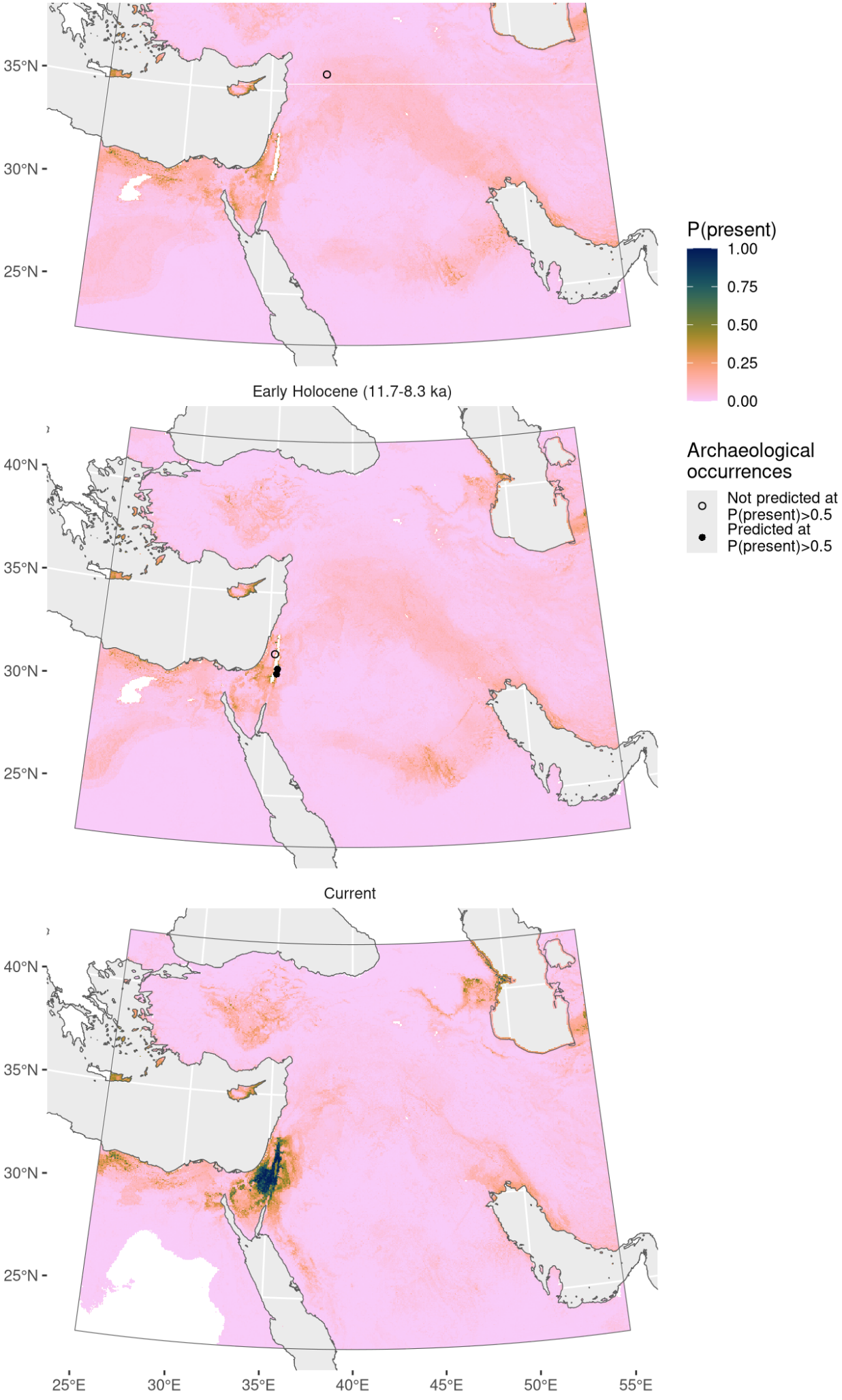
35°N
30°N
25°N
Early Holocene (11.7-8.3 ka)
40°N
35°N
30°N
25°N
Current
40°N
35°N
30°N
25°N
25°E
30°E
35°E
40°E
45°E
50°E
55°E
P(present)
1.00
0.75
0.50
0.25
0.00
Archaeological occurrences
Not predicted at P(present)>0.5
Predicted at P(present)>0.5

Figure 8: Predicted palaeodistributions of *Aizoanthemopsis hispanica*

Table 4: Archaeological occurrences of *Aizoanthemopsis hispanica*

Archaeological occurrences of *Aizoanthemopsis hispanica*

| Site | Age range | N assemblages | Average prop. | Source | Predicted? |
|---|---|---|---|---|---|
| Younger Dryas (12.9-11.7 ka) | | | | | |
| Abu Hureyra | 13.0–12.1 ka | 1 | 0.09% | ORIGINS | no |
| Early Holocene (11.7-8.3 ka) | | | | | |
| Netiv Hagdud | 11.6–10.6 ka | 1 | 5.16% | ORIGINS | no |
| Zahrat adh-Dhra 2 | 11.4–10.4 ka | 1 | 0.31% | ORIGINS | yes |
| El-Hemmeh | 11.1–10.5 ka | 1 | 0.11% | ORIGINS | yes |

# *Ammi majus*

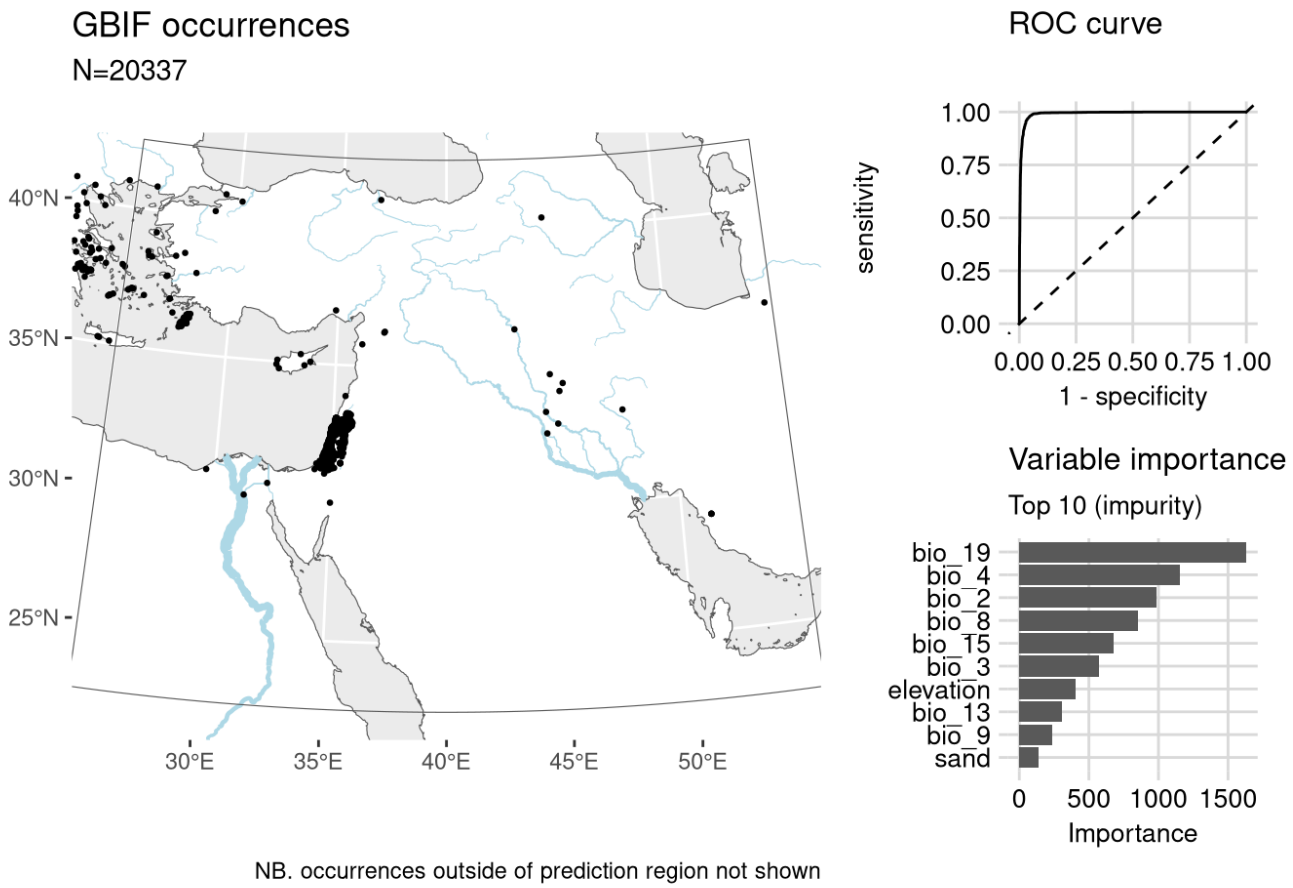


Figure 9: Fitted model summary for *Ammi majus*

Bølling-Allerød (14.7-12.9 ka)

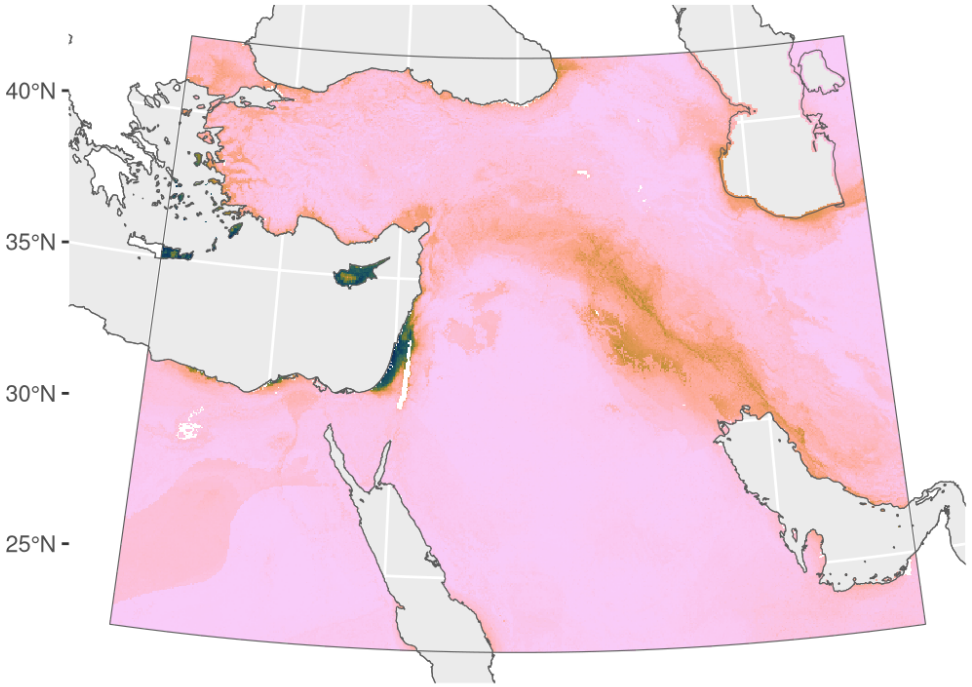


Younger Dryas (12.9-11.7 ka)

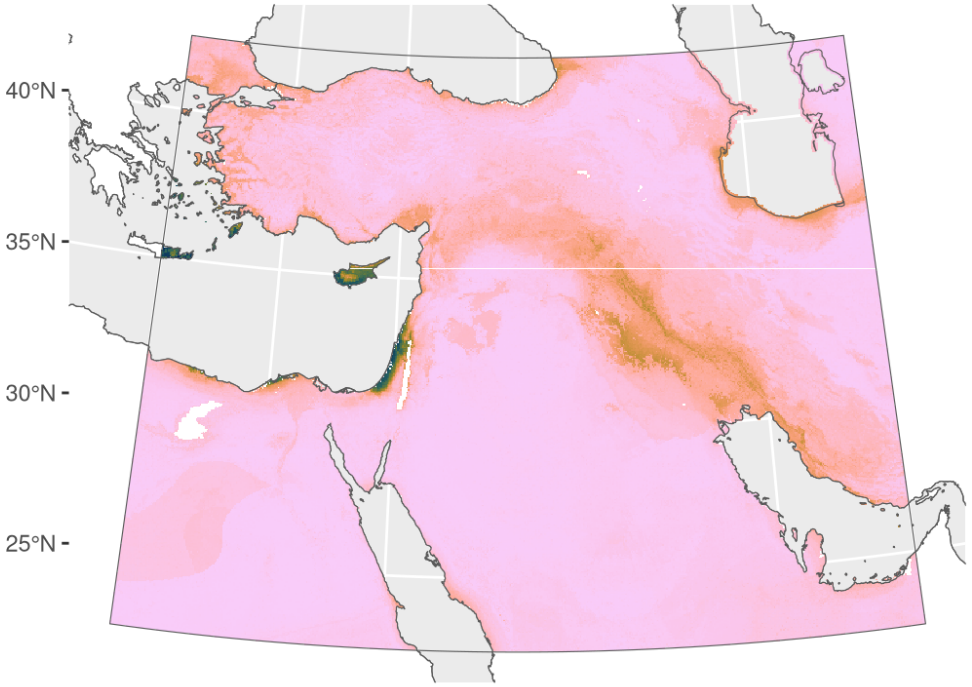


Early Holocene (11.7-8.3 ka)

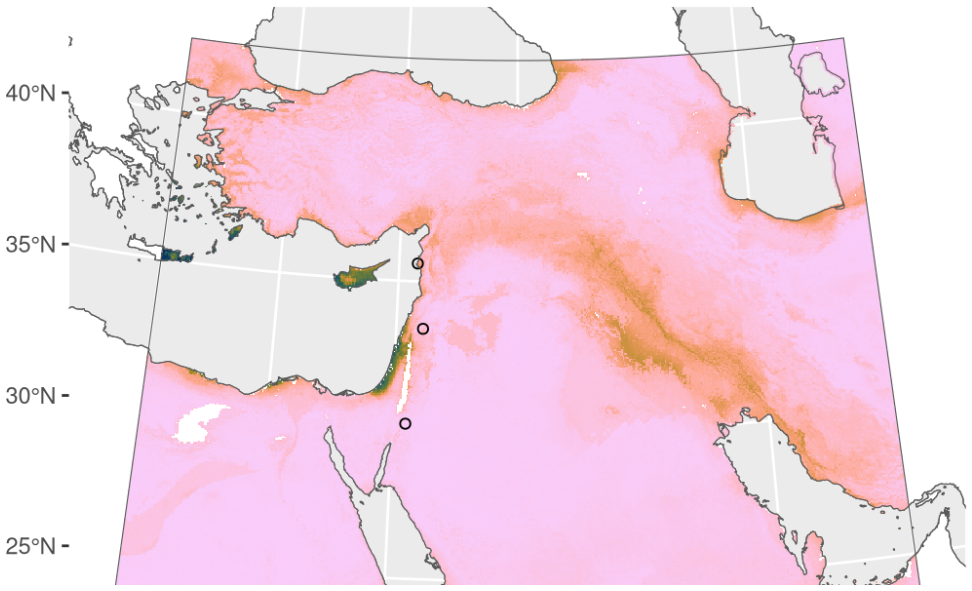


P(present)

1.00
0.75
0.50
0.25
0.00

Archaeological occurrences

Not predicted at P(present)>0.5

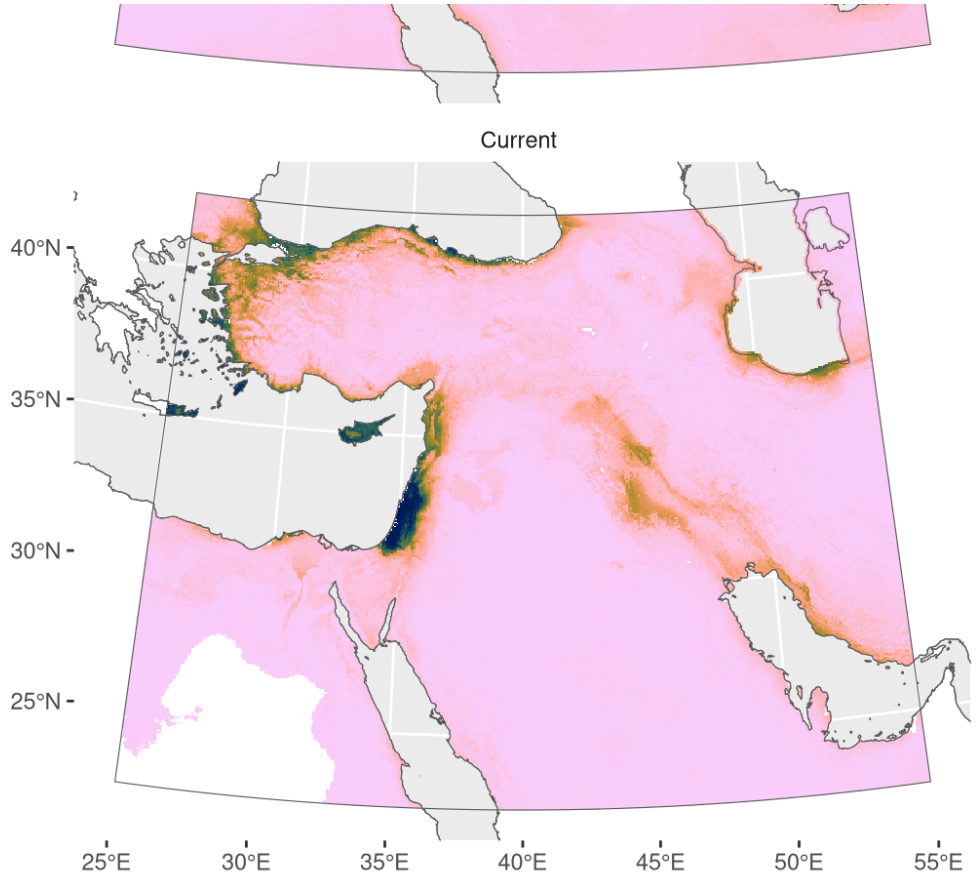


Figure 10: Predicted palaeodistributions of *Ammi majus*

Table 5: Archaeological occurrences of *Ammi majus*

Archaeological occurrences of *Ammi majus*

| Site | Age range | N assemblages | Average prop. | Source | Predicted? |
|---|---|---|---|---|---|
| Early Holocene (11.7-8.3 ka) | | | | | |
| Basta | 9.4–9.2 ka | 1 | 0.20% | ORIGINS | no |
| Tell Ramad | 9.3–8.6 ka | 2 | 0.02% | ORIGINS | no |
| Ras Shamra | 8.8–8.3 ka | 1 | 0.05% | ORIGINS | no |

# *Androsace maxima*

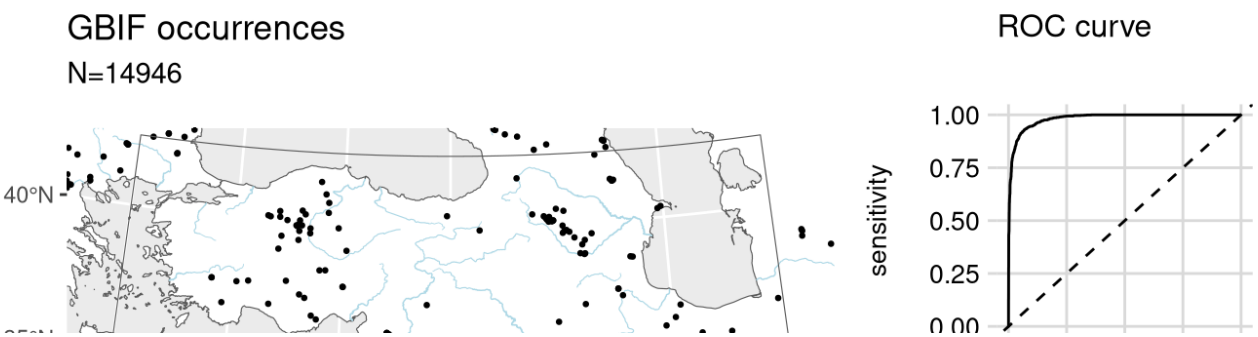

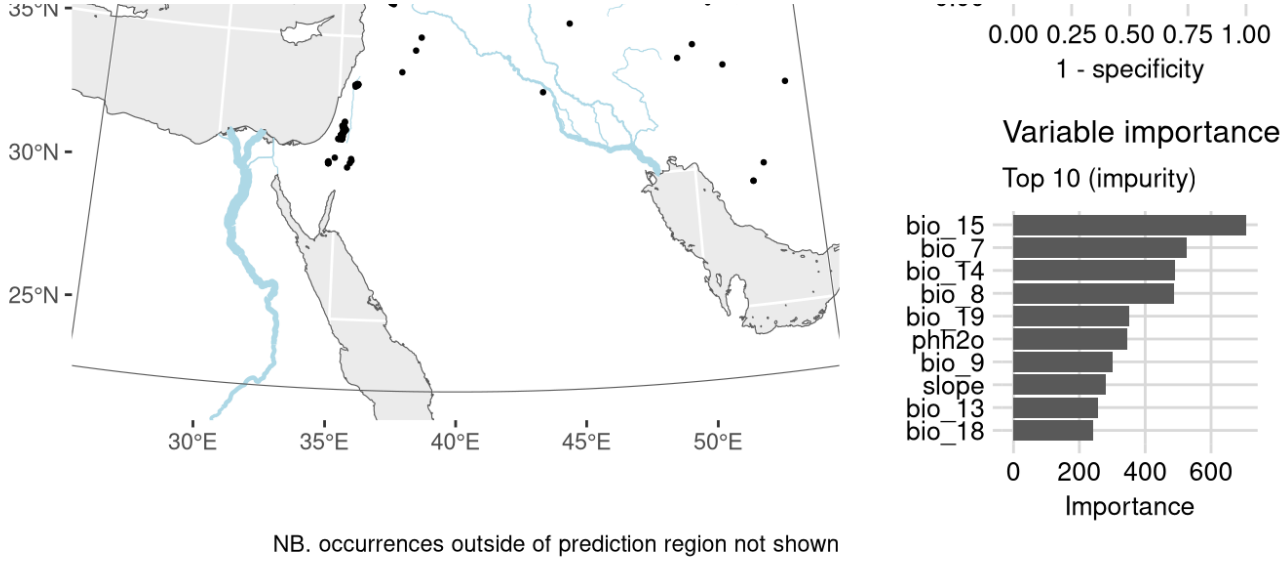


Figure 11: Fitted model summary for *Androsace maxima*

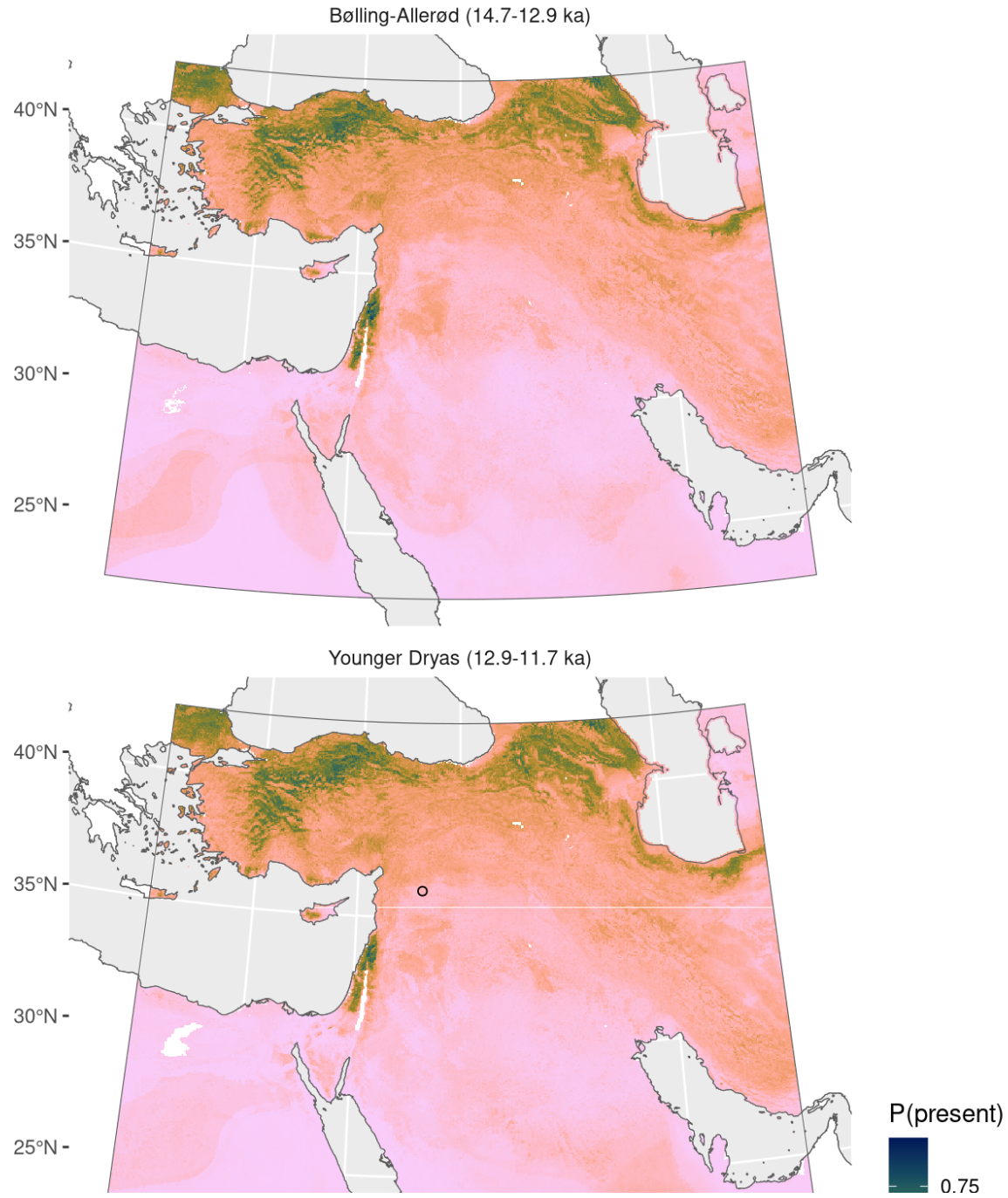

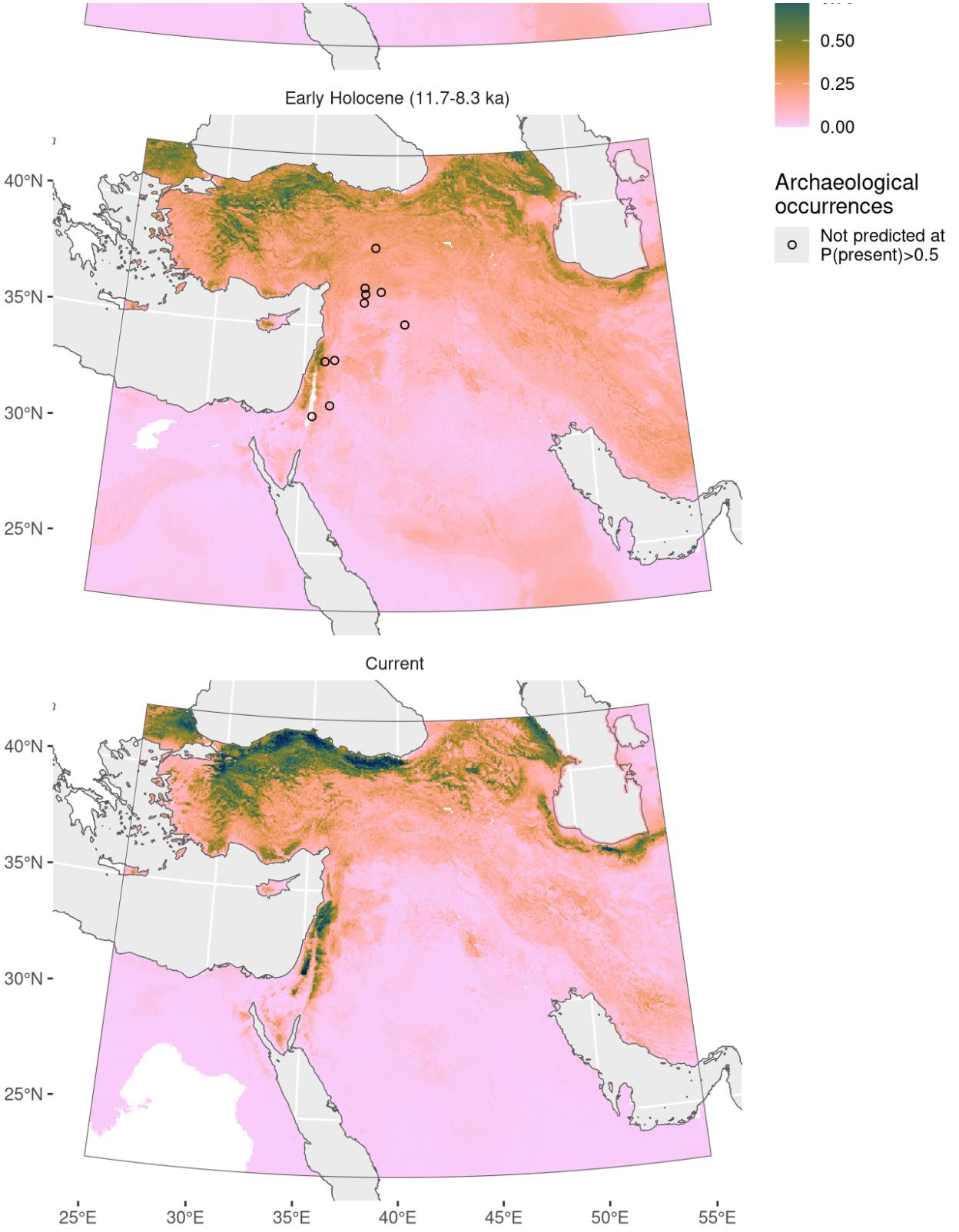


Figure 12: Predicted palaeodistributions of *Androsace maxima*

Table 6: Archaeological occurrences of *Androsace maxima*

Archaeological occurrences of *Androsace maxima*

| Site | Age range | N assemblages | Average prop. | Source | Predicted? |
|---|---|---|---|---|---|
| Younger Dryas (12.9-11.7 ka) | | | | | |
| Mureybet | 12.1–11.9 ka | 1 | 0.10% | ORIGINS | no |

| | | | | | |
|---|---|---|---|---|---|
| Early Holocene (11.7-8.3 ka) | | | | | |
| Mureybet | 11.7–10.8 ka | 2 | 1.05% | ORIGINS | no |
| Jerf el Ahmar | 11.4–10.7 ka | 1 | 0.06% | ORIGINS | no |
| Tell Aswad | 11.2–9.3 ka | 2 | 0.06% | ORIGINS | no |
| El-Hemmeh | 11.1–10.5 ka | 1 | 0.03% | ORIGINS | no |
| Dja'de | 10.7–10.2 ka | 1 | 0.02% | ORIGINS | no |
| Cafer Höyük | 10.6–9.1 ka | 2 | 0.14% | ORIGINS | no |
| Wadi Jilat 7 | 10.2–9.3 ka | 1 | 0.09% | ORIGINS | no |
| Sabi Abyad II | 9.5–8.8 ka | 1 | 0.07% | ORIGINS | no |
| Tell Ramad | 9.3–8.6 ka | 2 | 0.98% | ORIGINS | no |
| Bouqras | 9.2–8.6 ka | 1 | 0.03% | ORIGINS | no |
| Wadi Jilat 13 | 9.1–8.5 ka | 2 | 0.35% | ORIGINS | no |

## *Arenaria serpyllifolia*

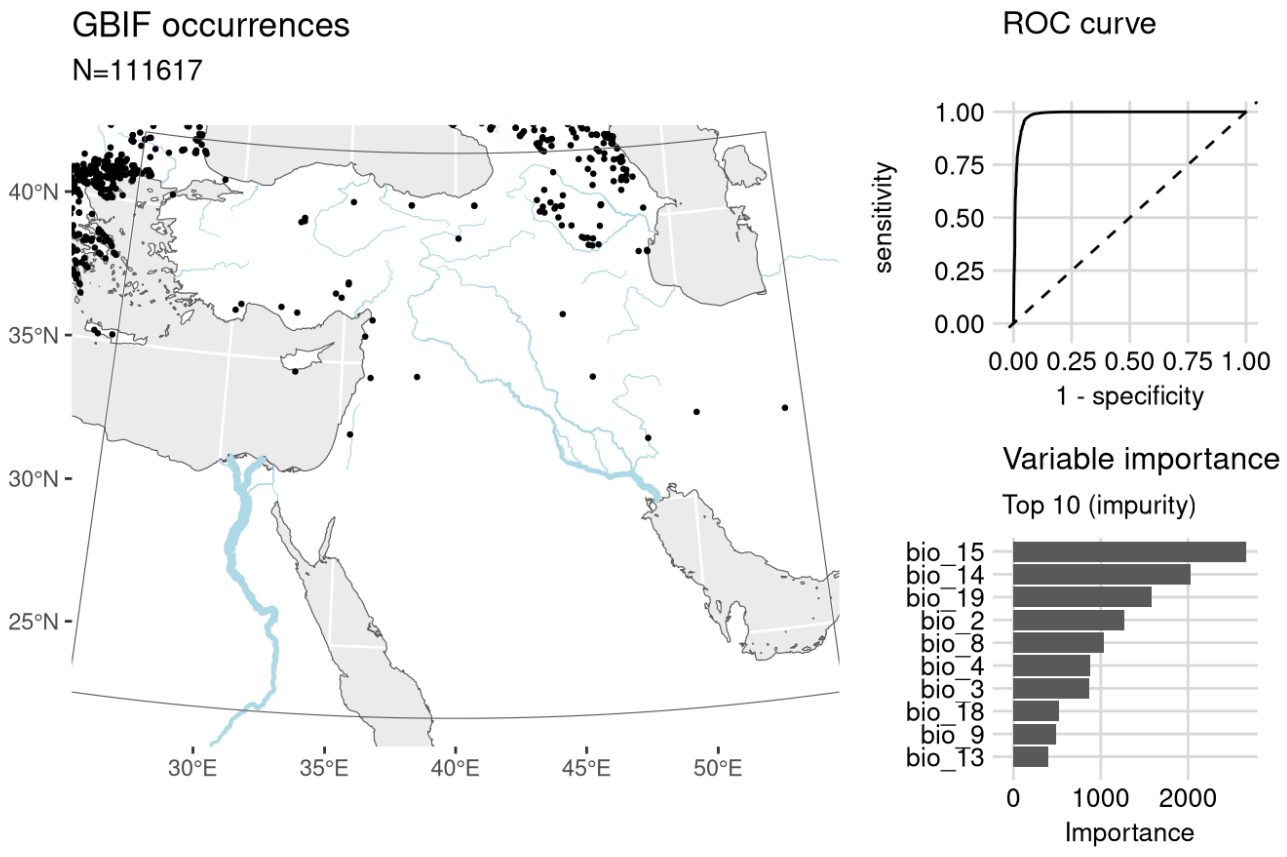


NB. occurrences outside of prediction region not shown

Figure 13: Fitted model summary for *Arenaria serpyllifolia*

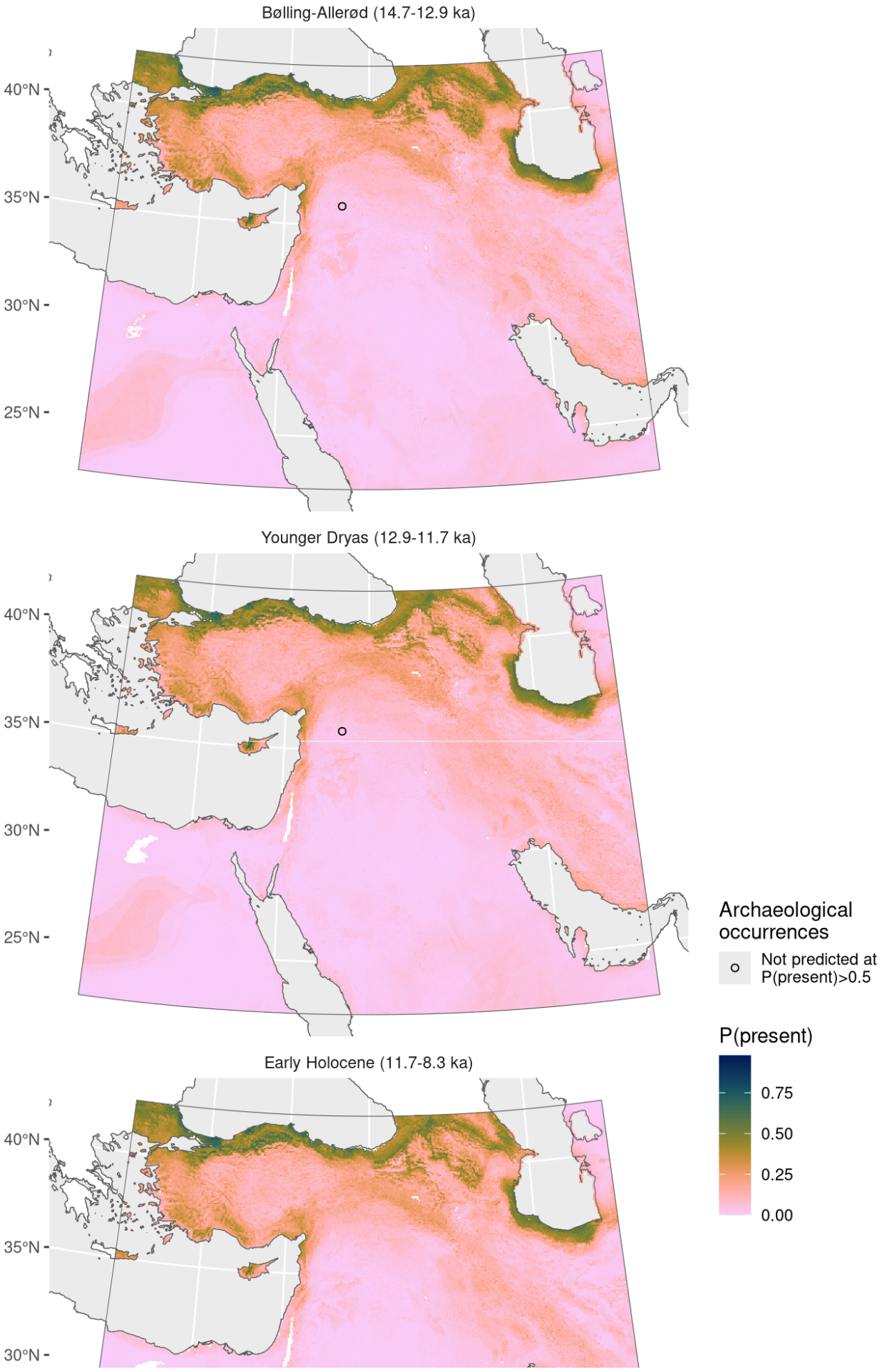

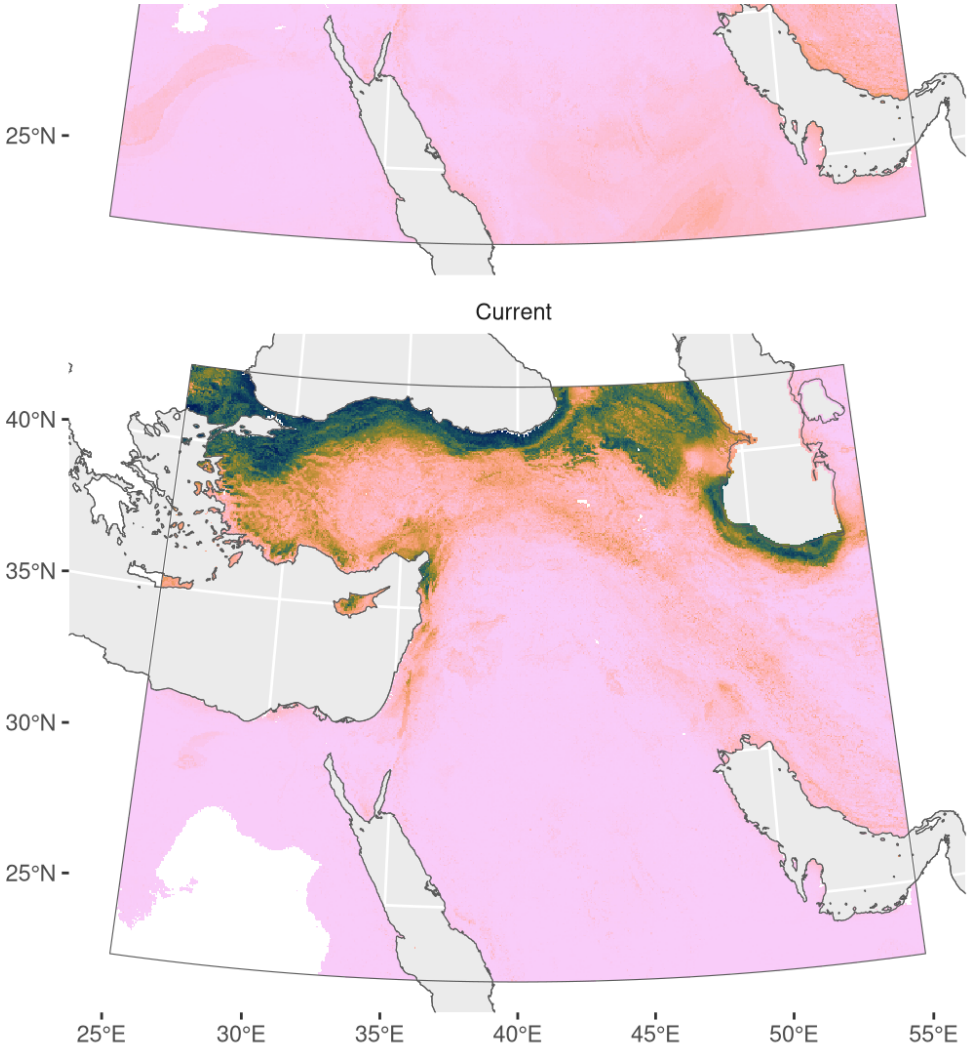


Figure 14: Predicted palaeodistributions of *Arenaria serpyllifolia*

Table 7: Archaeological occurrences of *Arenaria serpyllifolia*

Archaeological occurrences of *Arenaria serpyllifolia*

| Site | Age range | N assemblages | Average prop. | Source | Predicted? |
|---|---|---|---|---|---|
| Bølling-Allerød (14.7-12.9 ka) | | | | | |
| Abu Hureyra | 13.1–13.0 ka | 1 | 0.31% | ORIGINS | no |
| Younger Dryas (12.9-11.7 ka) | | | | | |
| Abu Hureyra | 13.0–11.8 ka | 2 | 0.15% | ORIGINS | no |

# *Arnebia decumbens*

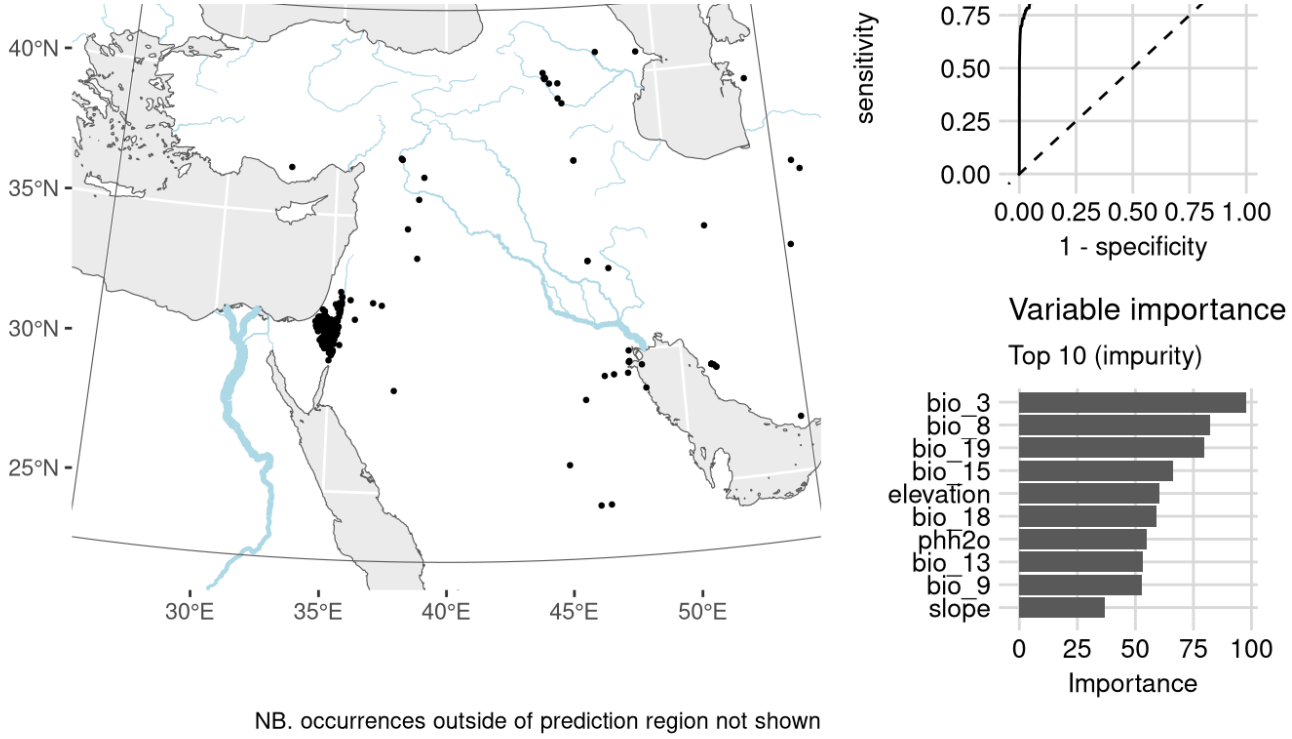


Figure 15: Fitted model summary for *Arnebia decumbens*

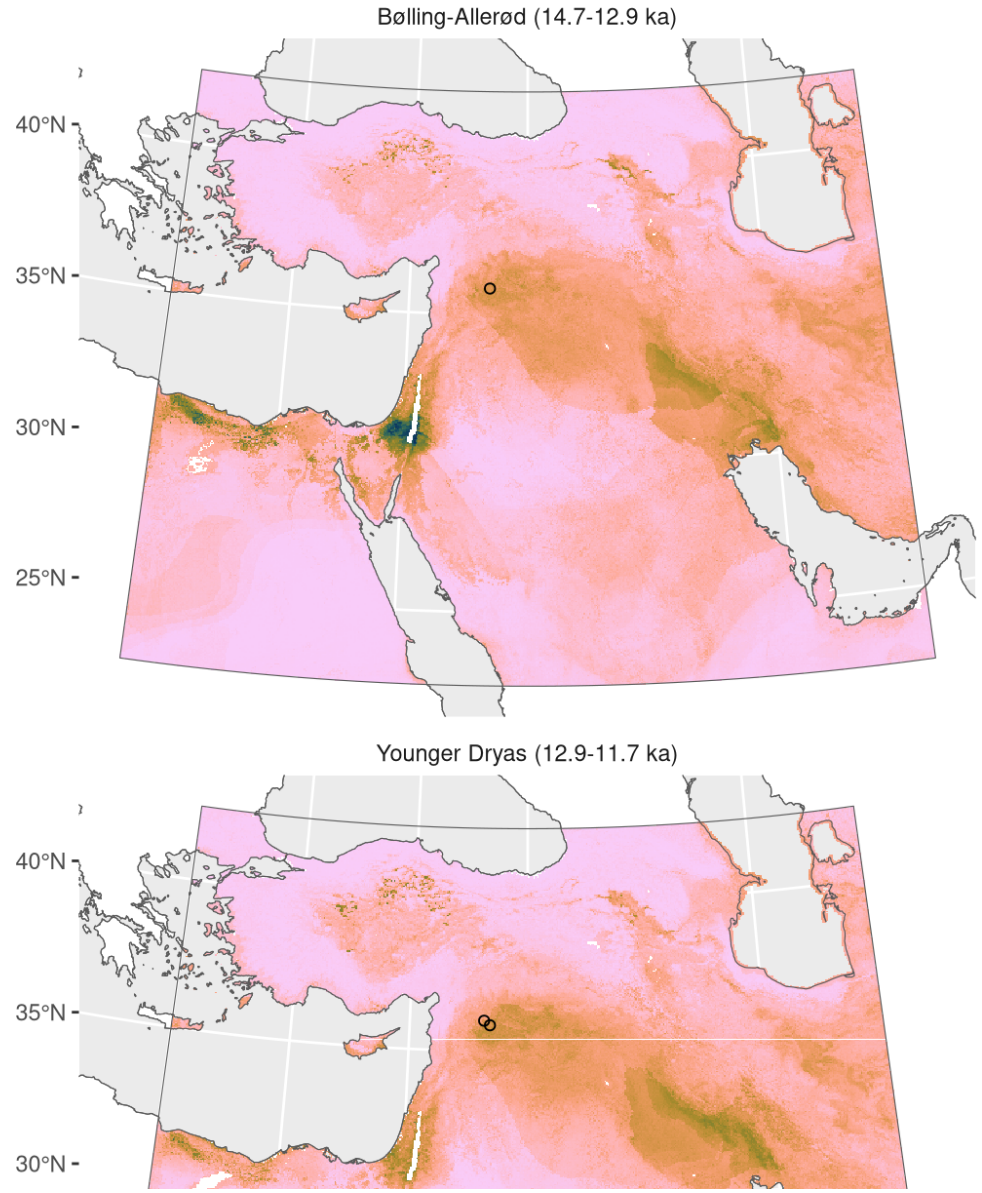

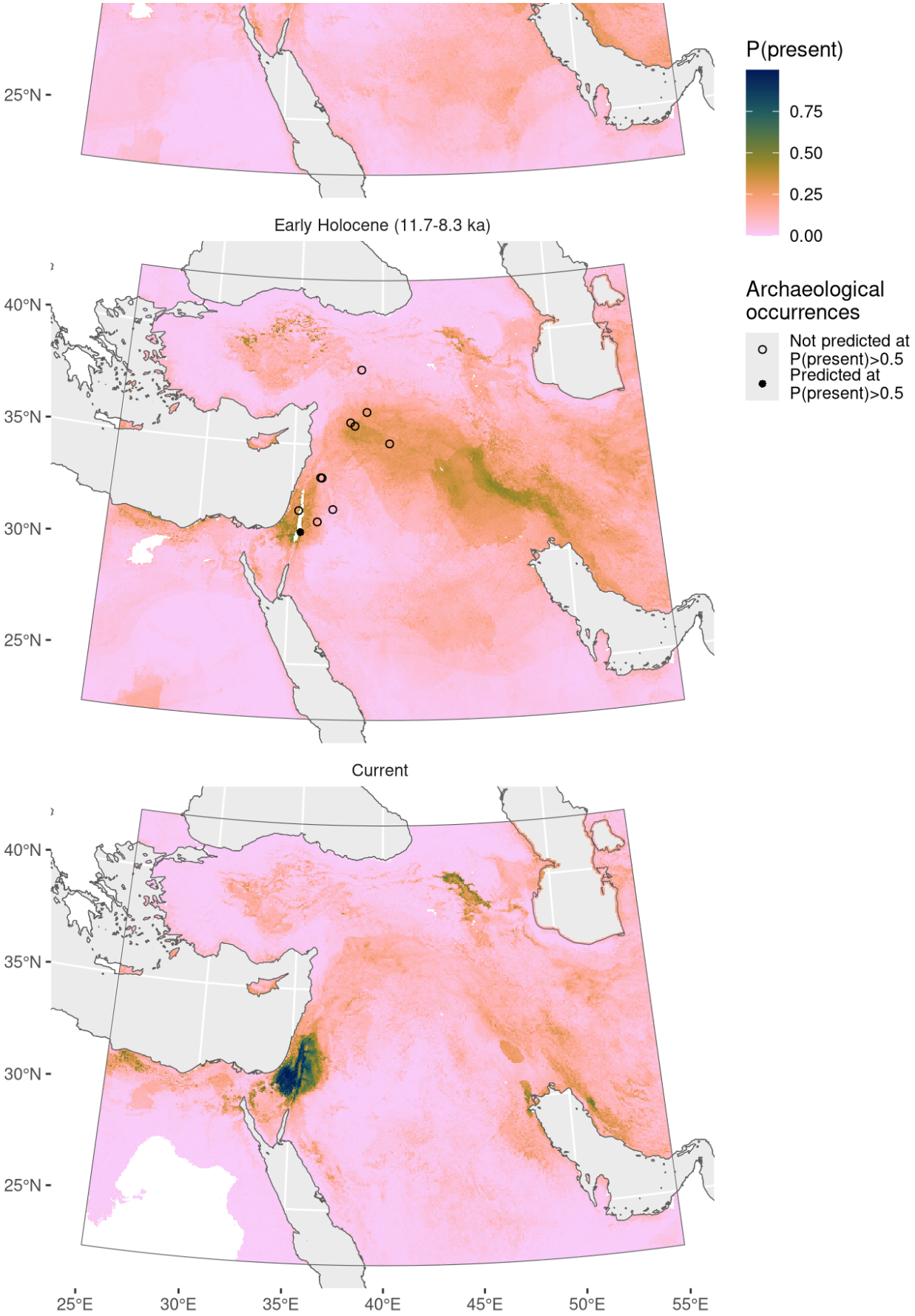


Figure 16: Predicted palaeodistributions of *Arnebia decumbens*

Table 8: Archaeological occurrences of *Arnebia decumbens*

Archaeological occurrences of *Arnebia decumbens*

| Site | Age range | N assemblages | Average prop. | Source | Predicted? |
|---|---|---|---|---|---|
| Bølling-Allerød (14.7-12.9 ka) | | | | | |
| Abu Hureyra | 13.1–13.0 ka | 1 | 3.19% | ORIGINS | no |
| Younger Dryas (12.9-11.7 ka) | | | | | |
| Abu Hureyra | 13.0–11.8 ka | 2 | 9.55% | ORIGINS | no |
| Mureybet | 12.1–11.9 ka | 1 | 8.00% | ORIGINS | no |
| Early Holocene (11.7-8.3 ka) | | | | | |
| Mureybet | 11.7–10.8 ka | 2 | 14.43% | ORIGINS | no |
| Netiv Hagdud | 11.6–10.6 ka | 1 | 0.07% | ORIGINS | no |
| El-Hemmeh | 11.1–10.5 ka | 1 | 0.85% | ORIGINS | yes |
| Cafer Höyük | 10.6–9.7 ka | 1 | 0.25% | ORIGINS | no |
| Wadi Jilat 7 | 10.2–9.3 ka | 3 | 1.07% | ORIGINS | no |
| Tell Aswad | 10.2–9.3 ka | 1 | 0.04% | ORIGINS | no |
| Sabi Abyad II | 9.5–8.8 ka | 1 | 0.79% | ORIGINS | no |
| Tell Ghoraifé | 9.5–8.6 ka | 1 | 0.10% | ORIGINS | no |
| Dhuweila | 9.4–9.1 ka | 1 | 1.56% | ORIGINS | no |
| Abu Hureyra | 9.3–8.2 ka | 1 | 35.61% | ORIGINS | no |
| Bouqras | 9.2–8.6 ka | 1 | 1.65% | ORIGINS | no |
| Wadi Jilat 13 | 9.1–8.4 ka | 3 | 1.48% | ORIGINS | no |

## *Arnebia linearifolia*

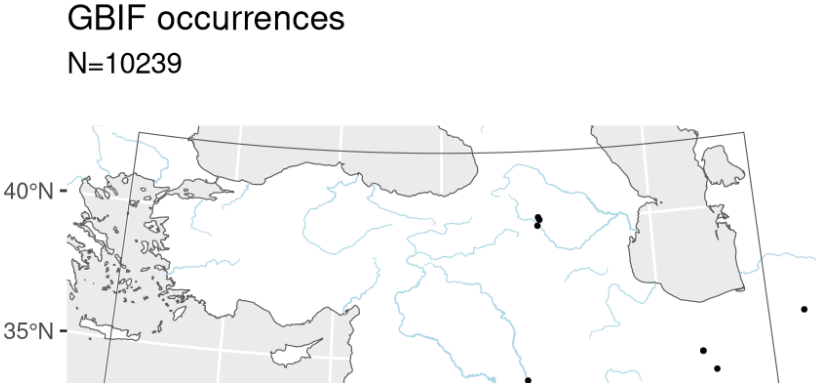


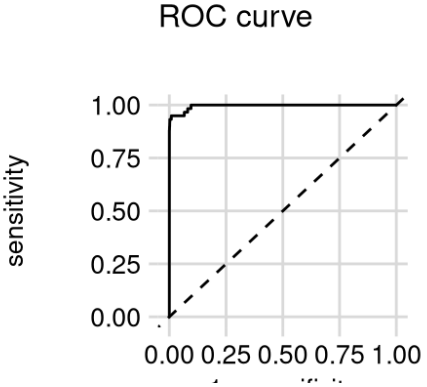

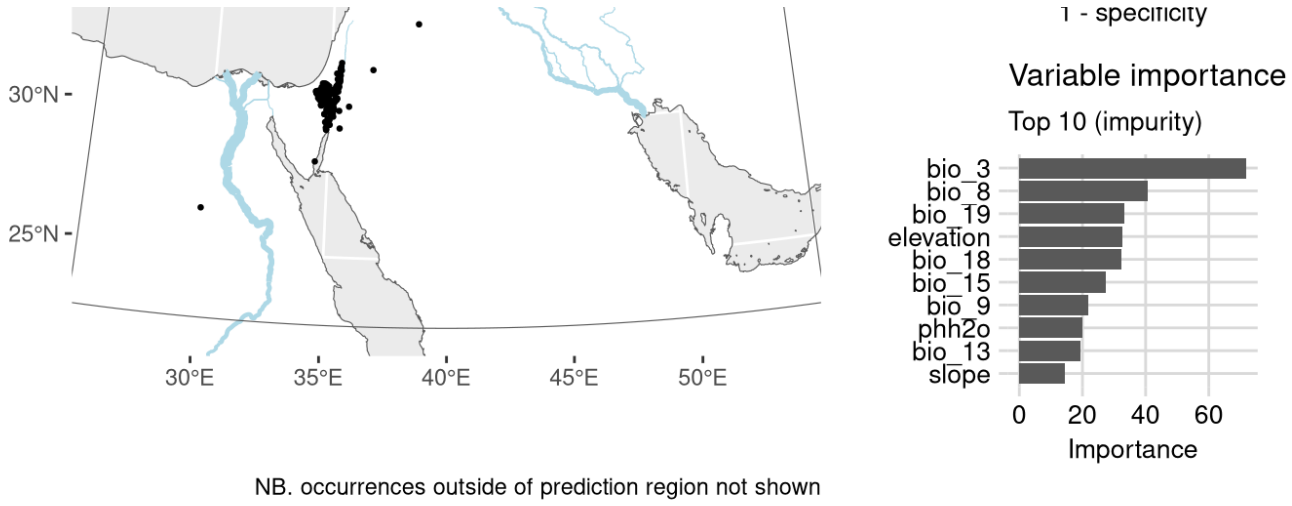


Figure 17: Fitted model summary for *Arnebia linearifolia*

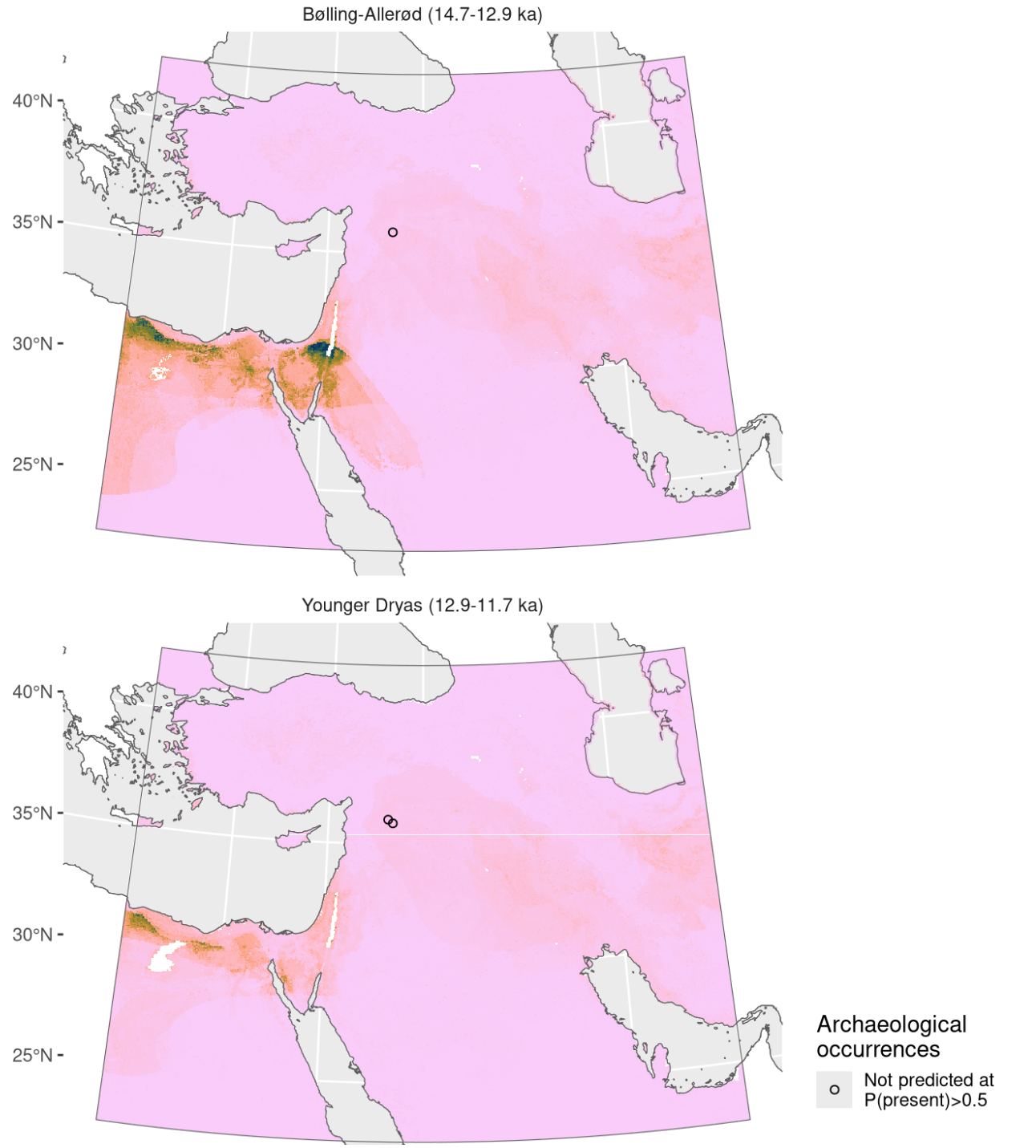

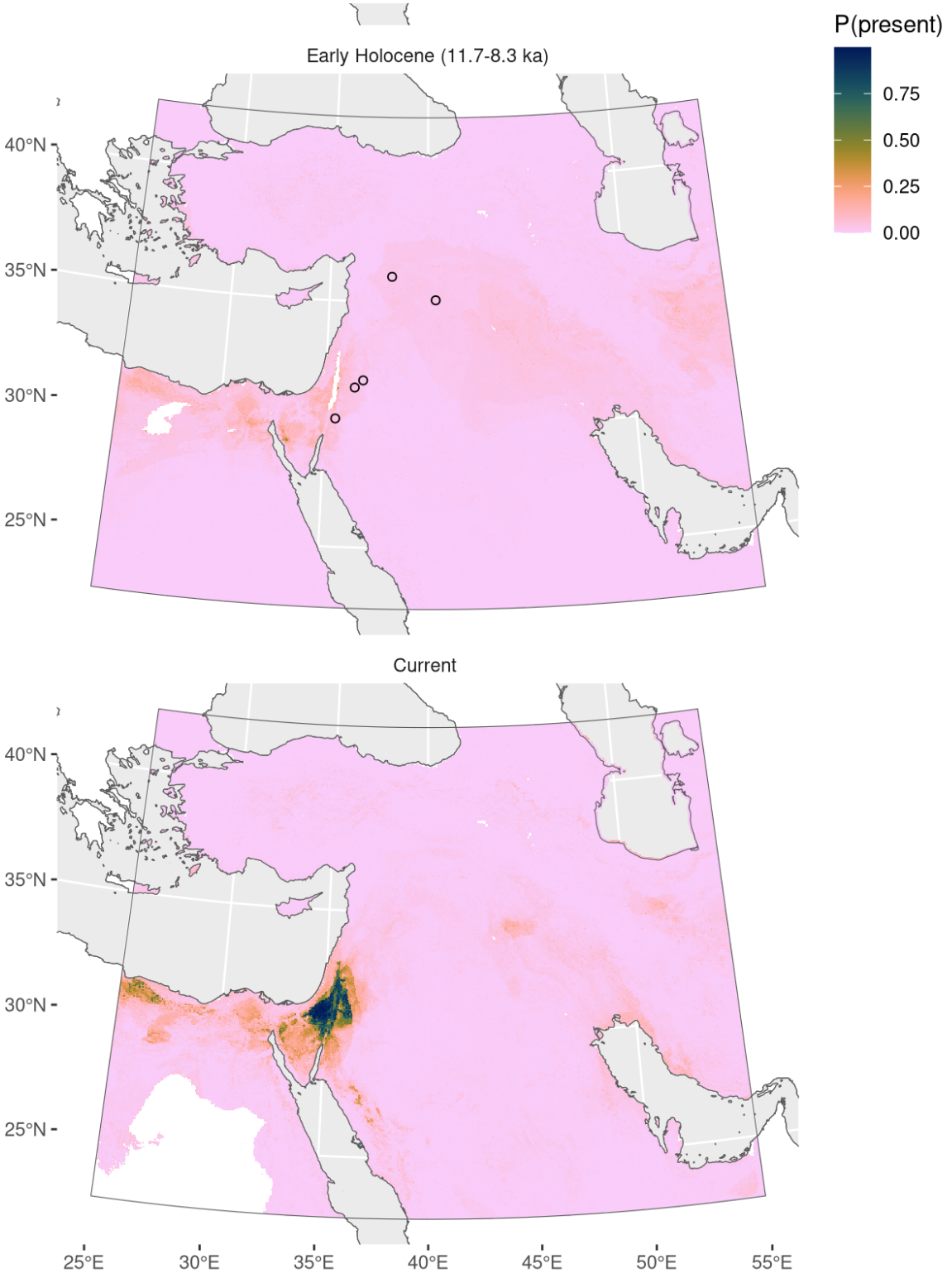


Figure 18: Predicted palaeodistributions of *Arnebia linearifolia*

Table 9: Archaeological occurrences of *Arnebia linearifolia*

Archaeological occurrences of *Arnebia linearifolia*

| Site | Age range | N assemblages | Average prop. | Source | Predicted? |
|---|---|---|---|---|---|
| Bølling-Allerød (14.7-12.9 ka) | | | | | |
| Abu Hureyra | 13.1–13.0 ka | 1 | 0.36% | ORIGINS | no |

| | | | | | |
|---|---|---|---|---|---|
| Younger Dryas (12.9-11.7 ka) | | | | | |
| Abu Hureyra | 13.0–11.8 ka | 2 | 0.45% | ORIGINS | no |
| Mureybet | 12.1–11.9 ka | 1 | 0.21% | ORIGINS | no |
| Early Holocene (11.7-8.3 ka) | | | | | |
| Mureybet | 11.7–10.8 ka | 2 | 0.41% | ORIGINS | no |
| Wadi Jilat 7 | 10.2–9.3 ka | 3 | 1.20% | ORIGINS | no |
| Basta | 9.4–9.2 ka | 1 | 1.81% | ORIGINS | no |
| Azraq 31 | 9.3–9.2 ka | 1 | 0.92% | ORIGINS | no |
| Bouqras | 9.2–8.6 ka | 1 | 0.12% | ORIGINS | no |
| Wadi Jilat 13 | 9.1–8.5 ka | 1 | 0.05% | ORIGINS | no |

## *Atriplex prostrata*

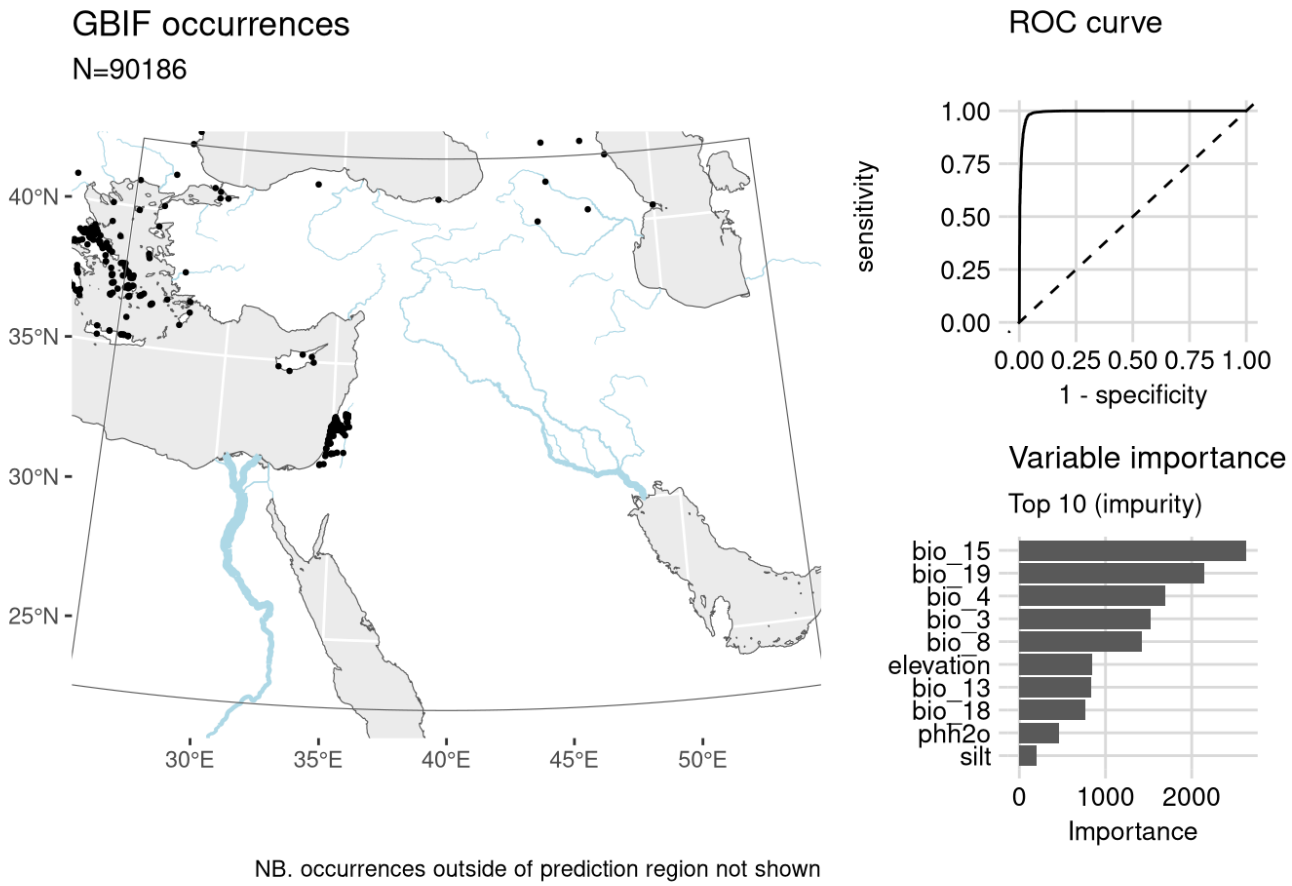


Figure 19: Fitted model summary for *Atriplex prostrata*

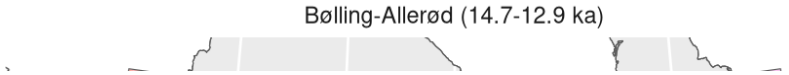

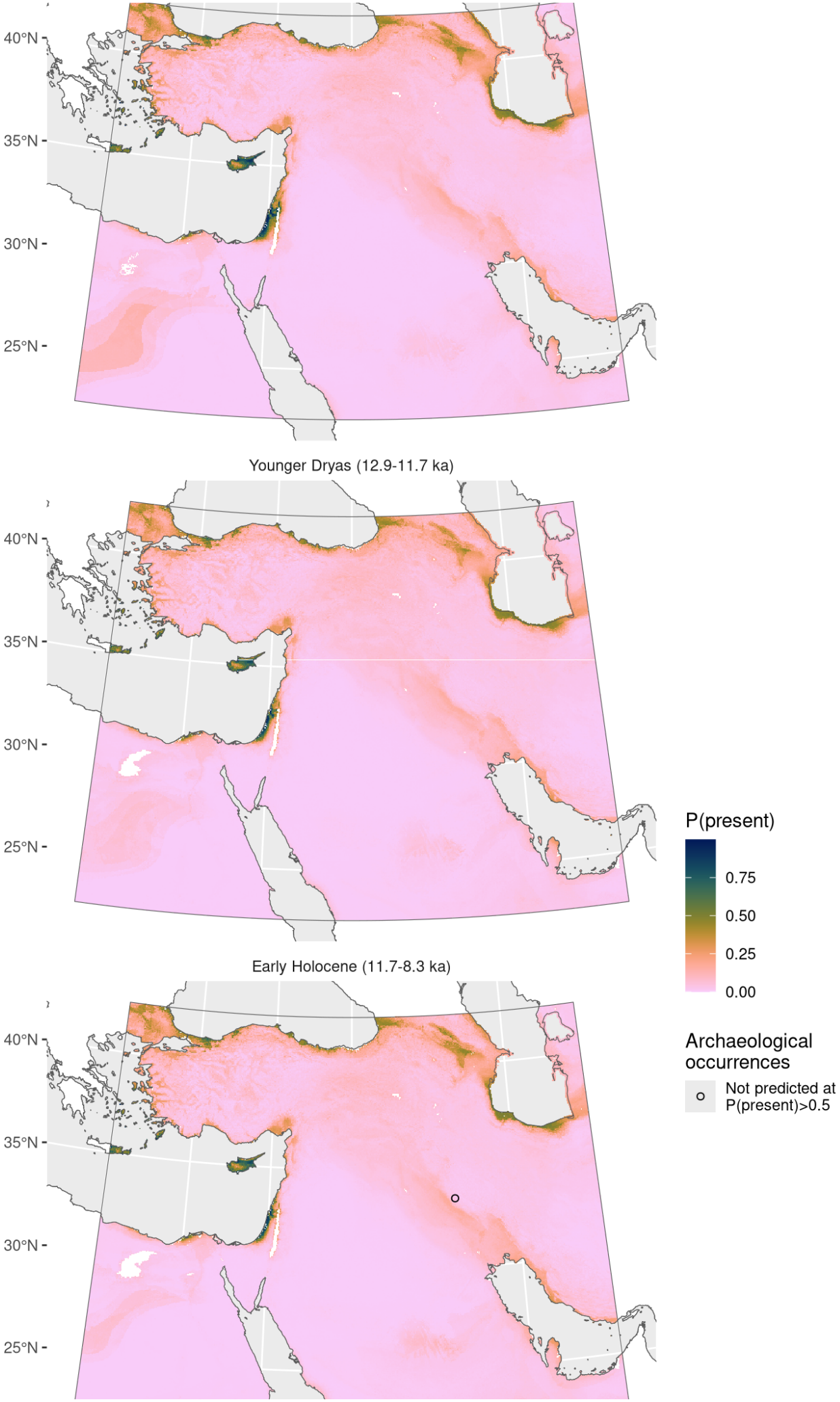
40°N
35°N
30°N
25°N
Younger Dryas (12.9-11.7 ka)
40°N
35°N
30°N
25°N
Early Holocene (11.7-8.3 ka)
40°N
35°N
30°N
25°N
P(present)
0.75
0.50
0.25
0.00
Archaeological occurrences
Not predicted at P(present)>0.5

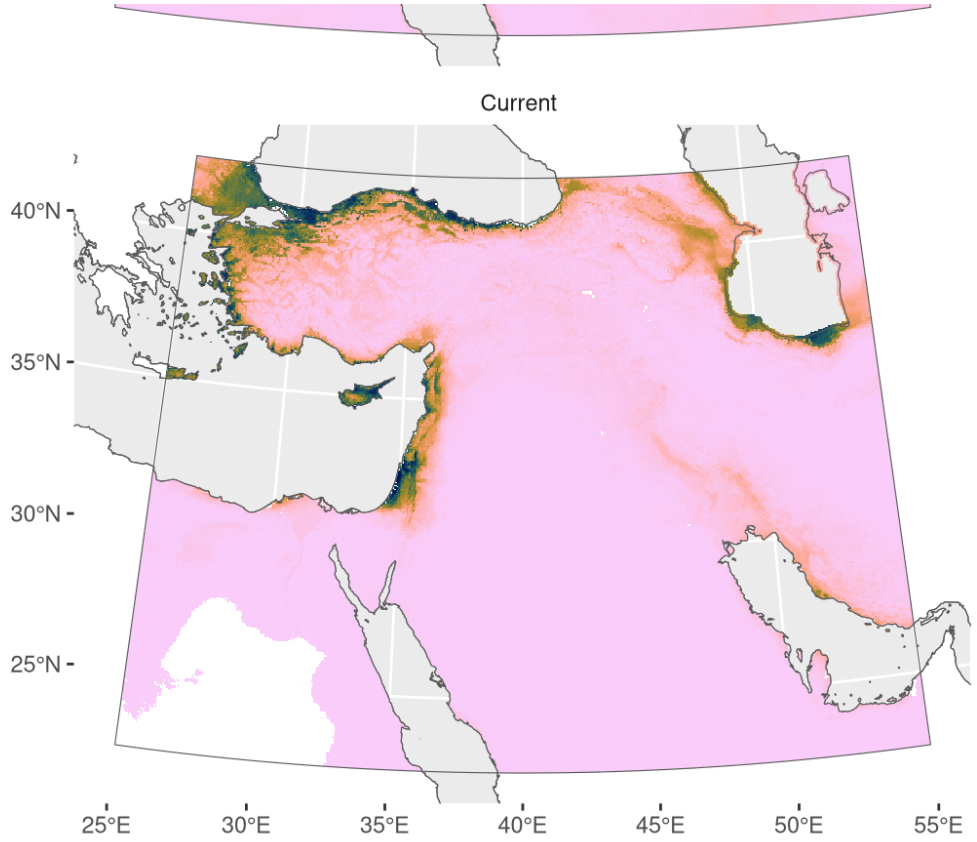


Figure 20: Predicted palaeodistributions of *Atriplex prostrata*

Table 10: Archaeological occurrences of *Atriplex prostrata*

Archaeological occurrences of *Atriplex prostrata*

| Site | Age range | N assemblages | Average prop. | Source | Predicted? |
|---|---|---|---|---|---|
| Early Holocene (11.7-8.3 ka) | | | | | |
| Chogha Golan | 11.2–9.9 ka | 4 | 0.18% | ORIGINS | no |

# *Avena sterilis*

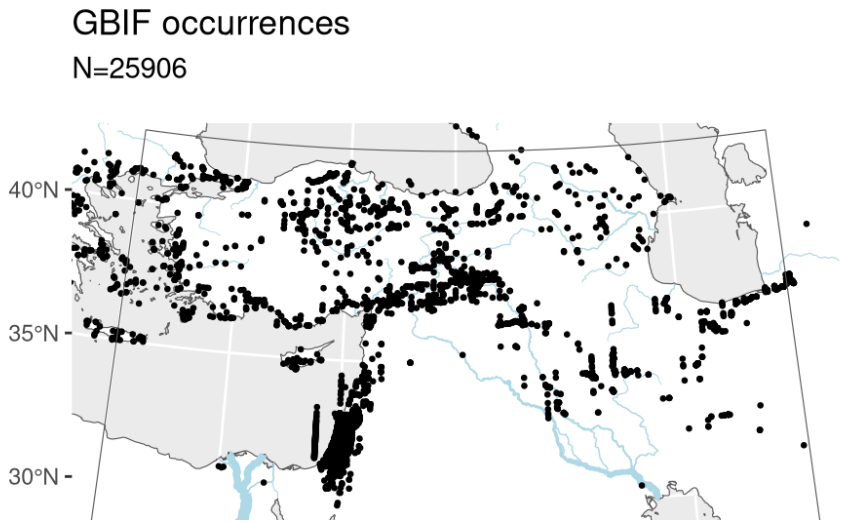


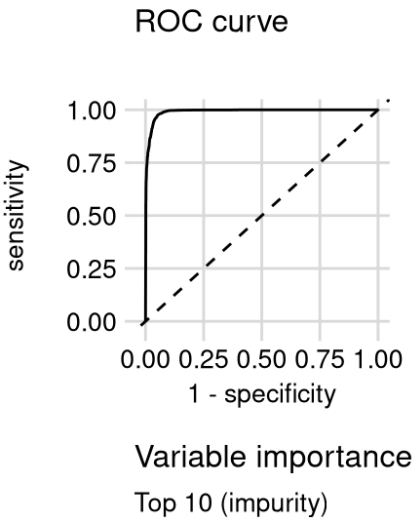

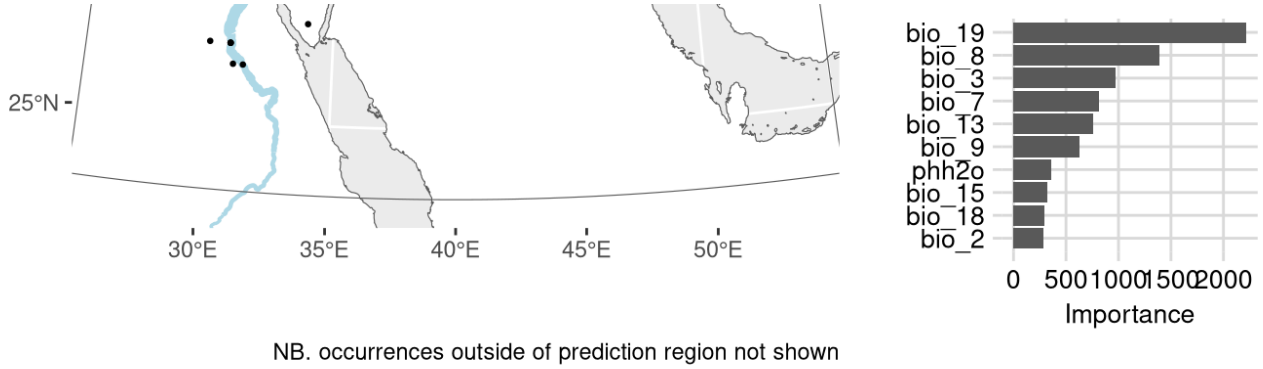


Figure 21: Fitted model summary for *Avena sterilis*

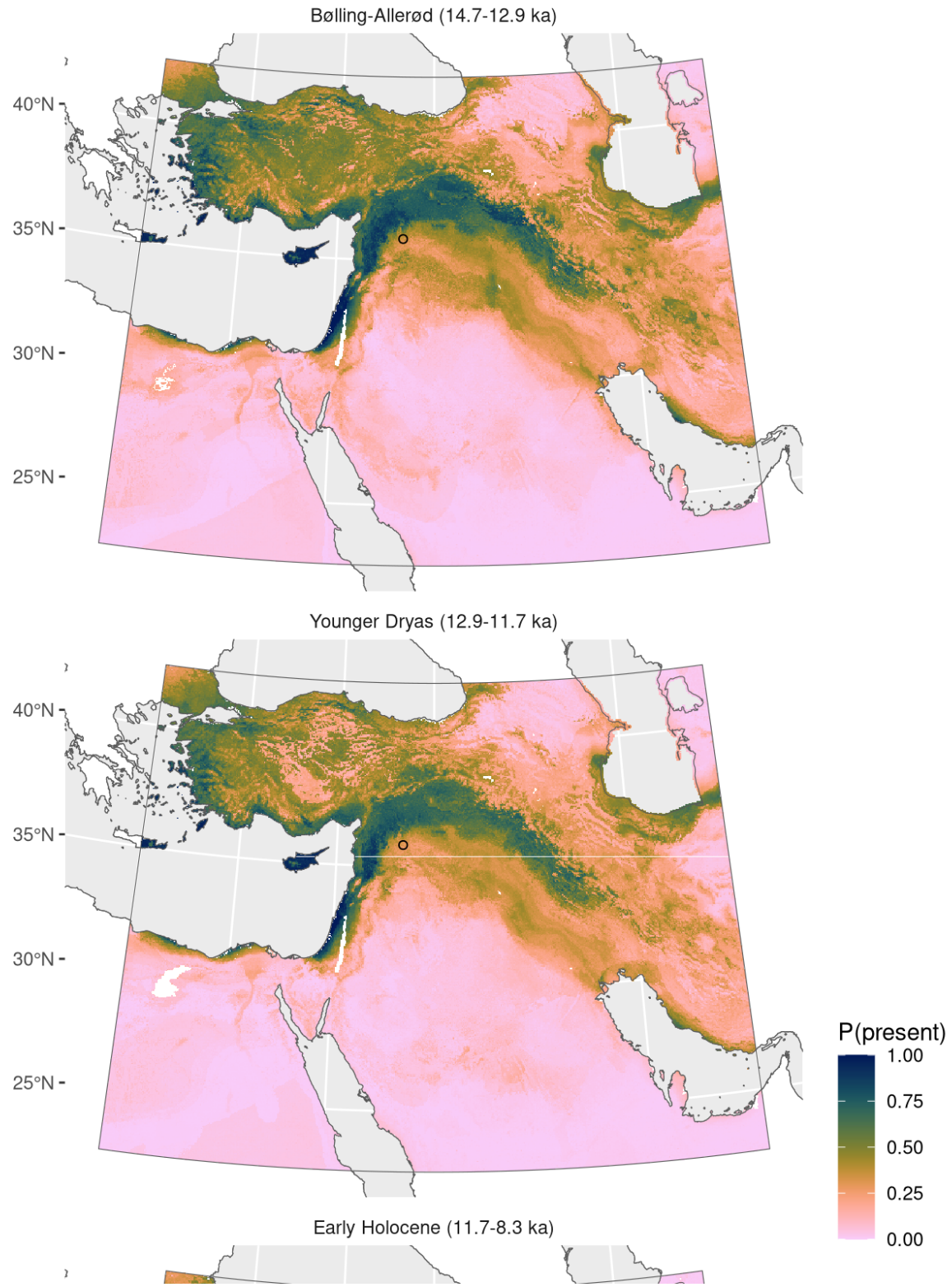

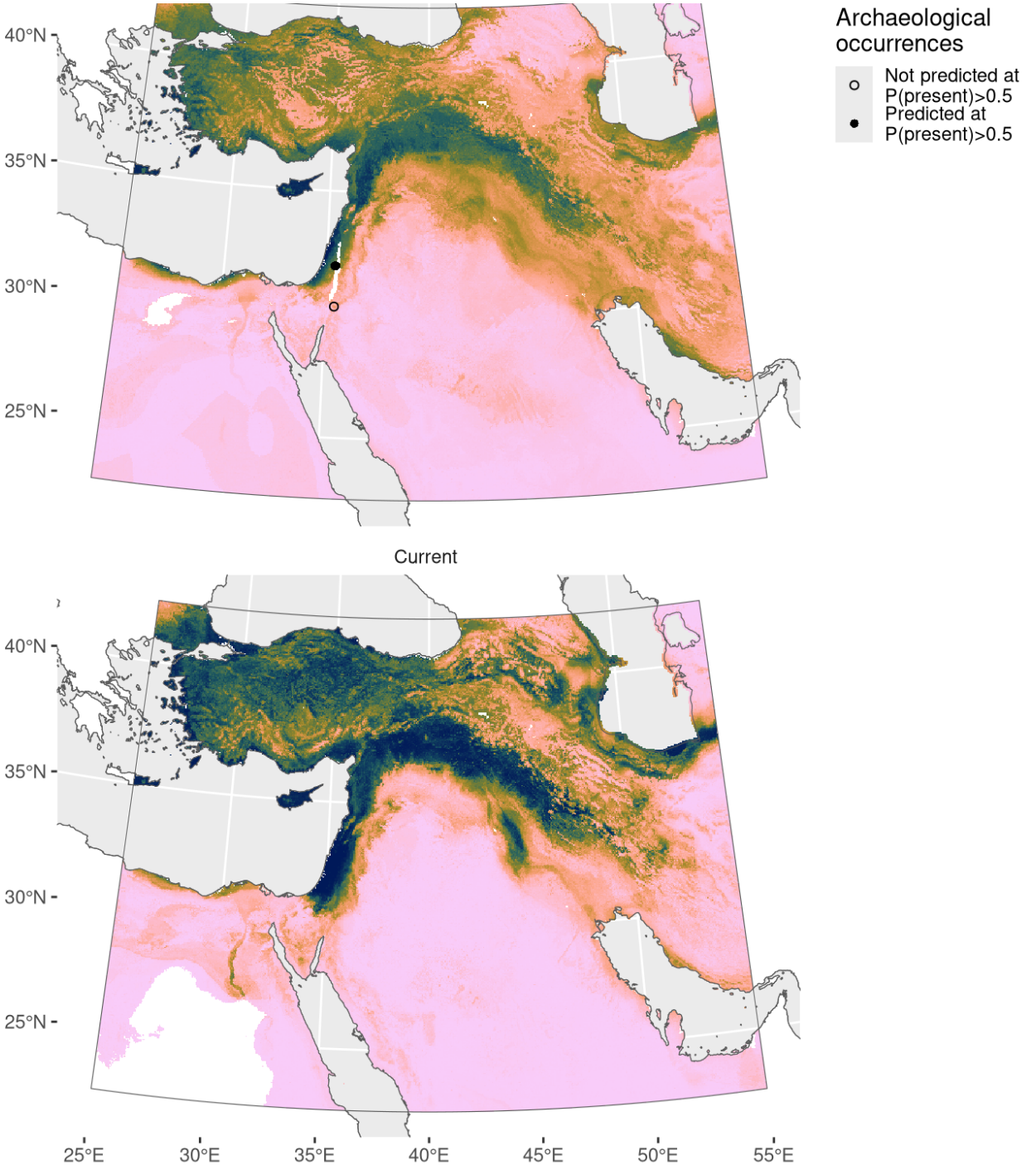


Figure 22: Predicted palaeodistributions of *Avena sterilis*

Table 11: Archaeological occurrences of *Avena sterilis*

Archaeological occurrences of *Avena sterilis*

| Site | Age range | N assemblages | Average prop. | Source | Predicted? |
|---|---|---|---|---|---|
| Bølling-Allerød (14.7-12.9 ka) | | | | | |
| Abu Hureyra | 13.1–13.0 ka | 1 | 0.05% | ORIGINS | no |
| Younger Dryas (12.9-11.7 ka) | | | | | |
| Abu Hureyra | 13.0–12.1 ka | 1 | 0.02% | ORIGINS | no |

| | | | | | |
|---|---|---|---|---|---|
| Early Holocene (11.7-8.3 ka) | | | | | |
| Netiv Hagdud | 11.6–10.6 ka | 1 | 0.39% | ORIGINS | yes |
| Gilgal I | 11.2–11.2 ka | 1 | 31.76% | ORIGINS | yes |
| Beidha | 10.1–9.5 ka | 1 | 0.01% | ORIGINS | no |

# *Bassia arabica*

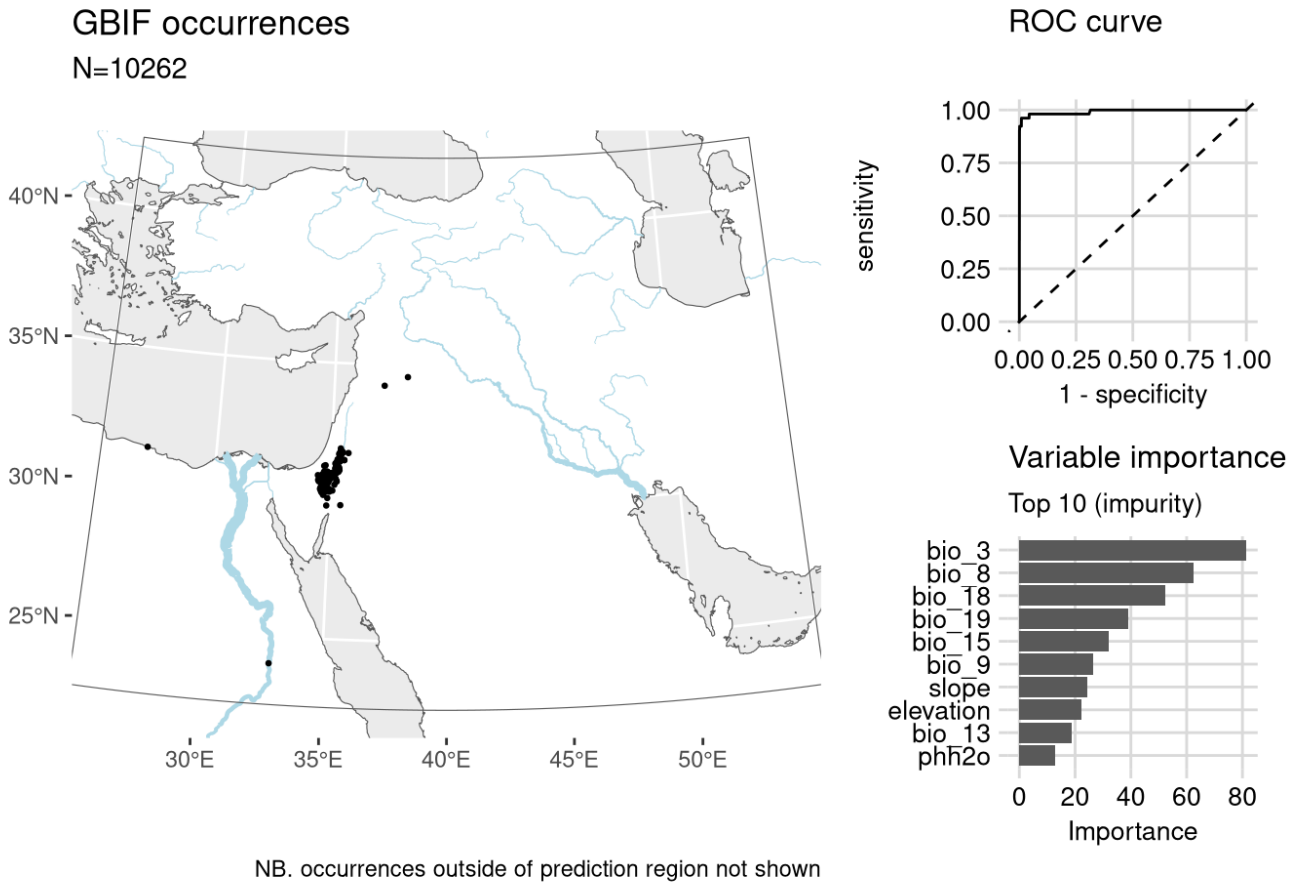


Figure 23: Fitted model summary for *Bassia arabica*

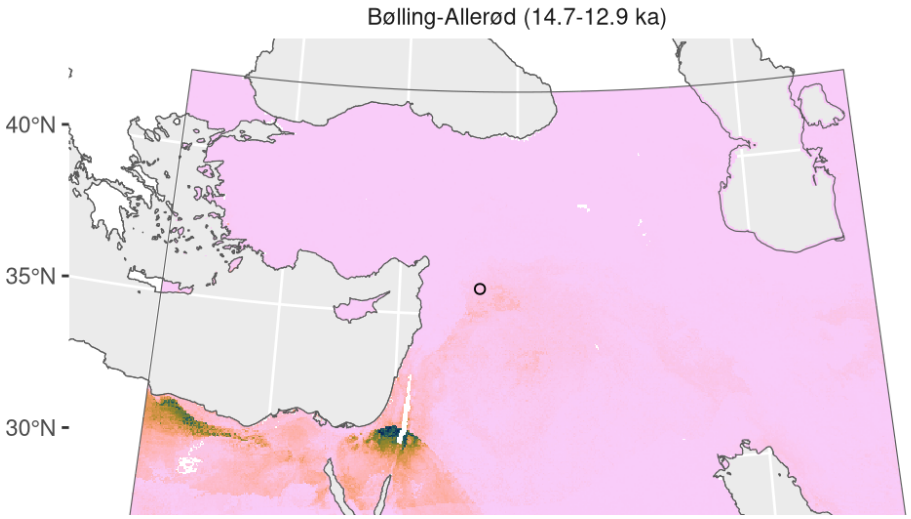

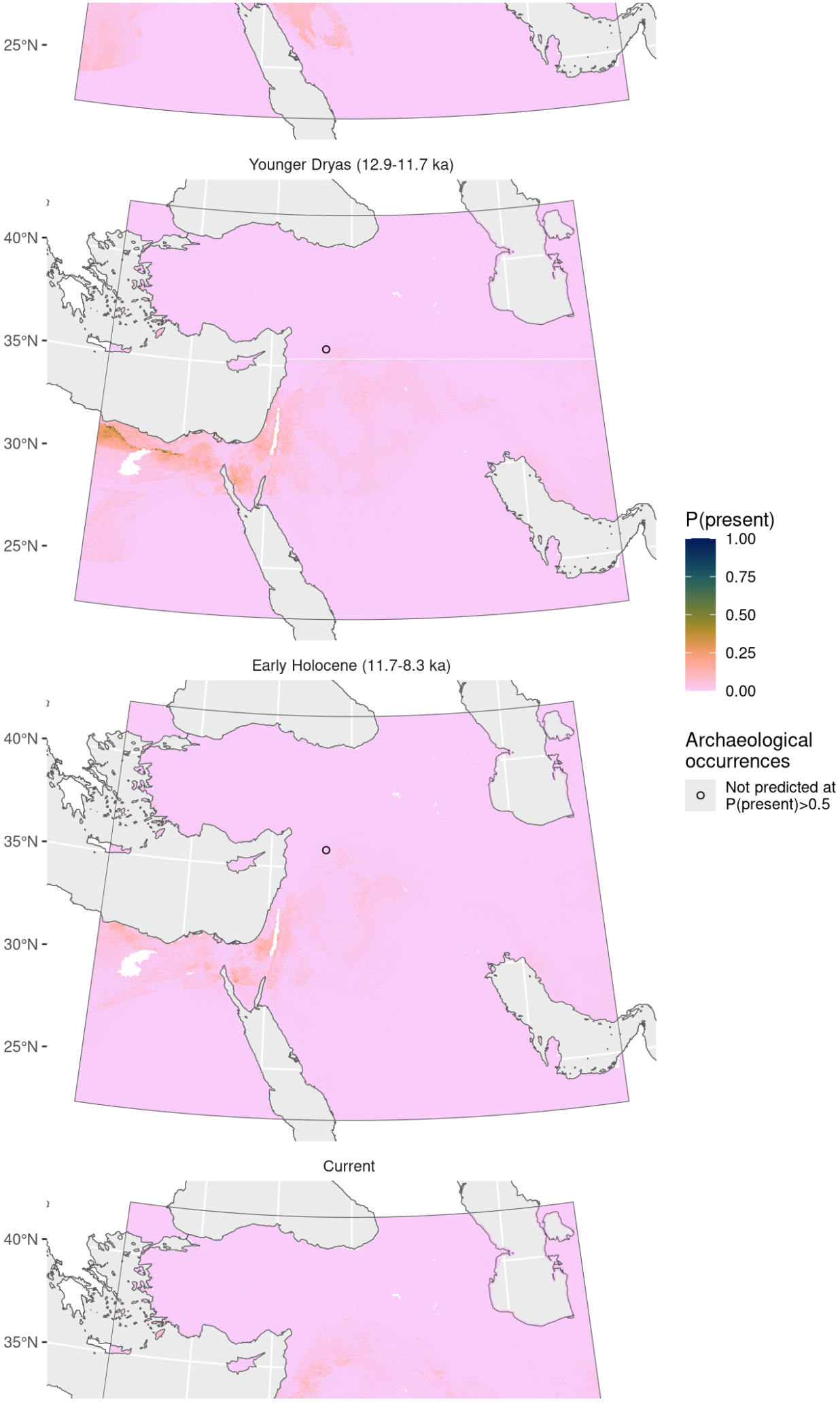
25°N
Younger Dryas (12.9-11.7 ka)
40°N
35°N
30°N
25°N
Early Holocene (11.7-8.3 ka)
40°N
35°N
30°N
25°N
Current
40°N
35°N
P(present)
1.00
0.75
0.50
0.25
0.00
Archaeological occurrences
Not predicted at P(present)>0.5

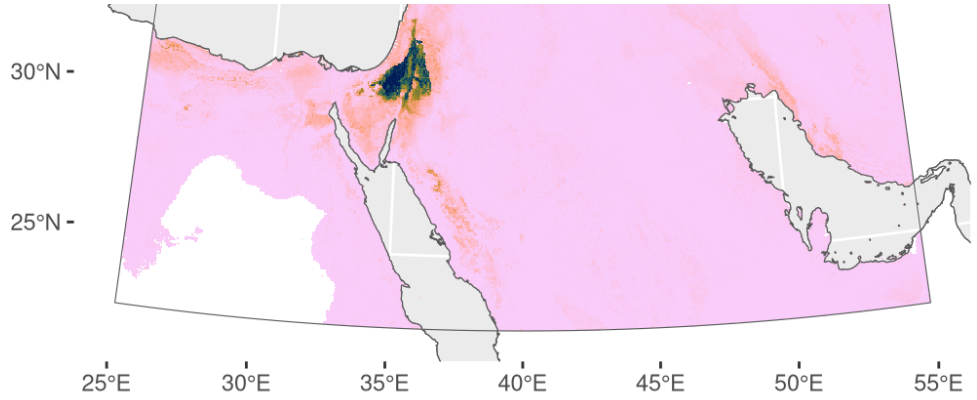


Figure 24: Predicted palaeodistributions of *Bassia arabica*

Table 12: Archaeological occurrences of *Bassia arabica*

Archaeological occurrences of *Bassia arabica*

| Site | Age range | N assemblages | Average prop. | Source | Predicted? |
|---|---|---|---|---|---|
| Bølling-Allerød (14.7-12.9 ka) | | | | | |
| Abu Hureyra | 13.1–13.0 ka | 1 | 0.05% | ORIGINS | no |
| Younger Dryas (12.9-11.7 ka) | | | | | |
| Abu Hureyra | 13.0–11.8 ka | 2 | 0.61% | ORIGINS | no |
| Early Holocene (11.7-8.3 ka) | | | | | |
| Abu Hureyra | 9.3–8.2 ka | 1 | 0.71% | ORIGINS | no |

# *Bolboschoenus glaucus*

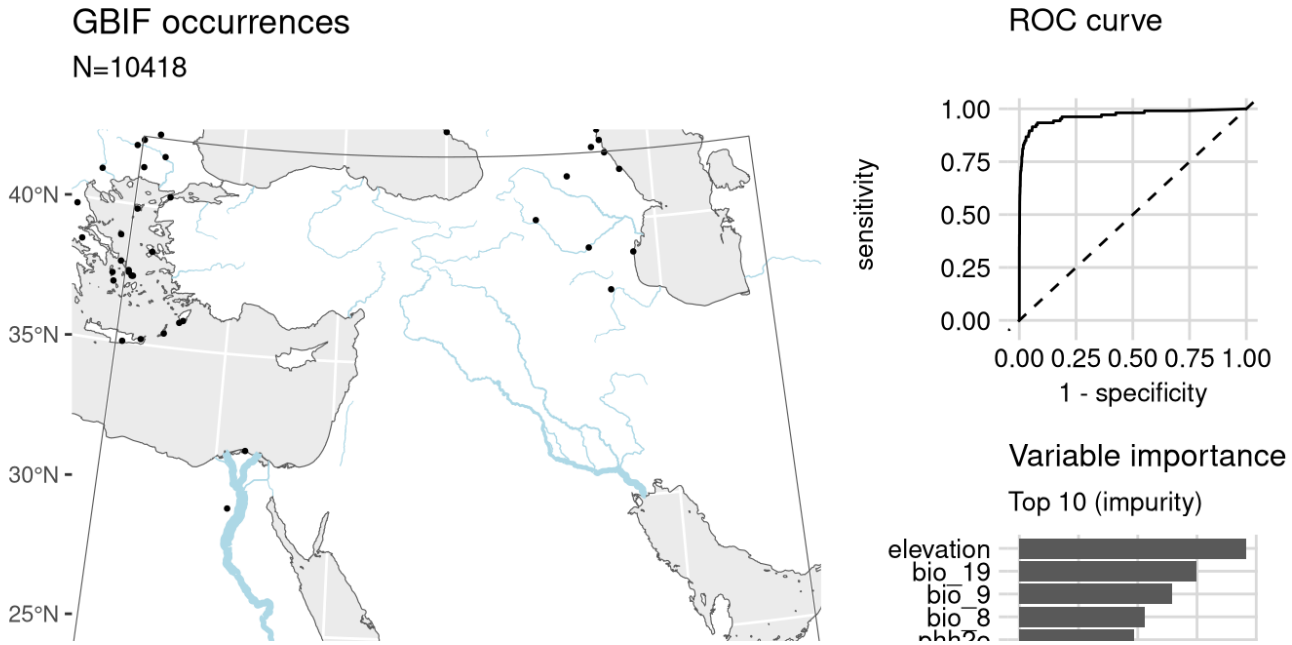

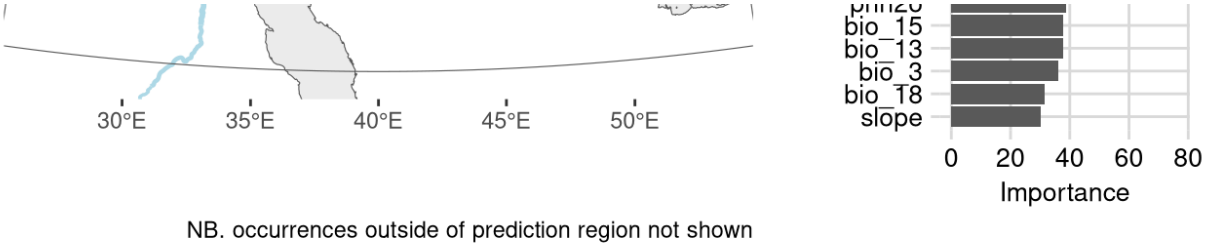


Figure 25: Fitted model summary for *Bolboschoenus glaucus*

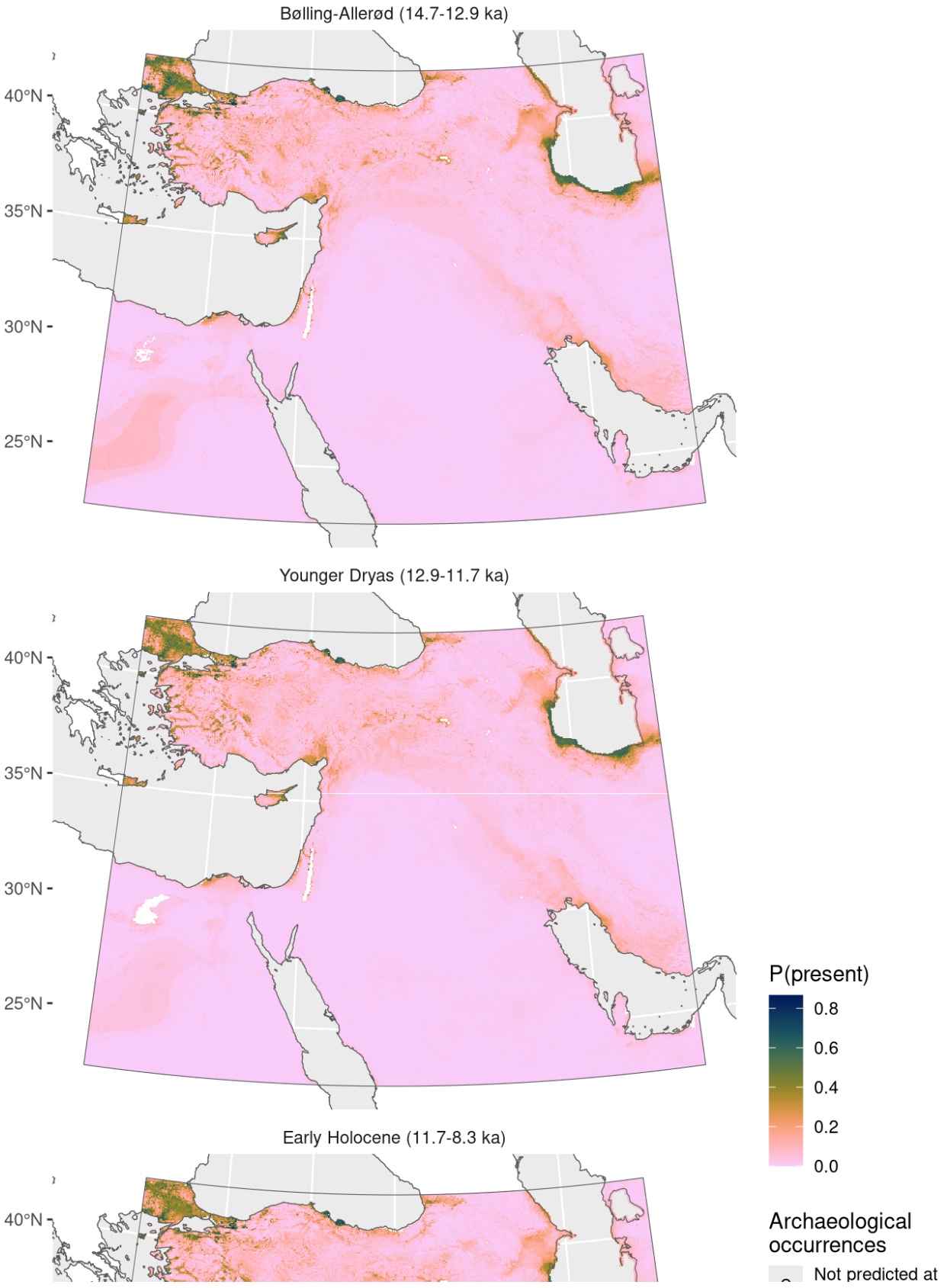

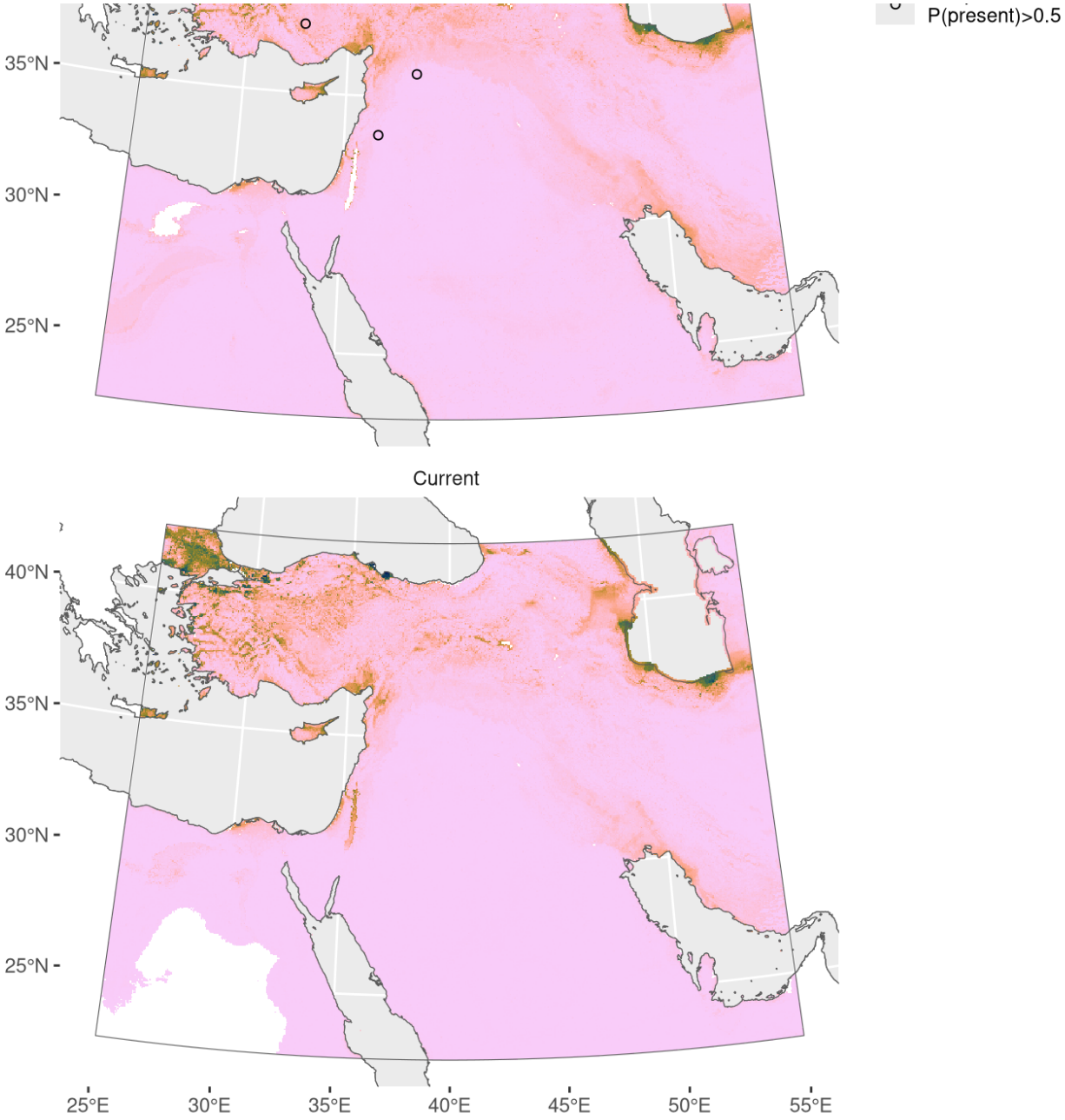


Figure 26: Predicted palaeodistributions of *Bolboschoenus glaucus*

Table 13: Archaeological occurrences of *Bolboschoenus glaucus*

Archaeological occurrences of *Bolboschoenus glaucus*

| Site | Age range | N assemblages | Average prop. | Source | Predicted? |
|---|---|---|---|---|---|
| Early Holocene (11.7-8.3 ka) | | | | | |
| Tell Aswad | 11.2–9.3 ka | 3 | 4.72% | ORIGINS | no |
| Abu Hureyra | 9.3–8.2 ka | 1 | 0.47% | ORIGINS | no |
| Çatalhöyük | 9.2–8.3 ka | 1 | 0.00% | ORIGINS | no |

## *Bolboschoenus maritimus*

# *Bolboschoenus maritimus*

Including Scirpus maritimus.

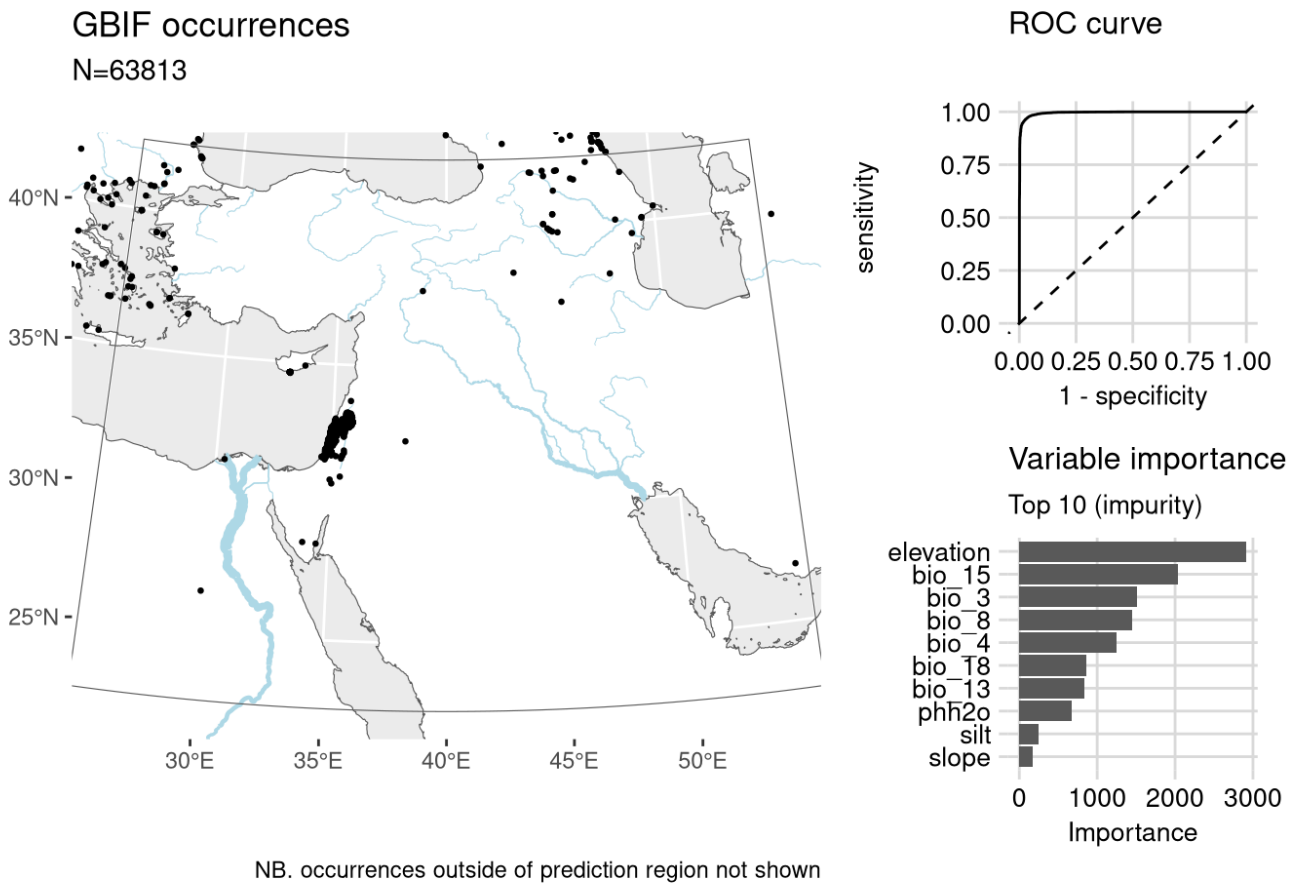


Figure 27: Fitted model summary for *Bolboschoenus maritimus*

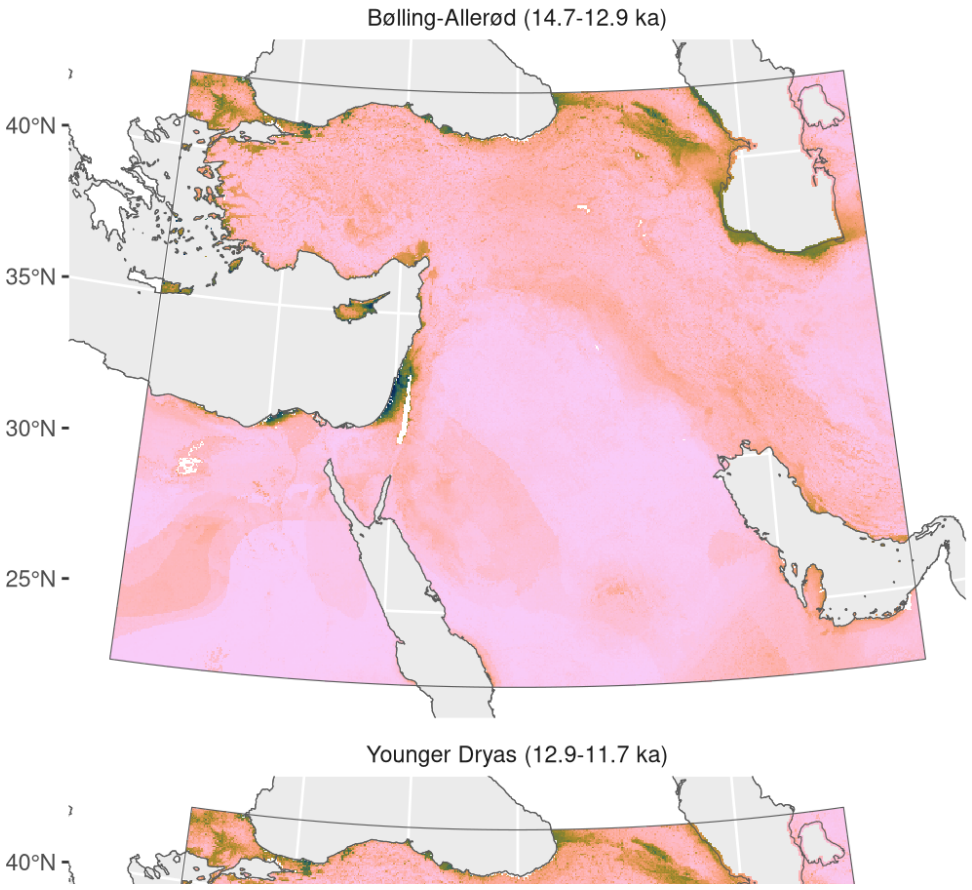

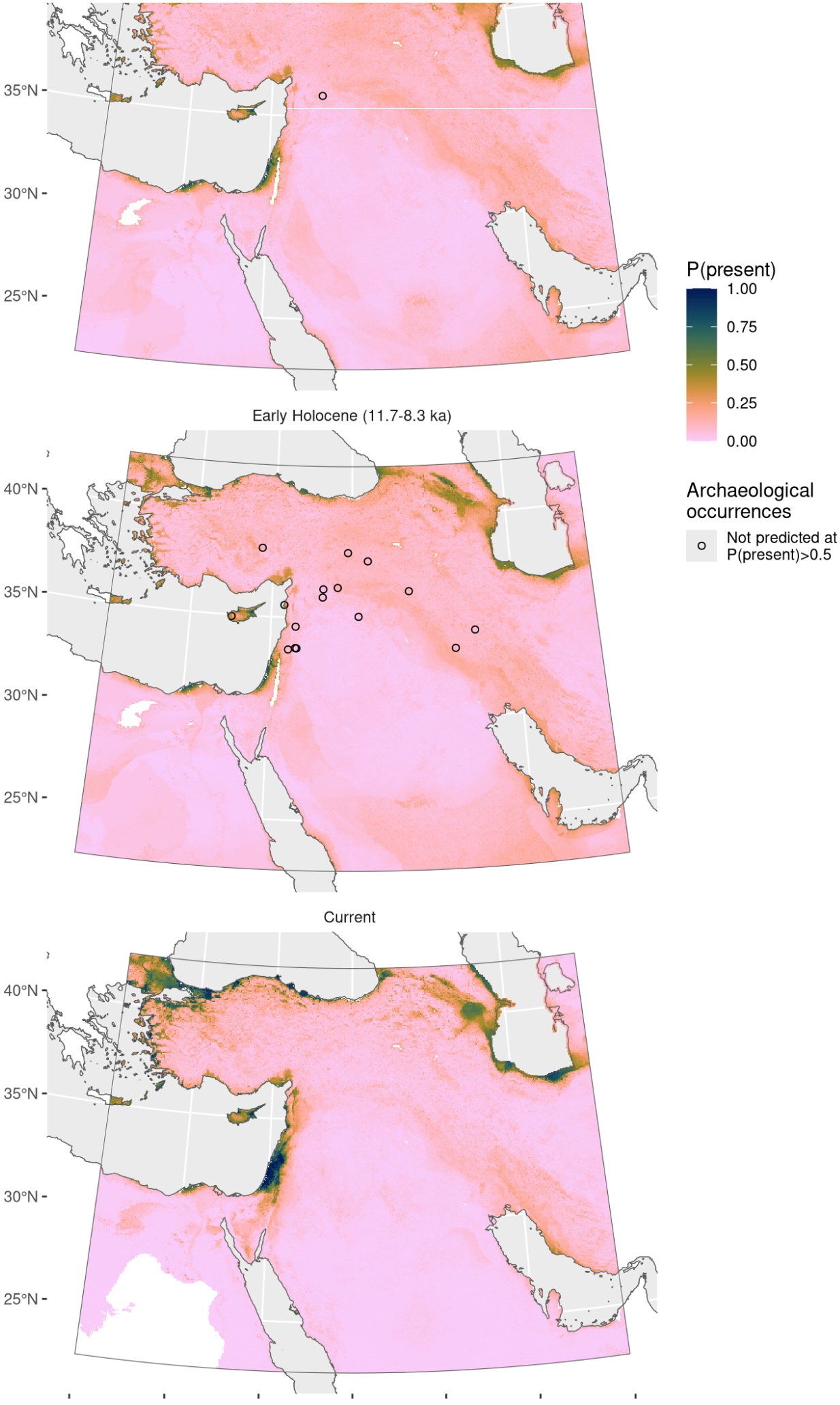
35°N
30°N
25°N
Early Holocene (11.7-8.3 ka)
40°N
35°N
30°N
25°N
Current
40°N
35°N
30°N
25°N
P(present)
1.00
0.75
0.50
0.25
0.00
Archaeological occurrences
Not predicted at P(present)>0.5

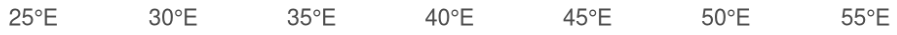


Figure 28: Predicted palaeodistributions of *Bolboschoenus maritimus*

Table 14: Archaeological occurrences of *Bolboschoenus maritimus*

Archaeological occurrences of *Bolboschoenus maritimus*

| Site | Age range | N assemblages | Average prop. | Source | Predicted? |
|---|---|---|---|---|---|
| Younger Dryas (12.9-11.7 ka) | | | | | |
| Mureybet | 12.1–11.9 ka | 1 | 3.74% | ORIGINS | no |
| Early Holocene (11.7-8.3 ka) | | | | | |
| Körtik Tepe | 11.7–11.2 ka | 1 | 9.43% | ORIGINS | no |
| Mureybet | 11.7–10.8 ka | 2 | 1.69% | ORIGINS | no |
| M'lefaat | 11.3–11.1 ka | 1 | 0.70% | ORIGINS | no |
| Chogha Golan | 11.2–9.8 ka | 4 | 0.27% | ORIGINS | no |
| Ganj Dareh | 10.3–9.2 ka | 5 | 6.72% | ORIGINS | no |
| Çayönü | 10.2–8.8 ka | 5 | 2.22% | ORIGINS | no |
| Tell Aswad | 10.2–9.3 ka | 1 | 0.36% | ORIGINS | no |
| Tell Ghoraifé | 10.1–8.6 ka | 2 | 4.73% | ORIGINS | no |
| Aşıklı Höyük | 9.9–9.4 ka | 1 | 0.01% | ORIGINS | no |
| Tell Halula | 9.9–9.1 ka | 1 | 0.93% | COMPAG | no |
| Ais Giorkis | 9.6–9.4 ka | 1 | 0.07% | ORIGINS | no |
| Sabi Abyad II | 9.5–8.8 ka | 1 | 0.72% | ORIGINS | no |
| Tell Ramad | 9.3–8.6 ka | 2 | 0.02% | ORIGINS | no |
| Bouqras | 9.2–8.6 ka | 1 | 2.50% | ORIGINS | no |
| Tell Nebi Mend | 9.0–8.6 ka | 1 | 5.62% | COMPAG | no |
| Ras Shamra | 8.8–8.3 ka | 1 | 1.98% | ORIGINS | no |

## *Brachypodium distachyon*

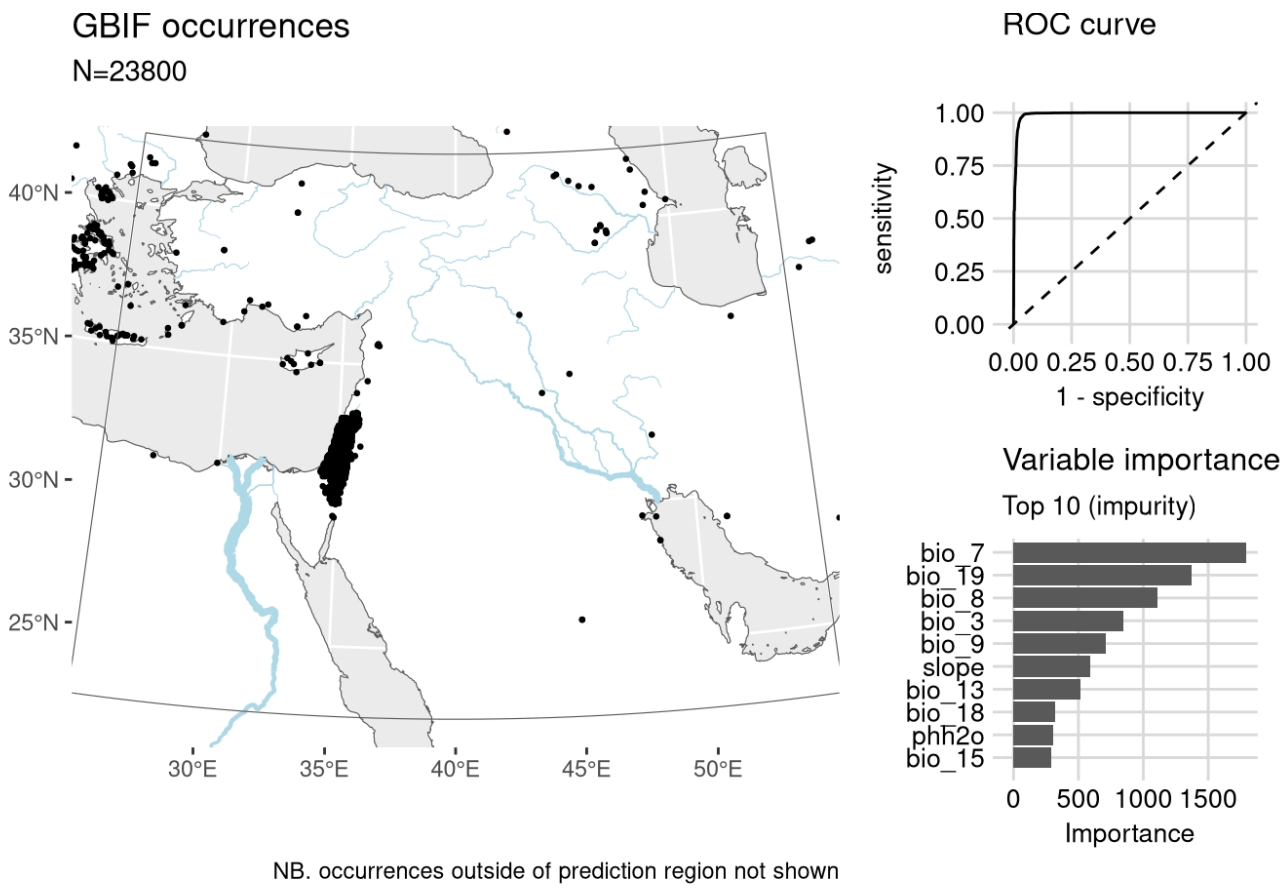


Figure 29: Fitted model summary for *Brachypodium distachyon*

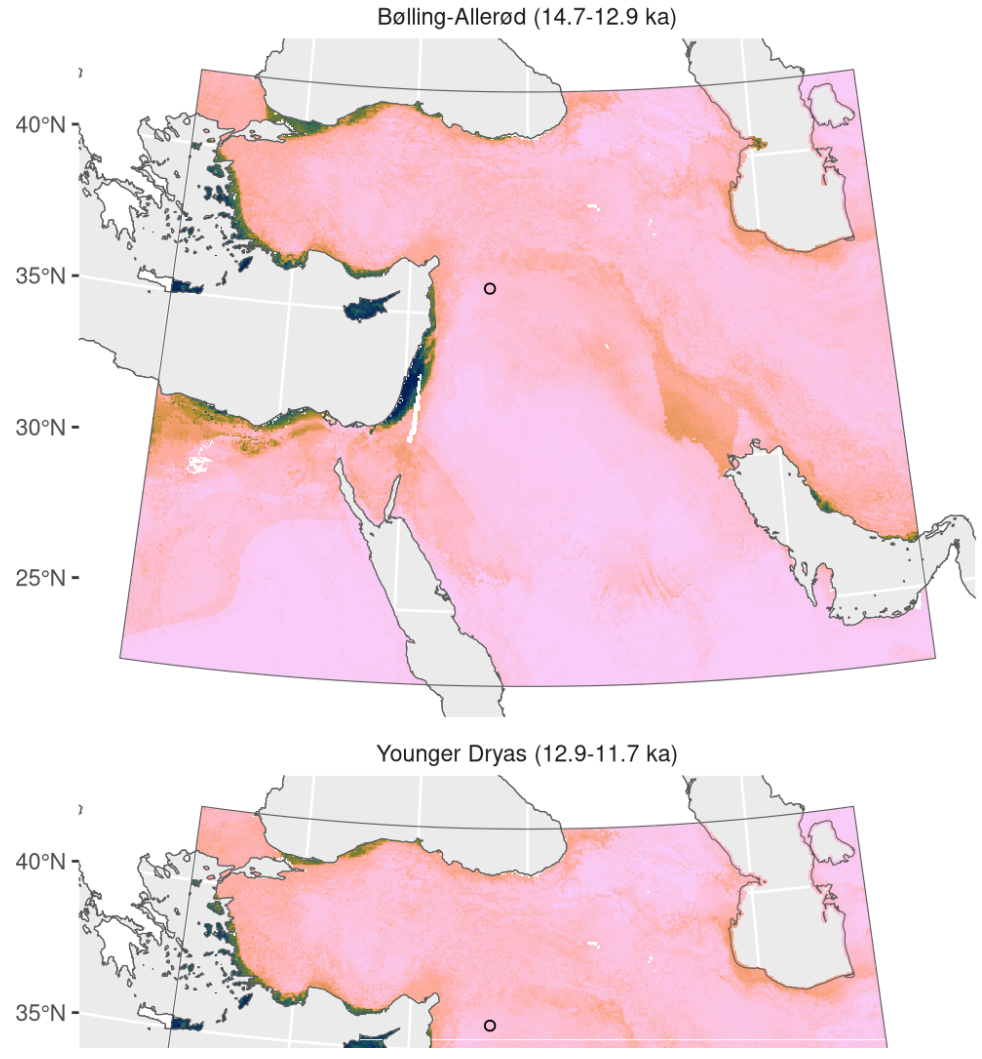

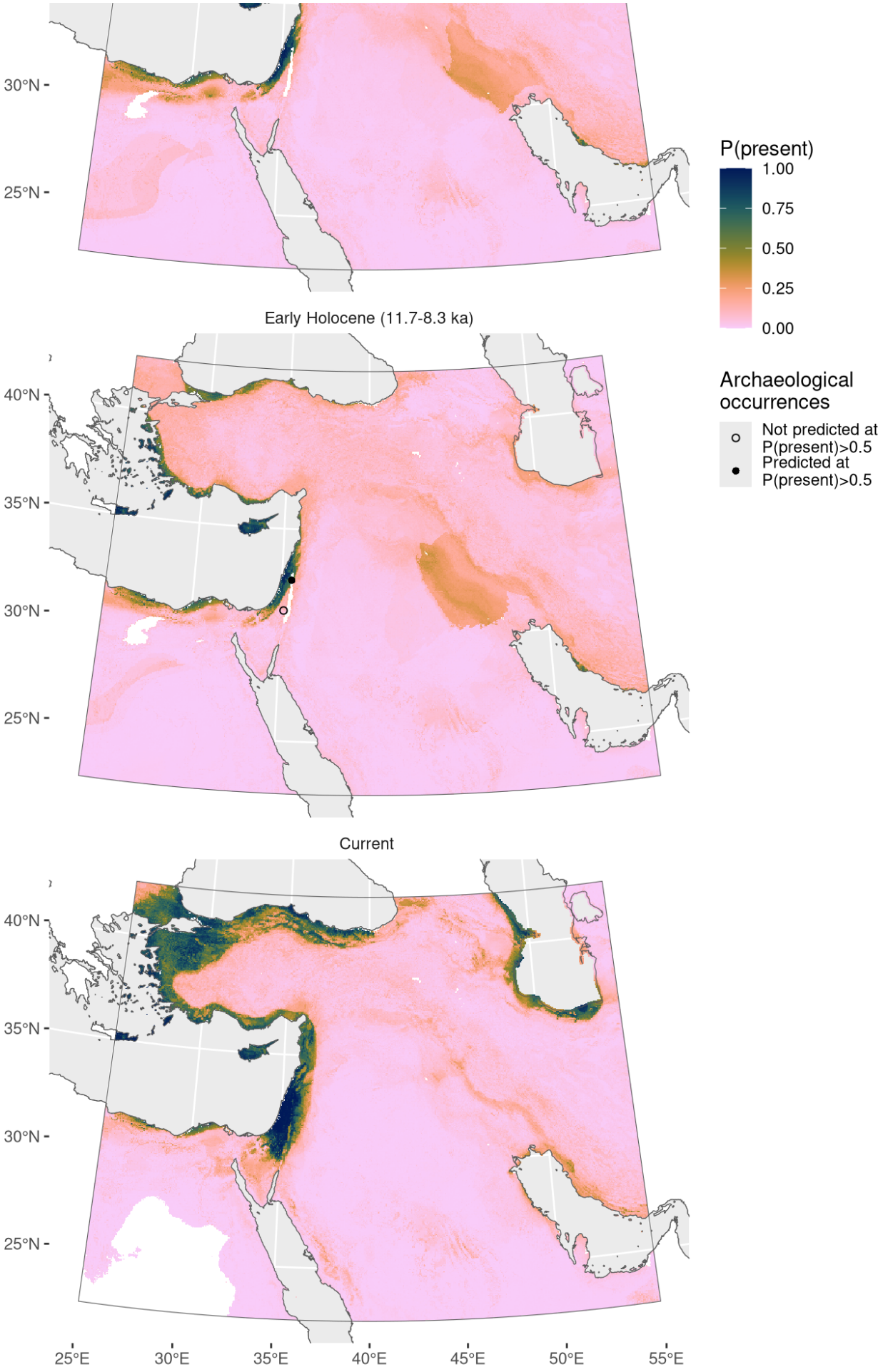


Figure 30: Predicted palaeodistributions of *Brachypodium distachyon*

Table 15: Archaeological occurrences of *Brachypodium distachyon*

Archaeological occurrences of *Brachypodium distachyon*

| Site | Age range | N assemblages | Average prop. | Source | Predicted? |
|---|---|---|---|---|---|
| Bølling-Allerød (14.7-12.9 ka) | | | | | |
| Abu Hureyra | 13.1–13.0 ka | 1 | 0.10% | ORIGINS | no |
| Younger Dryas (12.9-11.7 ka) | | | | | |
| Abu Hureyra | 13.0–11.8 ka | 2 | 0.46% | ORIGINS | no |
| Early Holocene (11.7-8.3 ka) | | | | | |
| Gesher | 11.5–11.2 ka | 1 | 0.50% | ORIGINS | yes |
| Nahal Hemar | 10.1–9.3 ka | 1 | 0.09% | ORIGINS | no |

# *Bromus sterilis*

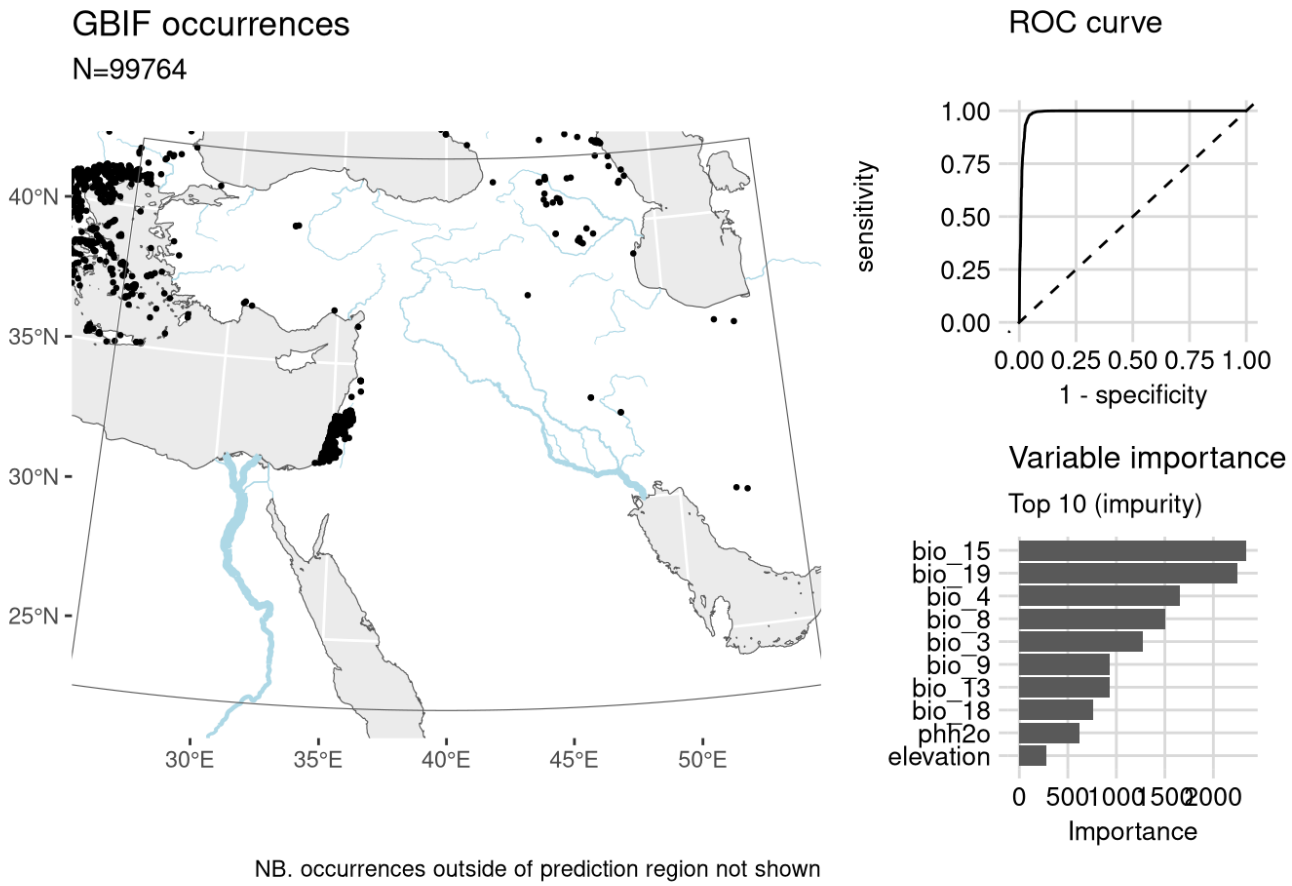


Figure 31: Fitted model summary for *Bromus sterilis*

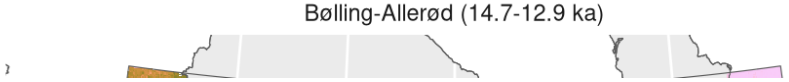

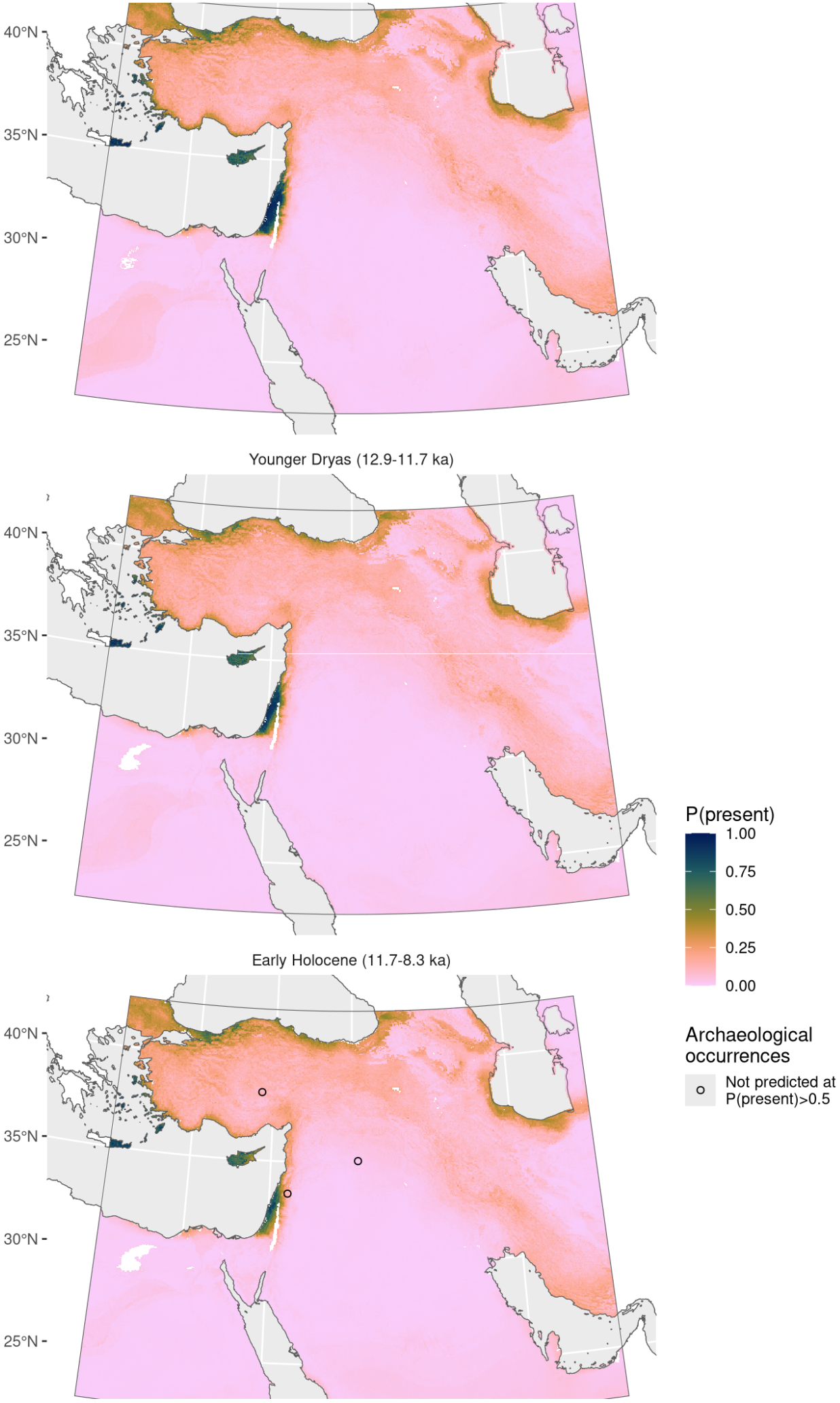
40°N
35°N
30°N
25°N
Younger Dryas (12.9-11.7 ka)
40°N
35°N
30°N
25°N
Early Holocene (11.7-8.3 ka)
40°N
35°N
30°N
25°N
P(present)
1.00
0.75
0.50
0.25
0.00
Archaeological occurrences
Not predicted at P(present)>0.5

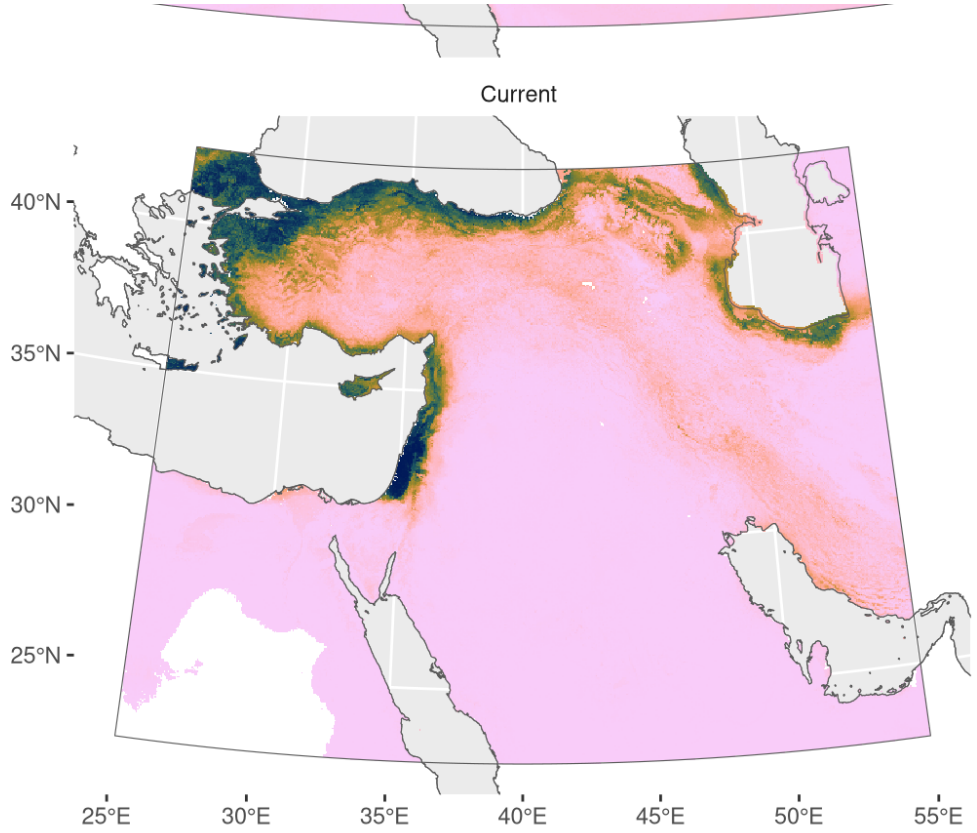


Figure 32: Predicted palaeodistributions of *Bromus sterilis*

Table 16: Archaeological occurrences of *Bromus sterilis*

Archaeological occurrences of *Bromus sterilis*

| Site | Age range | N assemblages | Average prop. | Source | Predicted? |
|---|---|---|---|---|---|
| Early Holocene (11.7-8.3 ka) | | | | | |
| Aşıklı Höyük | 9.9–9.4 ka | 1 | 0.01% | ORIGINS | no |
| Bouqras | 9.2–8.6 ka | 1 | 0.03% | ORIGINS | no |
| Tell Ramad | 8.9–8.6 ka | 1 | 0.00% | ORIGINS | no |

# *Buglossoides arvensis*

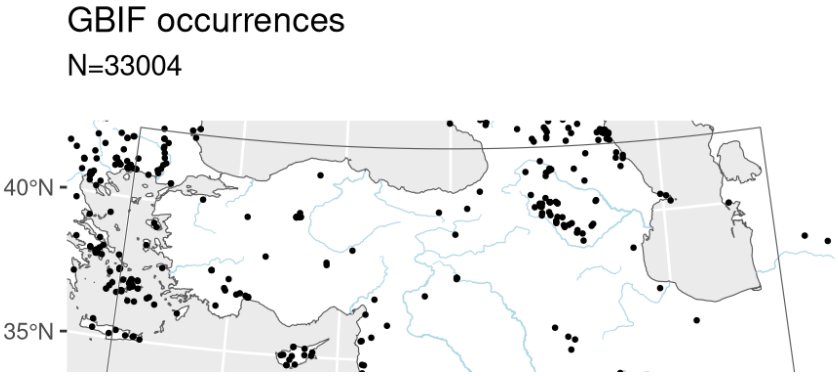


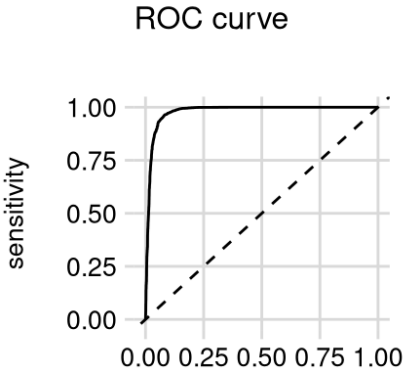

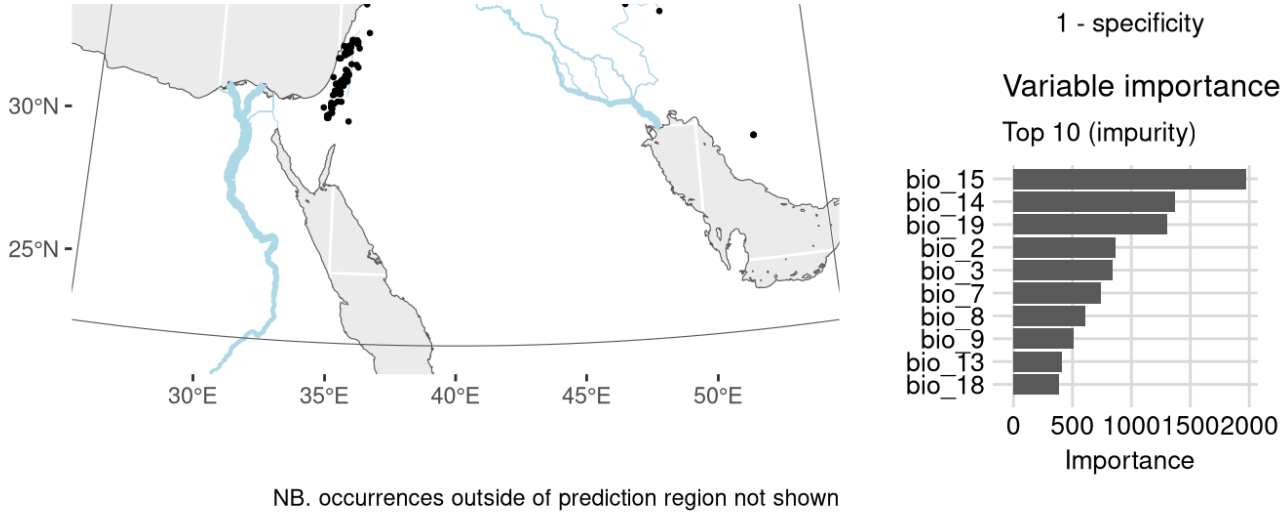


Figure 33: Fitted model summary for *Buglossoides arvensis*

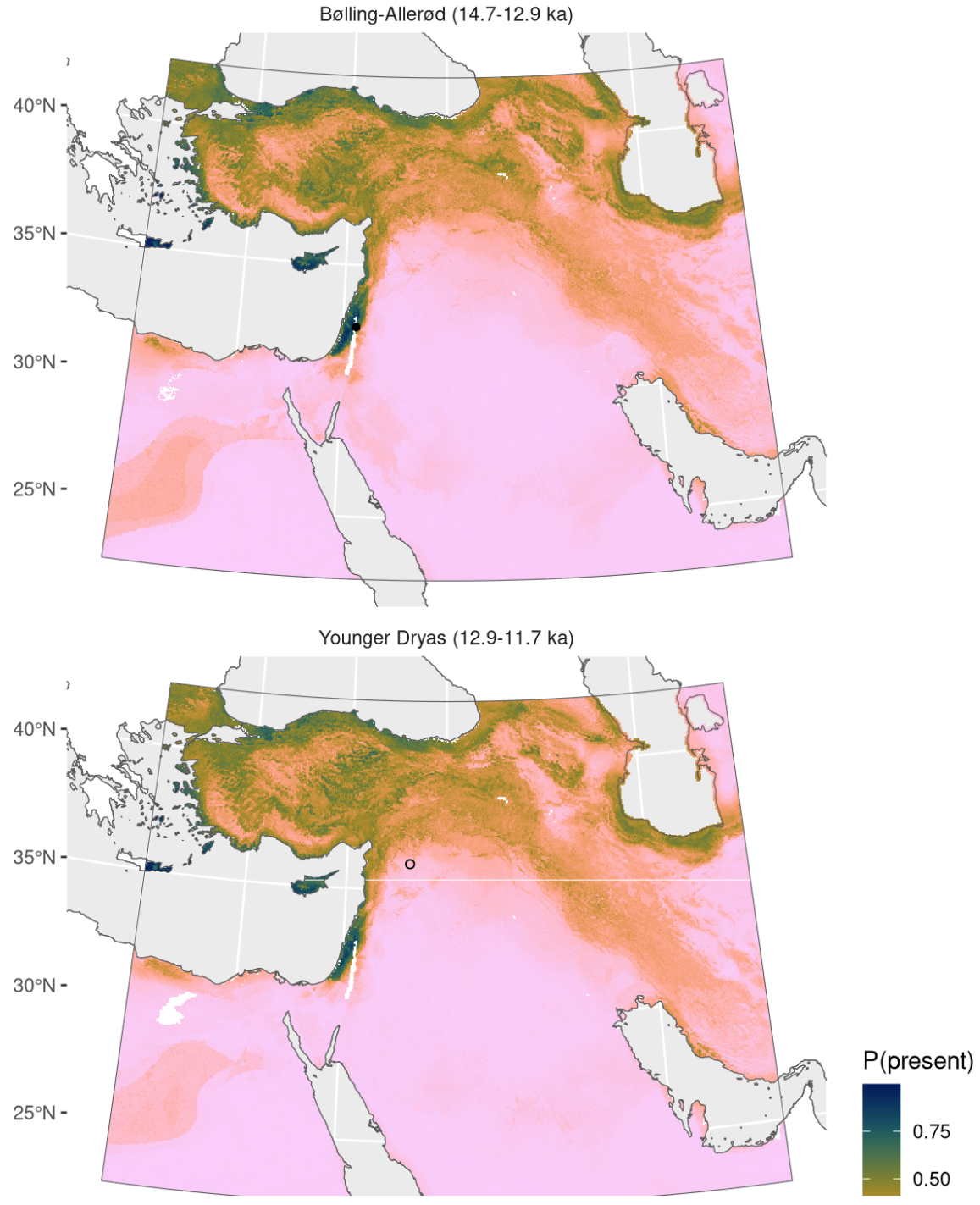

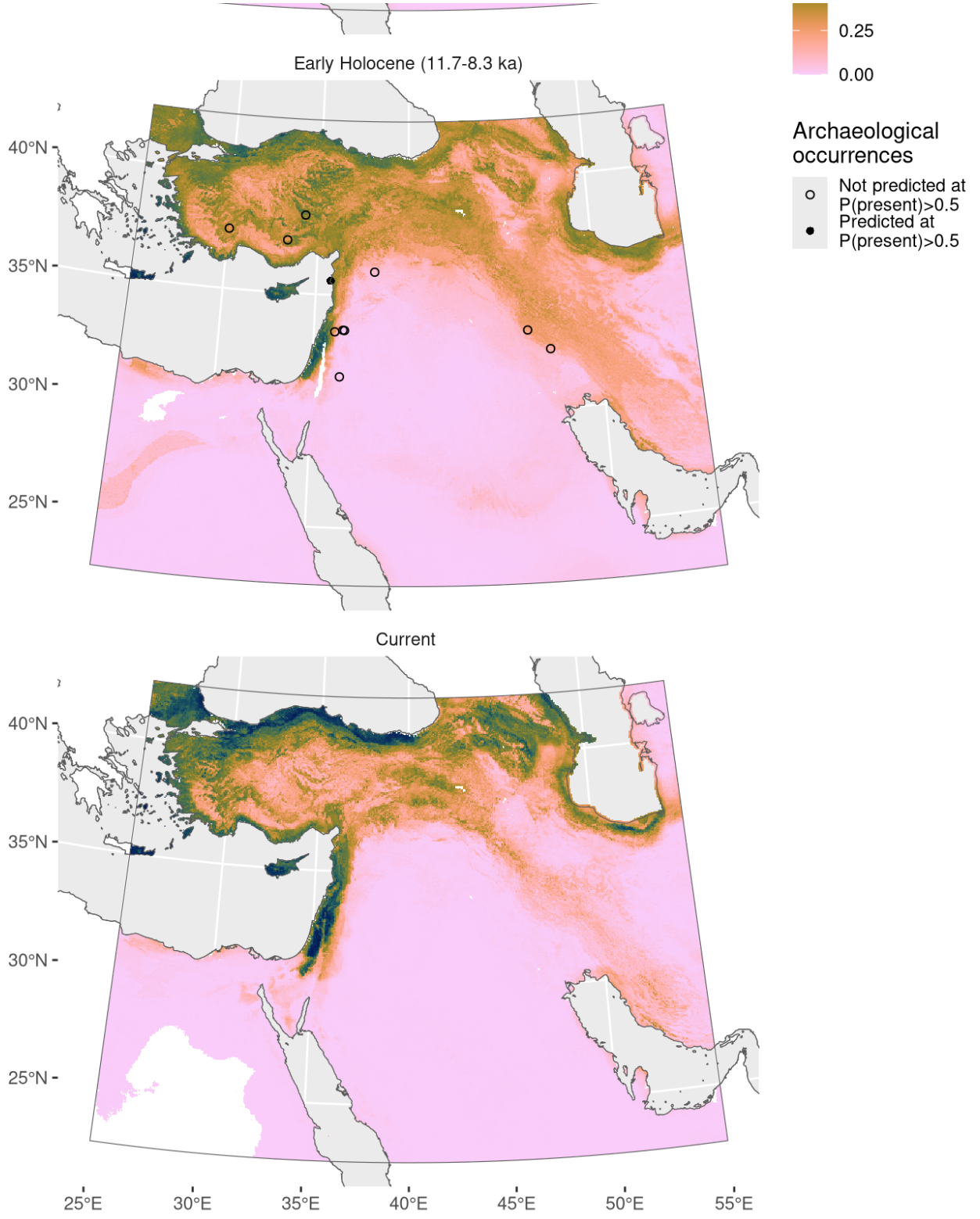


Figure 34: Predicted palaeodistributions of *Buglossoides arvensis*

Table 17: Archaeological occurrences of *Buglossoides arvensis*

Archaeological occurrences of *Buglossoides arvensis*

| Site | Age range | N assemblages | Average prop. | Source | Predicted? |
|---|---|---|---|---|---|
| Bølling-Allerød (14.7-12.9 ka) | | | | | |
| Wadi Hammeh 27 | 14.1–12.7 ka | 1 | 0.03% | ORIGINS | yes |

| | | | | | |
|---|---|---|---|---|---|
| Younger Dryas (12.9-11.7 ka) | | | | | |
| Mureybet | 12.1–11.9 ka | 1 | 0.13% | ORIGINS | no |
| Early Holocene (11.7-8.3 ka) | | | | | |
| Mureybet | 11.7–11.2 ka | 1 | 0.05% | ORIGINS | no |
| Chogha Golan | 11.2–9.6 ka | 3 | 1.07% | ORIGINS | no |
| Tell Aswad | 10.8–9.3 ka | 2 | 0.15% | ORIGINS | no |
| Wadi Jilat 7 | 10.2–9.3 ka | 1 | 0.03% | ORIGINS | no |
| Hacılar | 10.2–9.4 ka | 1 | 2.20% | ORIGINS | no |
| Tell Ghoraifé | 10.1–8.6 ka | 2 | 4.73% | ORIGINS | no |
| Ali Kosh | 10.1–8.0 ka | 3 | 0.27% | ORIGINS | no |
| Aşıklı Höyük | 9.9–9.4 ka | 1 | 19.19% | ORIGINS | no |
| Can Hasan III | 9.4–8.6 ka | 1 | 66.34% | ORIGINS | no |
| Tell Ramad | 9.3–8.6 ka | 2 | 0.21% | ORIGINS | no |
| Wadi Jilat 13 | 9.1–8.4 ka | 3 | 0.30% | ORIGINS | no |
| Ras Shamra | 8.8–8.3 ka | 1 | 0.05% | ORIGINS | yes |

## *Buglossoides tenuiflora*

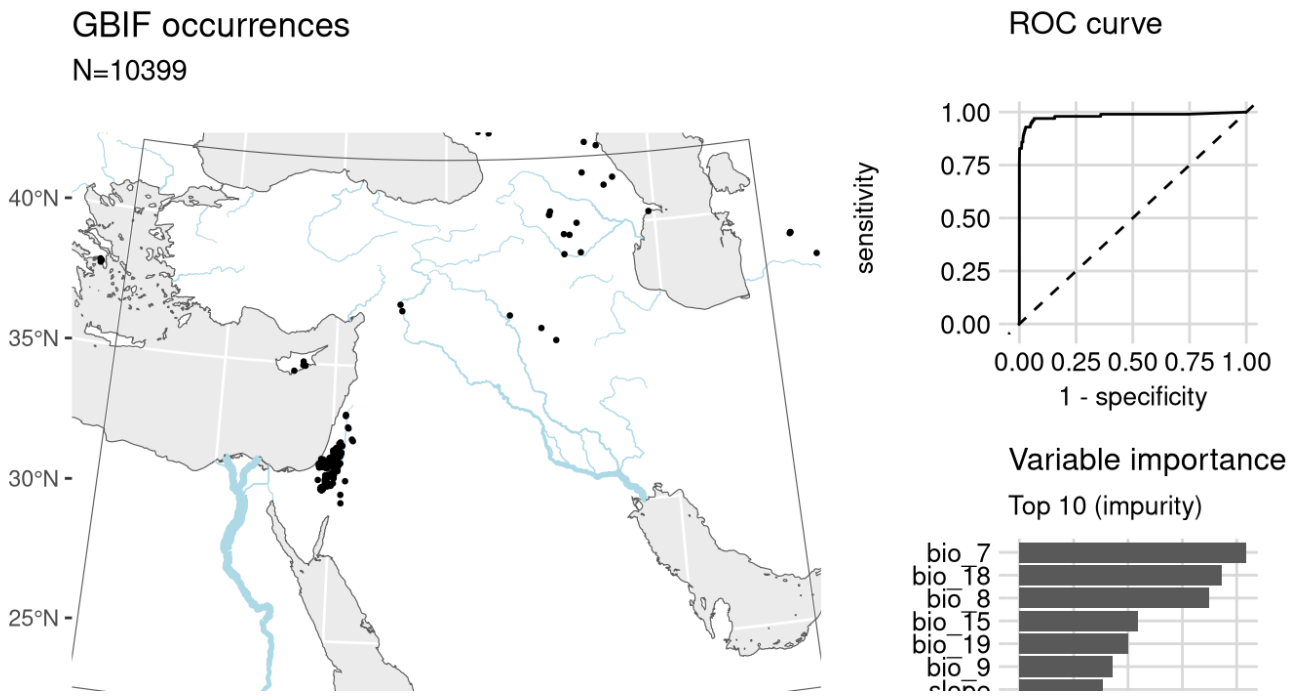

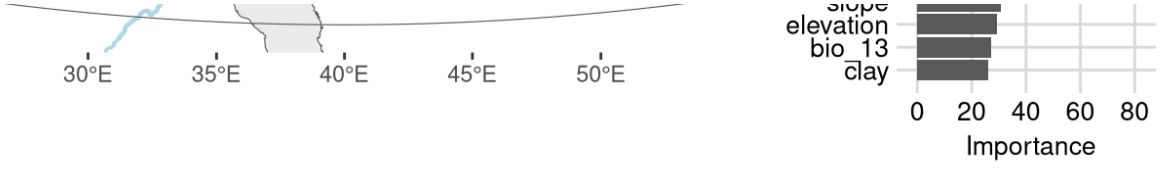


NB. occurrences outside of prediction region not shown

Figure 35: Fitted model summary for *Buglossoides tenuiflora*

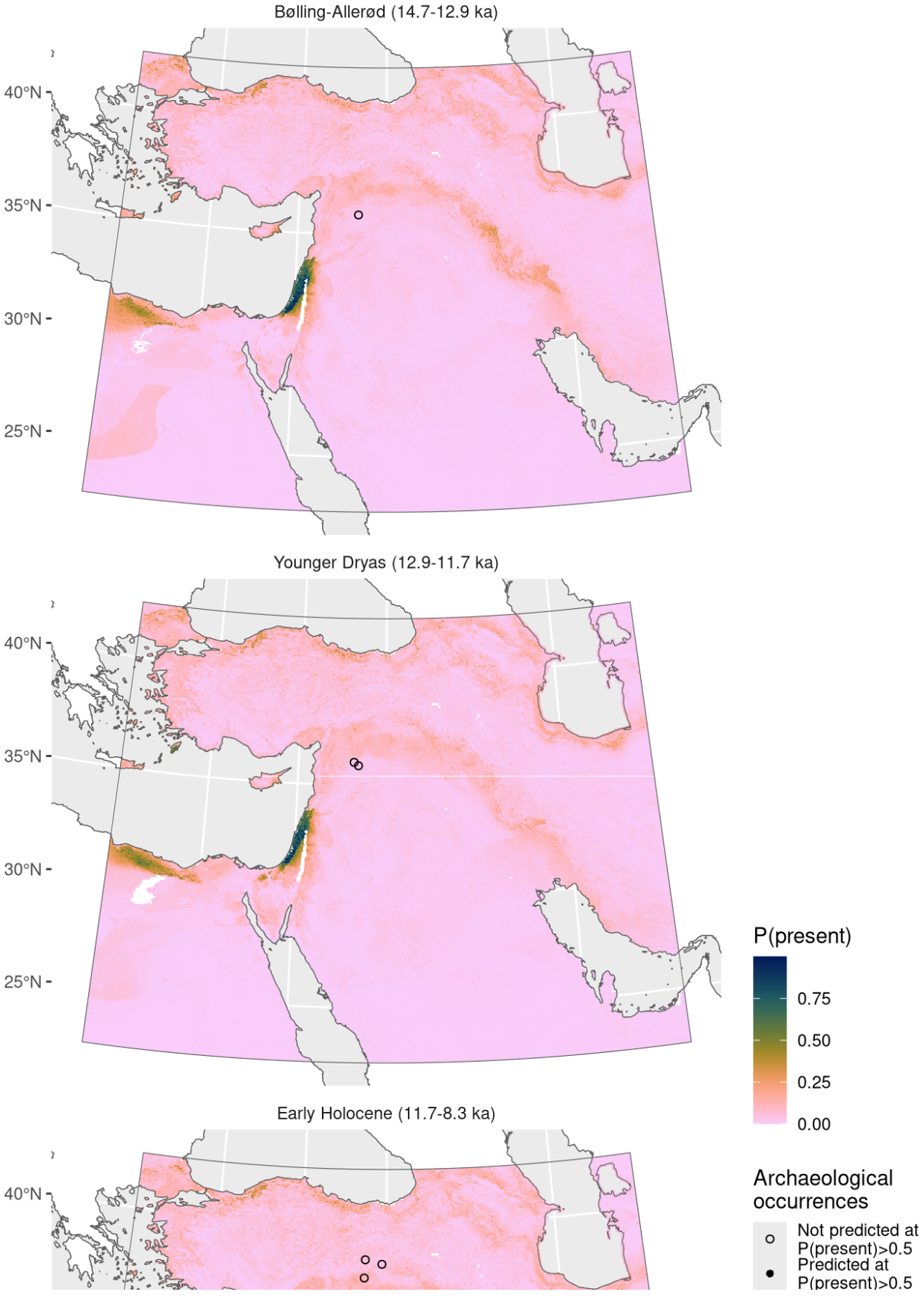

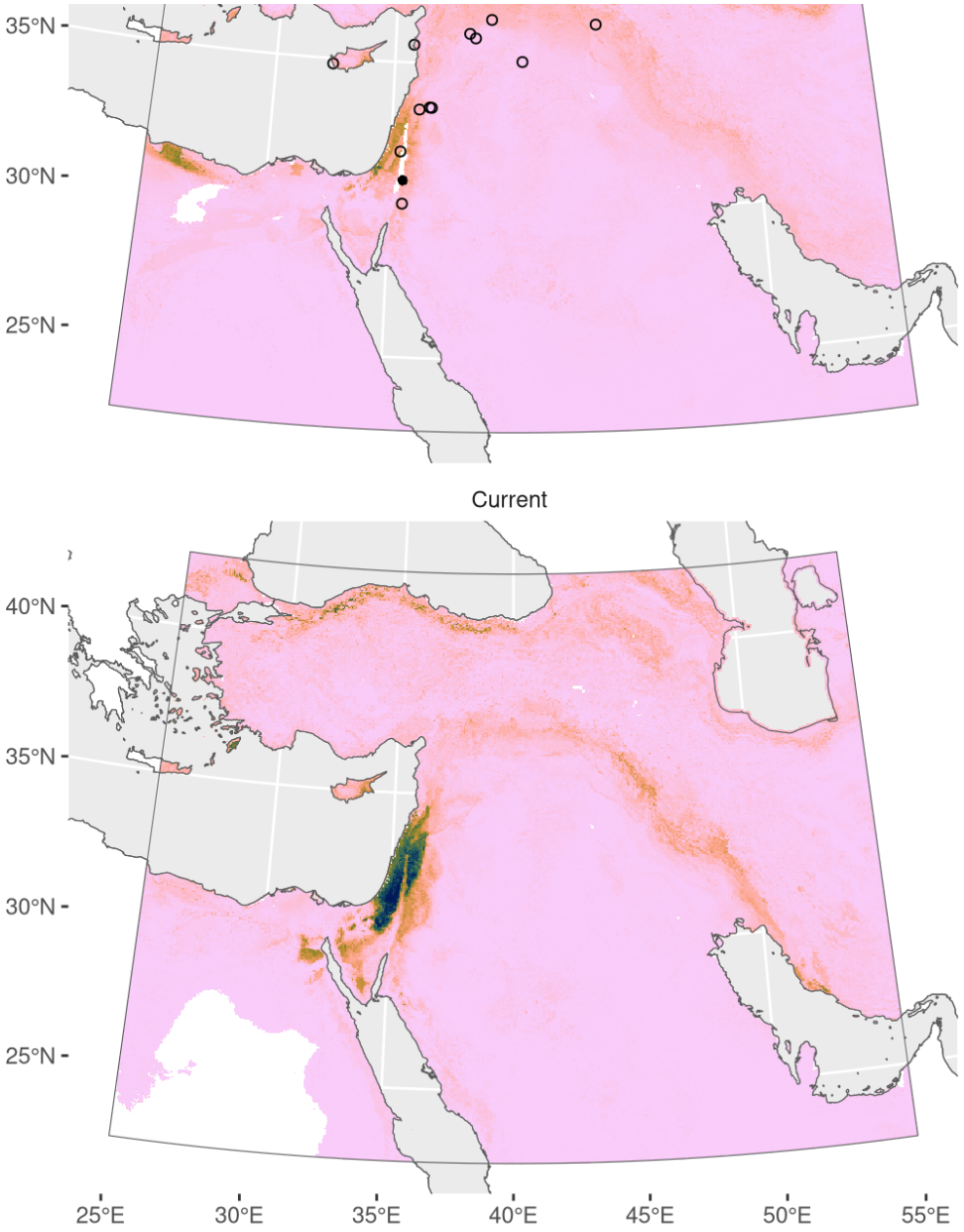


Figure 36: Predicted palaeodistributions of *Buglossoides tenuiflora*

Table 18: Archaeological occurrences of *Buglossoides tenuiflora*

Archaeological occurrences of *Buglossoides tenuiflora*

| Site | Age range | N assemblages | Average prop. | Source | Predicted? |
|---|---|---|---|---|---|
| Bølling-Allerød (14.7-12.9 ka) | | | | | |
| Abu Hureyra | 13.1–13.0 ka | 1 | 0.95% | ORIGINS | no |
| Younger Dryas (12.9-11.7 ka) | | | | | |
| Abu Hureyra | 13.0–11.8 ka | 2 | 1.74% | ORIGINS | no |
| Mureybet | 12.1–11.9 ka | 1 | 9.50% | ORIGINS | no |
| Early Holocene (11.7-8.3 ka) | | | | | |

| | | | | | |
|---|---|---|---|---|---|
| Mureybet | 11.7–10.8 ka | 2 | 10.47% | ORIGINS | no |
| Netiv Hagdud | 11.6–10.6 ka | 1 | 0.15% | ORIGINS | no |
| M'lefaat | 11.3–11.1 ka | 1 | 0.63% | ORIGINS | no |
| Tell Aswad | 11.2–9.3 ka | 3 | 0.23% | ORIGINS | no |
| El-Hemmeh | 11.1–10.5 ka | 1 | 1.01% | ORIGINS | yes |
| Cafer Höyük | 10.6–9.7 ka | 1 | 0.58% | ORIGINS | no |
| Mylouthkia | 10.6–10.2 ka | 1 | 0.21% | ORIGINS | no |
| Nevalı Çori | 10.4–10.2 ka | 1 | 0.35% | ORIGINS | no |
| Tell Ghoraifé | 10.1–8.6 ka | 2 | 2.01% | ORIGINS | no |
| Basta | 9.6–8.8 ka | 2 | 22.13% | ORIGINS | no |
| Sabi Abyad II | 9.5–8.8 ka | 1 | 0.07% | ORIGINS | no |
| Abu Hureyra | 9.3–8.2 ka | 1 | 4.48% | ORIGINS | no |
| Tell Ramad | 9.3–8.6 ka | 2 | 0.68% | ORIGINS | no |
| Çayönü | 9.2–8.9 ka | 1 | 0.05% | ORIGINS | no |
| Bouqras | 9.2–8.6 ka | 1 | 2.24% | ORIGINS | no |
| Ras Shamra | 8.8–8.3 ka | 1 | 0.05% | ORIGINS | no |

## *Capparis spinosa*

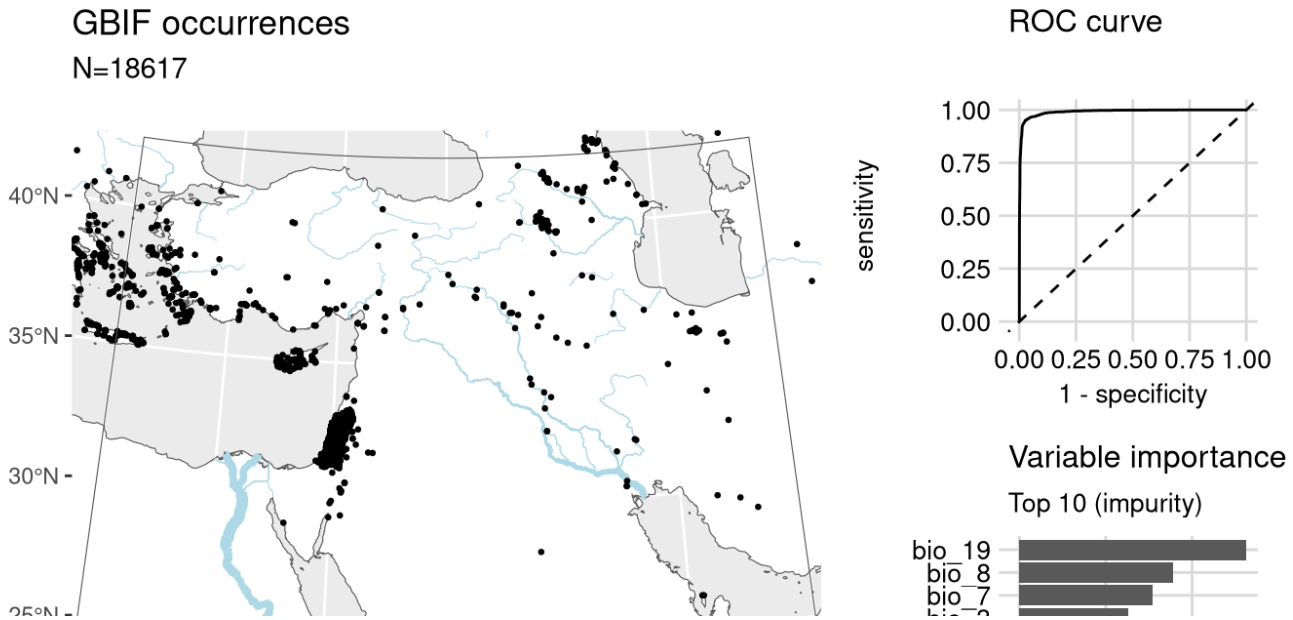

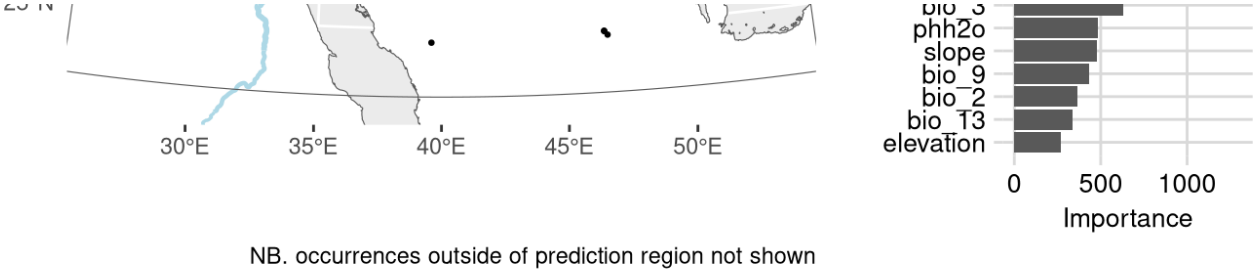


NB. occurrences outside of prediction region not shown

Figure 37: Fitted model summary for *Capparis spinosa*

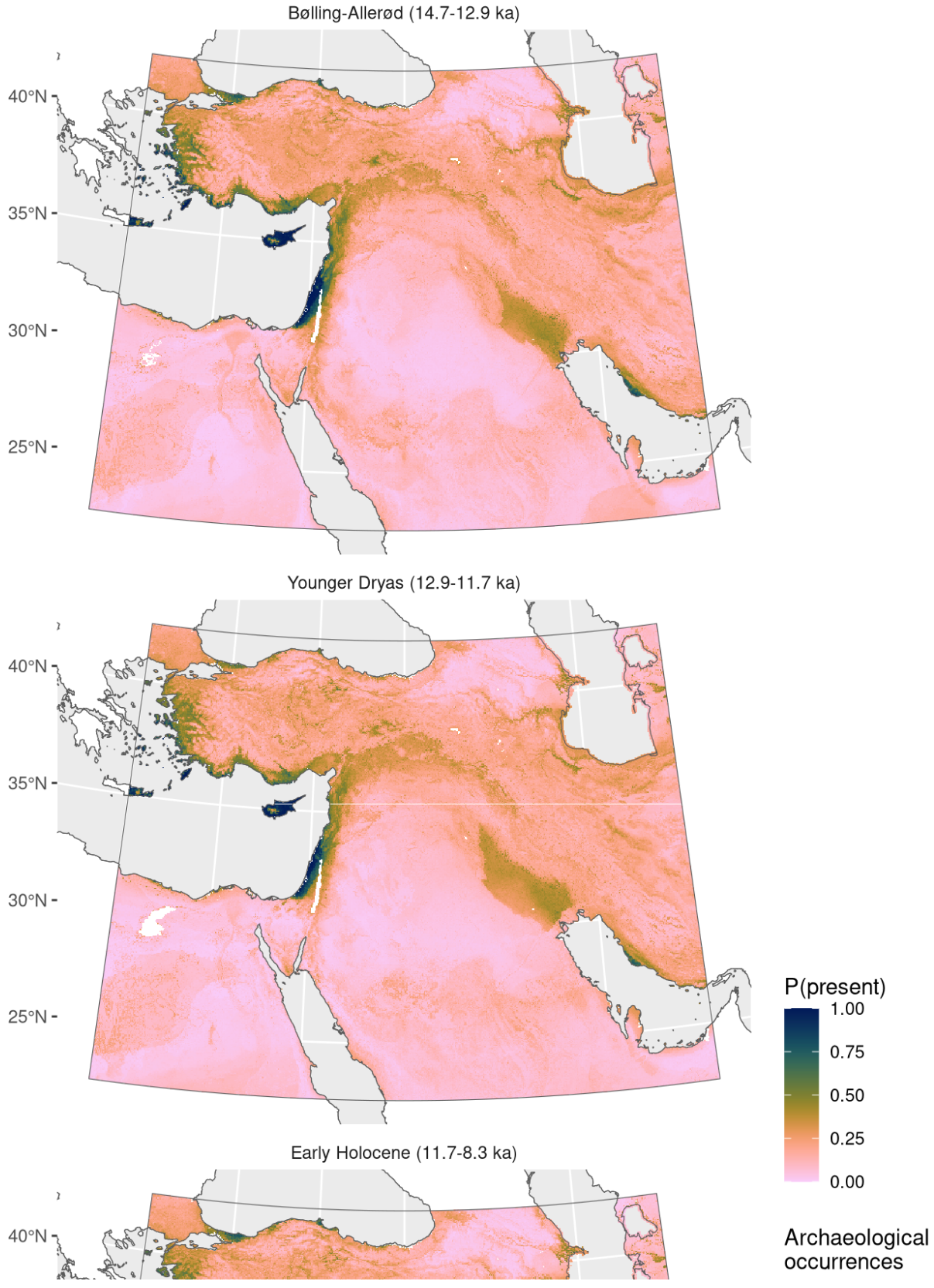

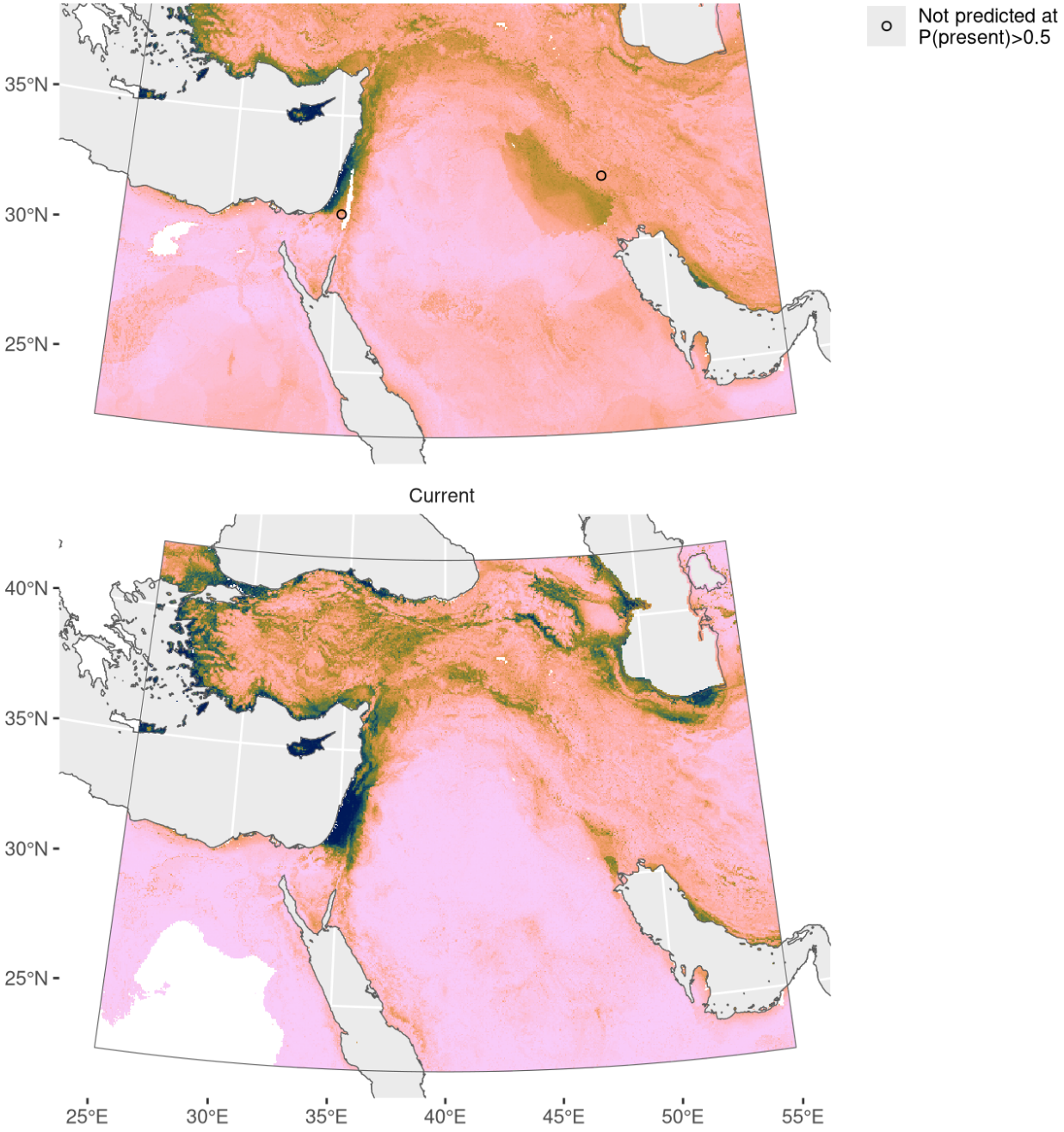


Figure 38: Predicted palaeodistributions of *Capparis spinosa*

Table 19: Archaeological occurrences of *Capparis spinosa*

Archaeological occurrences of *Capparis spinosa*

| Site | Age range | N assemblages | Average prop. | Source | Predicted? |
|---|---|---|---|---|---|
| Early Holocene (11.7-8.3 ka) | | | | | |
| Nahal Hemar | 10.1–9.3 ka | 1 | 0.09% | ORIGINS | no |
| Ali Kosh | 10.1–8.0 ka | 3 | 0.10% | ORIGINS | no |

## *Carex divisa*

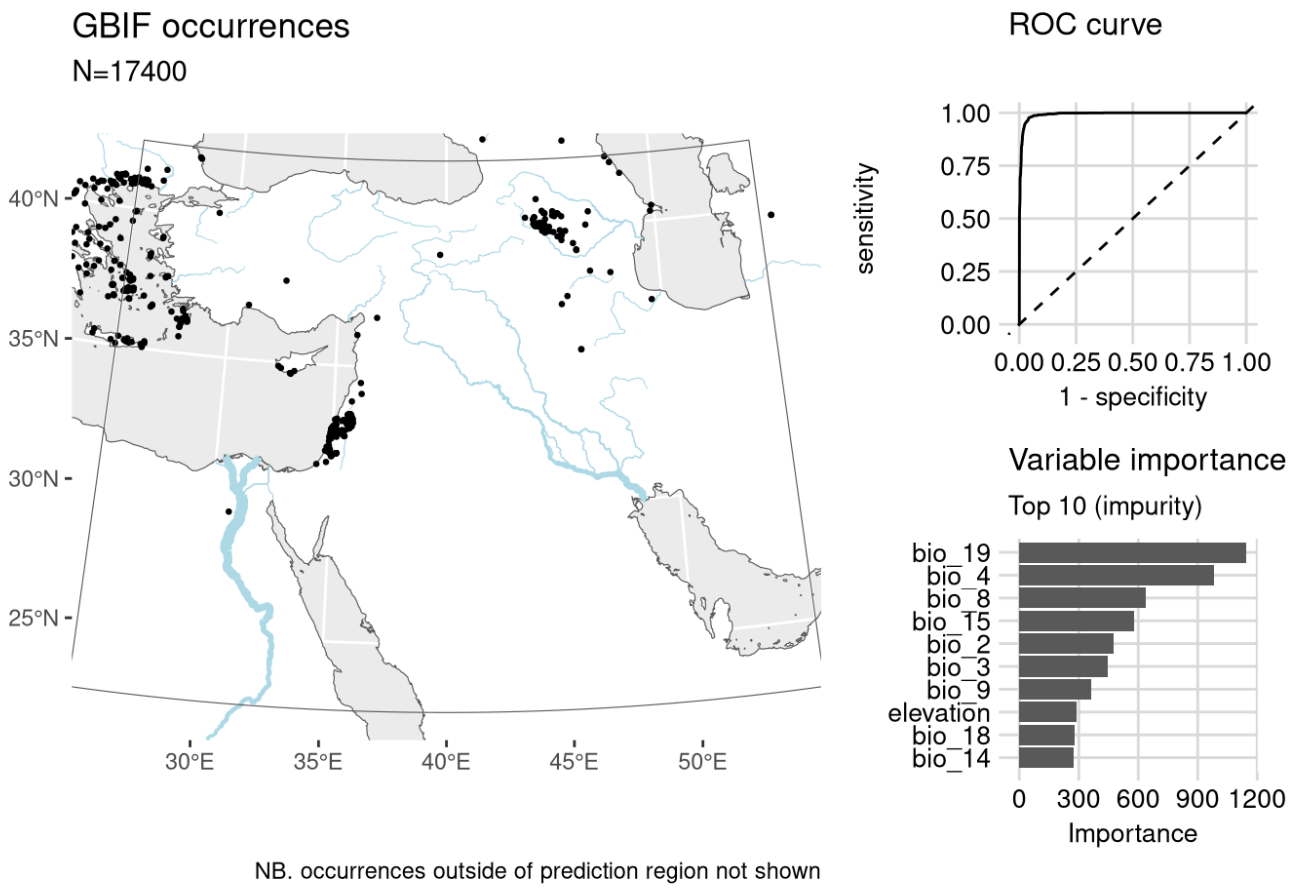


Figure 39: Fitted model summary for *Carex divisa*

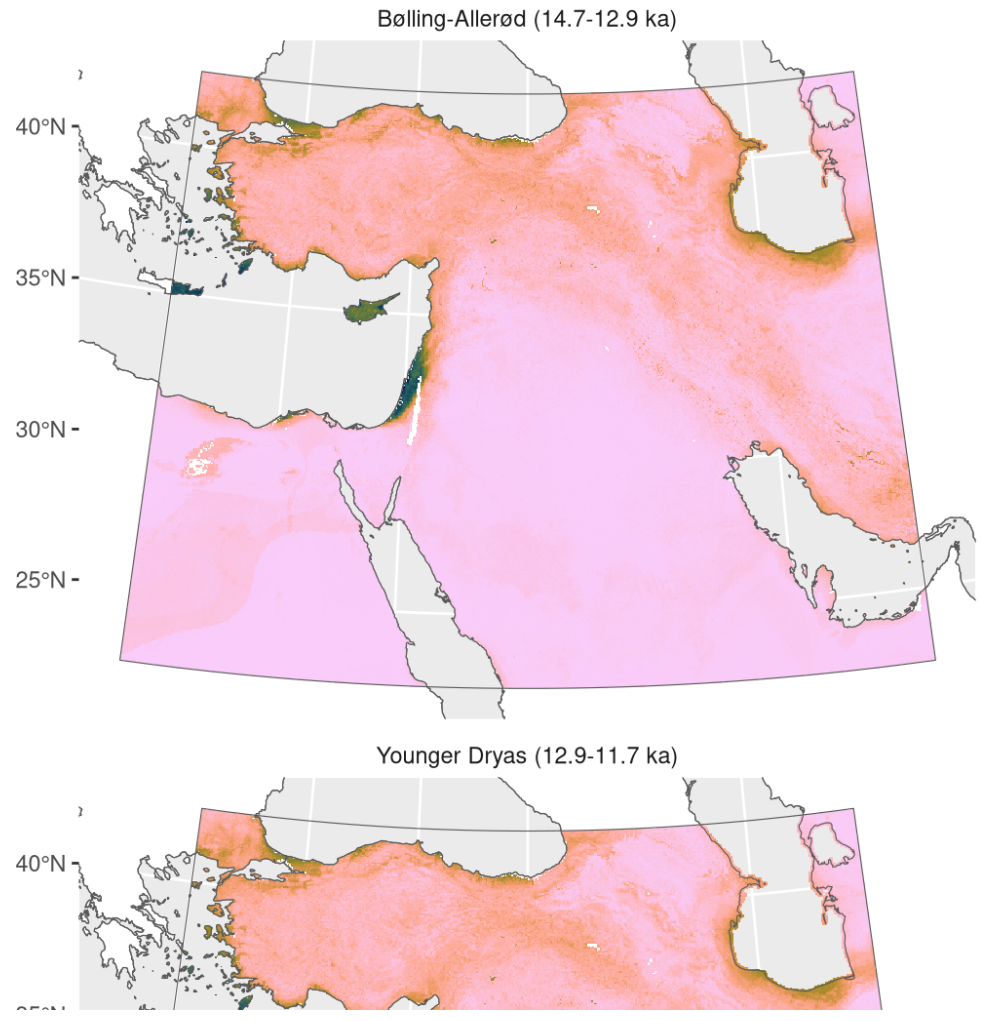

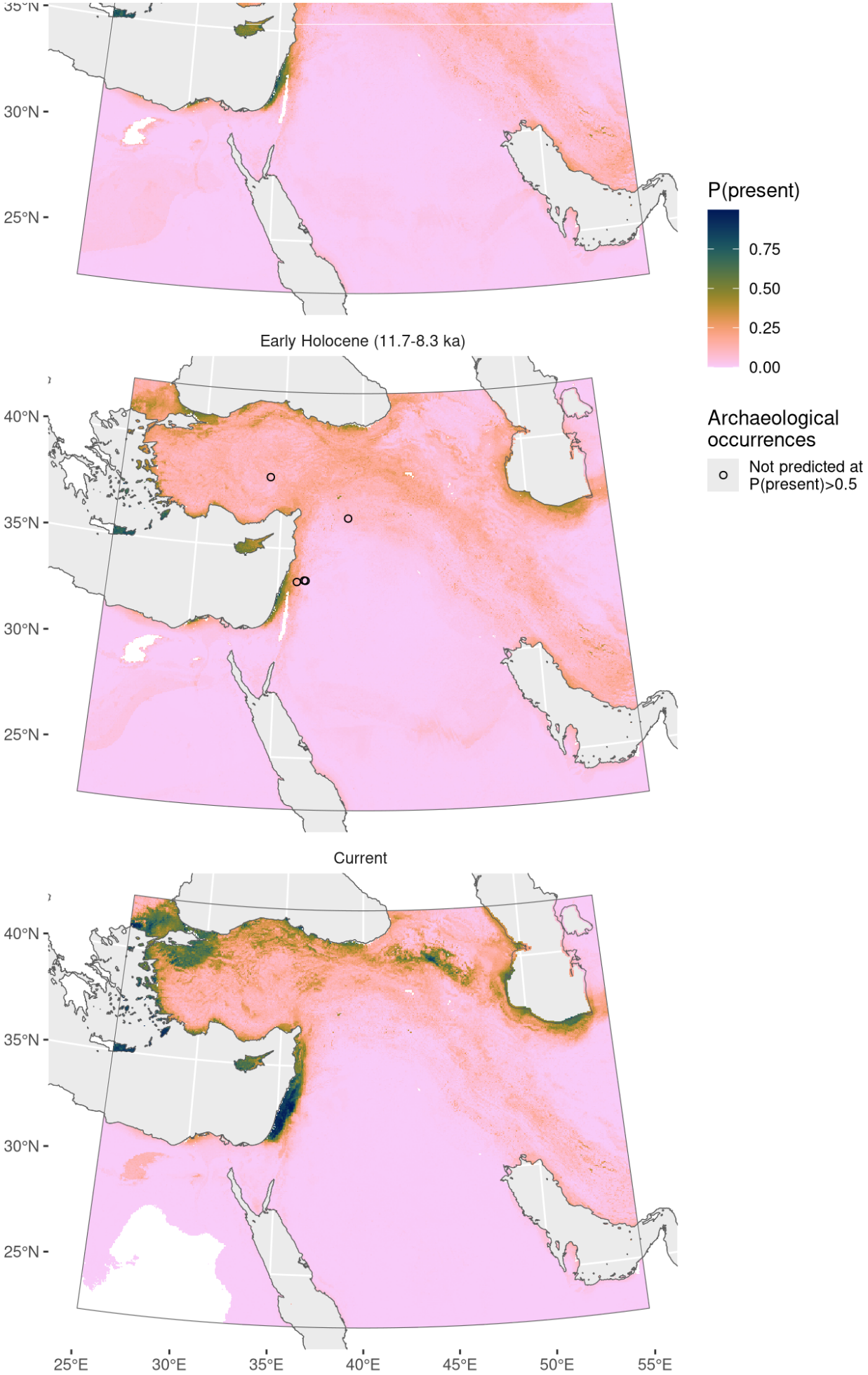


Figure 40: Predicted palaeodistributions of *Carex divisa*

Table 20: Archaeological occurrences of *Carex divisa*

Archaeological occurrences of *Carex divisa*

| Site | Age range | N assemblages | Average prop. | Source | Predicted? |
|---|---|---|---|---|---|
| Early Holocene (11.7-8.3 ka) | | | | | |
| Tell Aswad | 11.2–9.3 ka | 3 | 3.33% | ORIGINS | no |
| Tell Ghoraifé | 10.1–8.6 ka | 2 | 4.96% | ORIGINS | no |
| Aşıklı Höyük | 9.9–9.4 ka | 1 | 0.03% | ORIGINS | no |
| Sabi Abyad II | 9.5–8.8 ka | 1 | 1.62% | ORIGINS | no |
| Tell Ramad | 9.3–8.6 ka | 2 | 0.01% | ORIGINS | no |

# *Chenopodium album*

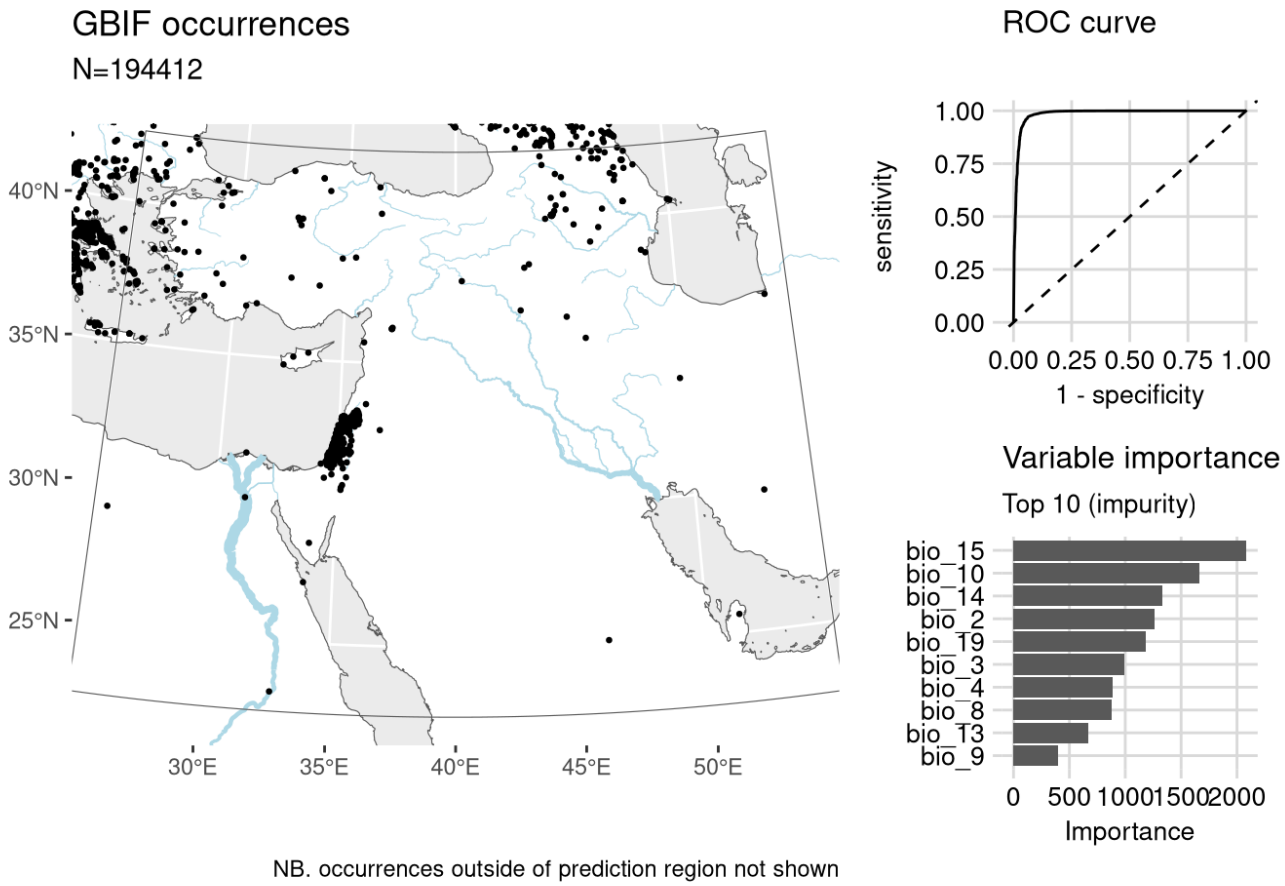


Figure 41: Fitted model summary for *Chenopodium album*

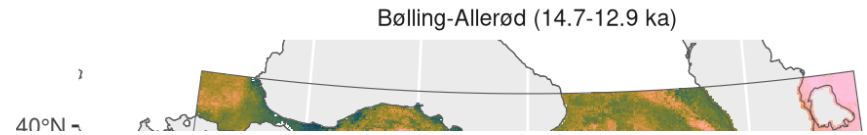

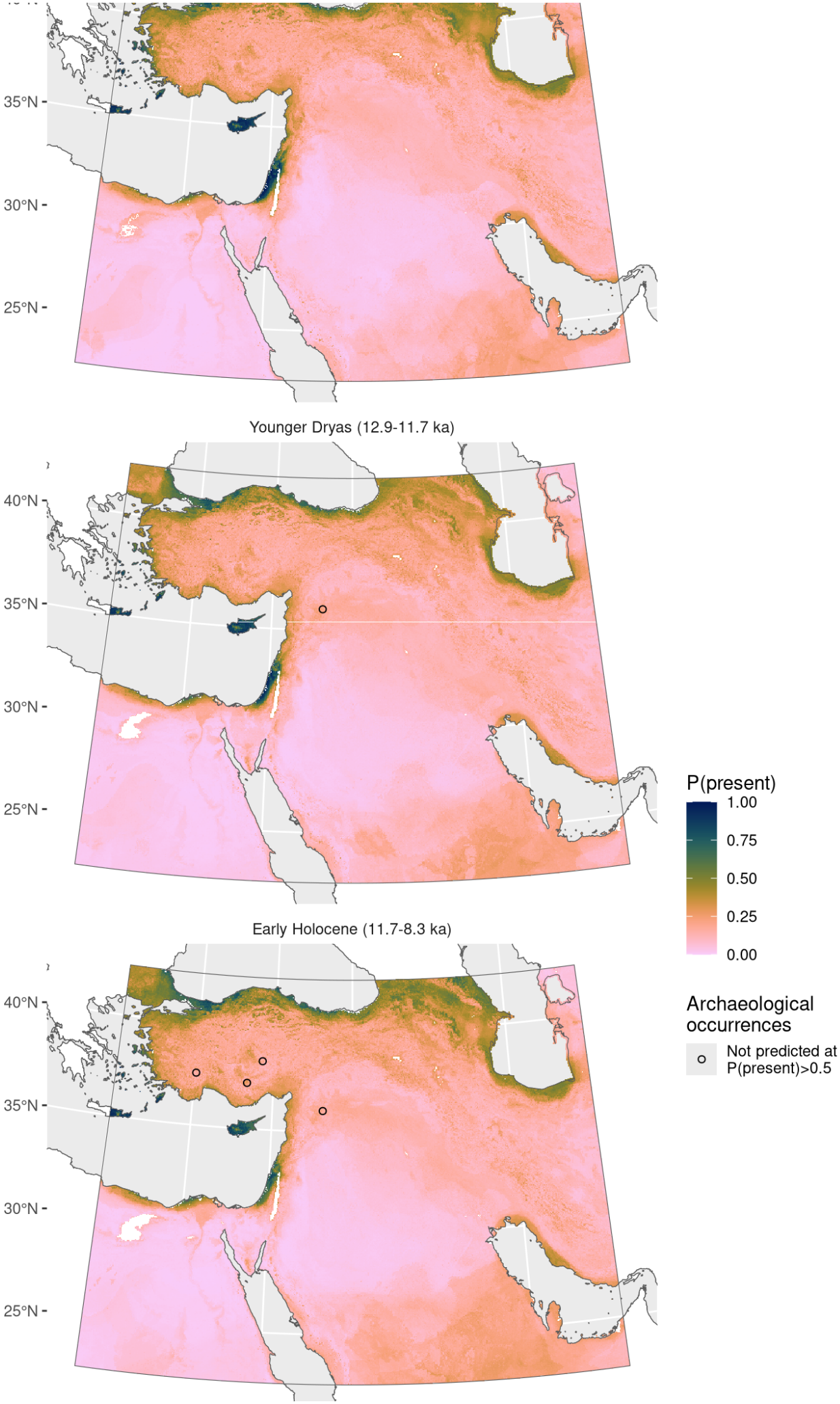
35°N
30°N
25°N
Younger Dryas (12.9-11.7 ka)
40°N
35°N
30°N
25°N
Early Holocene (11.7-8.3 ka)
40°N
35°N
30°N
25°N
P(present)
1.00
0.75
0.50
0.25
0.00
Archaeological occurrences
Not predicted at P(present)>0.5

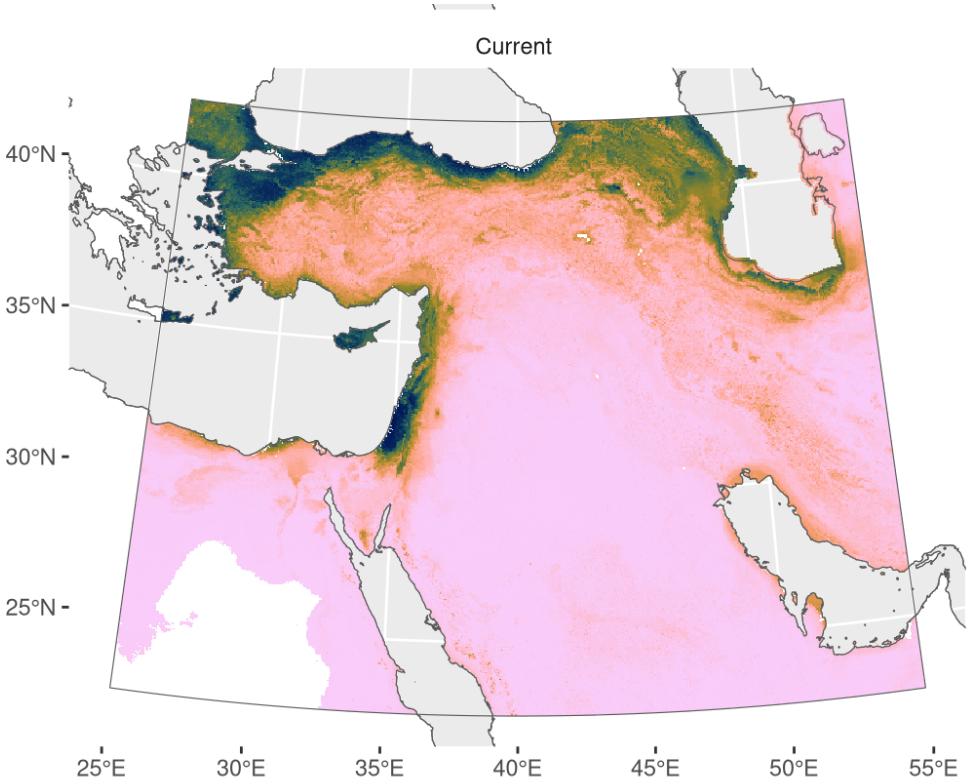


Figure 42: Predicted palaeodistributions of *Chenopodium album*

Table 21: Archaeological occurrences of *Chenopodium album*

Archaeological occurrences of *Chenopodium album*

| Site | Age range | N assemblages | Average prop. | Source | Predicted? |
|---|---|---|---|---|---|
| Younger Dryas (12.9-11.7 ka) | | | | | |
| Mureybet | 12.1–11.9 ka | 1 | 1.01% | ORIGINS | no |
| Early Holocene (11.7-8.3 ka) | | | | | |
| Mureybet | 11.7–11.2 ka | 1 | 0.05% | ORIGINS | no |
| Hacılar | 10.2–9.4 ka | 1 | 1.10% | ORIGINS | no |
| Aşıklı Höyük | 9.9–9.4 ka | 1 | 0.09% | ORIGINS | no |
| Can Hasan III | 9.4–8.6 ka | 1 | 0.02% | ORIGINS | no |

# *Cicer reticulatum*

Including Cicer arietinum.

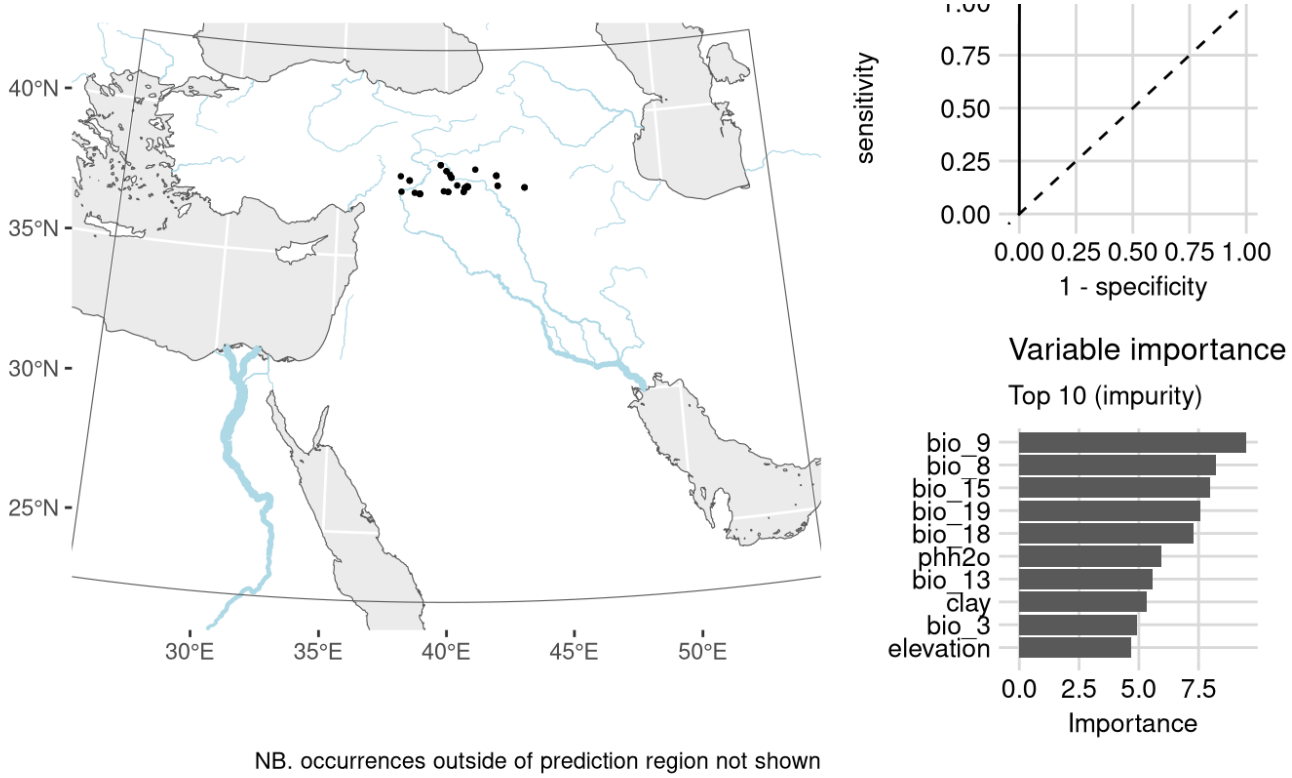


Figure 43: Fitted model summary for *Cicer reticulatum*

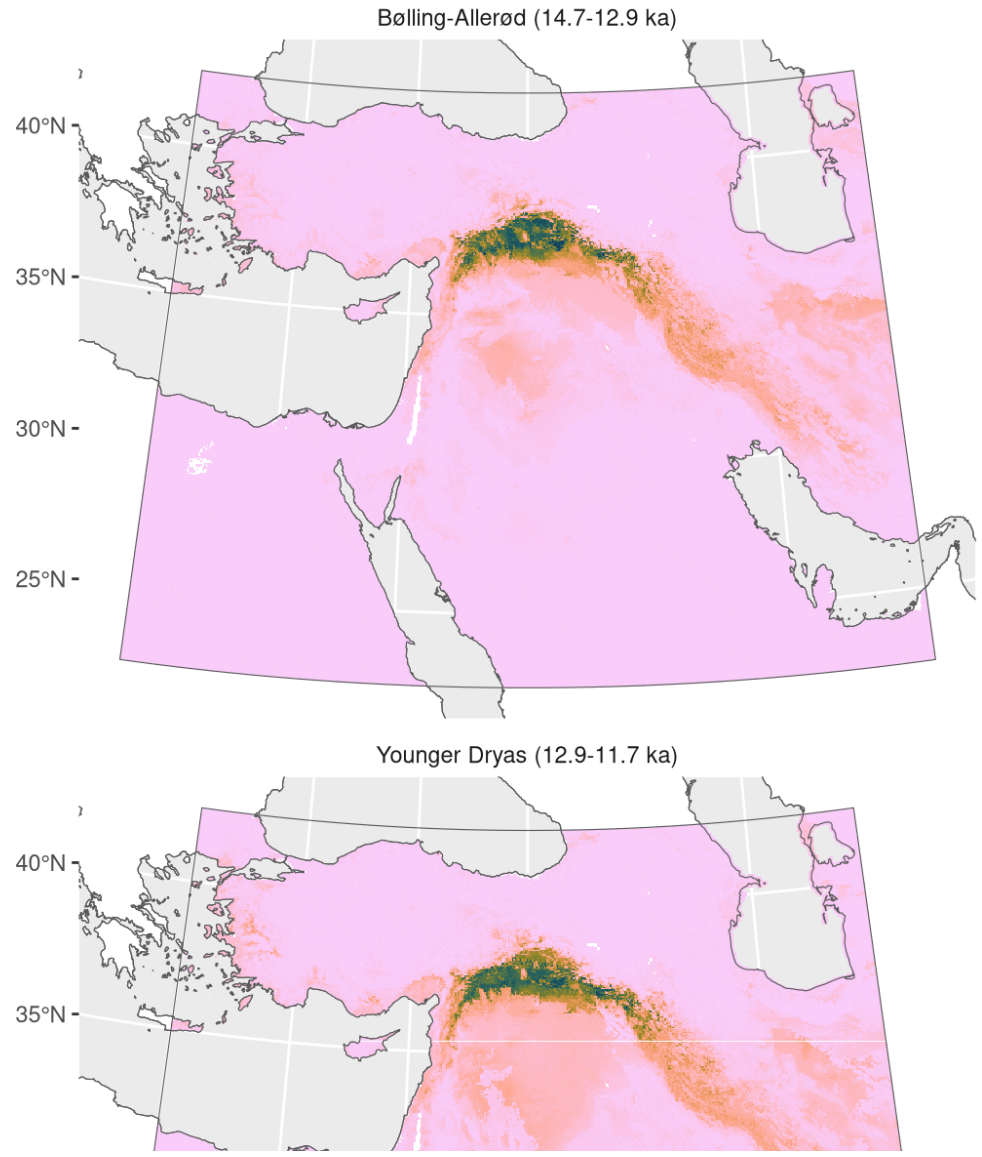

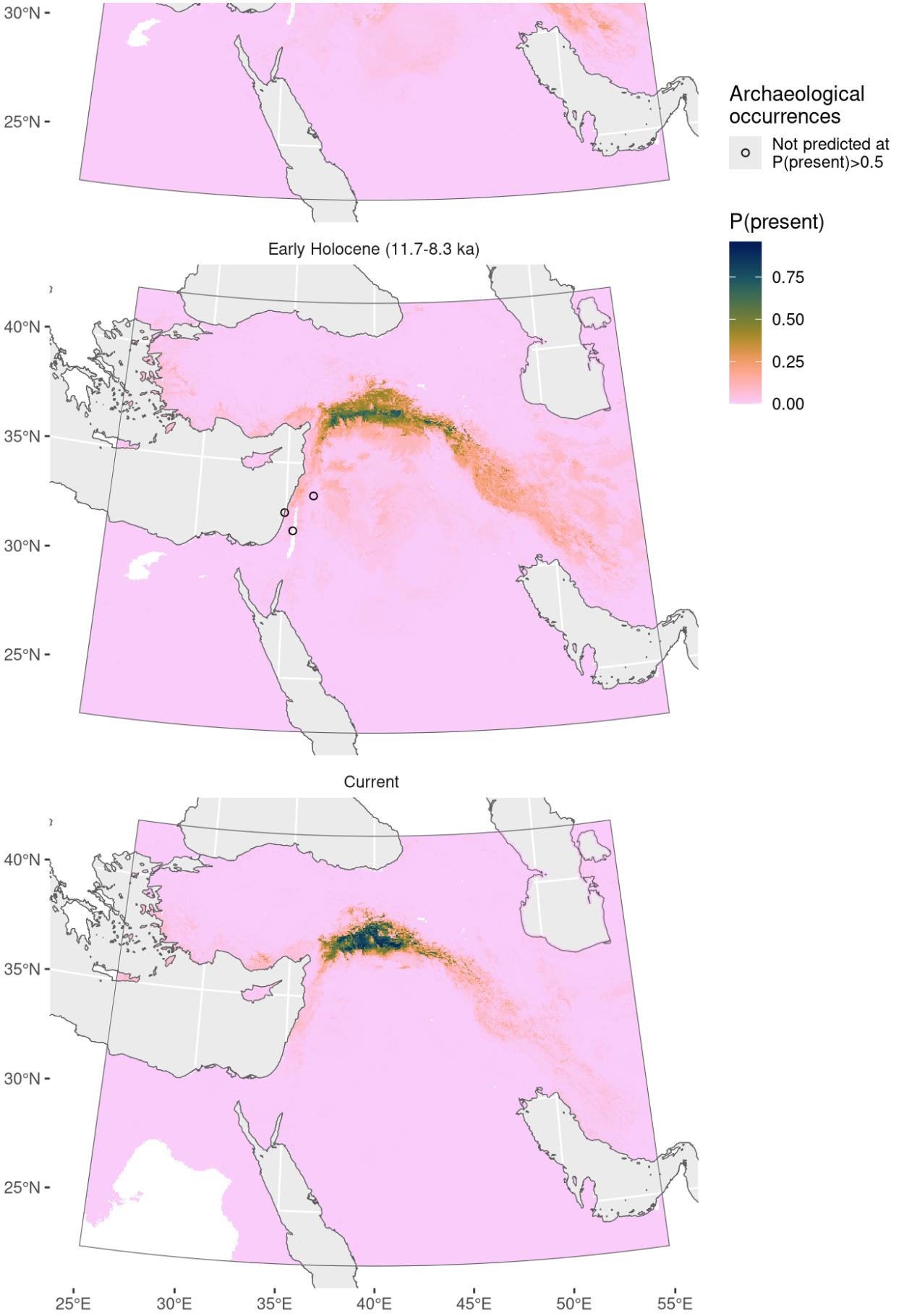


Figure 44: Predicted palaeodistributions of *Cicer reticulatum*

Table 22: Archaeological occurrences of *Cicer reticulatum*

Archaeological occurrences of *Cicer reticulatum*

| Site | Age range | N assemblages | Average prop. | Source | Predicted? |
|---|---|---|---|---|---|
| Early Holocene (11.7-8.3 ka) | | | | | |
| Tell Ghoraifé | 10.1–9.0 ka | 1 | 0.99% | ORIGINS | no |
| Atlit-Yam | 9.0–8.0 ka | 1 | 0.04% | ORIGINS | no |
| Tell es-Sultan | 8.9–8.2 ka | 1 | 0.03% | ORIGINS | no |

# *Citrullus colocynthis*

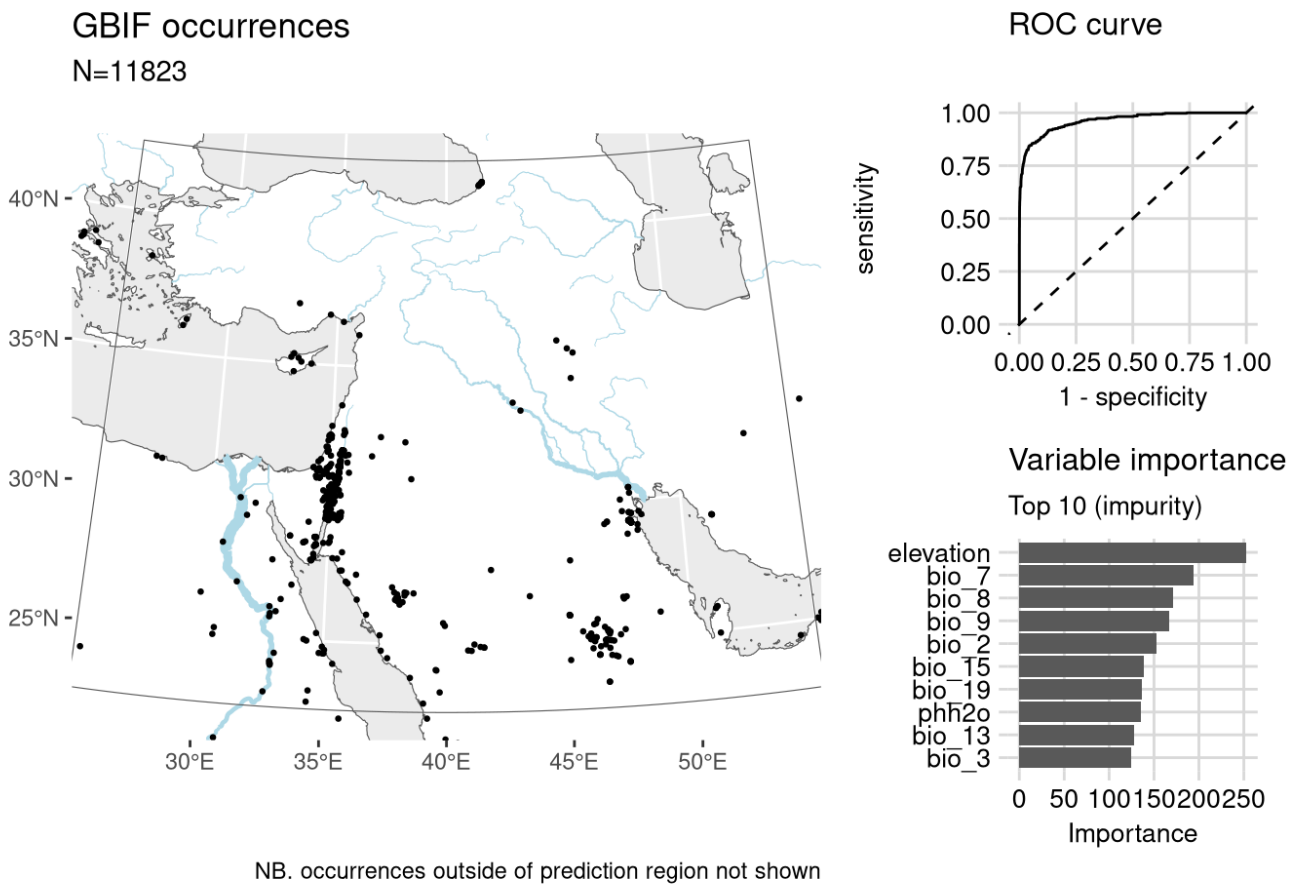


Figure 45: Fitted model summary for *Citrullus colocynthis*

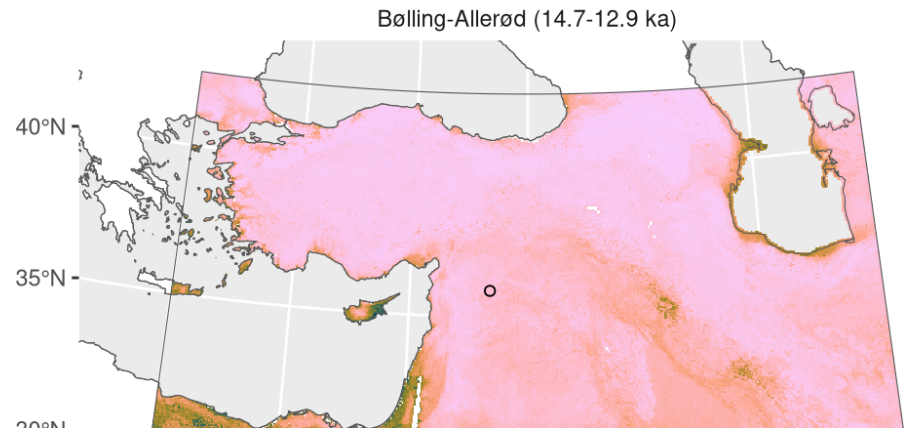

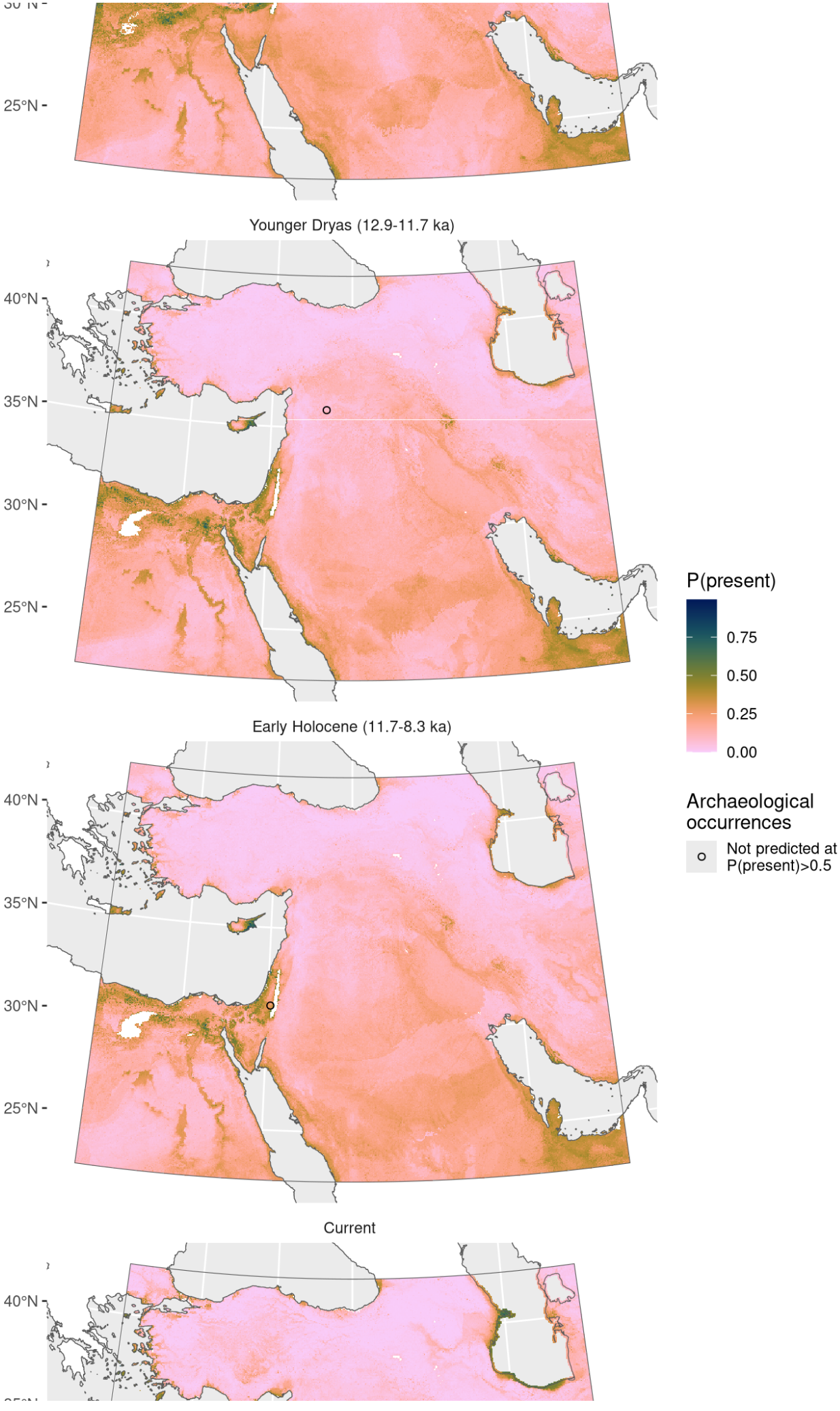
30°N
25°N
Younger Dryas (12.9-11.7 ka)
40°N
35°N
30°N
25°N
Early Holocene (11.7-8.3 ka)
40°N
35°N
30°N
25°N
Current
40°N
P(present)
0.75
0.50
0.25
0.00
Archaeological occurrences
Not predicted at P(present)>0.5

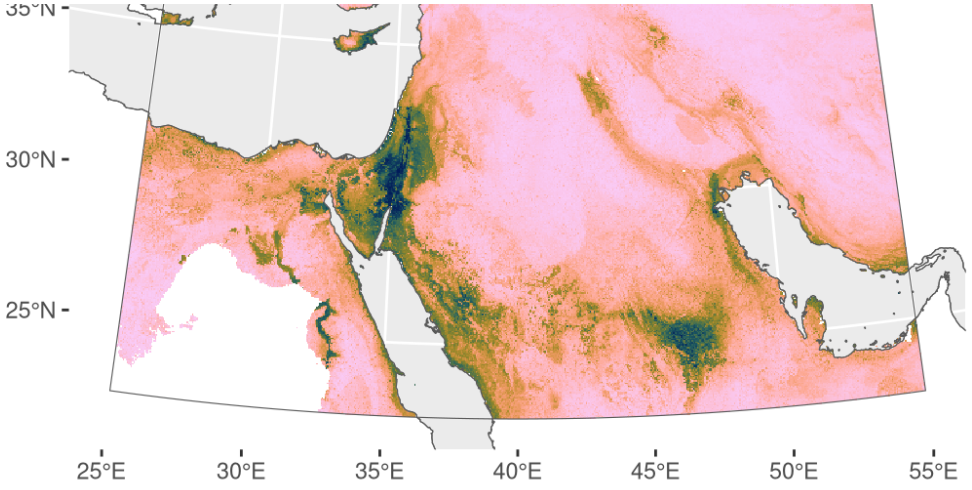


Figure 46: Predicted palaeodistributions of *Citrullus colocynthis*

Table 23: Archaeological occurrences of *Citrullus colocynthis*

Archaeological occurrences of *Citrullus colocynthis*

| Site | Age range | N assemblages | Average prop. | Source | Predicted? |
|---|---|---|---|---|---|
| Bølling-Allerød (14.7-12.9 ka) | | | | | |
| Abu Hureyra | 13.1–13.0 ka | 1 | 0.10% | ORIGINS | no |
| Younger Dryas (12.9-11.7 ka) | | | | | |
| Abu Hureyra | 13.0–11.8 ka | 2 | 0.13% | ORIGINS | no |
| Early Holocene (11.7-8.3 ka) | | | | | |
| Nahal Hemar | 10.1–9.3 ka | 1 | 1.96% | ORIGINS | no |

# *Crithopsis delileana*

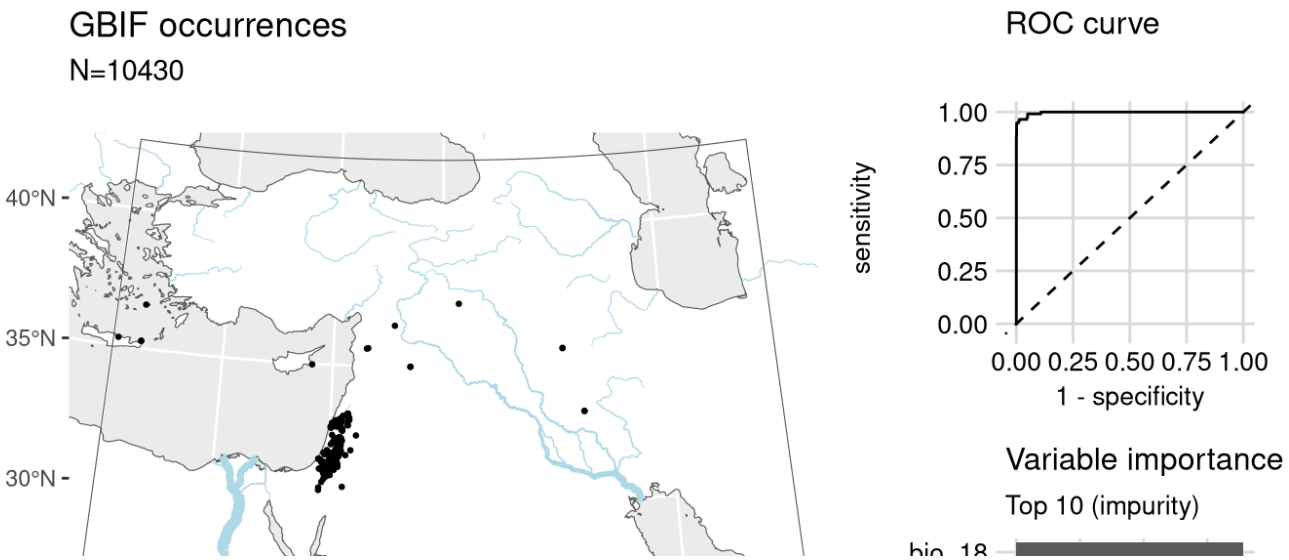

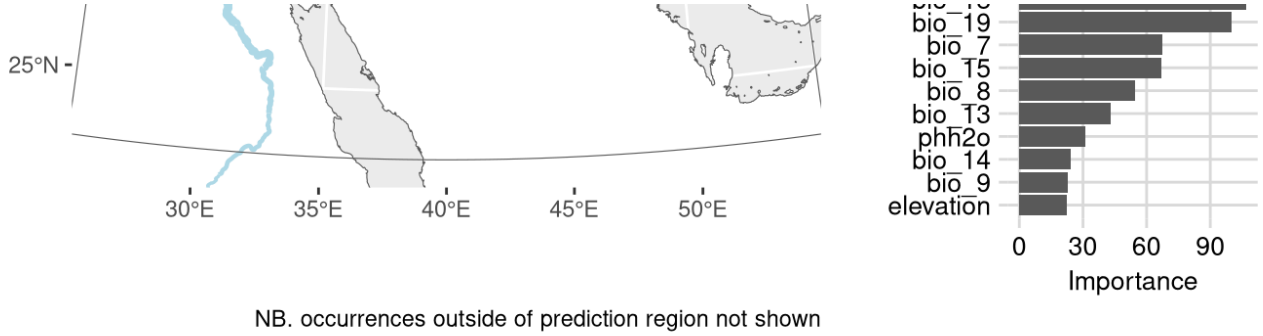


NB. occurrences outside of prediction region not shown

Figure 47: Fitted model summary for *Crithopsis delileana*

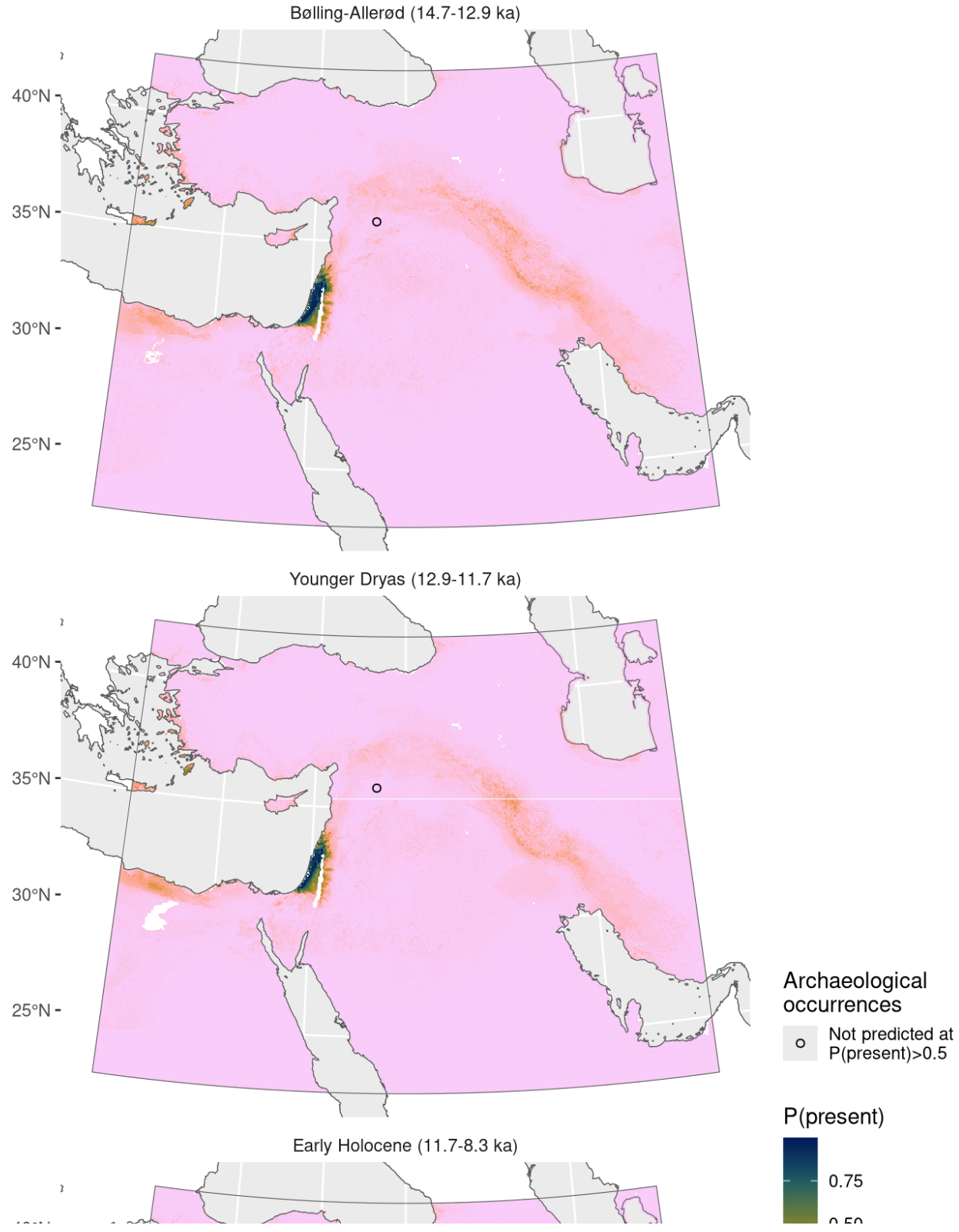

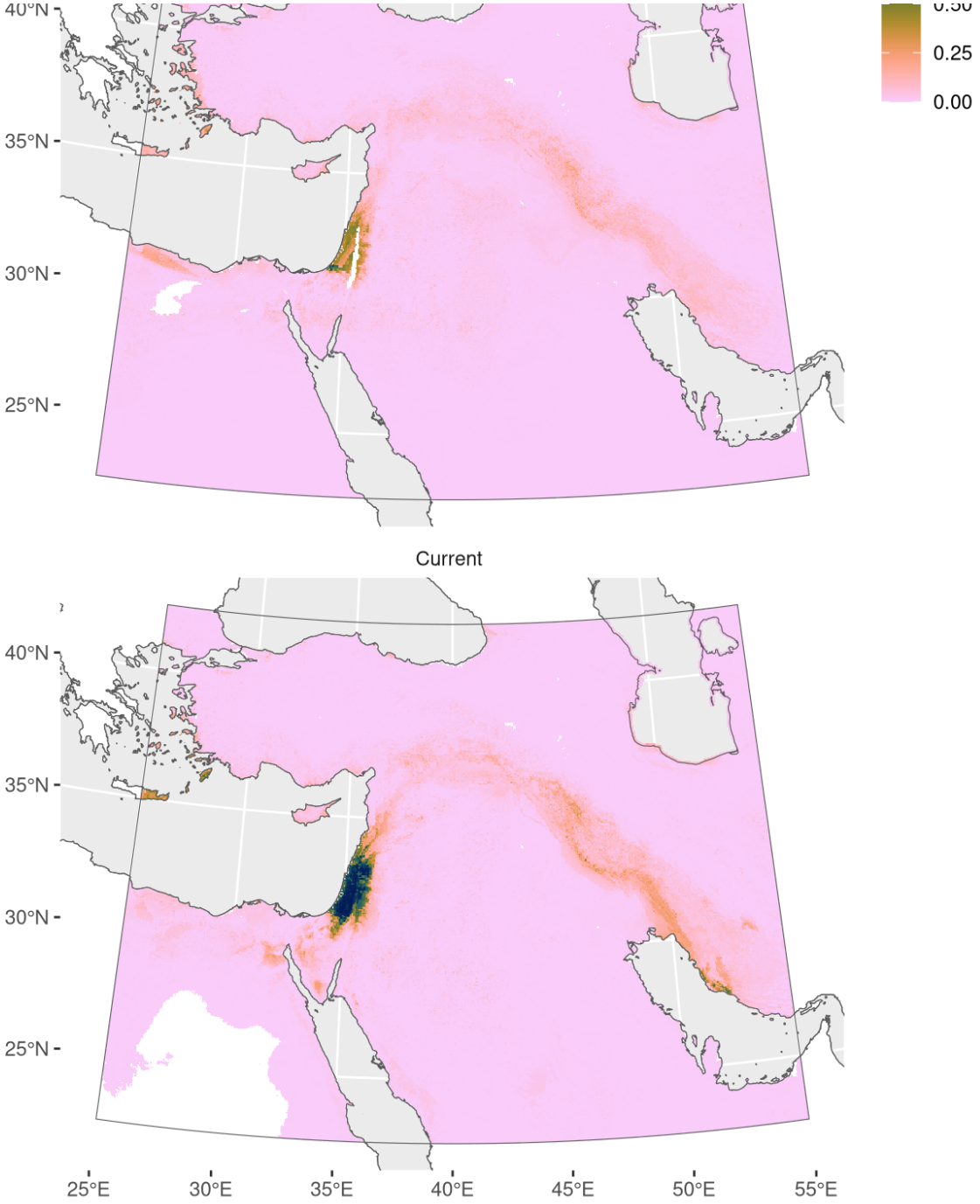


Figure 48: Predicted palaeodistributions of *Crithopsis delileana*

Table 24: Archaeological occurrences of *Crithopsis delileana*

Archaeological occurrences of *Crithopsis delileana*

| Site | Age range | N assemblages | Average prop. | Source | Predicted? |
|---|---|---|---|---|---|
| Bølling-Allerød (14.7-12.9 ka) | | | | | |
| Abu Hureyra | 13.1–13.0 ka | 1 | 0.05% | ORIGINS | no |
| Younger Dryas (12.9-11.7 ka) | | | | | |
| Abu Hureyra | 13.0–11.8 ka | 2 | 0.06% | ORIGINS | no |

# *Euclidium syriacum*

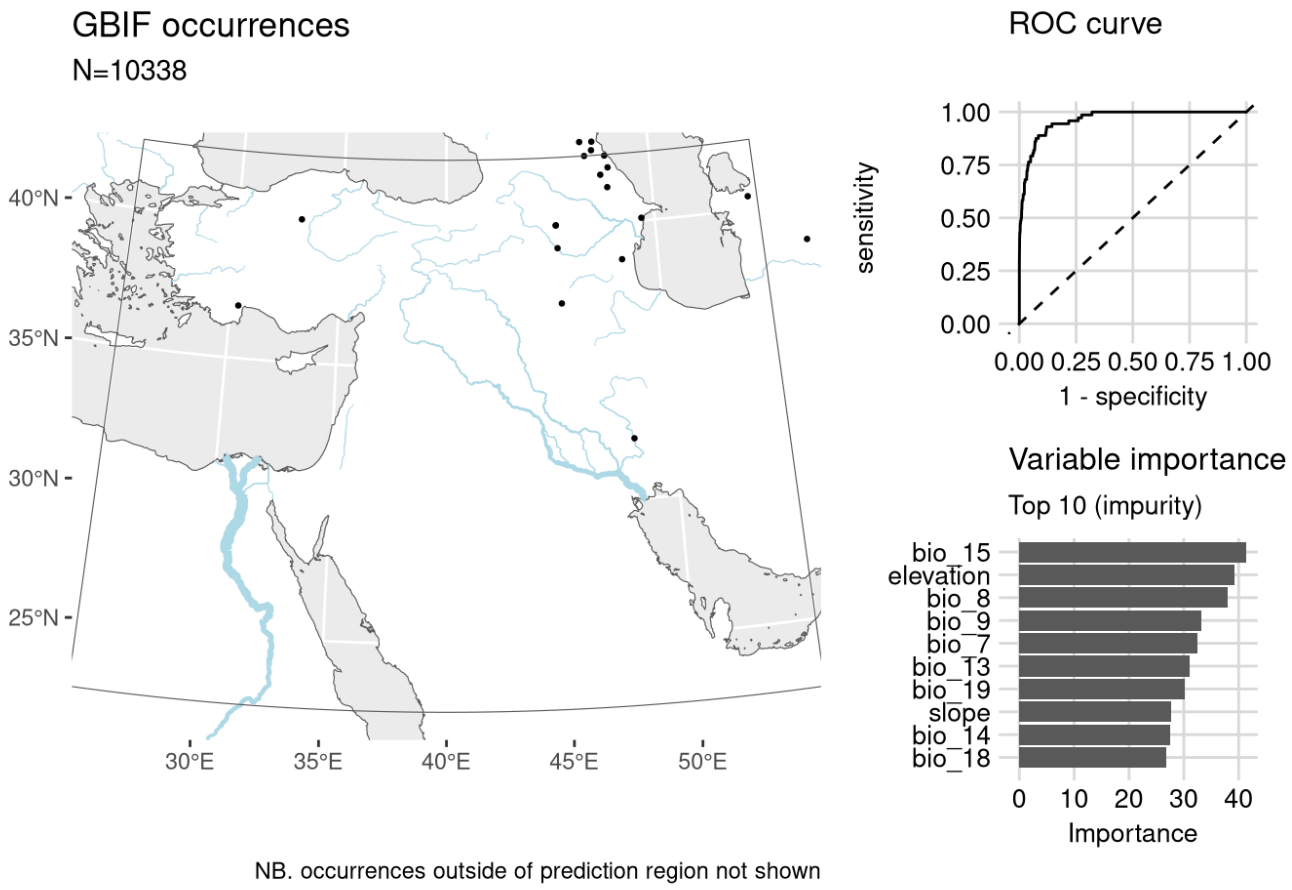


Figure 49: Fitted model summary for *Euclidium syriacum*

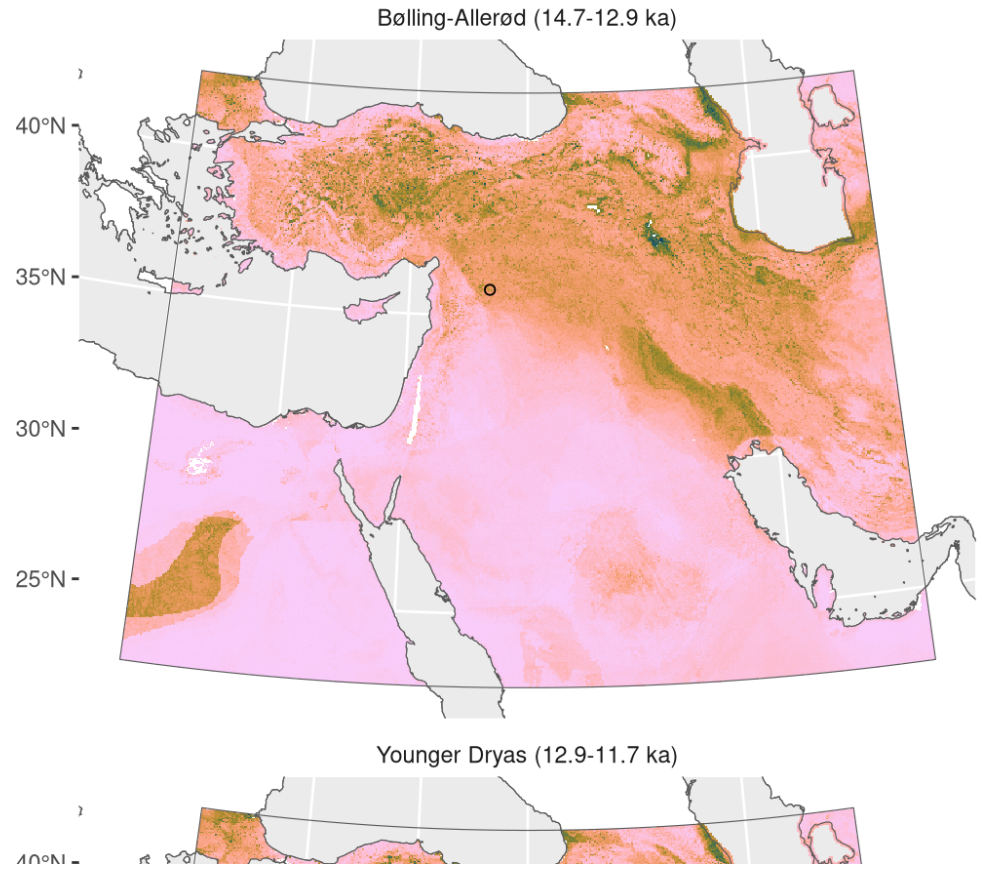

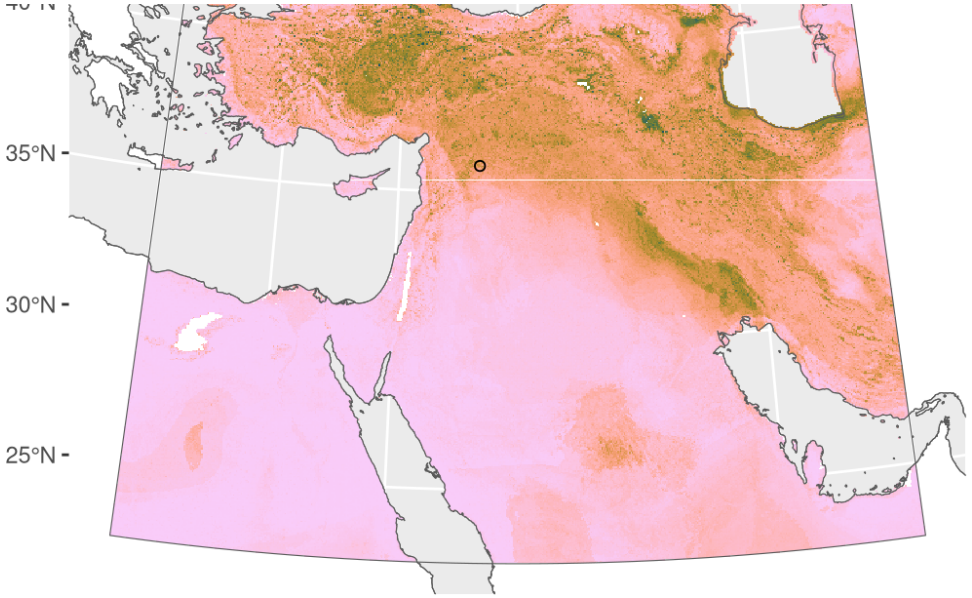


Early Holocene (11.7-8.3 ka)

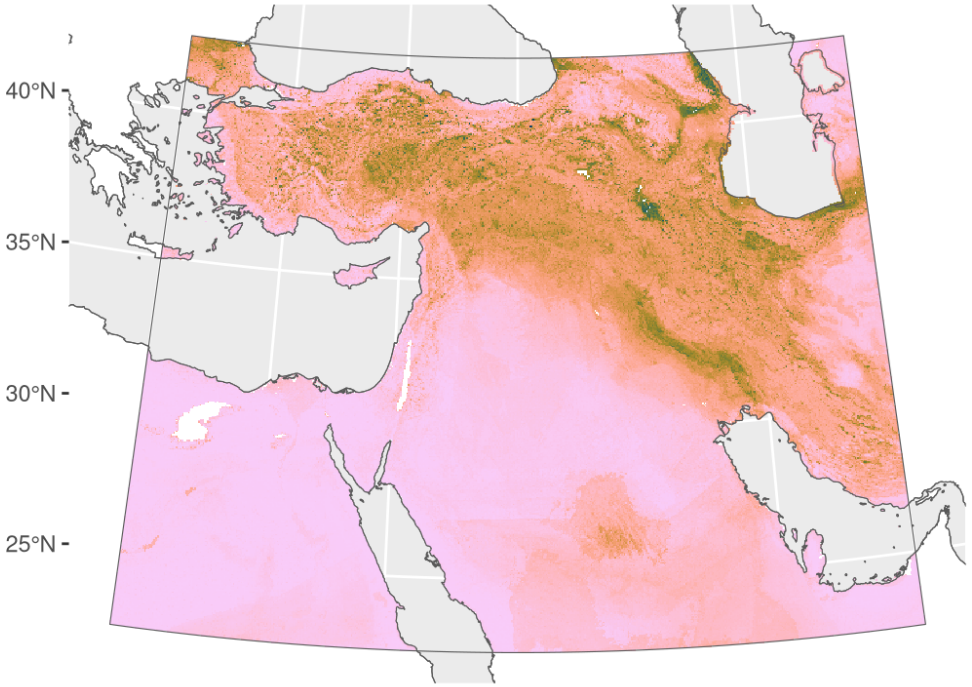


Current

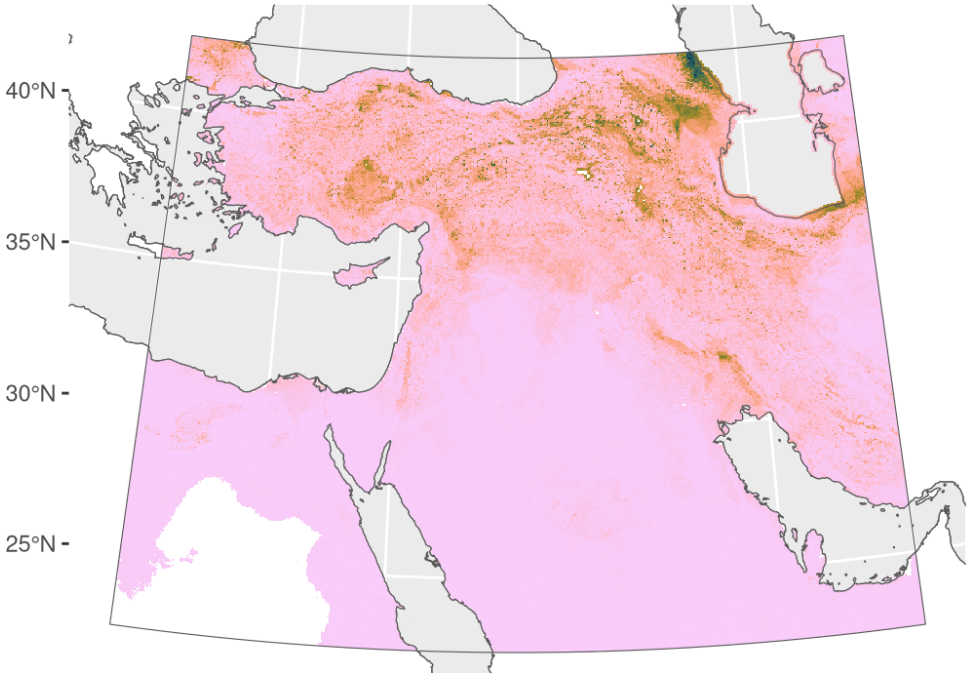


Archaeological occurrences

Not predicted at P(present)>0.5

P(present)

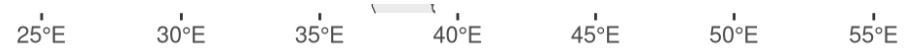


Figure 50: Predicted palaeodistributions of *Euclidium syriacum*

Table 25: Archaeological occurrences of *Euclidium syriacum*

Archaeological occurrences of *Euclidium syriacum*

| Site | Age range | N assemblages | Average prop. | Source | Predicted? |
|---|---|---|---|---|---|
| Bølling-Allerød (14.7-12.9 ka) | | | | | |
| Abu Hureyra | 13.1–13.0 ka | 1 | 0.16% | ORIGINS | no |
| Younger Dryas (12.9-11.7 ka) | | | | | |
| Abu Hureyra | 13.0–11.8 ka | 2 | 0.17% | ORIGINS | no |

# *Ficus carica*

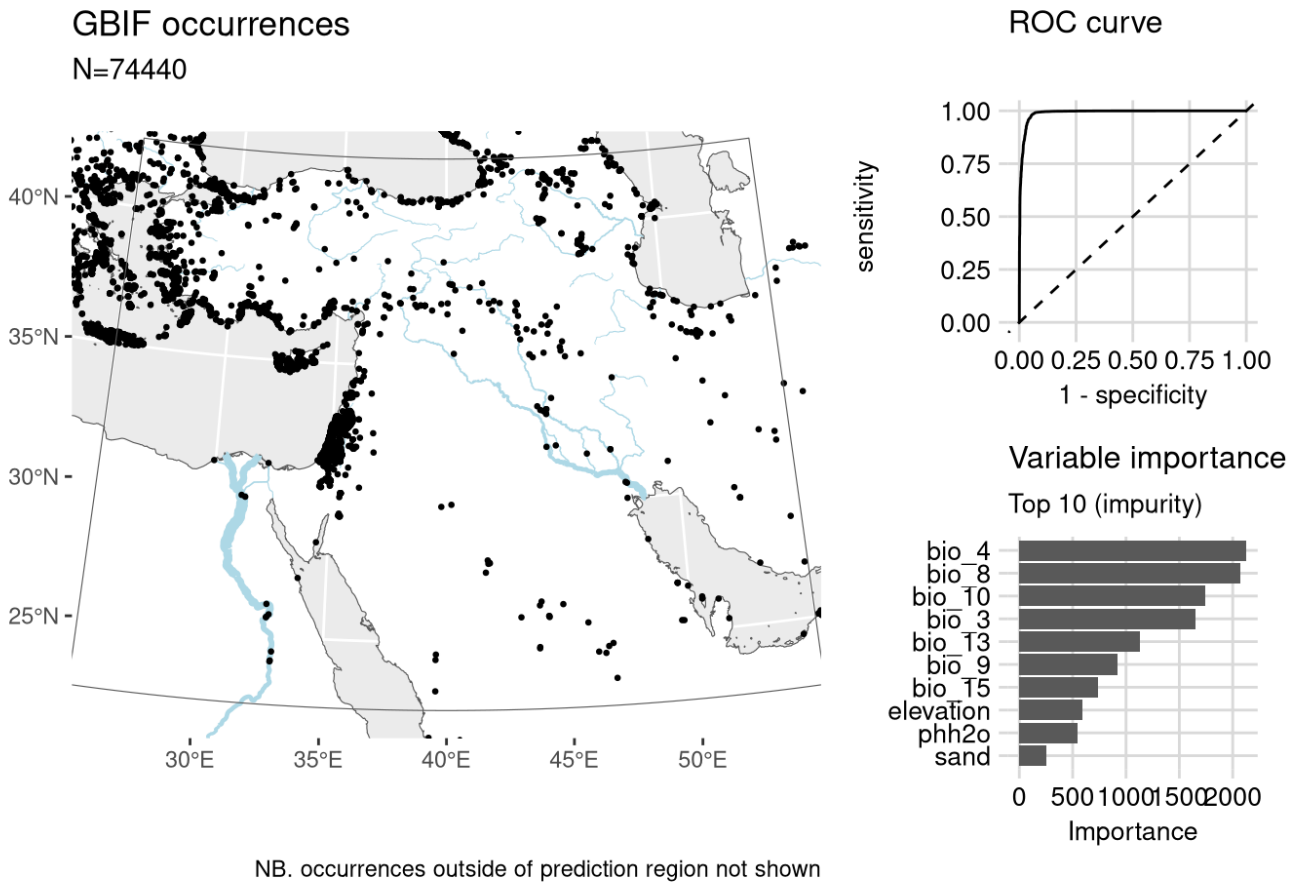


Figure 51: Fitted model summary for *Ficus carica*

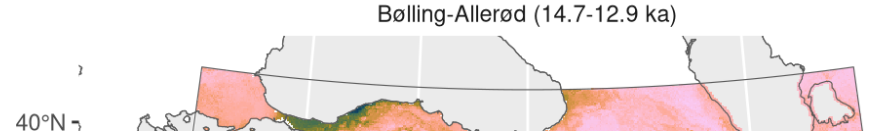

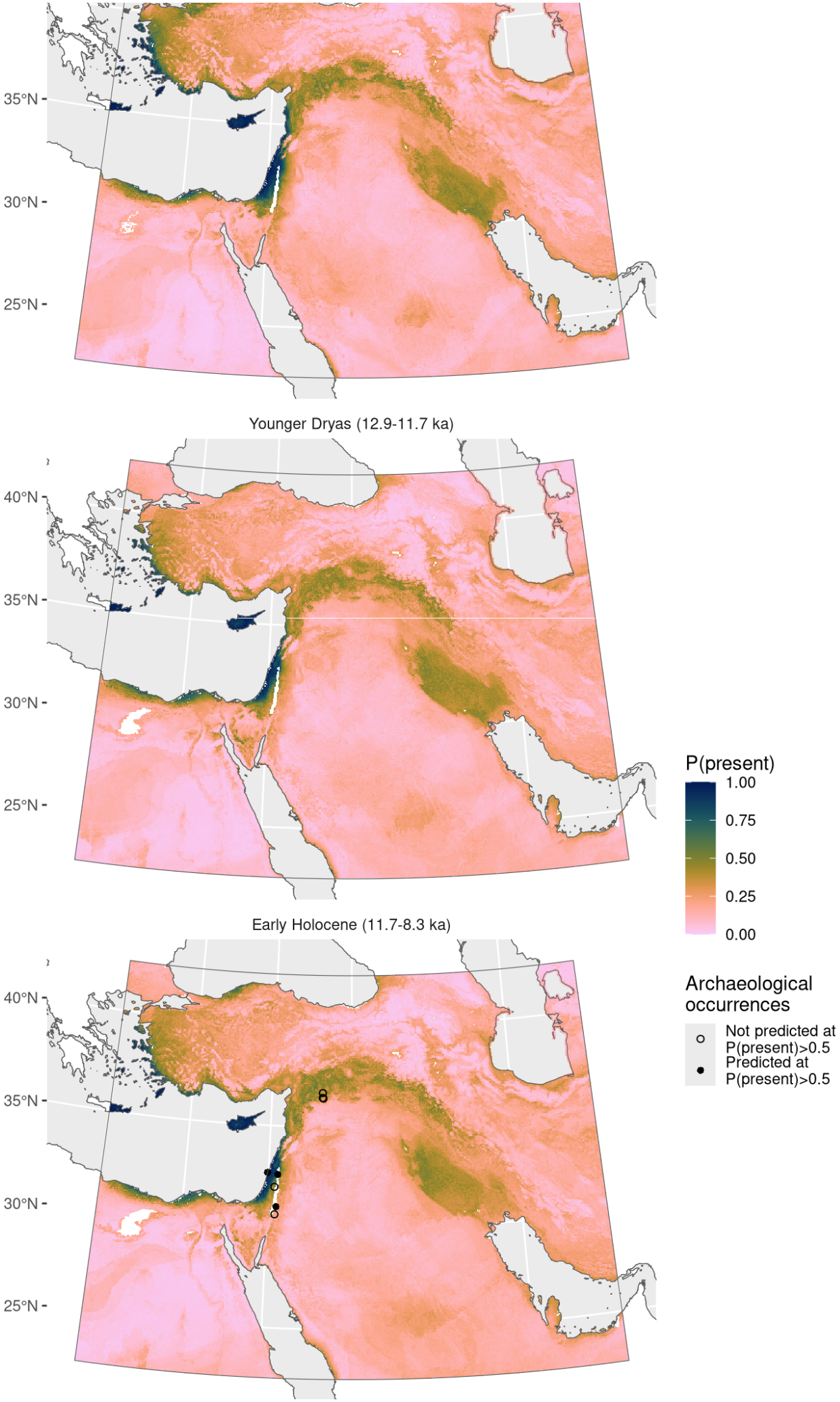
35°N
30°N
25°N
Younger Dryas (12.9-11.7 ka)
40°N
35°N
30°N
25°N
Early Holocene (11.7-8.3 ka)
40°N
35°N
30°N
25°N
8
P(present)
1.00
0.75
0.50
0.25
0.00
Archaeological occurrences
Not predicted at P(present)>0.5
Predicted at P(present)>0.5

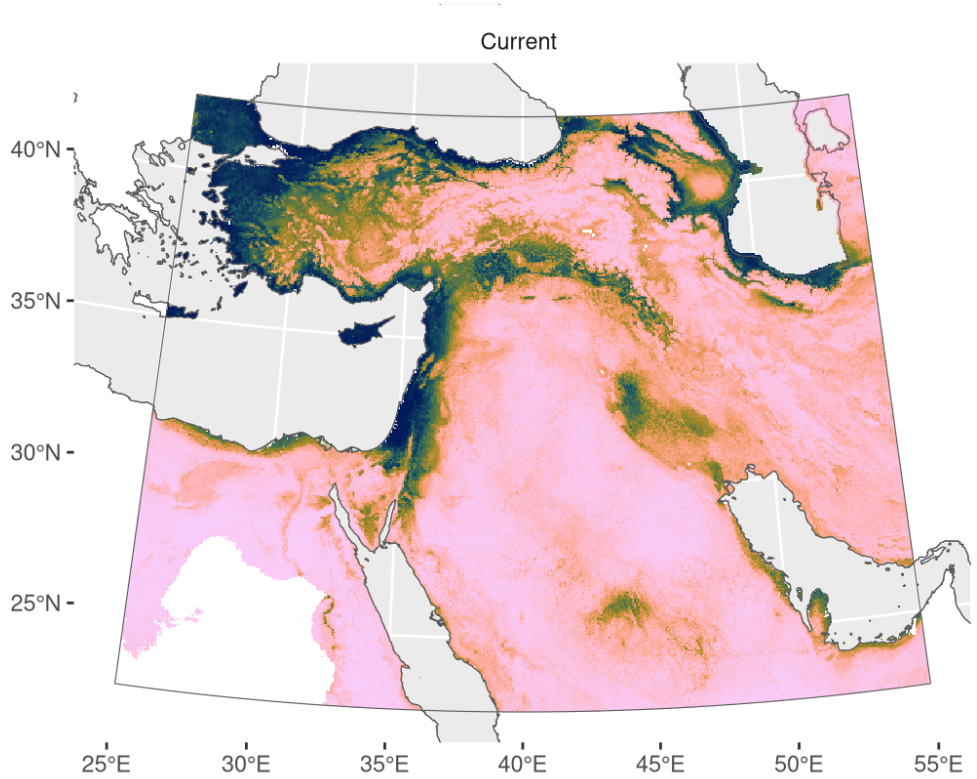


Figure 52: Predicted palaeodistributions of *Ficus carica*

Table 26: Archaeological occurrences of *Ficus carica*

Archaeological occurrences of *Ficus carica*

| Site | Age range | N assemblages | Average prop. | Source | Predicted? |
|---|---|---|---|---|---|
| Early Holocene (11.7-8.3 ka) | | | | | |
| Netiv Hagdud | 11.6–10.6 ka | 1 | 28.06% | ORIGINS | no |
| Wadi Faynan 16 | 11.6–11.2 ka | 1 | 16.71% | ORIGINS | no |
| Gesher | 11.5–11.2 ka | 1 | 17.91% | ORIGINS | yes |
| Jerf el Ahmar | 11.4–10.7 ka | 1 | 0.02% | ORIGINS | no |
| El-Hemmeh | 11.1–10.5 ka | 1 | 15.77% | ORIGINS | yes |
| Dja'de | 10.7–10.2 ka | 1 | 0.13% | ORIGINS | no |
| Halula | 9.9–9.5 ka | 1 | 0.55% | ORIGINS | no |
| Atlit-Yam | 9.0–8.0 ka | 1 | 67.76% | ORIGINS | yes |

## *Fumaria densiflora*

GBIF occurrences

ROC curve

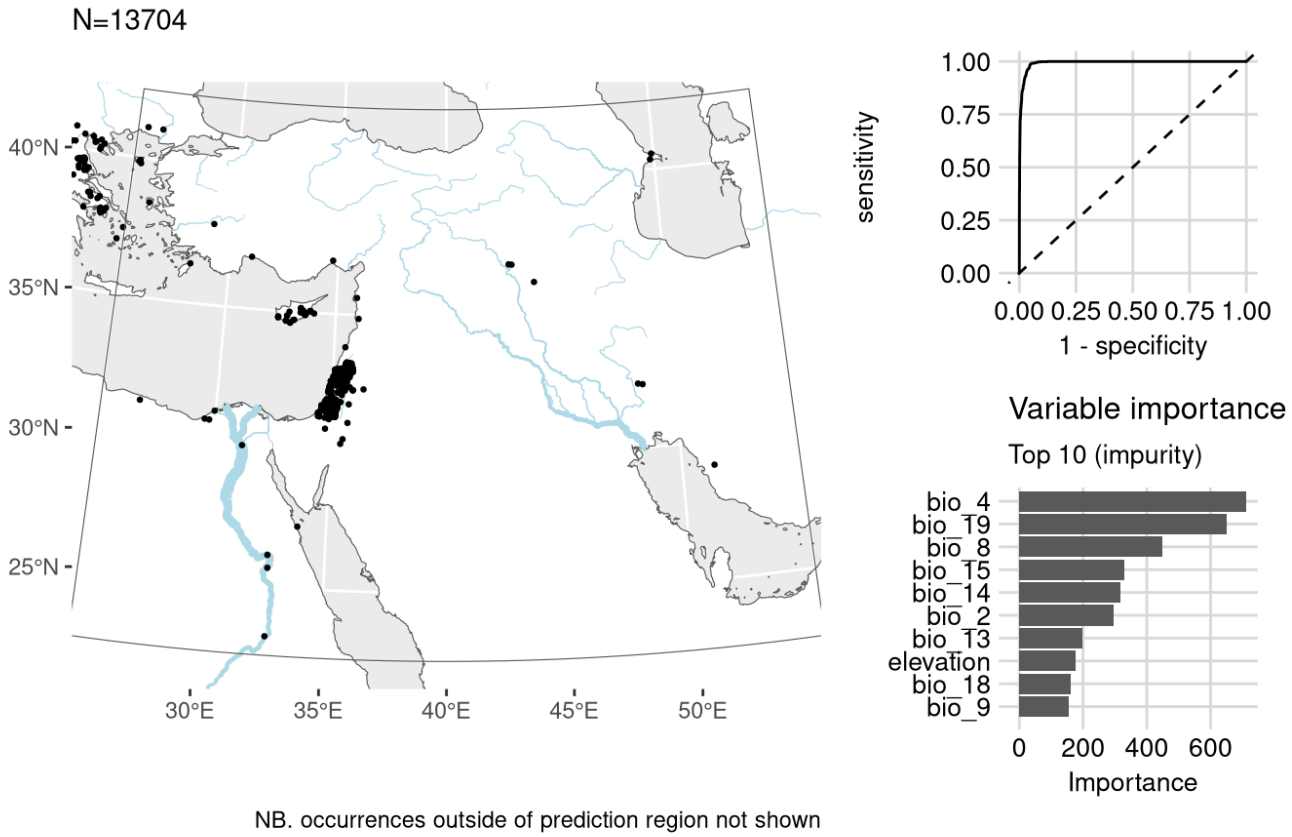


Figure 53: Fitted model summary for *Fumaria densiflora*

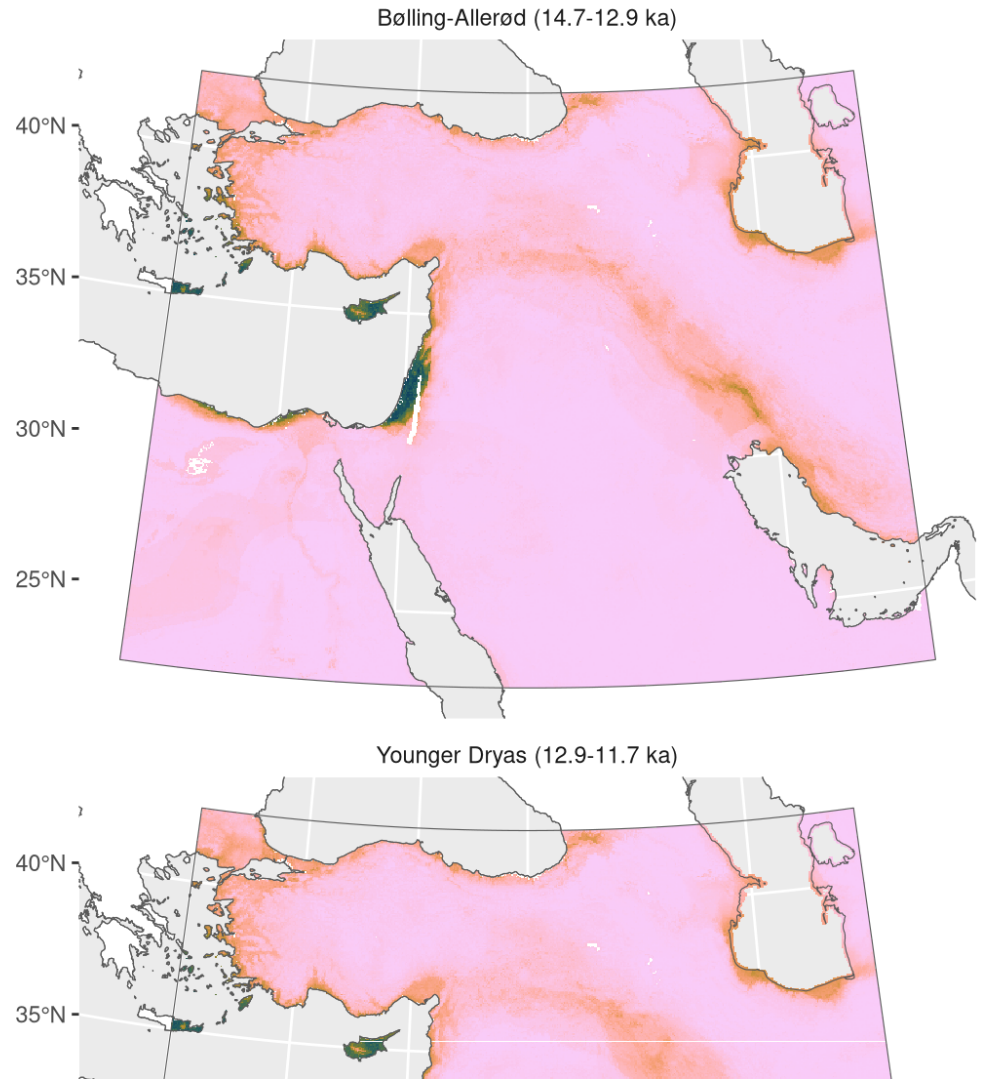

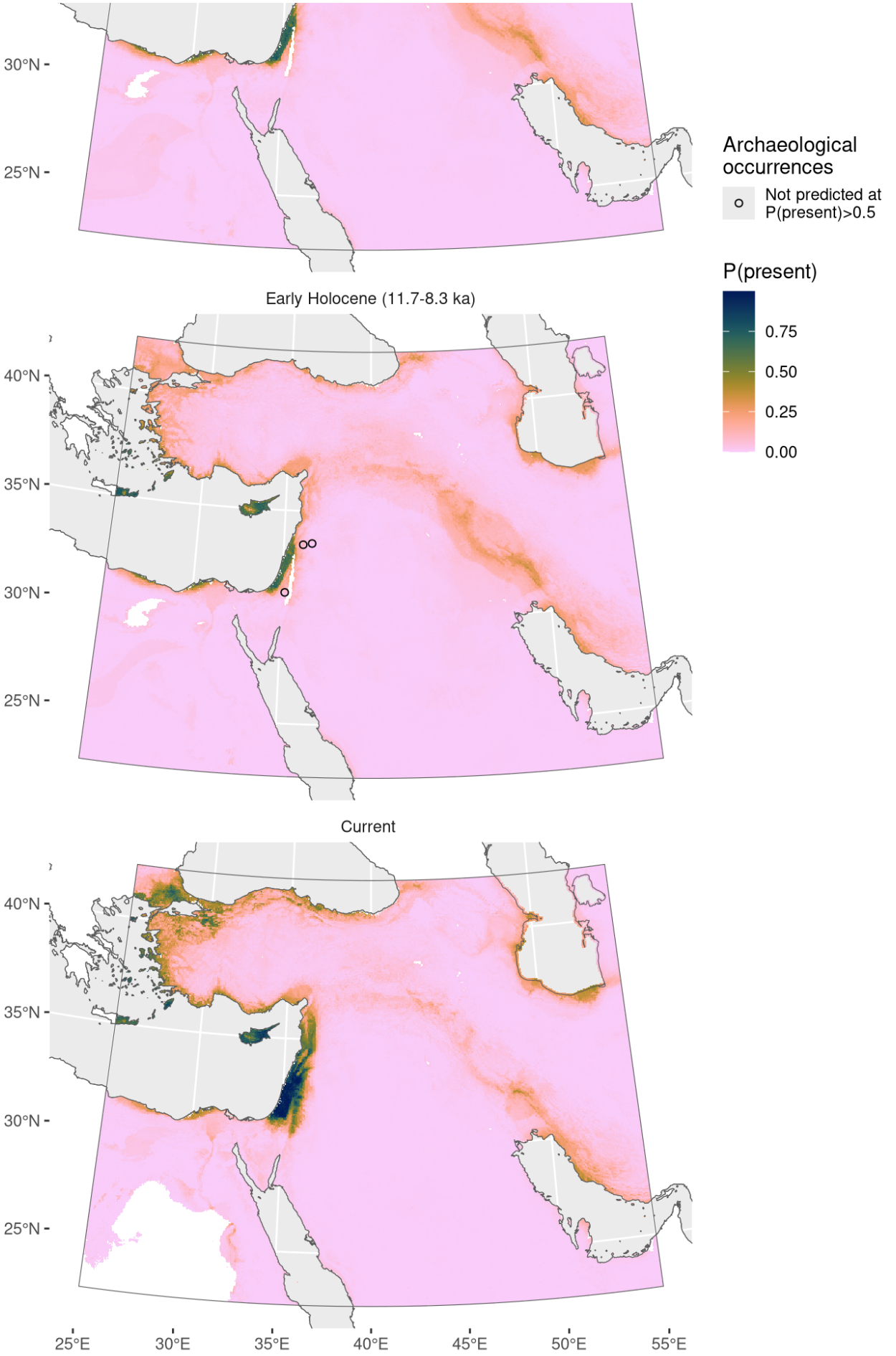


Figure 54: Predicted palaeodistributions of *Fumaria densiflora*

Table 27: Archaeological occurrences of *Fumaria densiflora*

Archaeological occurrences of *Fumaria densiflora*

| Site | Age range | N assemblages | Average prop. | Source | Predicted? |
|---|---|---|---|---|---|
| Early Holocene (11.7-8.3 ka) | | | | | |
| Tell Aswad | 10.2–9.3 ka | 1 | 0.00% | ORIGINS | no |
| Nahal Hemar | 10.1–9.3 ka | 1 | 0.56% | ORIGINS | no |
| Tell Ramad | 9.3–8.6 ka | 2 | 0.01% | ORIGINS | no |

# *Gypsophila elegans*

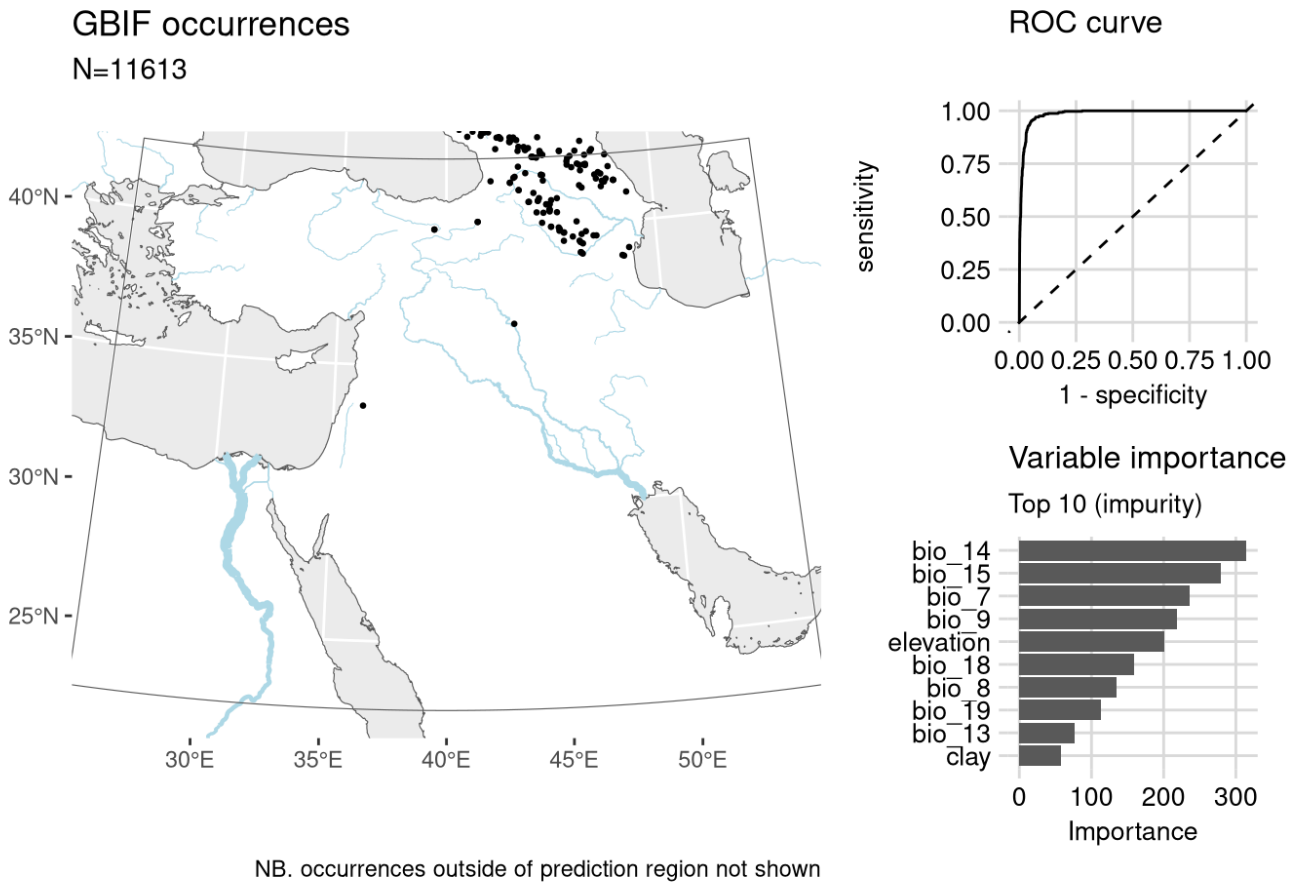


Figure 55: Fitted model summary for *Gypsophila elegans*

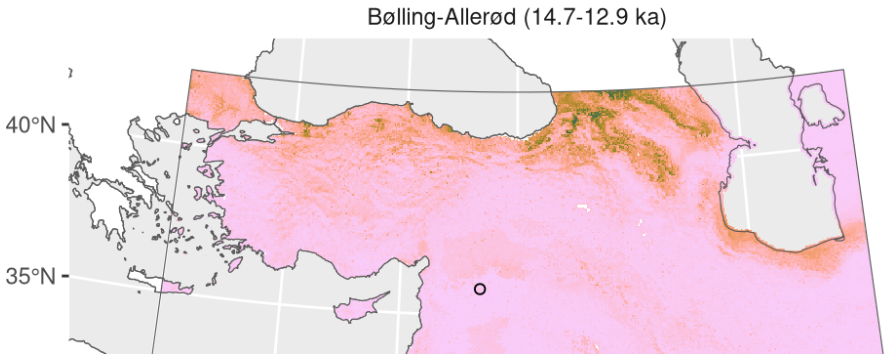

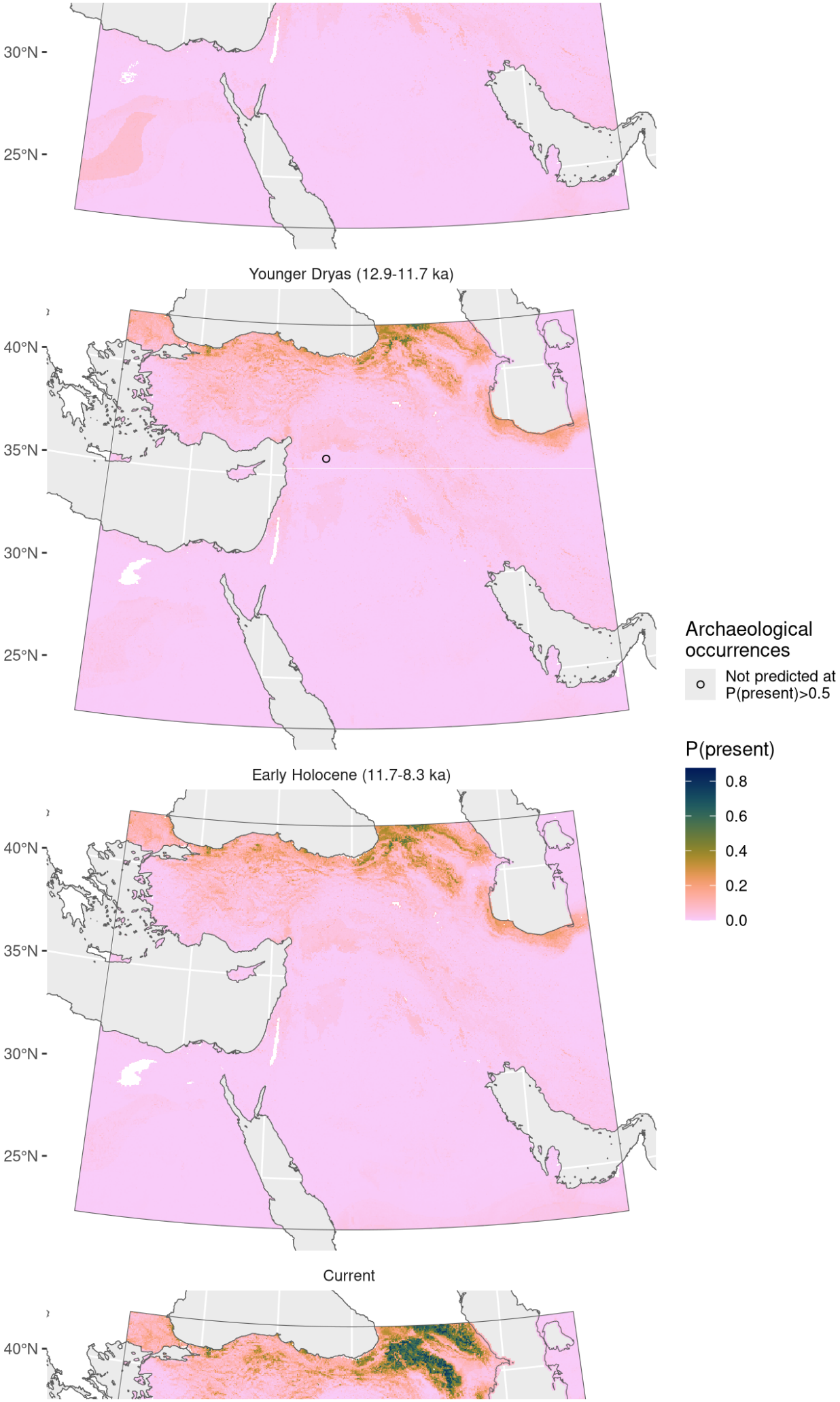
30°N
25°N
Younger Dryas (12.9-11.7 ka)
40°N
35°N
30°N
25°N
Early Holocene (11.7-8.3 ka)
40°N
35°N
30°N
25°N
Current
40°N
Archaeological occurrences
Not predicted at P(present)>0.5
P(present)
0.8
0.6
0.4
0.2
0.0

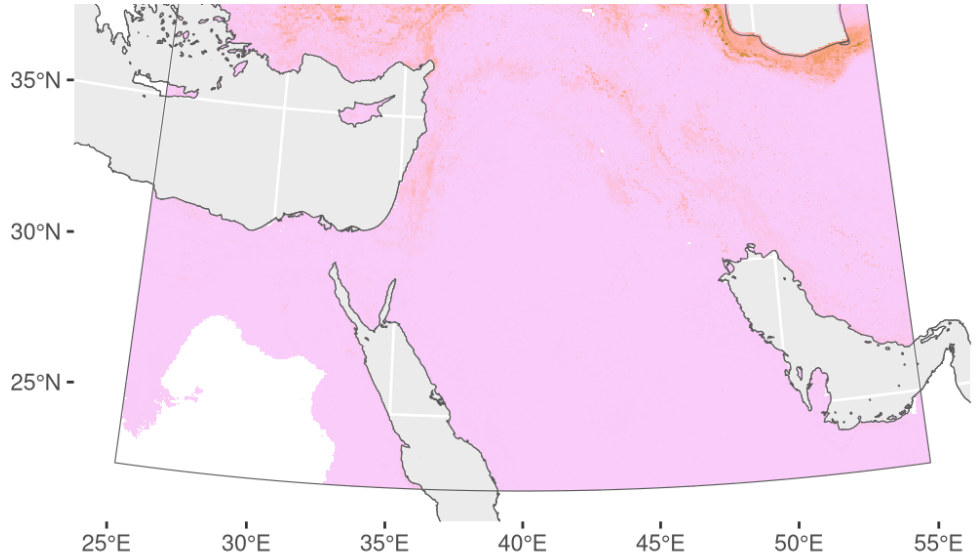


Figure 56: Predicted palaeodistributions of *Gypsophila elegans*

Table 28: Archaeological occurrences of *Gypsophila elegans*

Archaeological occurrences of *Gypsophila elegans*

| Site | Age range | N assemblages | Average prop. | Source | Predicted? |
|---|---|---|---|---|---|
| Bølling-Allerød (14.7-12.9 ka) | | | | | |
| Abu Hureyra | 13.1–13.0 ka | 1 | 0.31% | ORIGINS | no |
| Younger Dryas (12.9-11.7 ka) | | | | | |
| Abu Hureyra | 13.0–11.8 ka | 2 | 0.43% | ORIGINS | no |

# *Gypsophila pilosa*

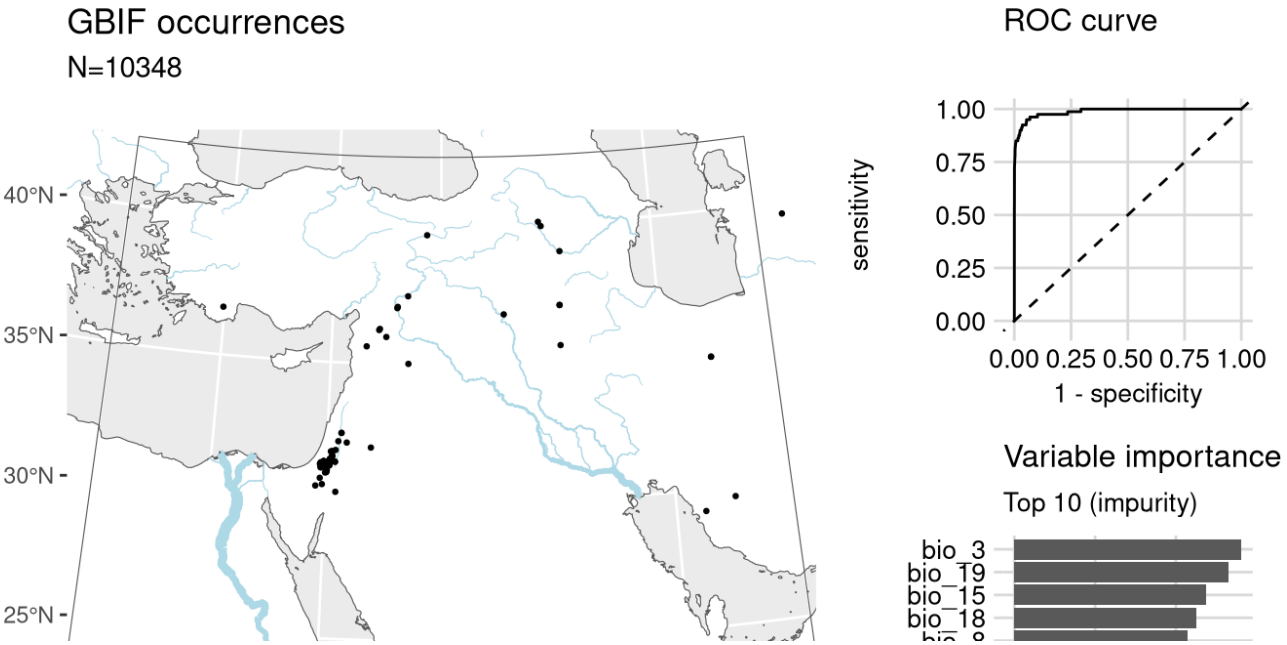

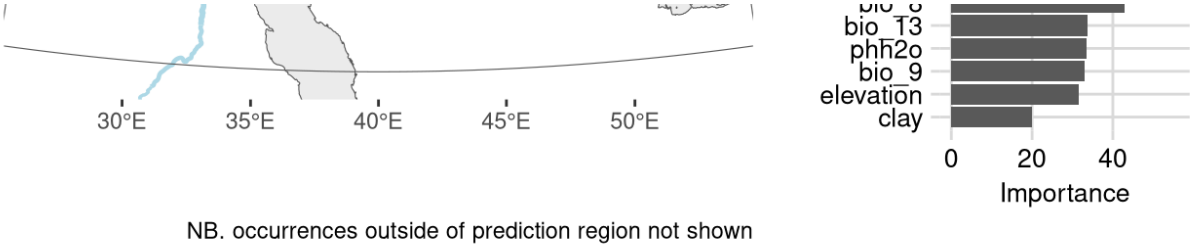


Figure 57: Fitted model summary for *Gypsophila pilosa*

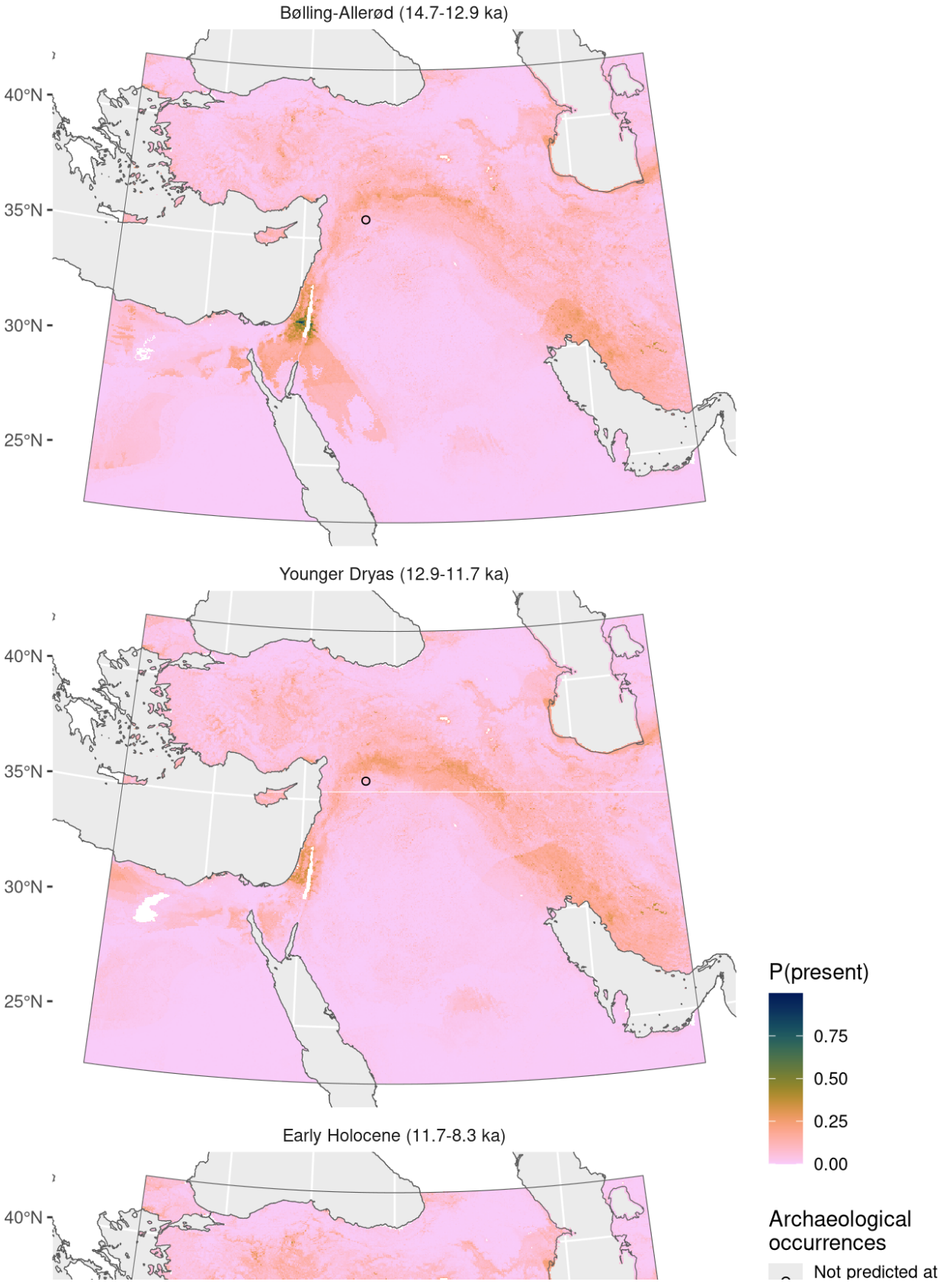

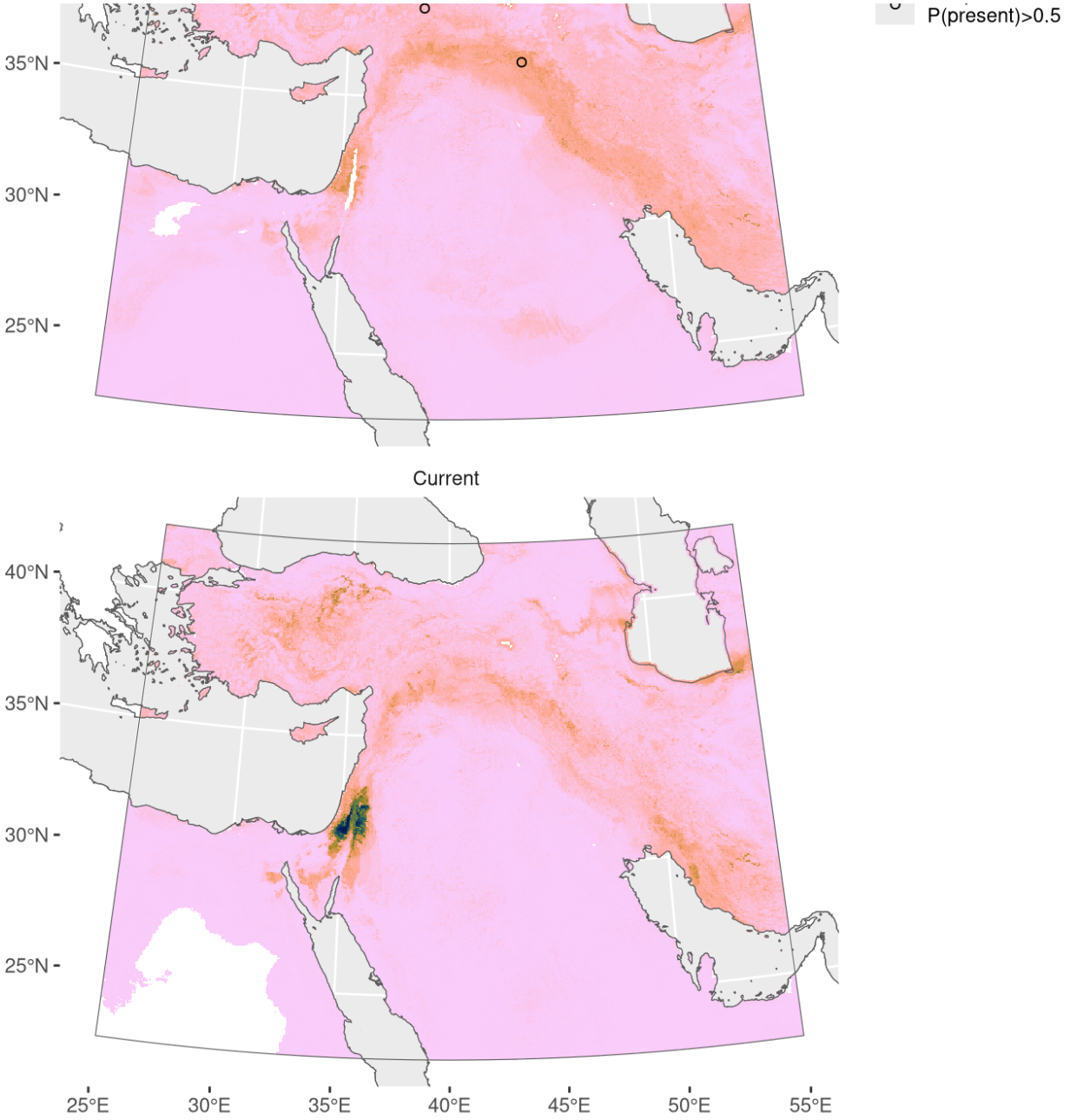


Figure 58: Predicted palaeodistributions of *Gypsophila pilosa*

Table 29: Archaeological occurrences of *Gypsophila pilosa*

Archaeological occurrences of *Gypsophila pilosa*

| Site | Age range | N assemblages | Average prop. | Source | Predicted? |
|---|---|---|---|---|---|
| Bølling-Allerød (14.7-12.9 ka) | | | | | |
| Abu Hureyra | 13.1–13.0 ka | 1 | 0.33% | ORIGINS | no |
| Younger Dryas (12.9-11.7 ka) | | | | | |
| Abu Hureyra | 13.0–11.8 ka | 2 | 0.46% | ORIGINS | no |
| Early Holocene (11.7-8.3 ka) | | | | | |
| M'lefaat | 11.3–11.1 ka | 1 | 3.55% | ORIGINS | no |

| | | | | | |
|---|---|---|---|---|---|
| Mlefaat | 11.3–11.1 ka | 1 | 3.33% | ORIGINS | no |
| Cafer Höyük | 10.6–9.7 ka | 1 | 0.33% | ORIGINS | no |

# *Gypsophila vaccaria*

Including Vaccaria pyramidata.

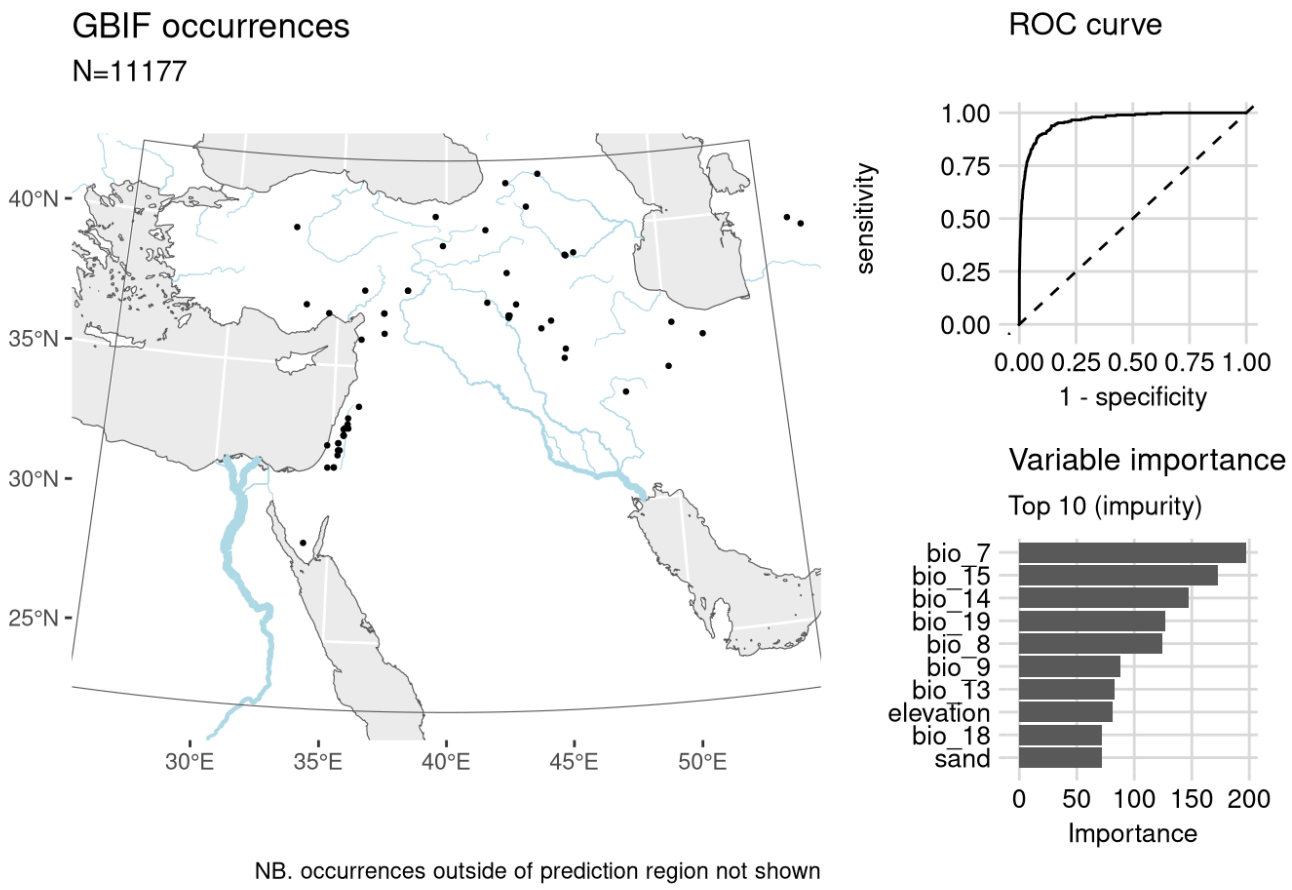


Figure 59: Fitted model summary for *Gypsophila vaccaria*

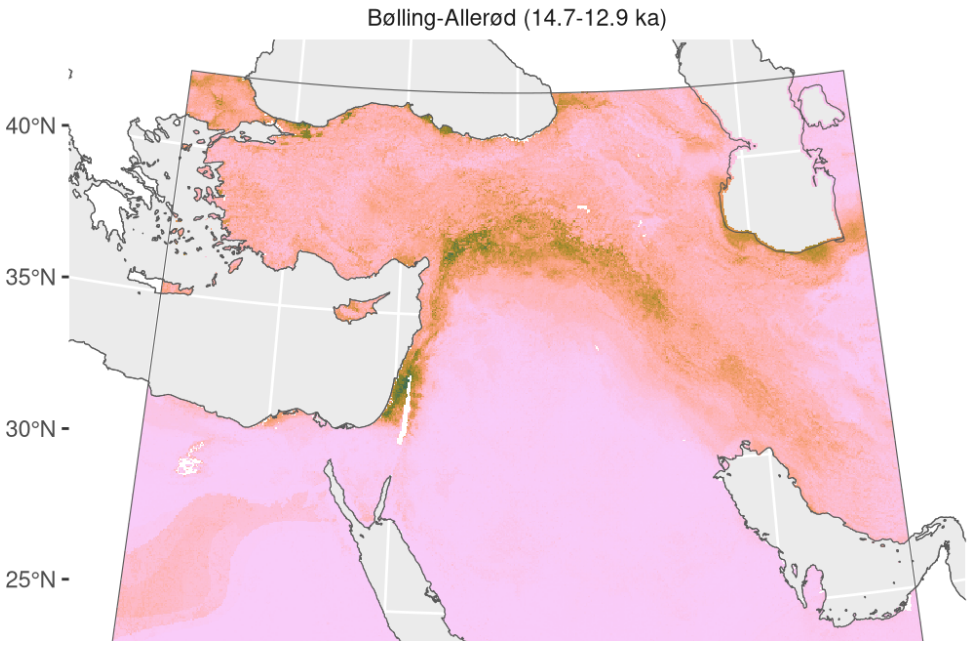

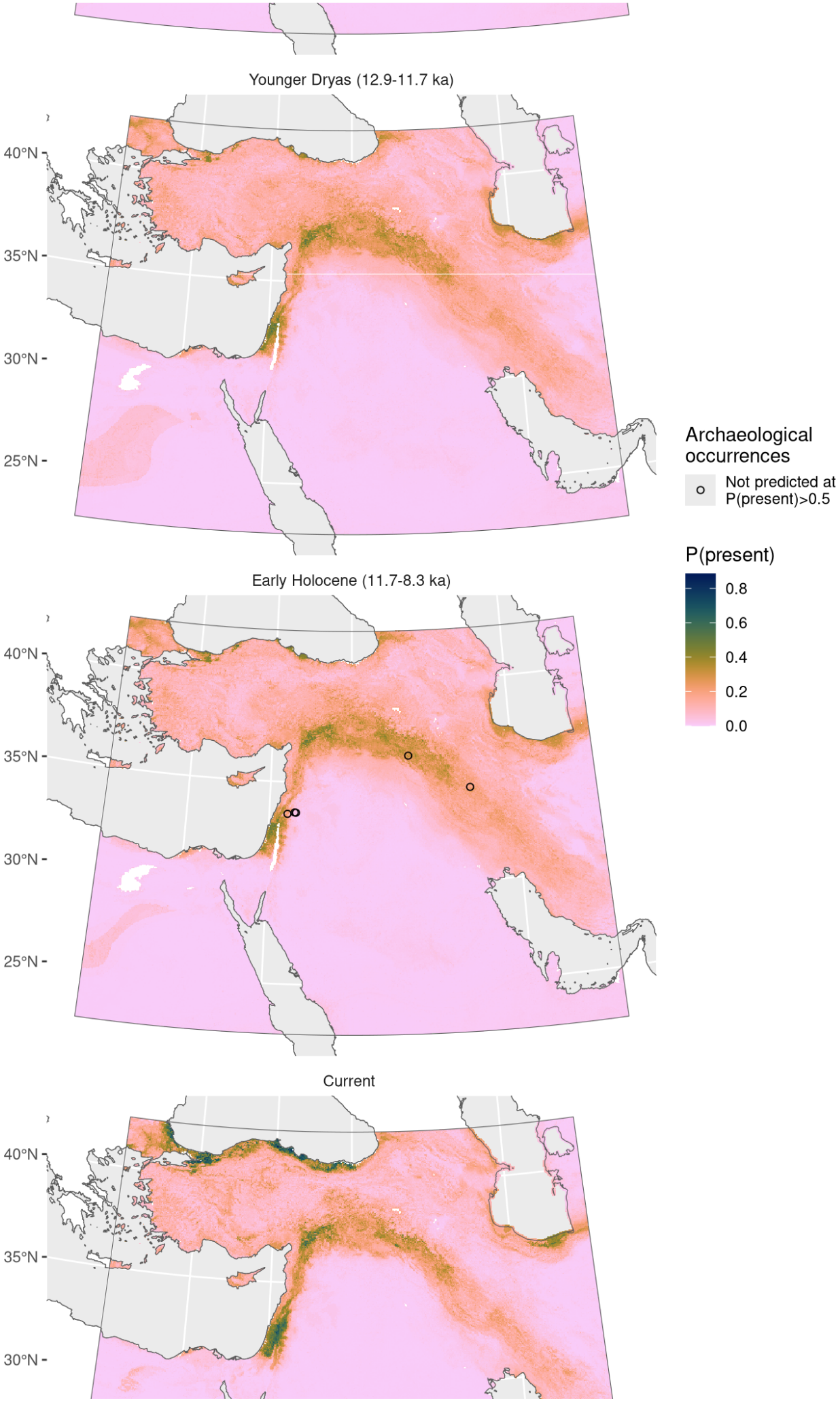
Younger Dryas (12.9-11.7 ka)
40°N
35°N
30°N
25°N
Early Holocene (11.7-8.3 ka)
40°N
35°N
30°N
25°N
Current
40°N
35°N
30°N
Archaeological occurrences
Not predicted at P(present)>0.5
P(present)
0.8
0.6
0.4
0.2
0.0

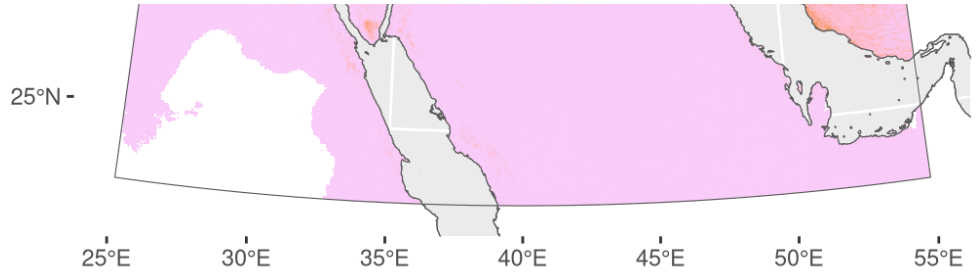


Figure 60: Predicted palaeodistributions of *Gypsophila vaccaria*

Table 30: Archaeological occurrences of *Gypsophila vaccaria*

Archaeological occurrences of *Gypsophila vaccaria*

| Site | Age range | N assemblages | Average prop. | Source | Predicted? |
|---|---|---|---|---|---|
| Early Holocene (11.7-8.3 ka) | | | | | |
| Sheikh-e Abad | 11.8–8.4 ka | 2 | 0.58% | ADEMNES | no |
| M'lefaat | 11.3–11.1 ka | 1 | 0.40% | ORIGINS | no |
| Tell Aswad | 10.2–9.3 ka | 1 | 0.04% | ORIGINS | no |
| Tell Ghoraifé | 10.1–8.6 ka | 2 | 0.22% | ORIGINS | no |
| Tell Ramad | 9.3–8.6 ka | 2 | 0.02% | ORIGINS | no |

# *Hordeum bulbosum*

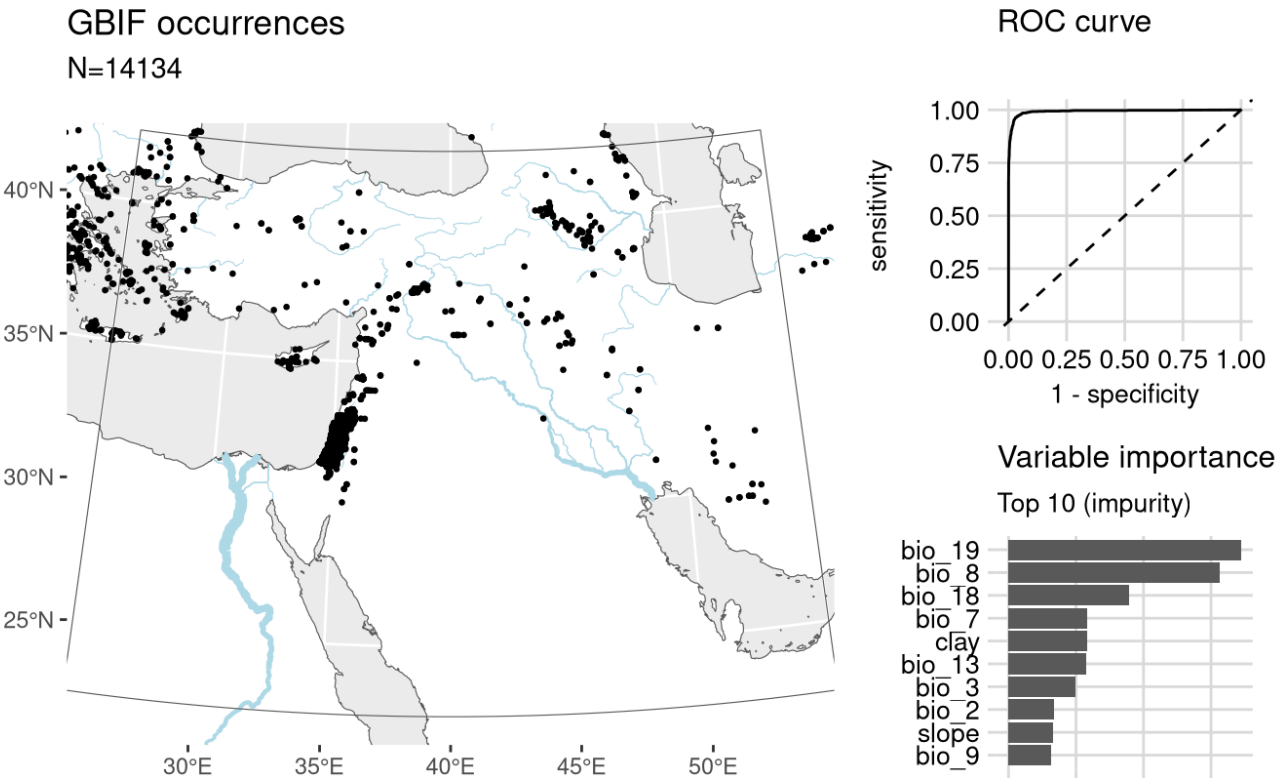

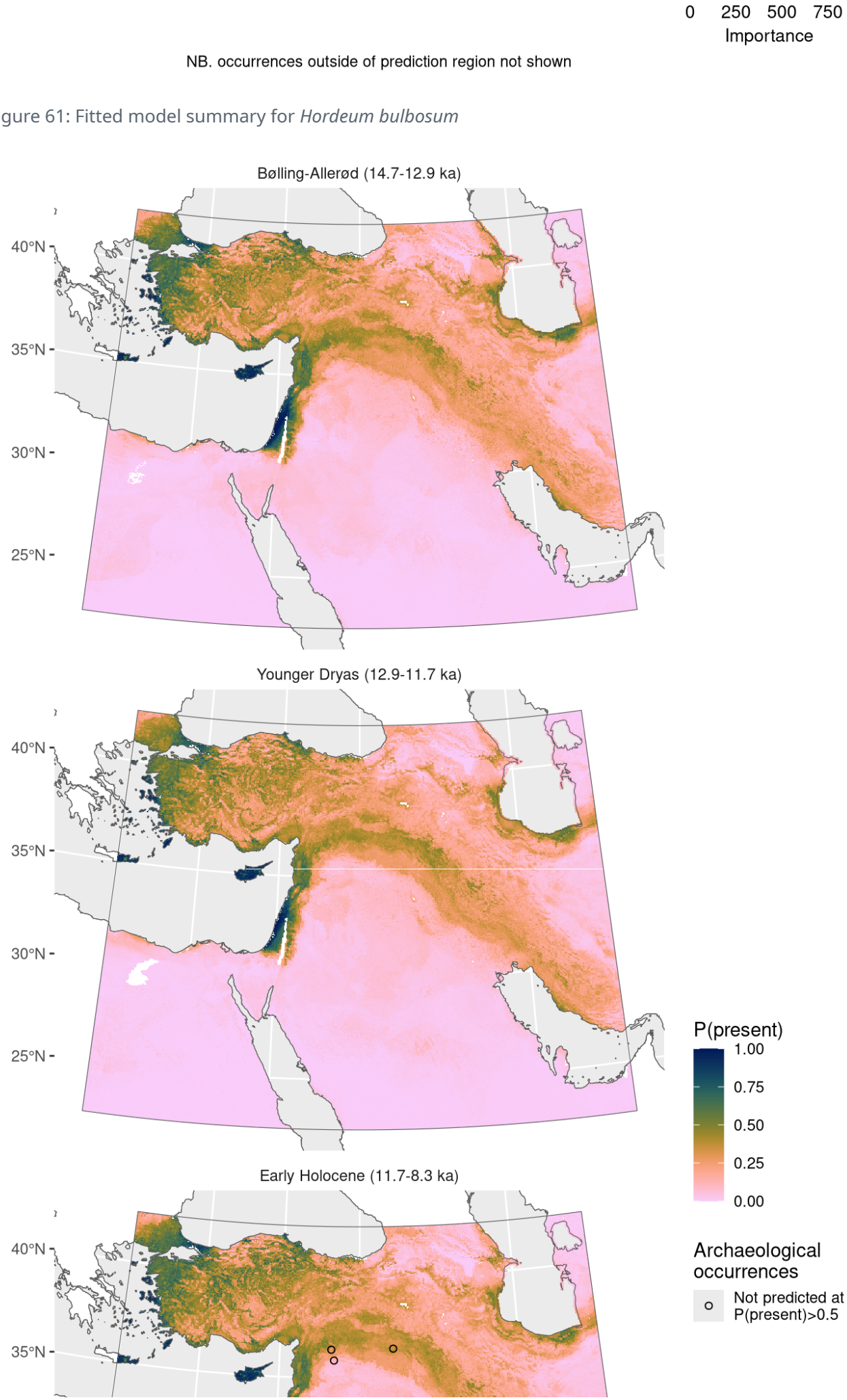


Figure 61: Fitted model summary for *Hordeum bulbosum*

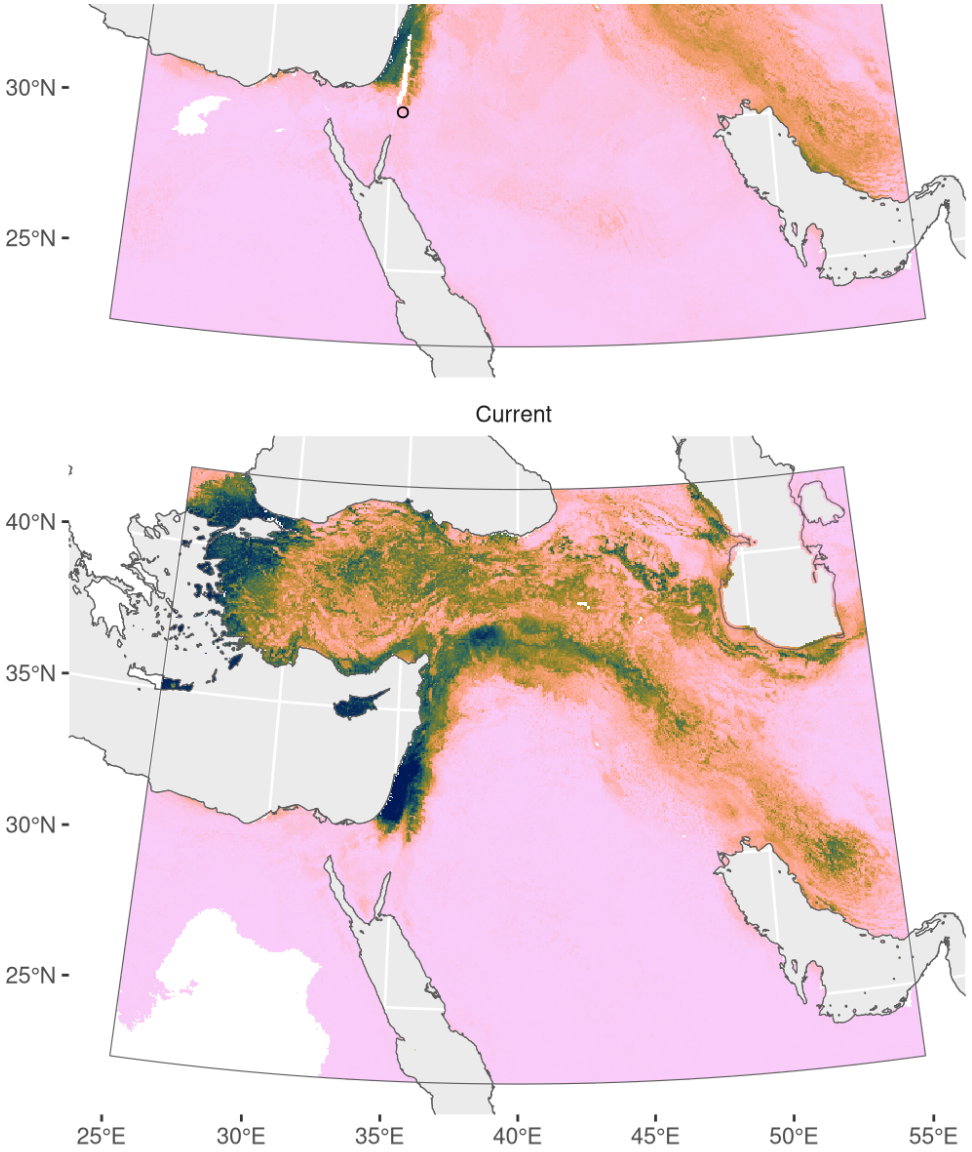


Figure 62: Predicted palaeodistributions of *Hordeum bulbosum*

Table 31: Archaeological occurrences of *Hordeum bulbosum*

Archaeological occurrences of *Hordeum bulbosum*

| Site | Age range | N assemblages | Average prop. | Source | Predicted? |
|---|---|---|---|---|---|
| Early Holocene (11.7-8.3 ka) | | | | | |
| Jerf el Ahmar | 11.4–10.7 ka | 1 | 0.24% | ORIGINS | no |
| Beidha | 10.1–9.5 ka | 1 | 0.00% | ORIGINS | no |
| Abu Hureyra | 9.3–8.2 ka | 1 | 4.01% | ORIGINS | no |
| Tell Maghzaliyeh | 9.0–8.2 ka | 1 | 0.14% | ORIGINS | no |

## *Hordeum murinum*

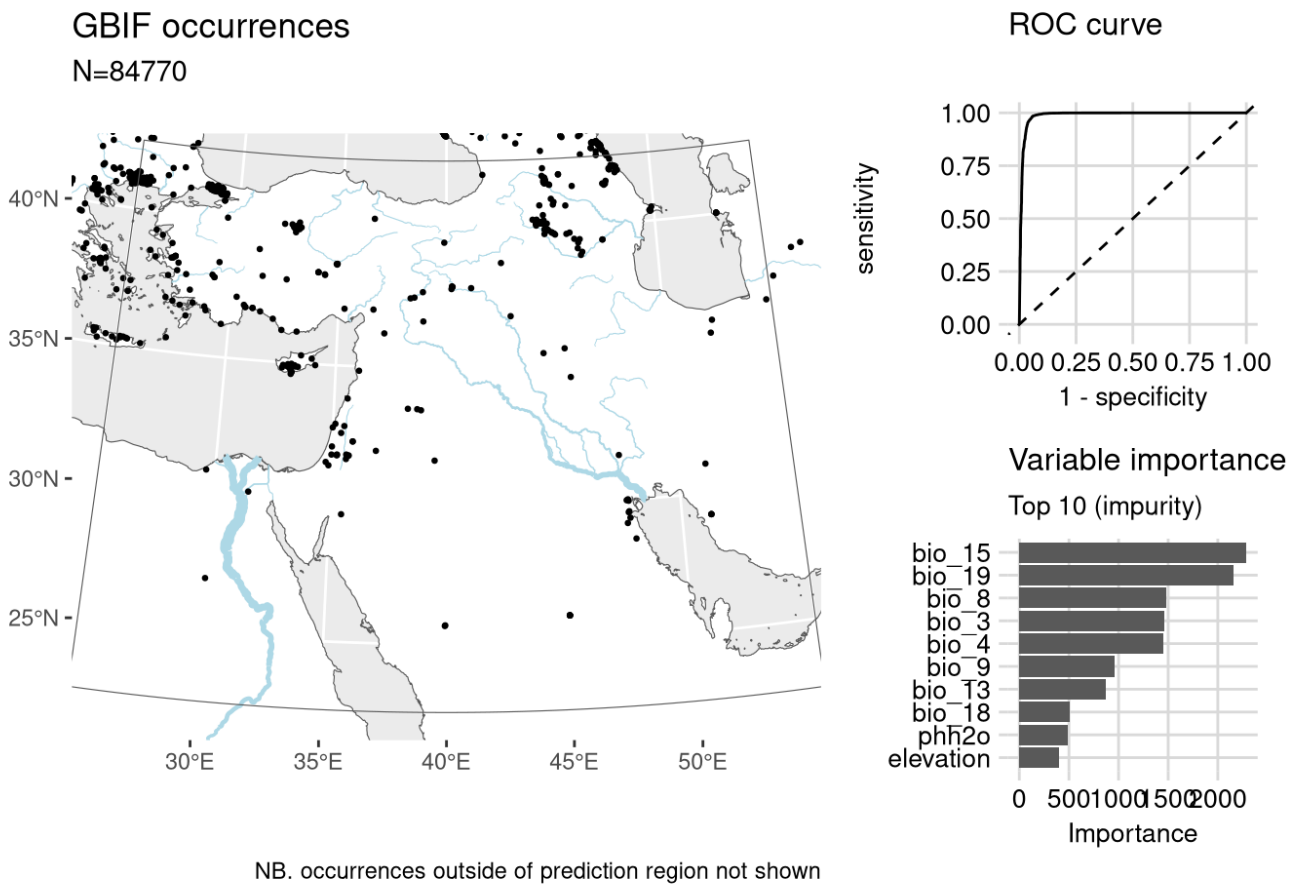


Figure 63: Fitted model summary for *Hordeum murinum*

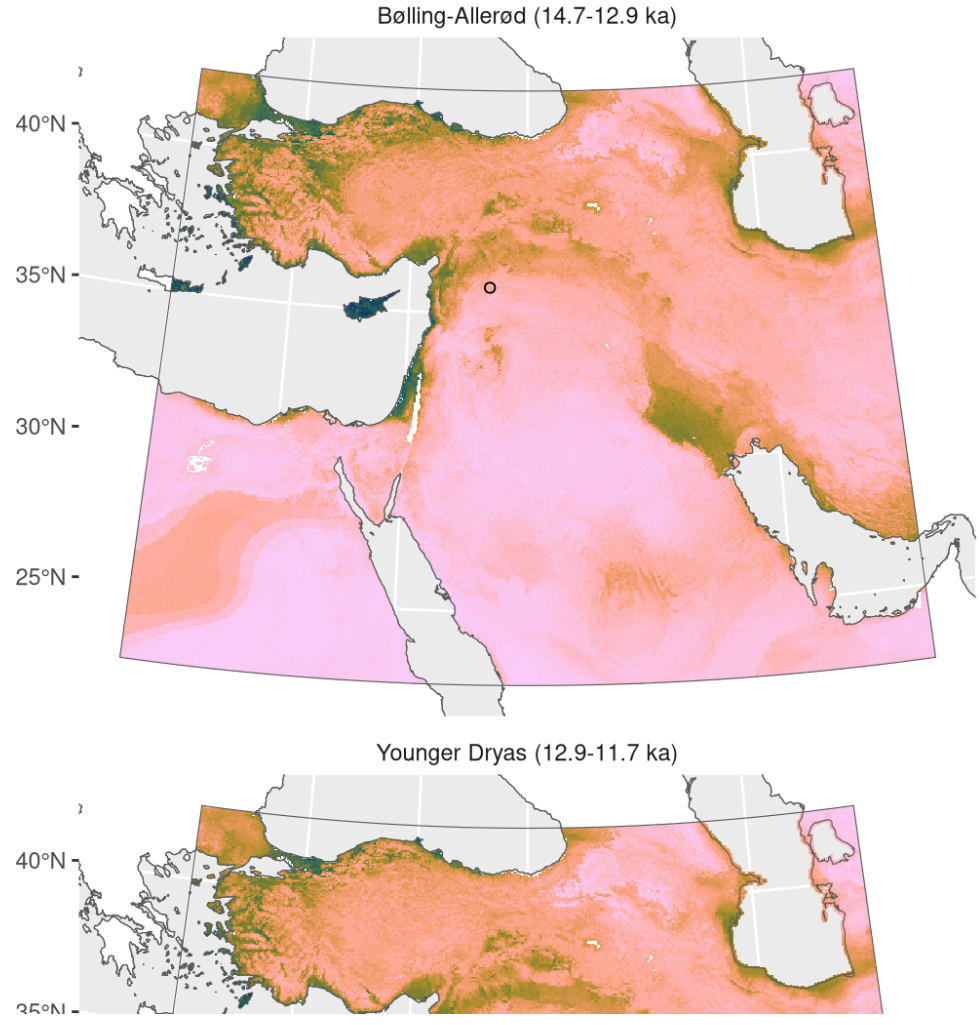

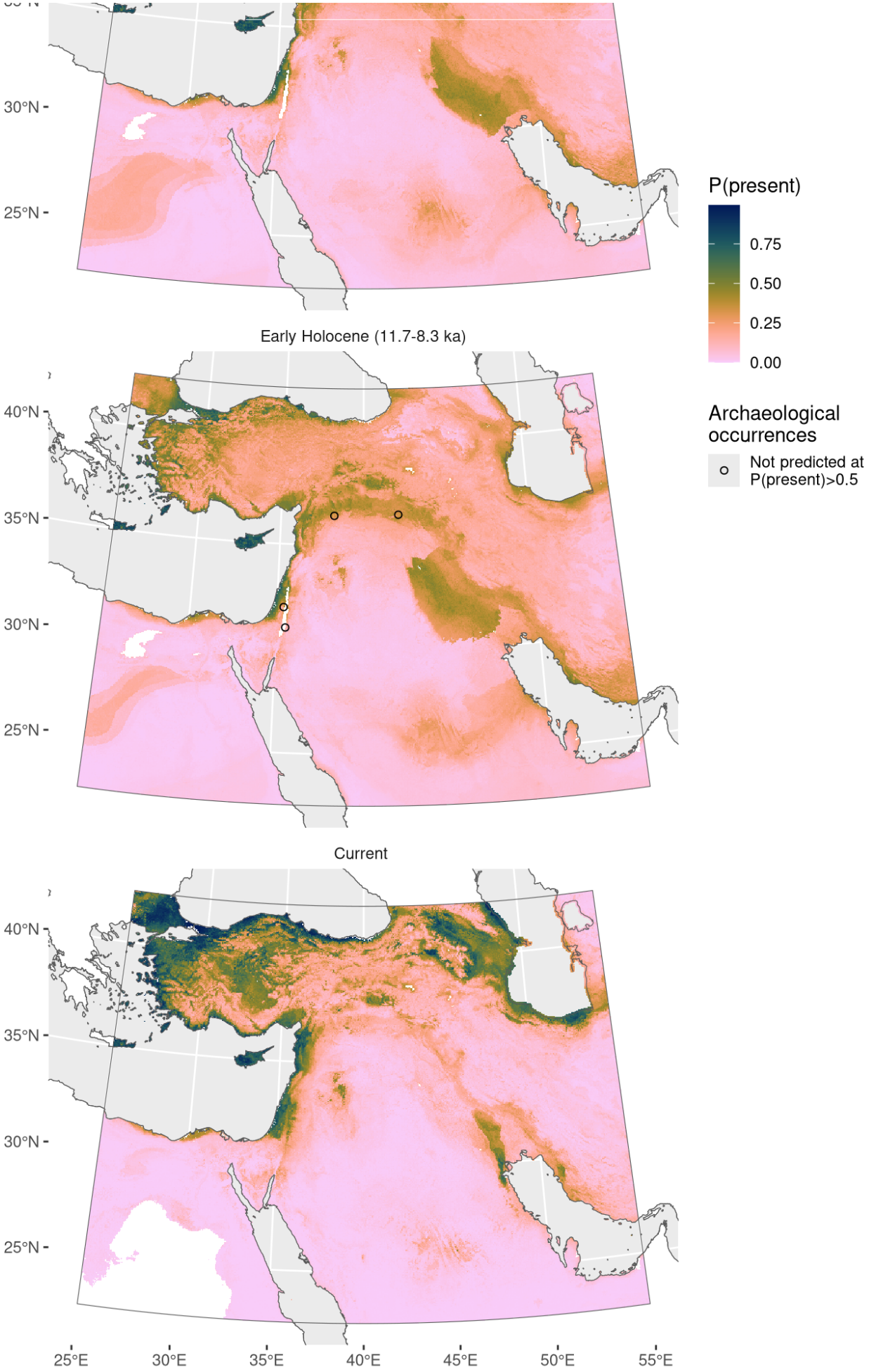


Figure 64: Predicted palaeodistributions of *Hordeum murinum*

Table 32: Archaeological occurrences of *Hordeum murinum*

Archaeological occurrences of *Hordeum murinum*

| Site | Age range | N assemblages | Average prop. | Source | Predicted? |
|---|---|---|---|---|---|
| Bølling-Allerød (14.7-12.9 ka) | | | | | |
| Abu Hureyra | 13.1–13.0 ka | 1 | 0.21% | ORIGINS | no |
| Early Holocene (11.7-8.3 ka) | | | | | |
| Netiv Hagdud | 11.6–10.6 ka | 1 | 0.13% | ORIGINS | no |
| Jerf el Ahmar | 11.4–10.7 ka | 1 | 2.55% | ORIGINS | no |
| El-Hemmeh | 11.1–10.5 ka | 1 | 0.32% | ORIGINS | no |
| Tell Maghzaliyeh | 9.0–8.2 ka | 1 | 29.97% | ORIGINS | no |

# *Hordeum spontaneum*

Including Hordeum vulgare.

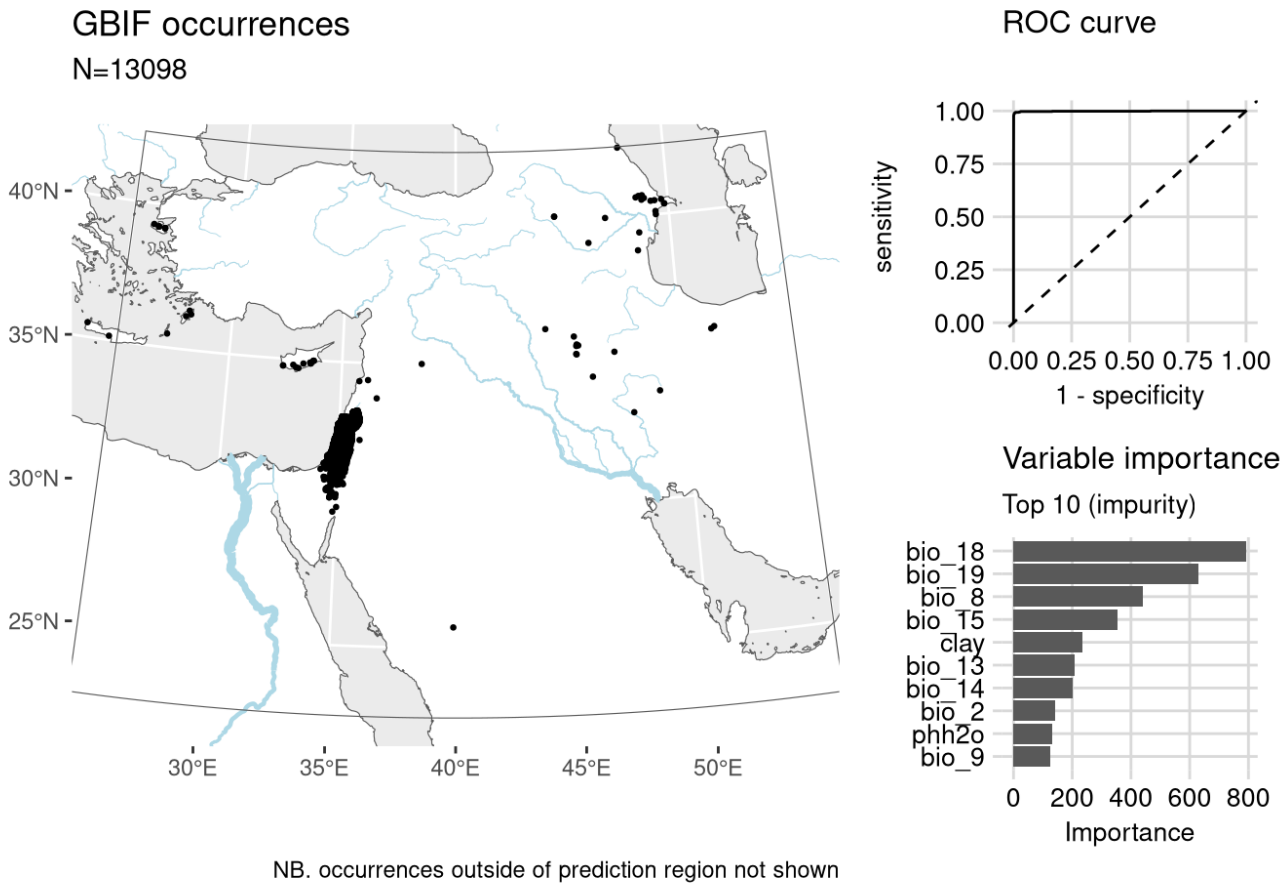


Figure 65: Fitted model summary for *Hordeum spontaneum*

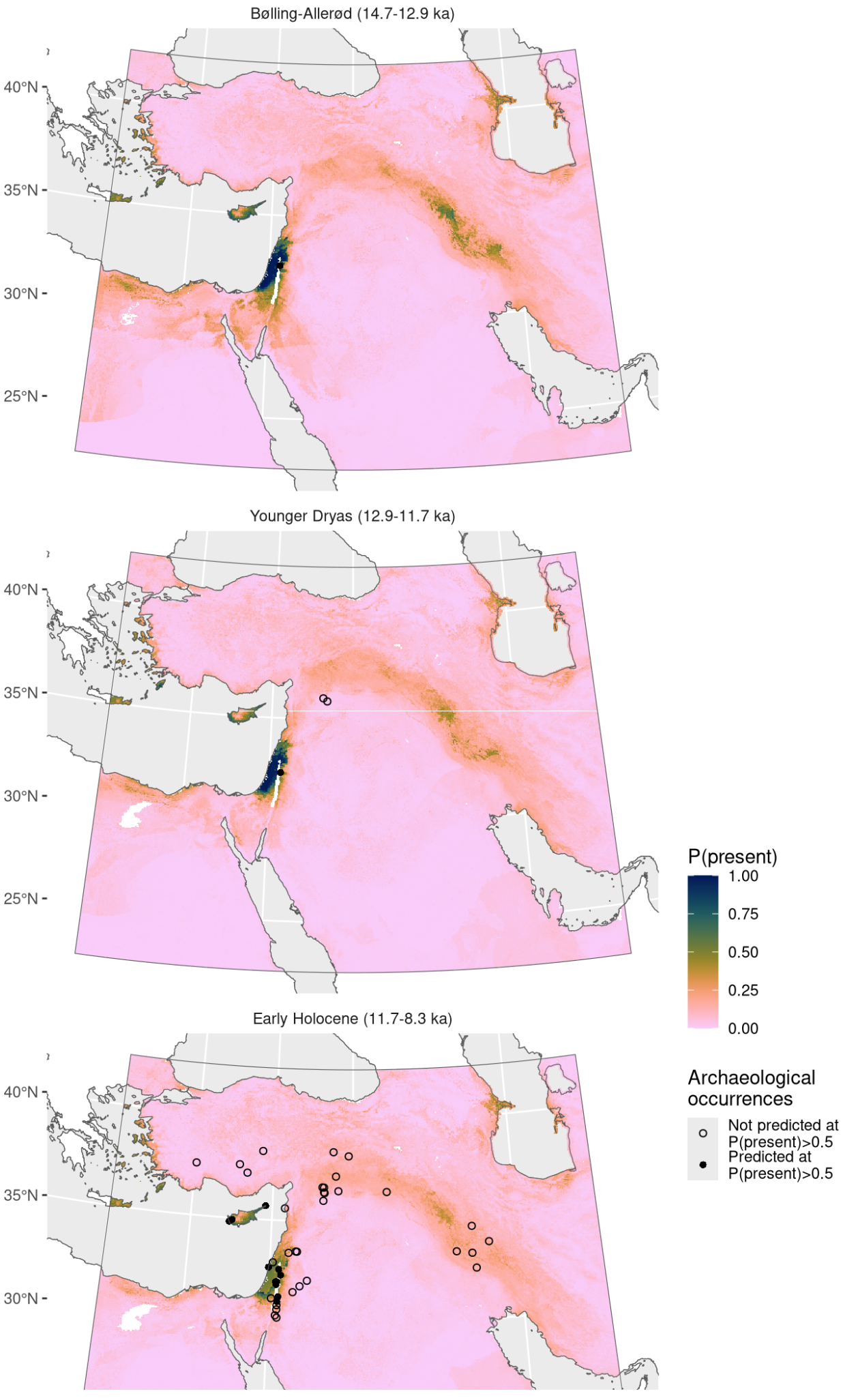
Bølling-Allerød (14.7-12.9 ka)
Younger Dryas (12.9-11.7 ka)
Early Holocene (11.7-8.3 ka)
40°N
35°N
30°N
25°N
P(present)
1.00
0.75
0.50
0.25
0.00
Archaeological occurrences
Not predicted at P(present)>0.5
Predicted at P(present)>0.5

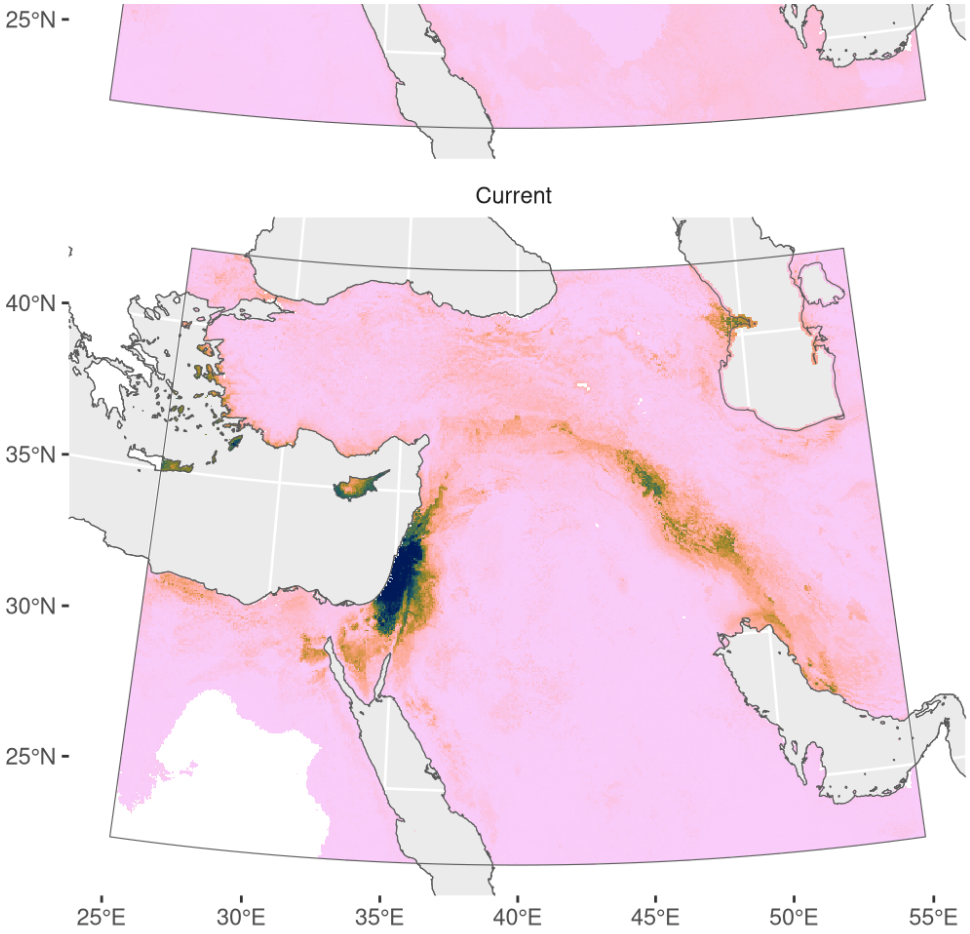


Figure 66: Predicted palaeodistributions of *Hordeum spontaneum*

Table 33: Archaeological occurrences of *Hordeum spontaneum*

Archaeological occurrences of *Hordeum spontaneum*

| Site | Age range | N assemblages | Average prop. | Source | Predicted? |
|---|---|---|---|---|---|
| Bølling-Allerød (14.7-12.9 ka) | | | | | |
| Wadi Hammeh 27 | 14.1–12.7 ka | 1 | 0.18% | ORIGINS | yes |
| Younger Dryas (12.9-11.7 ka) | | | | | |
| Iraq ed-Dubb | 13.2–12.2 ka | 1 | 0.59% | ORIGINS | yes |
| Abu Hureyra | 13.0–11.8 ka | 2 | 0.17% | ORIGINS | no |
| Mureybet | 12.1–11.9 ka | 1 | 0.18% | ORIGINS | no |
| Early Holocene (11.7-8.3 ka) | | | | | |

| | | | | | |
|---|---|---|---|---|---|
| Tell es-Sultan | 12.2–8.2 ka | 2 | 17.05% | ORIGINS | yes |
| Hayonim Cave | 12.2–10.9 ka | 1 | 100.00% | ORIGINS | no |
| Iraq ed-Dubb | 11.7–11.2 ka | 1 | 0.18% | ORIGINS | yes |
| Mureybet | 11.7–10.8 ka | 2 | 1.05% | ORIGINS | no |
| Netiv Hagdud | 11.6–10.6 ka | 1 | 29.33% | ORIGINS | yes |
| Gesher | 11.5–11.2 ka | 1 | 0.50% | ORIGINS | yes |
| Jerf el Ahmar | 11.4–10.7 ka | 1 | 0.01% | ORIGINS | no |
| Zahrat adh-Dhra 2 | 11.4–10.4 ka | 1 | 0.07% | ORIGINS | yes |
| Chogha Golan | 11.2–9.7 ka | 10 | 4.89% | ORIGINS | no |
| Gilgal I | 11.2–11.2 ka | 1 | 68.24% | ORIGINS | yes |
| Tell 'Abr | 11.2–10.8 ka | 1 | 4.20% | ORIGINS | no |
| El-Hemmeh | 11.1–10.5 ka | 1 | 4.65% | ORIGINS | yes |
| Kastros | 10.8–9.9 ka | 1 | 2.36% | ORIGINS | yes |
| Kissonerga Mosphilia | 10.8–10.3 ka | 1 | 1.00% | ADEMNES | yes |
| Göbekli Tepe | 10.8–9.6 ka | 1 | 16.00% | ORIGINS | no |
| Dja'de | 10.7–10.2 ka | 1 | 0.01% | ORIGINS | no |
| Sheikh-e Abad | 10.7–8.4 ka | 1 | 0.12% | ADEMNES | no |
| Mylouthkia | 10.6–8.8 ka | 2 | 11.31% | ORIGINS | yes |
| Cafer Höyük | 10.6–9.1 ka | 2 | 0.14% | ORIGINS | no |
| East Chia Sabz | 10.4–9.6 ka | 1 | 7.43% | ORIGINS | no |

| | | | | | |
|---|---|---|---|---|---|
| Tepe Abdul Hosein | 10.3–9.1 ka | 1 | 66.67% | ORIGINS | no |
| Wadi Jilat 7 | 10.2–9.3 ka | 3 | 1.33% | ORIGINS | no |
| Hacılar | 10.2–9.4 ka | 1 | 1.10% | ORIGINS | no |
| Tell Aswad | 10.2–9.3 ka | 1 | 0.04% | ORIGINS | no |
| Nahal Hemar | 10.1–9.3 ka | 1 | 0.33% | ORIGINS | no |
| Ali Kosh | 10.1–8.0 ka | 3 | 1.29% | ORIGINS | no |
| Beidha | 10.1–9.5 ka | 1 | 30.11% | ORIGINS | no |
| Aşıklı Höyük | 9.9–9.4 ka | 1 | 0.06% | ORIGINS | no |
| Çayönü | 9.9–8.8 ka | 4 | 0.43% | ORIGINS | no |
| Halula | 9.9–9.5 ka | 1 | 0.22% | ORIGINS | no |
| Ais Giorkis | 9.6–9.4 ka | 1 | 4.68% | ORIGINS | yes |
| Wadi Fidan A | 9.5–8.6 ka | 1 | 3.06% | ORIGINS | no |
| Sabi Abyad II | 9.5–8.8 ka | 1 | 0.51% | ORIGINS | no |
| Tell Ghoraifé | 9.5–8.6 ka | 1 | 0.10% | ORIGINS | no |
| Basta | 9.4–9.2 ka | 1 | 3.93% | ORIGINS | no |
| Ras Shamra | 9.4–8.3 ka | 2 | 0.50% | ORIGINS | no |
| Wadi Fidan | 9.4–8.4 ka | 2 | 3.00% | ADEMNES | no |
| Dhuweila | 9.4–9.1 ka | 1 | 3.12% | ORIGINS | no |
| Can Hasan III | 9.4–8.6 ka | 1 | 0.88% | ORIGINS | no |
| Azraq 31 | 9.3–9.2 ka | 1 | 2.29% | ORIGINS | no |
| Tell Ramad | 9.3–8.6 ka | 2 | 0.16% | ORIGINS | no |
| Çatalhöyük | 9.2–8.3 ka | 1 | 0.00% | ORIGINS | no |
| Wadi Fidan C | 9.2–8.2 ka | 1 | 2.83% | ORIGINS | no |
| Wadi Jilat 13 | 9.1–8.4 ka | 3 | 0.52% | ORIGINS | no |
| Atlit-Yam | 9.0–8.0 ka | 1 | 1.52% | ORIGINS | yes |
| Tell Maghzaliyeh | 9.0–8.2 ka | 1 | 12.53% | ORIGINS | no |

# *Lathyrus aphaca*

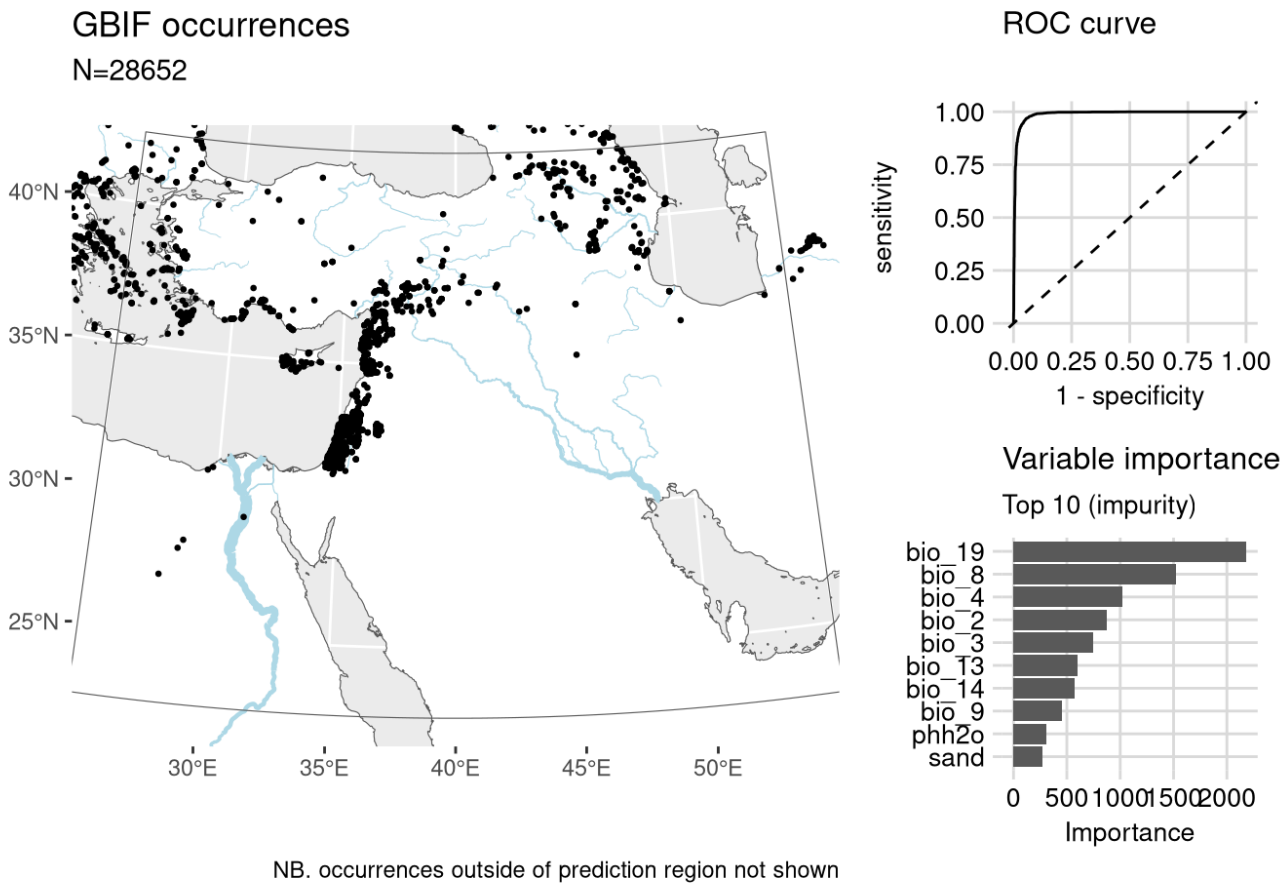


Figure 67: Fitted model summary for *Lathyrus aphaca*

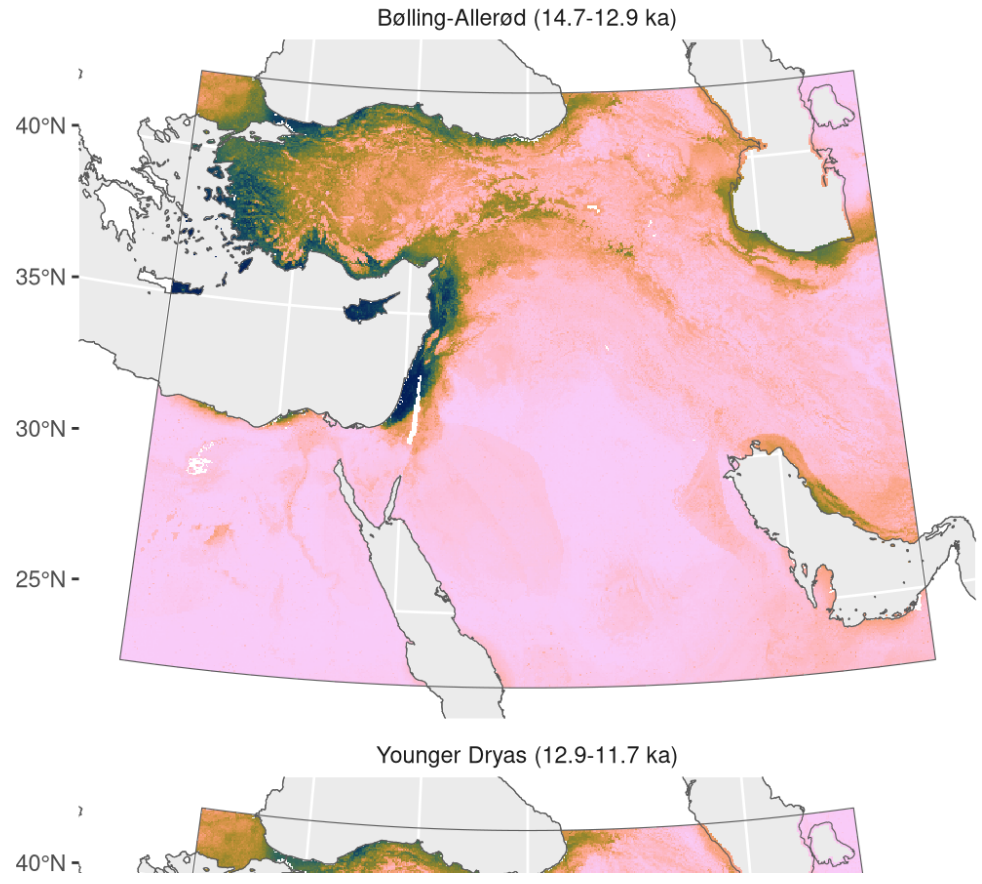

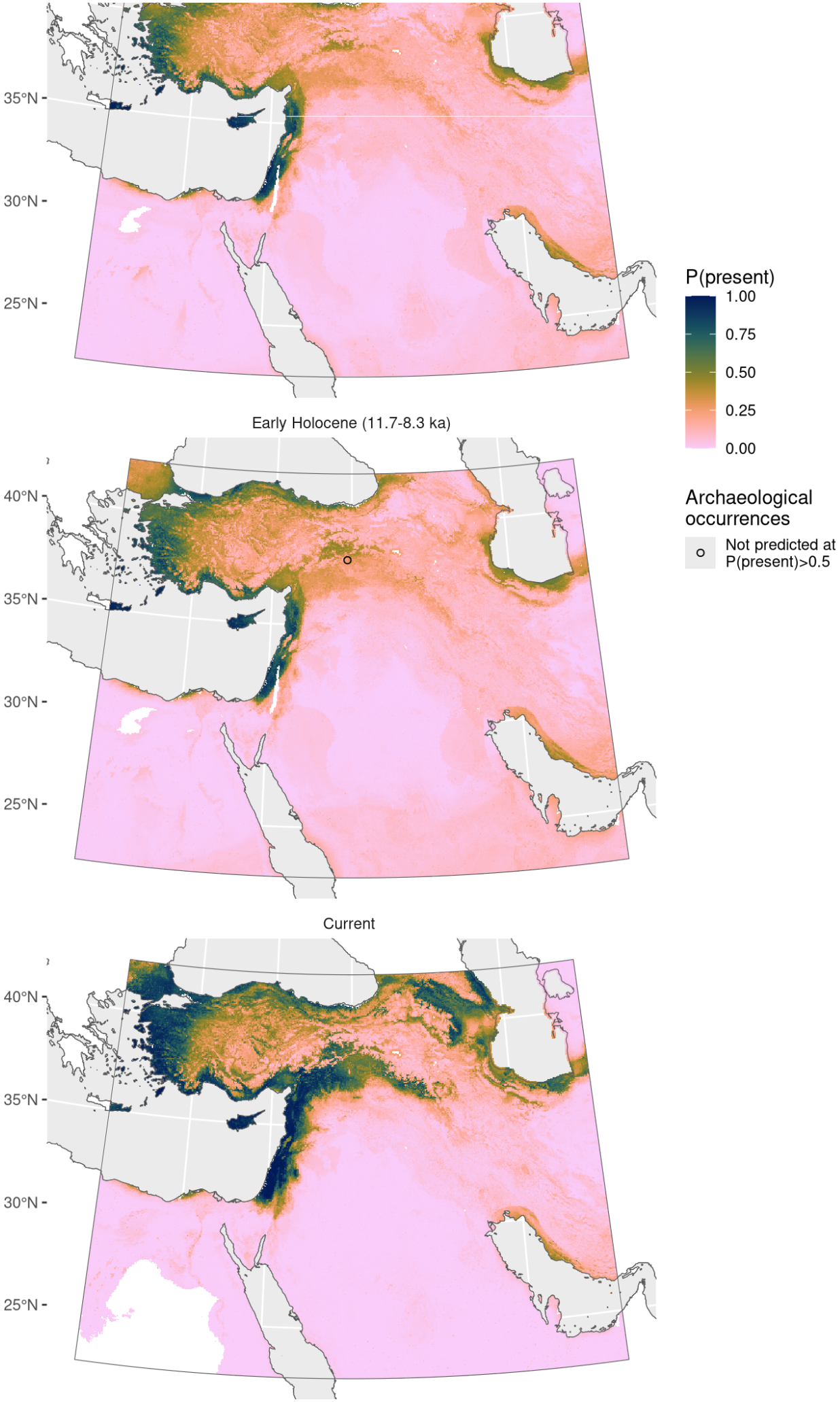
35°N
30°N
25°N
Early Holocene (11.7-8.3 ka)
40°N
35°N
30°N
25°N
Current
40°N
35°N
30°N
25°N
P(present)
1.00
0.75
0.50
0.25
0.00
Archaeological occurrences
Not predicted at P(present)>0.5

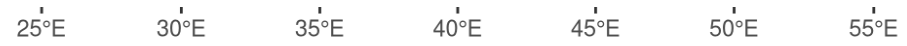


Figure 68: Predicted palaeodistributions of *Lathyrus aphaca*

Table 34: Archaeological occurrences of *Lathyrus aphaca*

Archaeological occurrences of *Lathyrus aphaca*

| Site | Age range | N assemblages | Average prop. | Source | Predicted? |
|---|---|---|---|---|---|
| Early Holocene (11.7-8.3 ka) | | | | | |
| Çayönü | 10.2–8.8 ka | 4 | 1.51% | ORIGINS | no |

# *Lathyrus oleraceus*

Including Pisum sativum and Pisum elatius.

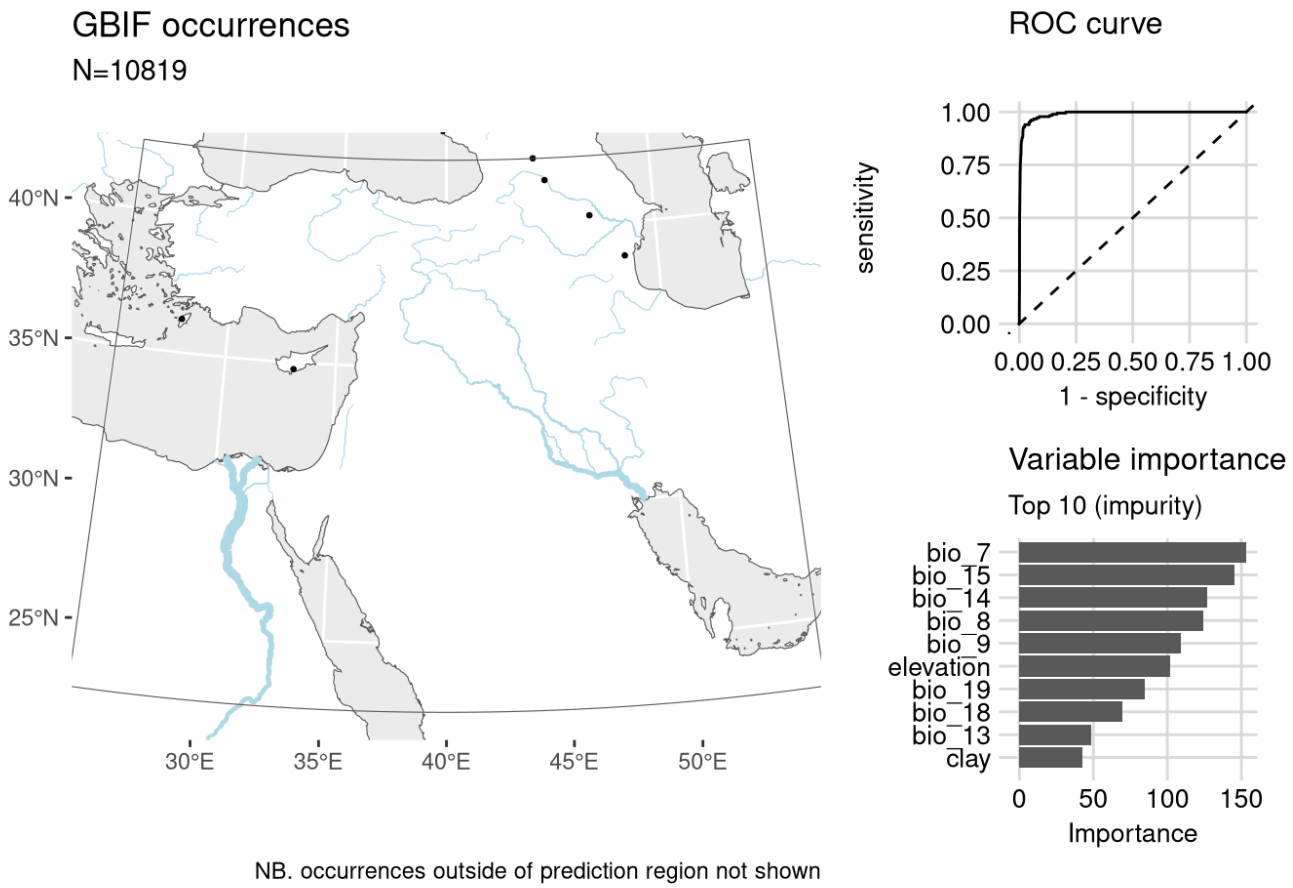


Figure 69: Fitted model summary for *Lathyrus oleraceus*

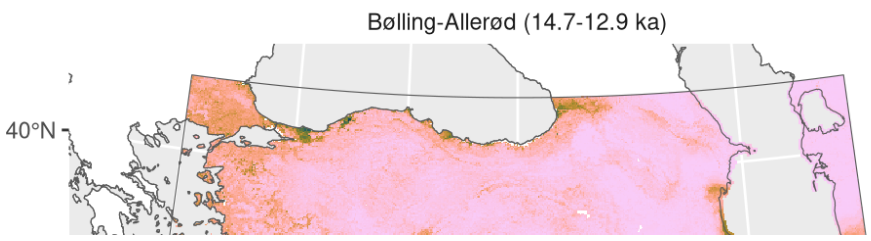

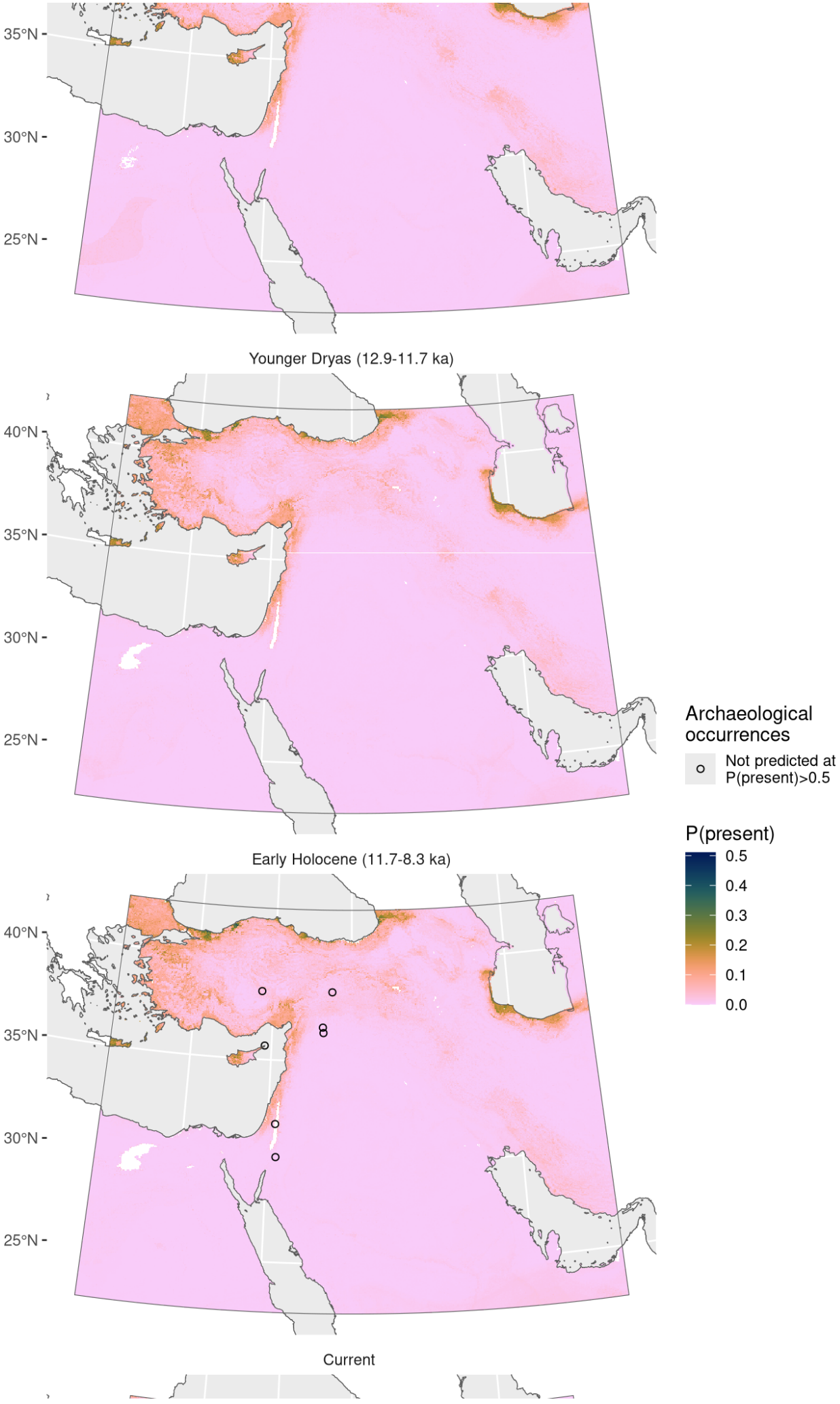
35°N
30°N
25°N
Younger Dryas (12.9-11.7 ka)
40°N
35°N
30°N
25°N
Early Holocene (11.7-8.3 ka)
40°N
35°N
30°N
25°N
Current
Archaeological occurrences
Not predicted at P(present)>0.5
P(present)
0.5
0.4
0.3
0.2
0.1
0.0

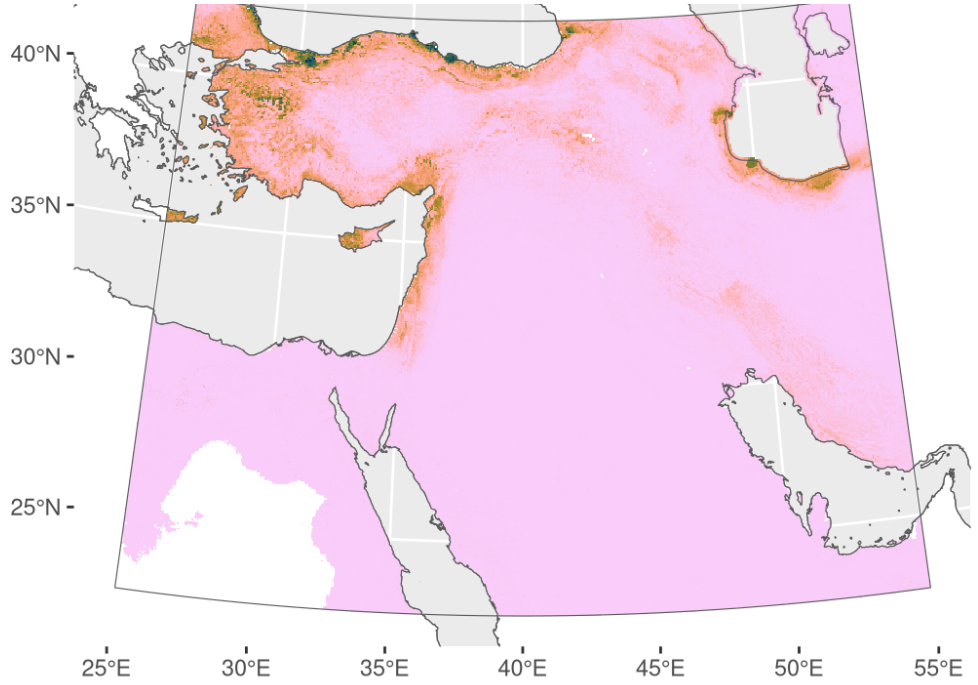


Figure 70: Predicted palaeodistributions of *Lathyrus oleraceus*

Table 35: Archaeological occurrences of *Lathyrus oleraceus*

Archaeological occurrences of *Lathyrus oleraceus*

| Site | Age range | N assemblages | Average prop. | Source | Predicted? |
|---|---|---|---|---|---|
| Early Holocene (11.7-8.3 ka) | | | | | |
| Jerf el Ahmar | 11.4–10.7 ka | 1 | 0.01% | ORIGINS | no |
| Kastros | 10.8–9.9 ka | 1 | 0.37% | ORIGINS | no |
| Dja'de | 10.7–10.2 ka | 1 | 0.04% | ORIGINS | no |
| Cafer Höyük | 10.6–9.7 ka | 1 | 0.42% | ORIGINS | no |
| Aşıklı Höyük | 9.9–9.4 ka | 1 | 0.01% | ORIGINS | no |
| Basta | 9.4–9.2 ka | 2 | 1.94% | ORIGINS | no |
| Tell es-Sultan | 8.9–8.2 ka | 1 | 4.52% | ORIGINS | no |

# *Lathyrus sativus*

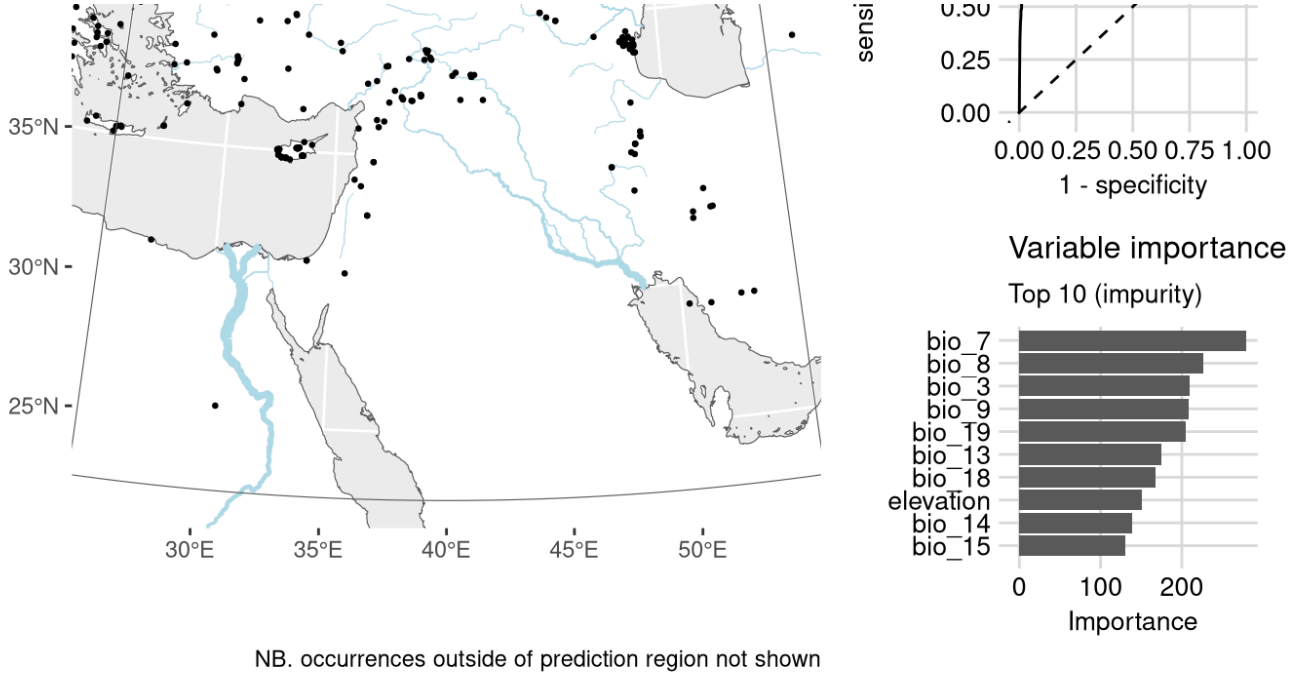


Figure 71: Fitted model summary for *Lathyrus sativus*

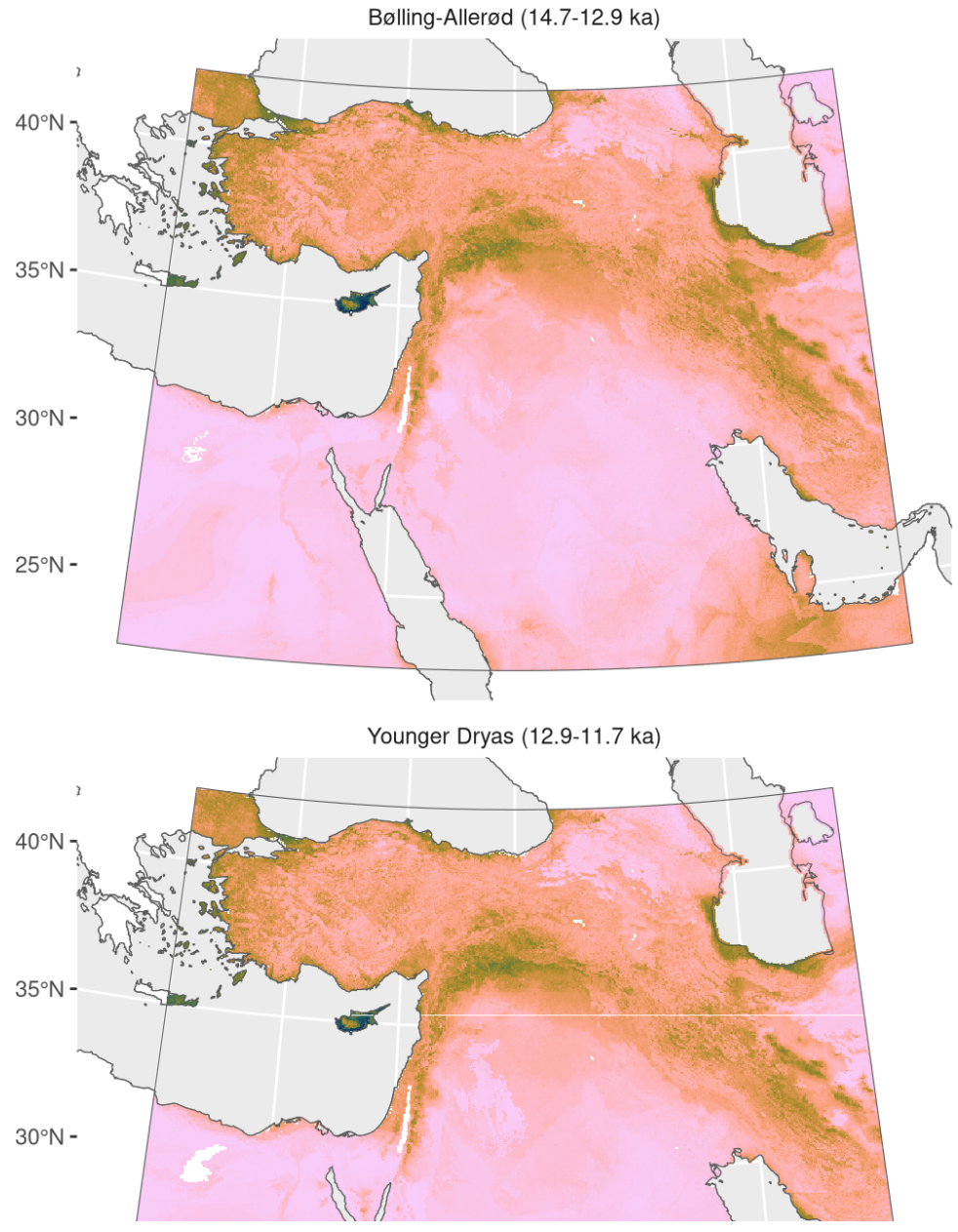

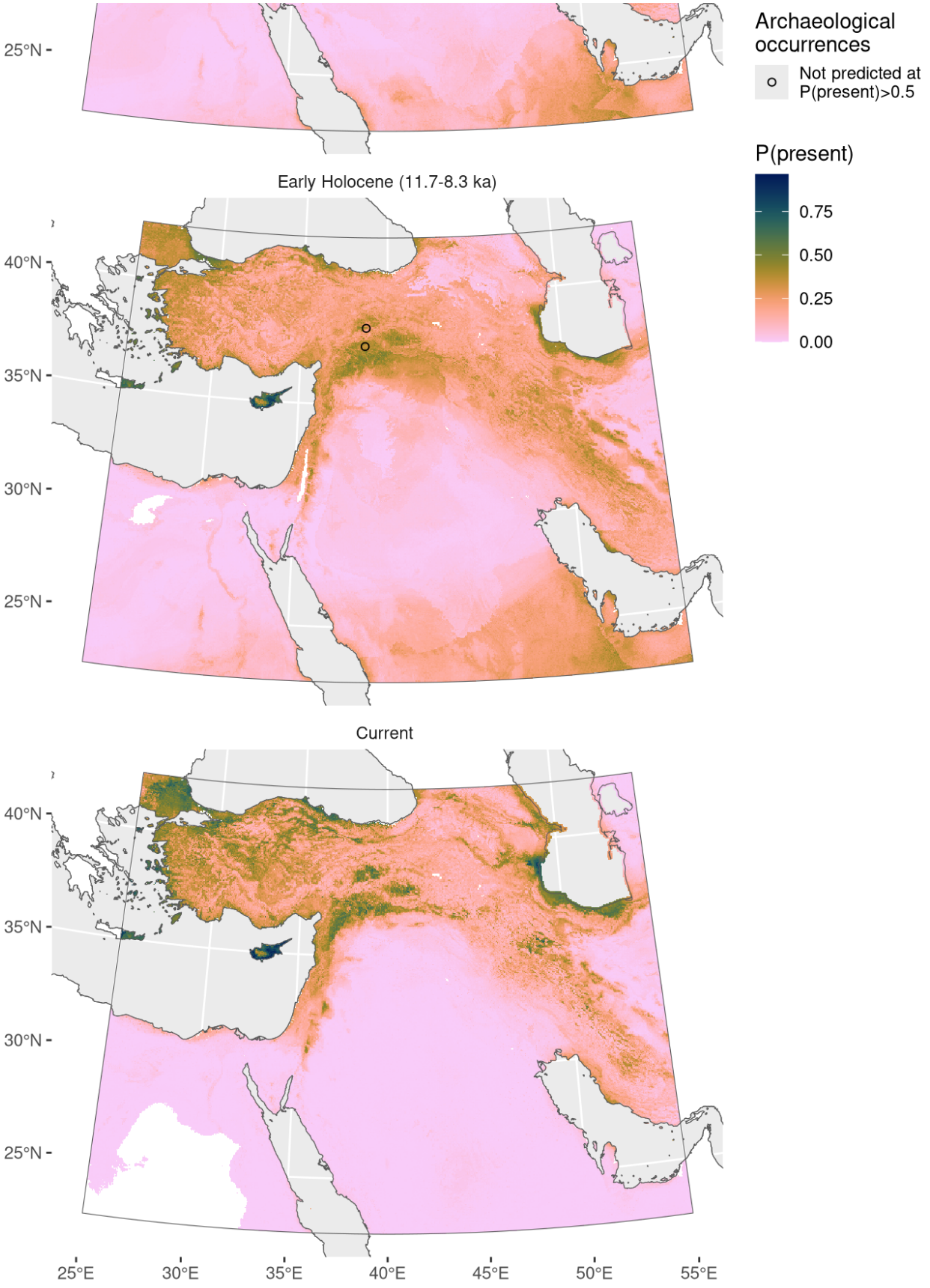


Figure 72: Predicted palaeodistributions of *Lathyrus sativus*

Table 36: Archaeological occurrences of *Lathyrus sativus*

Archaeological occurrences of *Lathyrus sativus*

| Site | Age range | N assemblages | Average prop. | Source | Predicted? |
|---|---|---|---|---|---|

| | | | | | |
|---|---|---|---|---|---|
| Early Holocene (11.7-8.3 ka) | | | | | |
| Cafer Höyük | 10.6–9.1 ka | 3 | 0.96% | ORIGINS | no |
| Nevalı Çori | 10.4–10.2 ka | 1 | 0.37% | ORIGINS | no |

# *Lepidium perfoliatum*

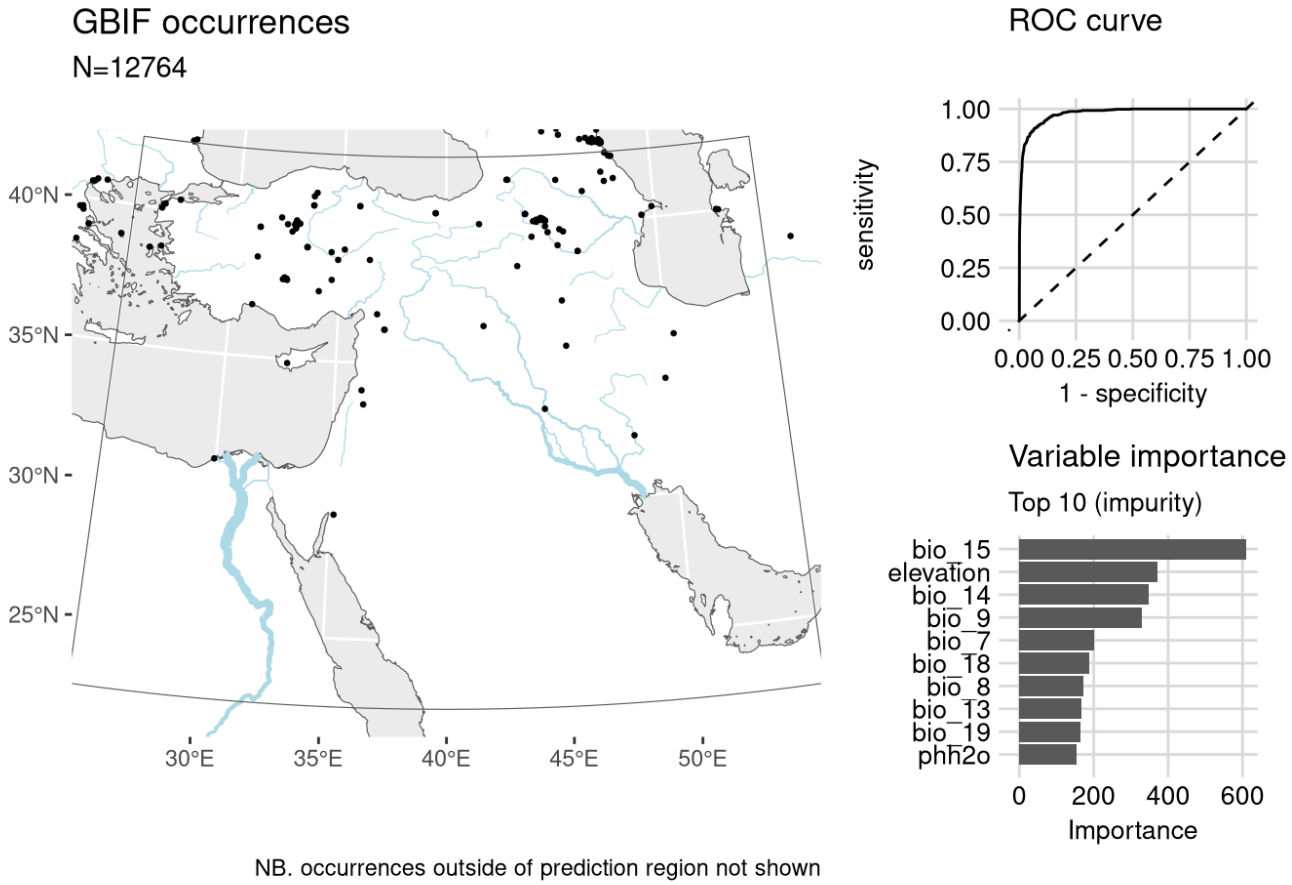


Figure 73: Fitted model summary for *Lepidium perfoliatum*

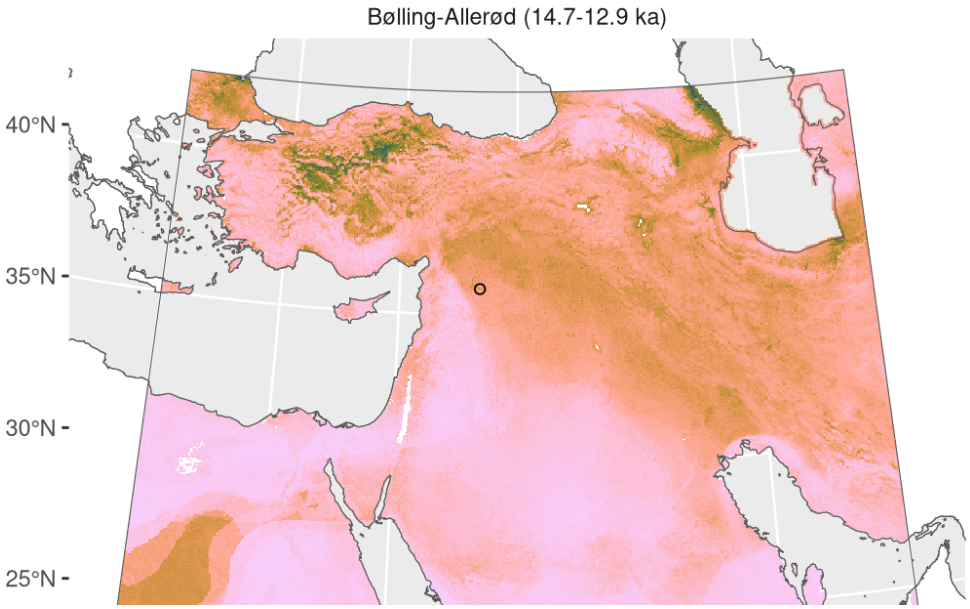

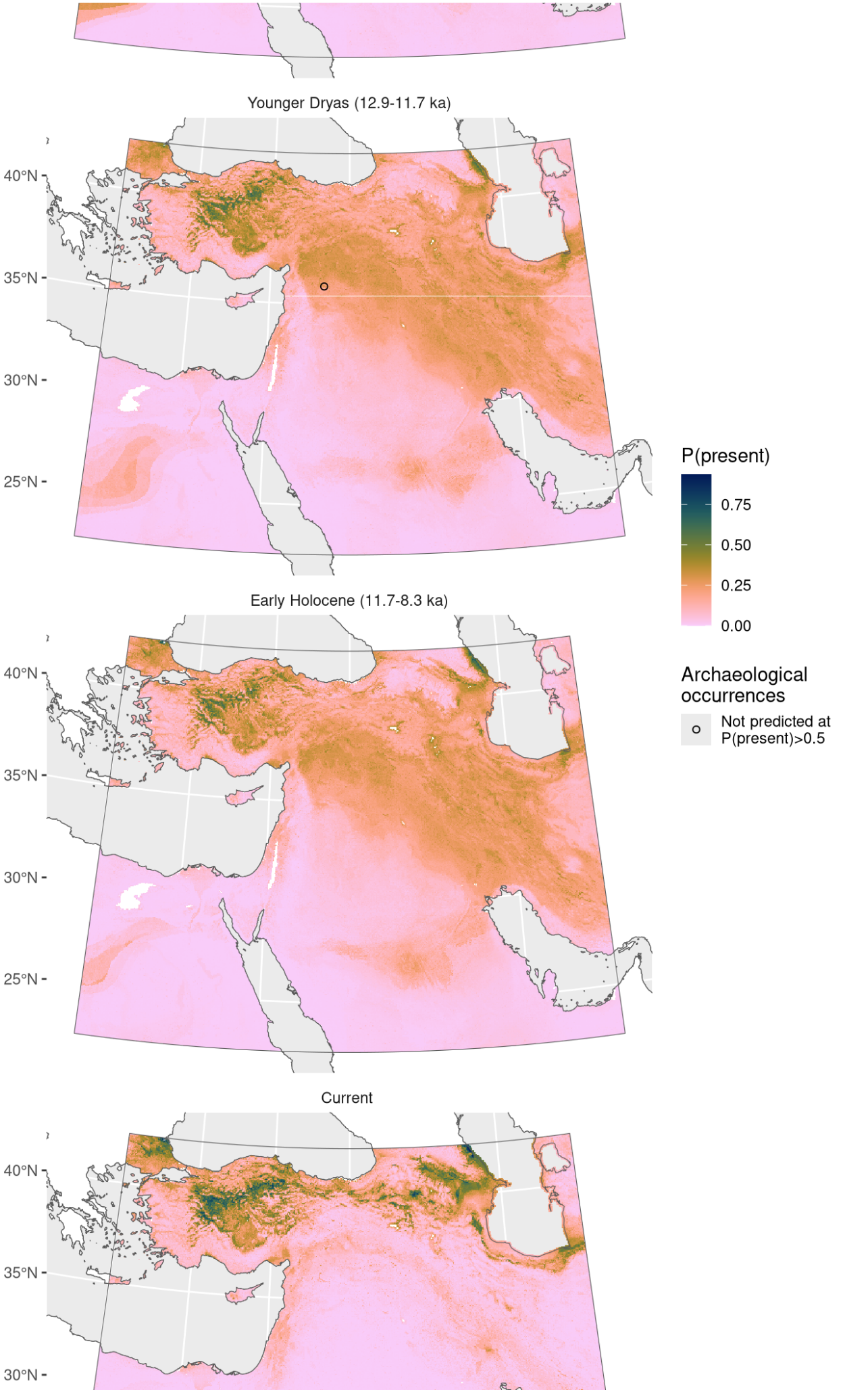
Younger Dryas (12.9-11.7 ka)
Early Holocene (11.7-8.3 ka)
Current
40°N
35°N
30°N
25°N
P(present)
0.75
0.50
0.25
0.00
Archaeological occurrences
Not predicted at P(present)>0.5

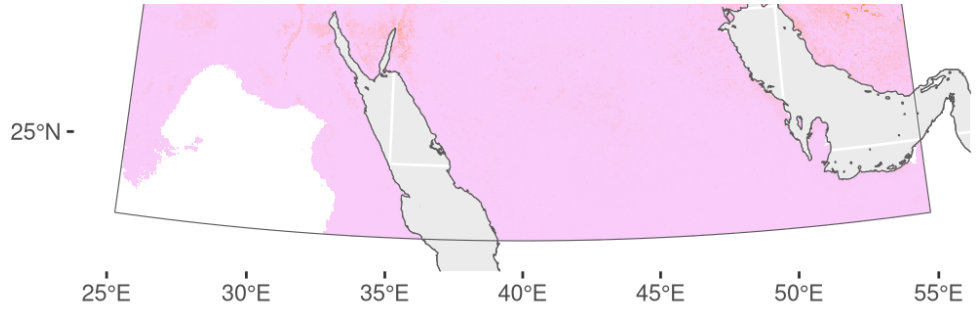


Figure 74: Predicted palaeodistributions of *Lepidium perfoliatum*

Table 37: Archaeological occurrences of *Lepidium perfoliatum*

Archaeological occurrences of *Lepidium perfoliatum*

| Site | Age range | N assemblages | Average prop. | Source | Predicted? |
|---|---|---|---|---|---|
| Bølling-Allerød (14.7-12.9 ka) | | | | | |
| Abu Hureyra | 13.1–13.0 ka | 1 | 2.65% | ORIGINS | no |
| Younger Dryas (12.9-11.7 ka) | | | | | |
| Abu Hureyra | 13.0–11.8 ka | 2 | 1.12% | ORIGINS | no |

# *Linum bienne*

Including Linum usitatissimum.

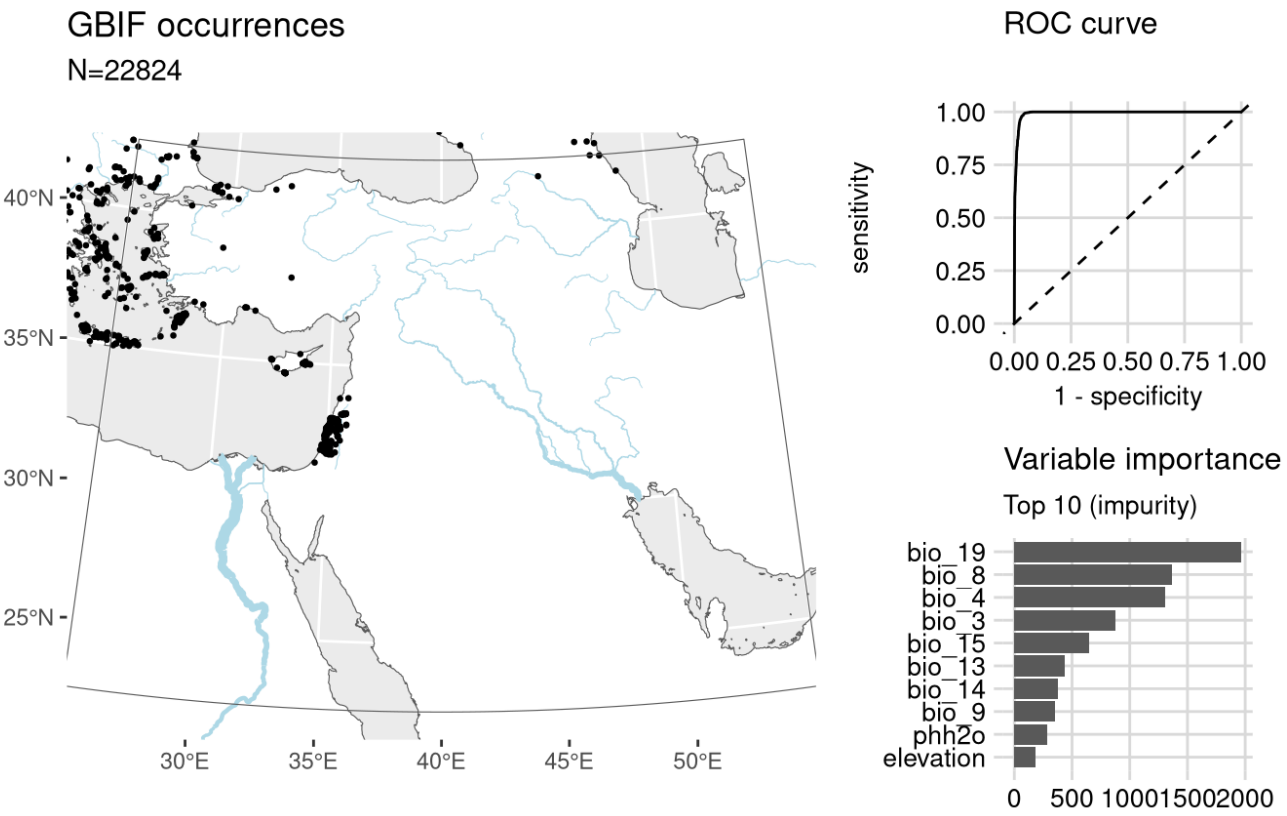

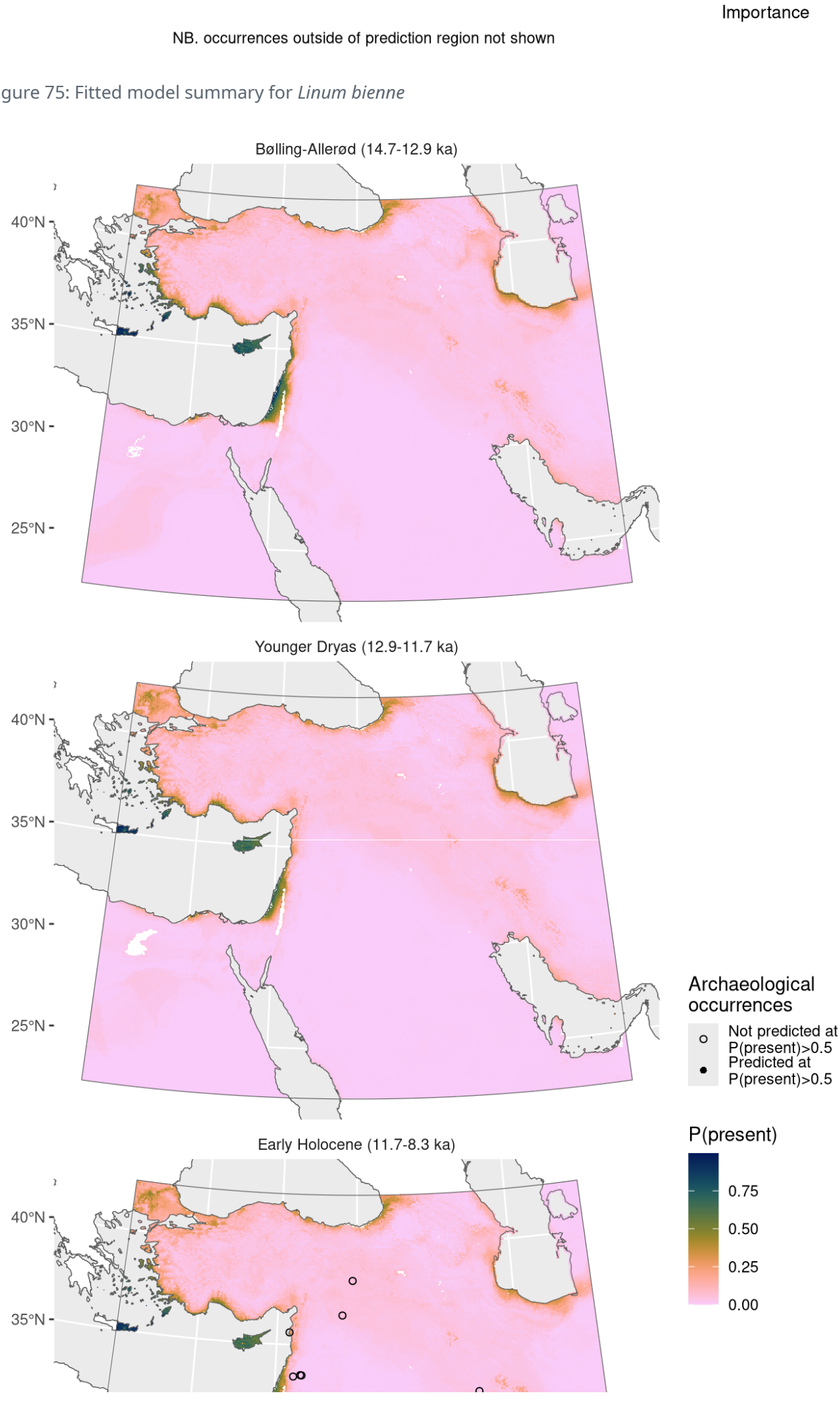


Figure 75: Fitted model summary for *Linum bienne*

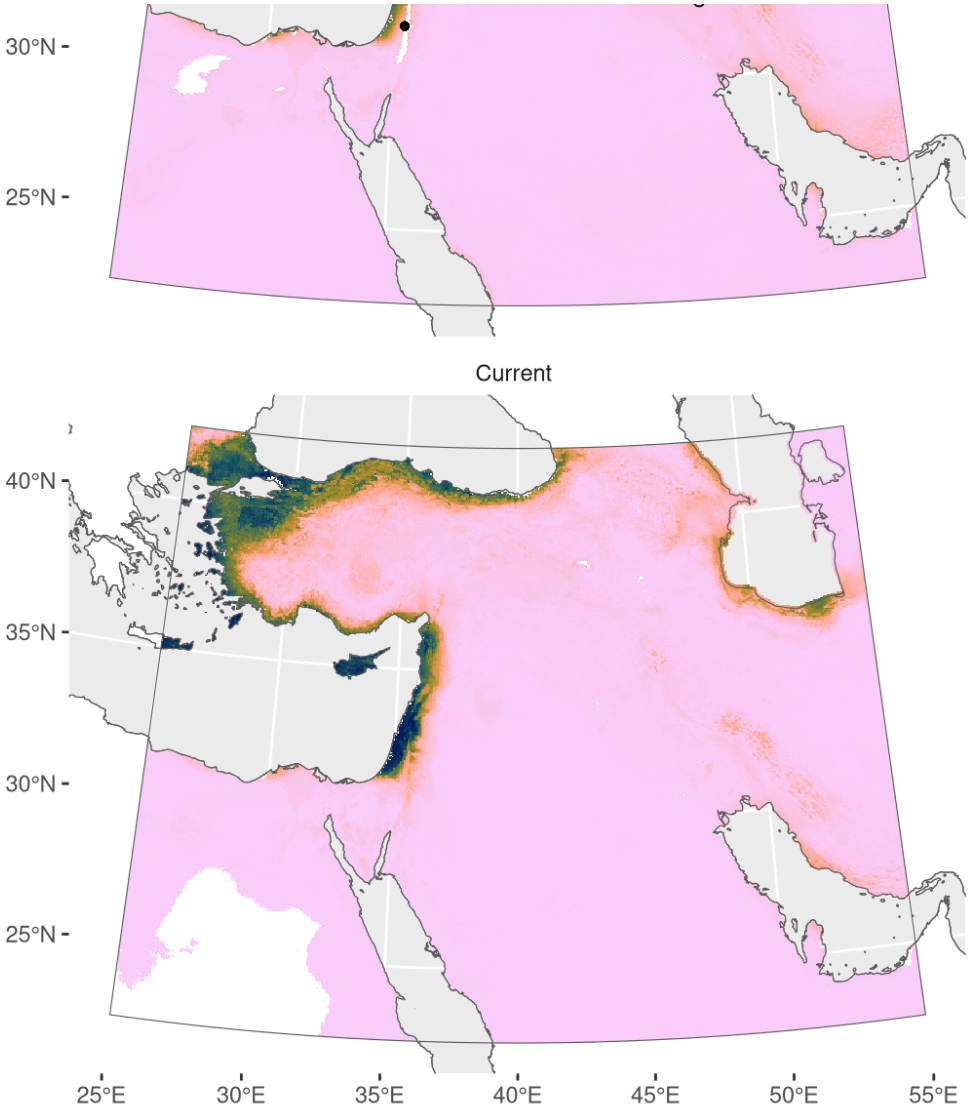


Figure 76: Predicted palaeodistributions of *Linum bienne*

Table 38: Archaeological occurrences of *Linum bienne*

Archaeological occurrences of *Linum bienne*

| Site | Age range | N assemblages | Average prop. | Source | Predicted? |
|---|---|---|---|---|---|
| Early Holocene (11.7-8.3 ka) | | | | | |
| Tell Aswad | 10.2–9.3 ka | 1 | 0.04% | ORIGINS | no |
| Tell Ghoraifé | 10.1–8.6 ka | 2 | 0.87% | ORIGINS | no |
| Ali Kosh | 10.1–8.0 ka | 3 | 0.02% | ORIGINS | no |
| Sabi Abyad II | 9.5–8.8 ka | 1 | 45.23% | ORIGINS | no |
| Ras Shamra | 9.4–8.3 ka | 2 | 0.31% | ORIGINS | no |
| Tell Ramad | 9.3–8.6 ka | 2 | 0.35% | ORIGINS | no |
| Çayönü | 9.2–8.8 ka | 2 | 4.38% | ORIGINS | no |

| | | | | | |
|---|---|---|---|---|---|
| Tell es-Sultan | 8.9–8.2 ka | 1 | 0.01% | ORIGINS | yes |

# *Lolium rigidum*

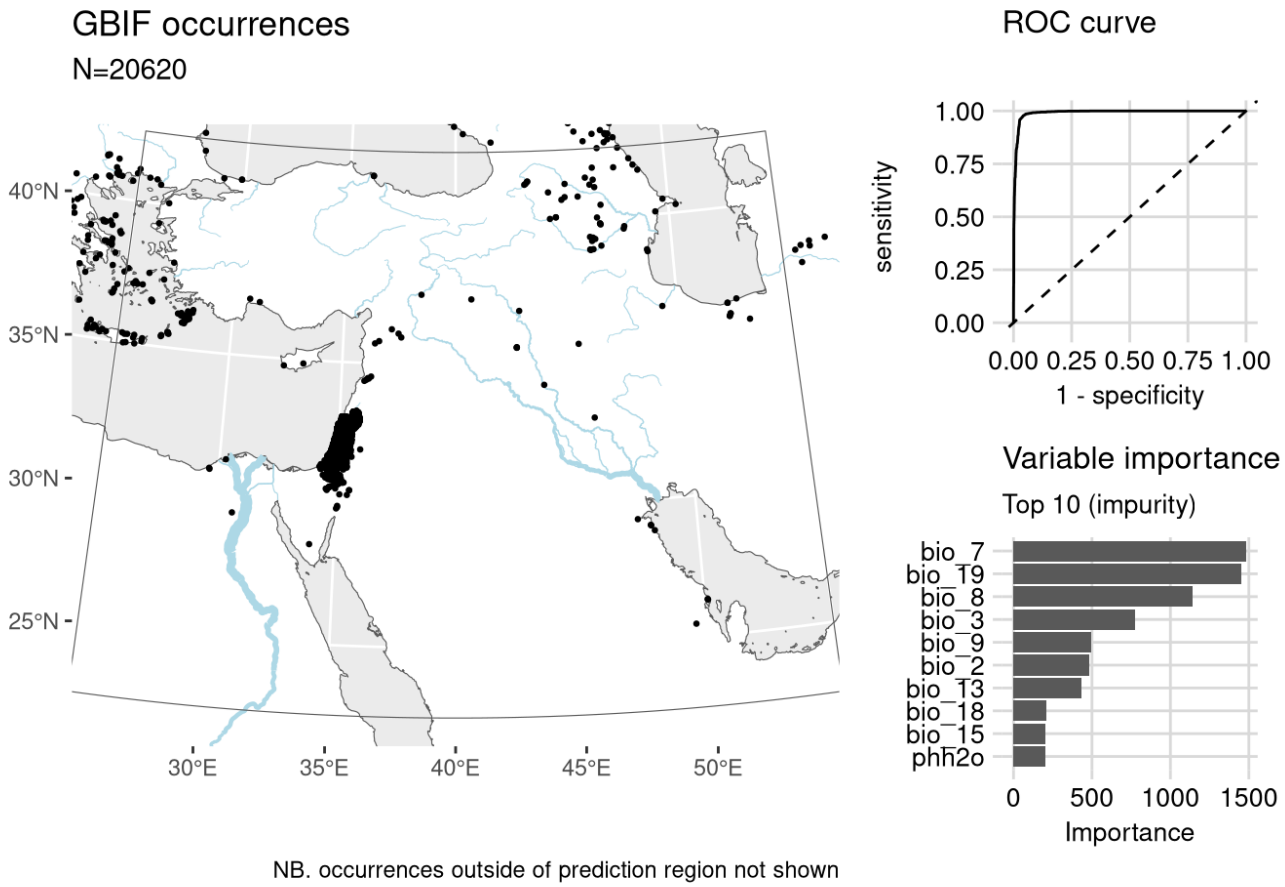


Figure 77: Fitted model summary for *Lolium rigidum*

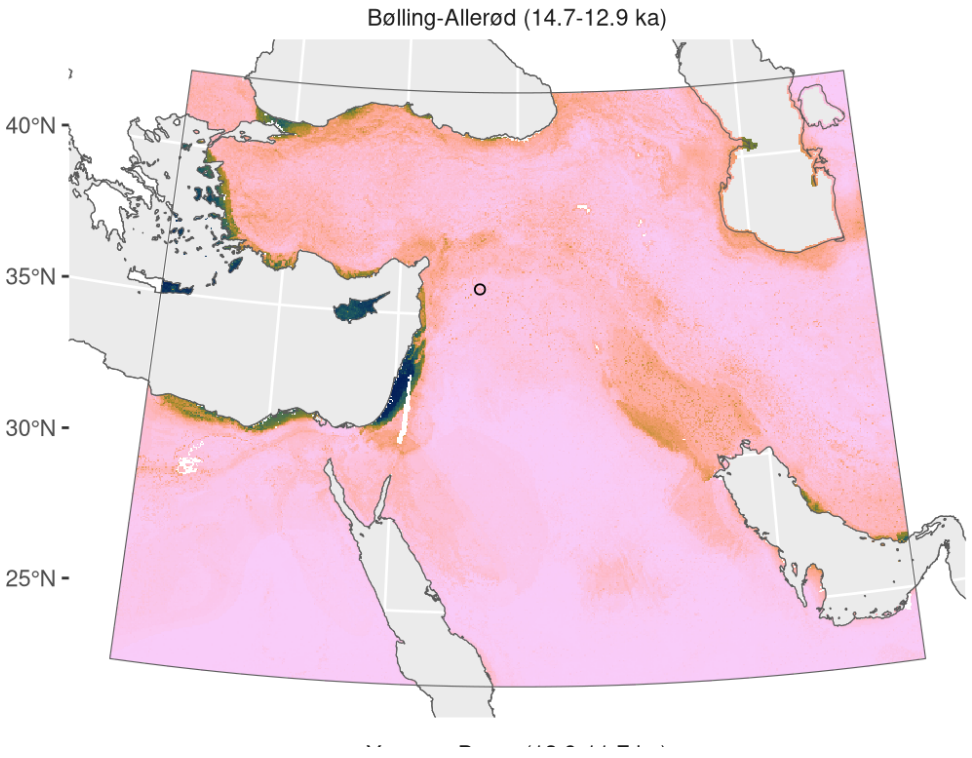

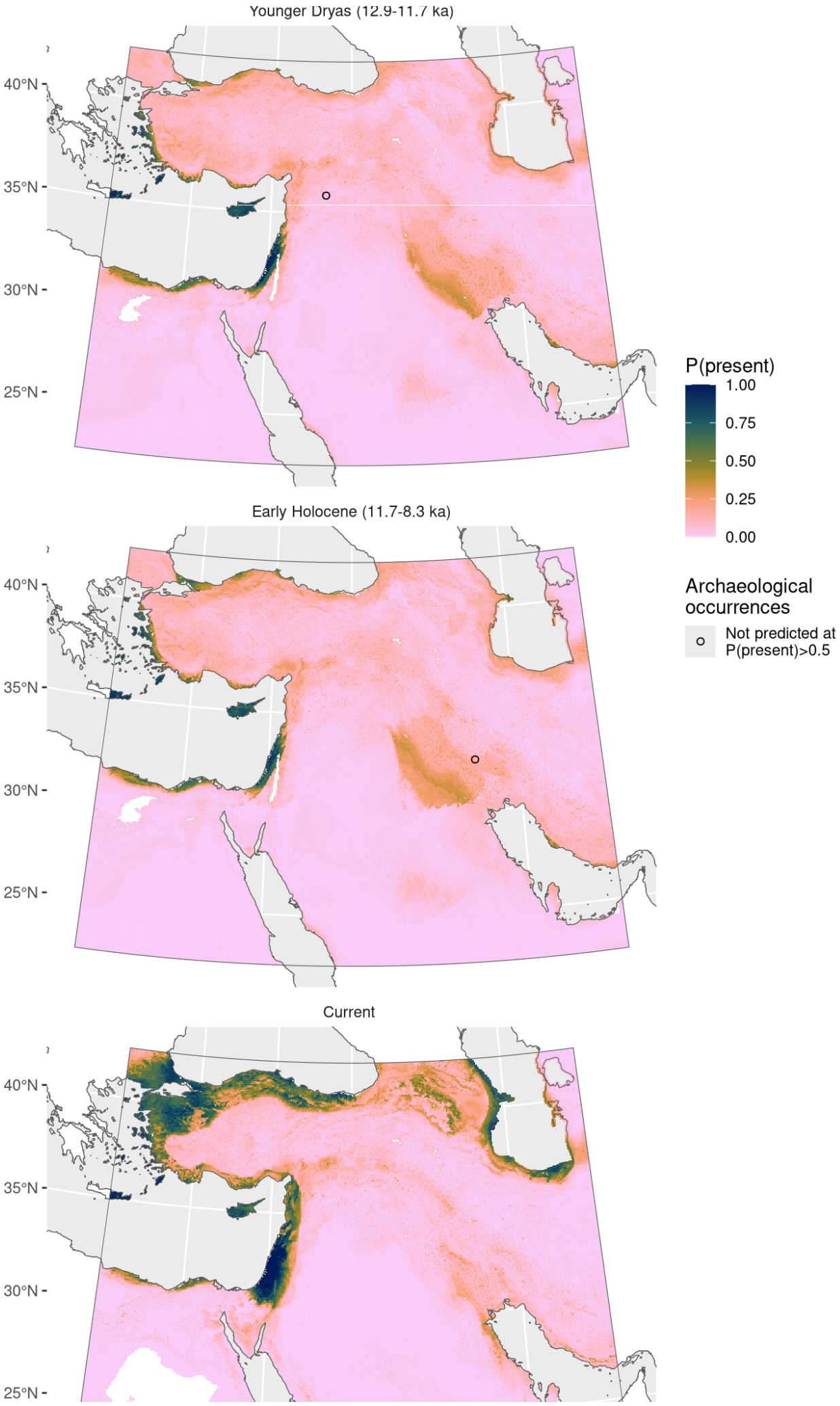
Younger Dryas (12.9-11.7 ka)
Early Holocene (11.7-8.3 ka)
Current
40°N
35°N
30°N
25°N
P(present)
1.00
0.75
0.50
0.25
0.00
Archaeological occurrences
Not predicted at P(present)>0.5

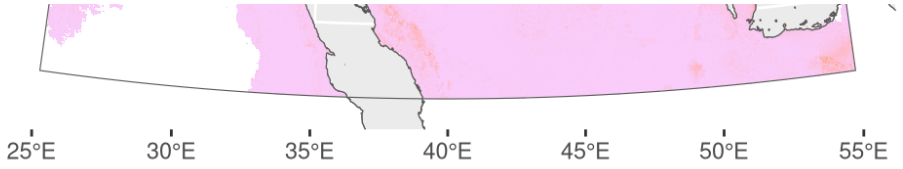


Figure 78: Predicted palaeodistributions of *Lolium rigidum*

Table 39: Archaeological occurrences of *Lolium rigidum*

Archaeological occurrences of *Lolium rigidum*

| Site | Age range | N assemblages | Average prop. | Source | Predicted? |
|---|---|---|---|---|---|
| Bølling-Allerød (14.7-12.9 ka) | | | | | |
| Abu Hureyra | 13.1–13.0 ka | 1 | 0.05% | ORIGINS | no |
| Younger Dryas (12.9-11.7 ka) | | | | | |
| Abu Hureyra | 12.1–11.8 ka | 1 | 0.15% | ORIGINS | no |
| Early Holocene (11.7-8.3 ka) | | | | | |
| Ali Kosh | 10.1–8.0 ka | 3 | 0.95% | ORIGINS | no |

# *Lolium temulentum*

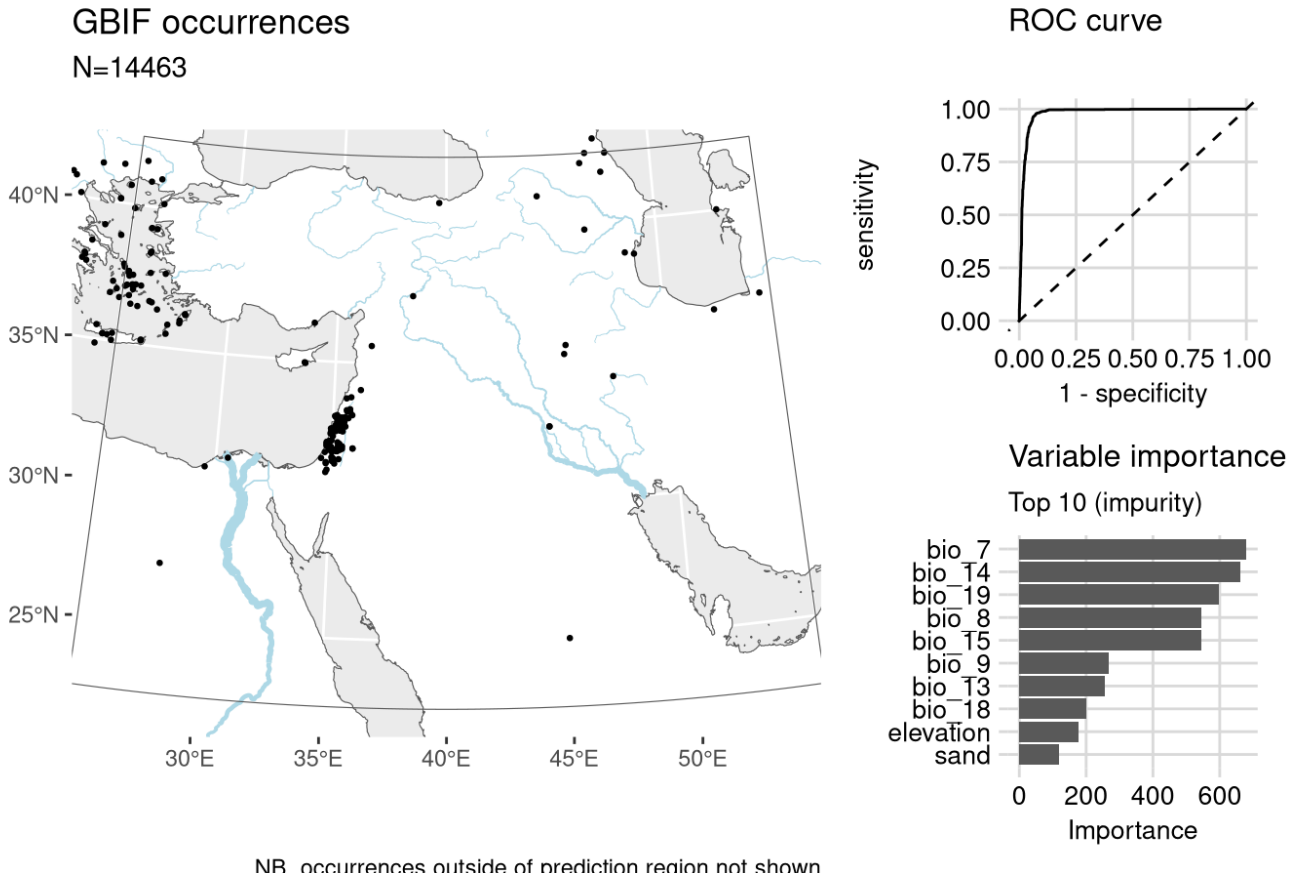

Figure 79: Fitted model summary for *Lolium temulentum*

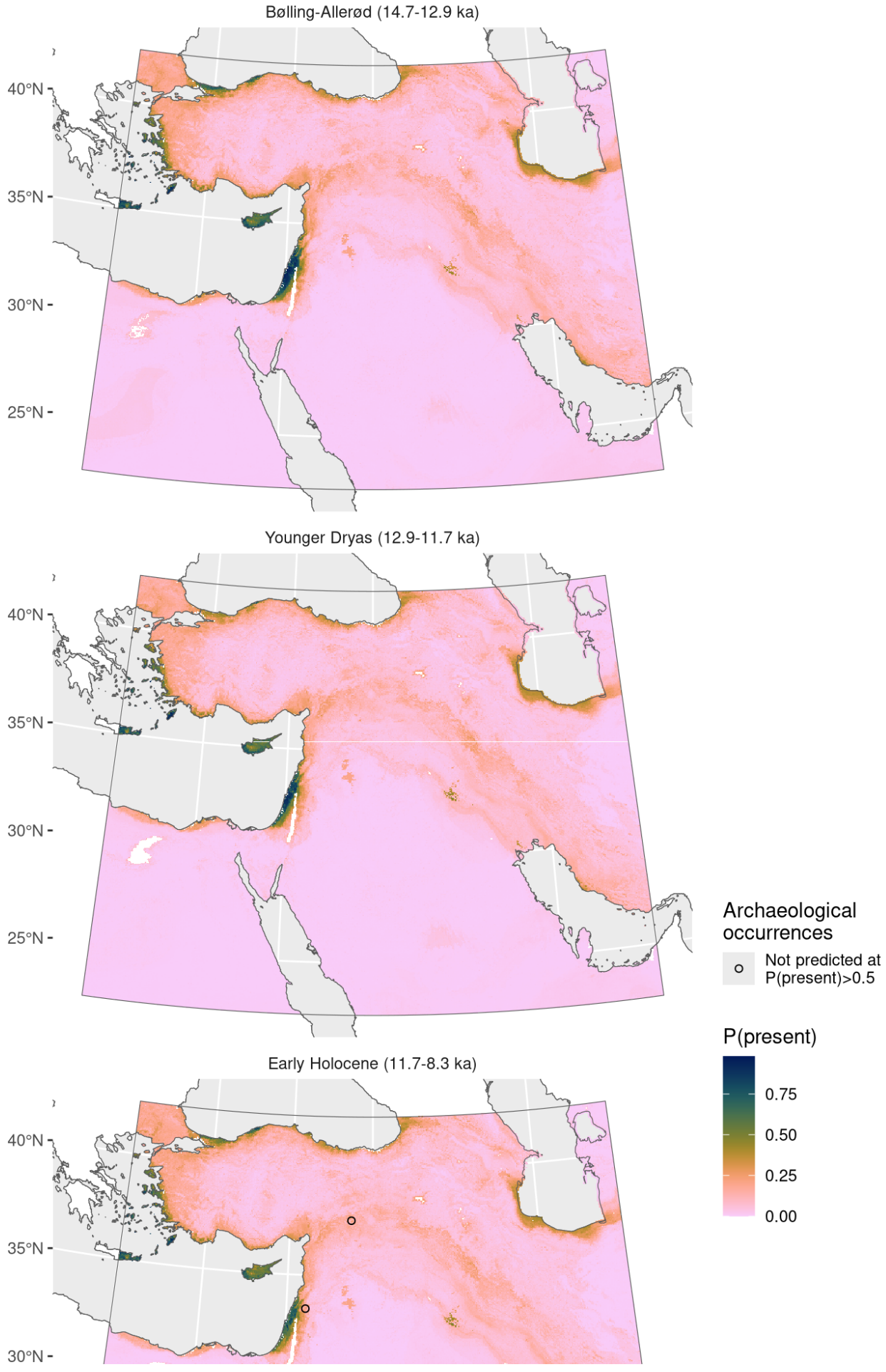

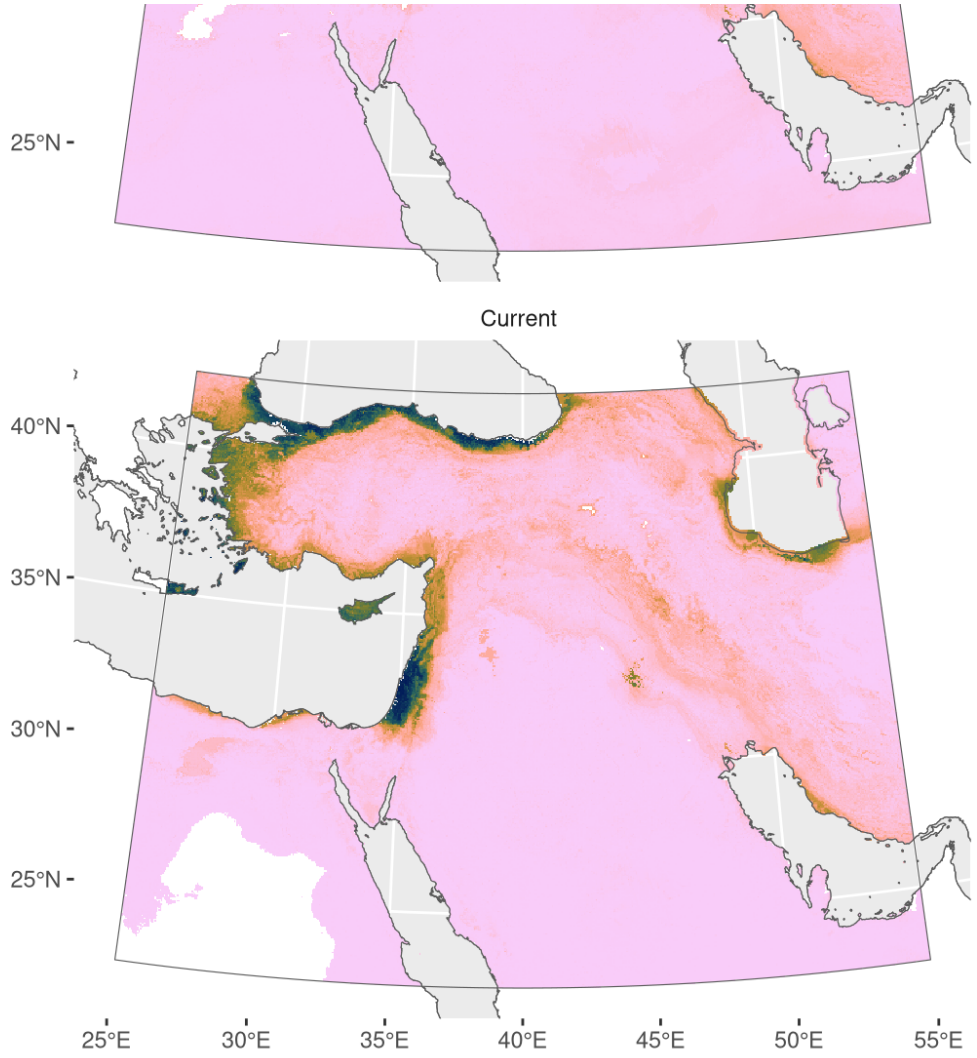


Figure 80: Predicted palaeodistributions of *Lolium temulentum*

Table 40: Archaeological occurrences of *Lolium temulentum*

Archaeological occurrences of *Lolium temulentum*

| Site | Age range | N assemblages | Average prop. | Source | Predicted? |
|---|---|---|---|---|---|
| Early Holocene (11.7-8.3 ka) | | | | | |
| Nevalı Çori | 10.4–10.2 ka | 1 | 0.00% | ORIGINS | no |
| Tell Ramad | 9.3–8.6 ka | 2 | 0.58% | ORIGINS | no |

# *Medicago radiata*

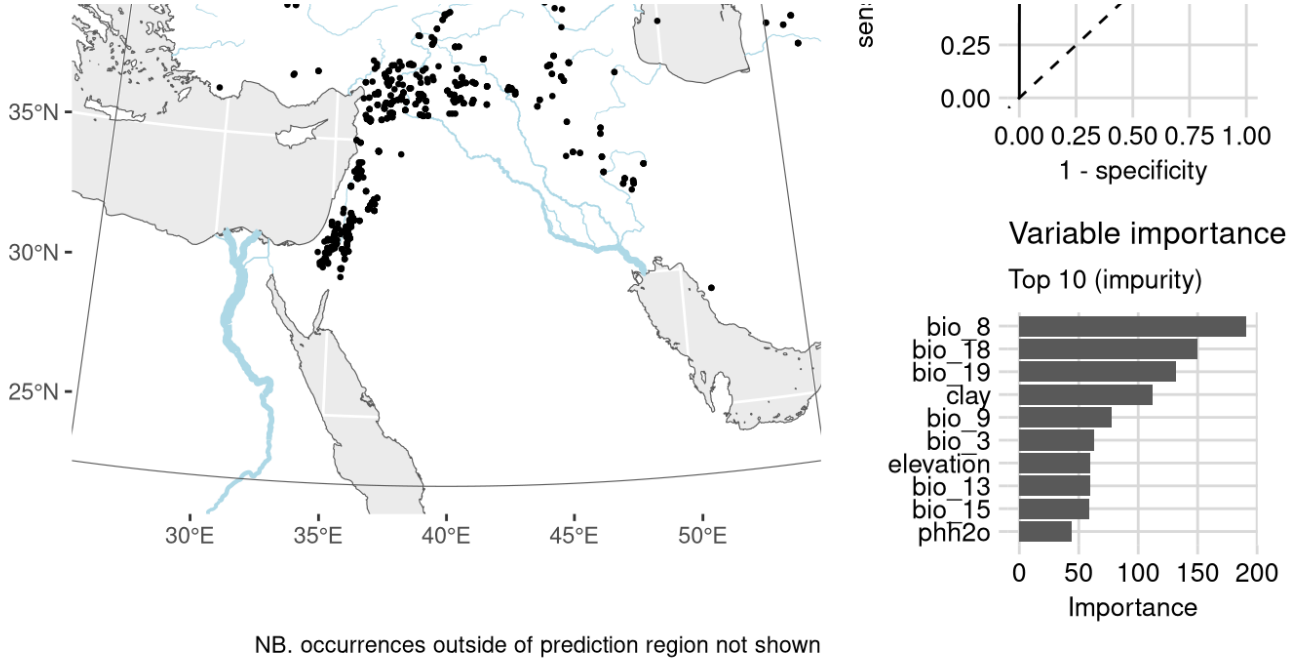


Figure 81: Fitted model summary for *Medicago radiata*

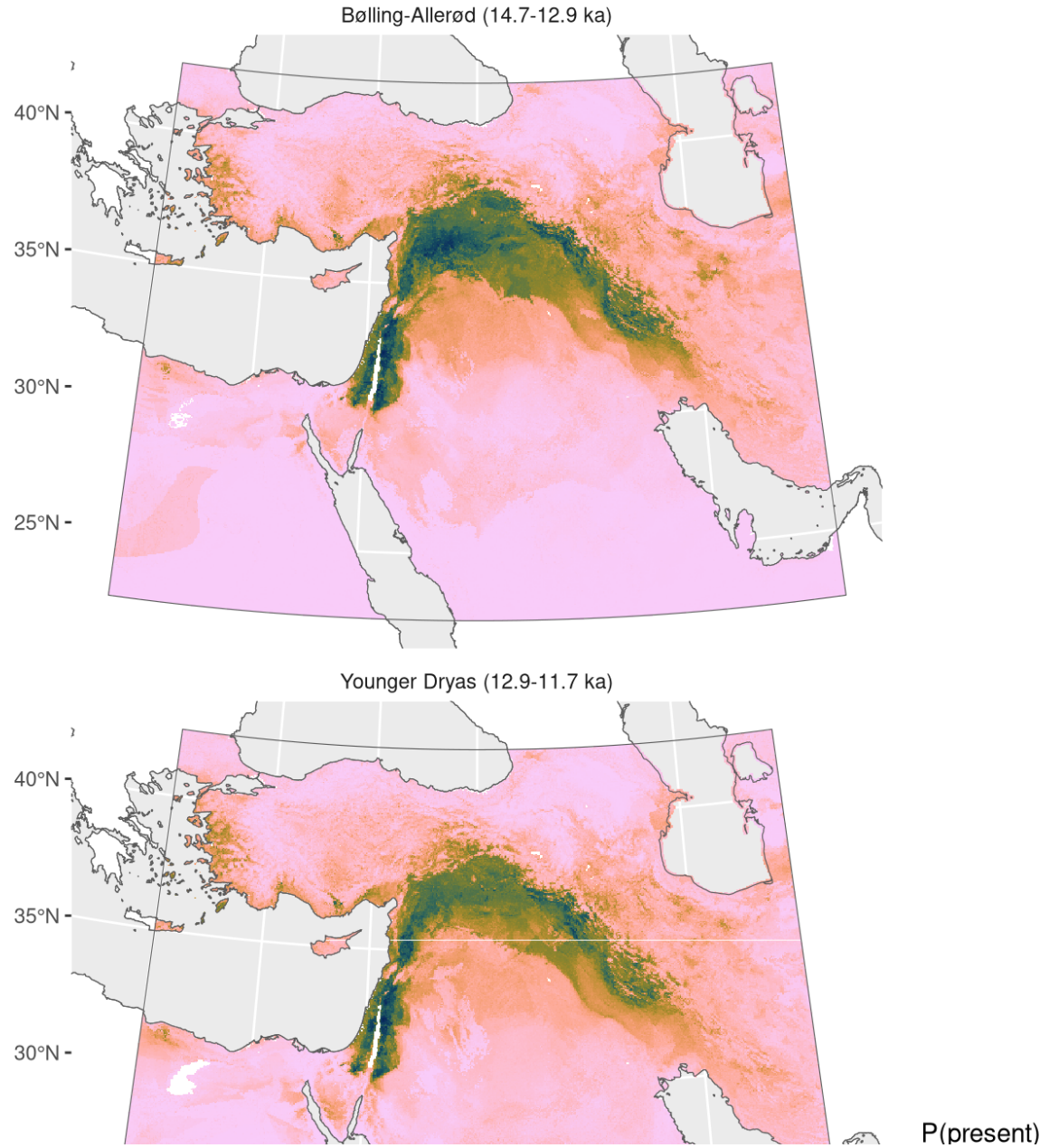

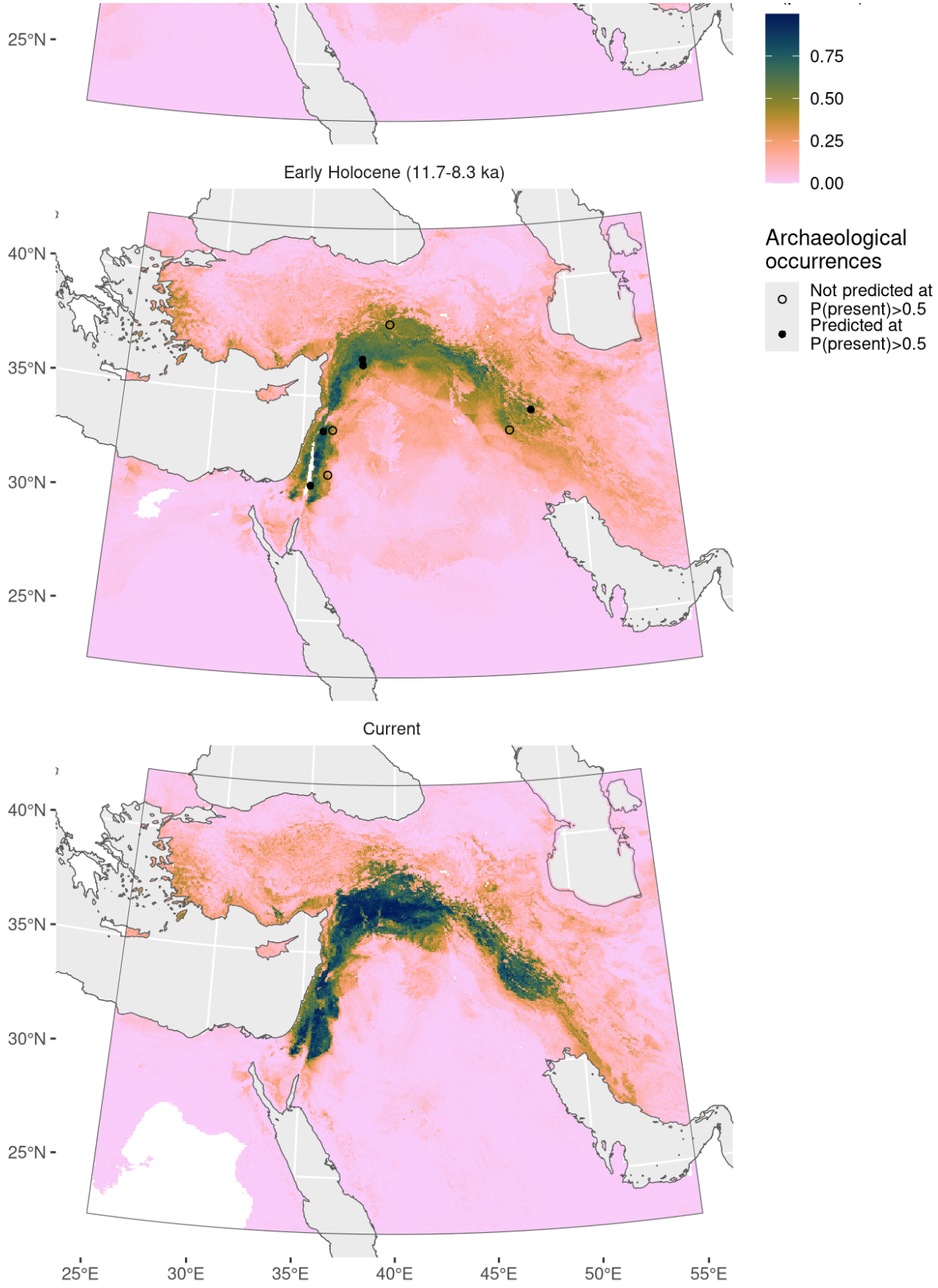


Figure 82: Predicted palaeodistributions of *Medicago radiata*

Table 41: Archaeological occurrences of *Medicago radiata*

Archaeological occurrences of *Medicago radiata*

| Site | Age range | N assemblages | Average prop. | Source | Predicted? |
|---|---|---|---|---|---|

| Early Holocene (11.7-8.3 ka) | | | | | |
|---|---|---|---|---|---|
| Jerf el Ahmar | 11.4–10.7 ka | 1 | 0.01% | ORIGINS | yes |
| Chogha Golan | 11.2–9.6 ka | 9 | 0.50% | ORIGINS | no |
| Tell Aswad | 11.2–9.3 ka | 2 | 1.63% | ORIGINS | no |
| El-Hemmeh | 11.1–10.5 ka | 1 | 0.24% | ORIGINS | yes |
| Dja'de | 10.7–10.2 ka | 1 | 0.02% | ORIGINS | yes |
| Ganj Dareh | 10.2–9.2 ka | 1 | 0.14% | ORIGINS | yes |
| Tell Ramad | 9.3–8.6 ka | 2 | 0.27% | ORIGINS | yes |
| Çayönü | 9.2–8.8 ka | 2 | 0.06% | ORIGINS | no |
| Wadi Jilat 13 | 9.1–8.5 ka | 1 | 0.17% | ORIGINS | no |

# *Phalaris paradoxa*

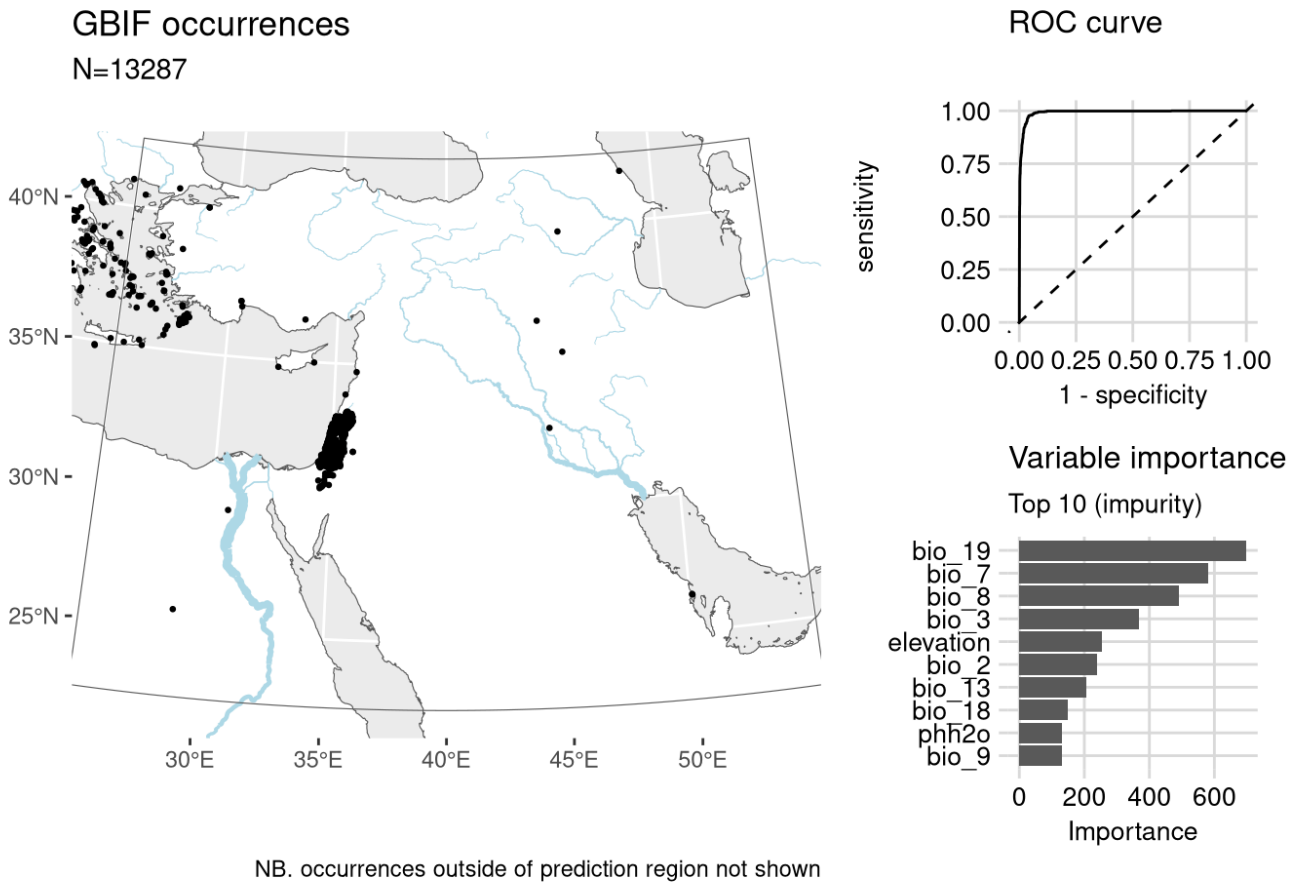


Figure 83: Fitted model summary for *Phalaris paradoxa*

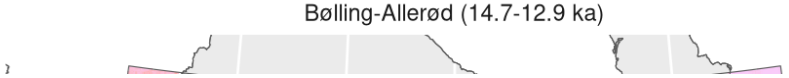

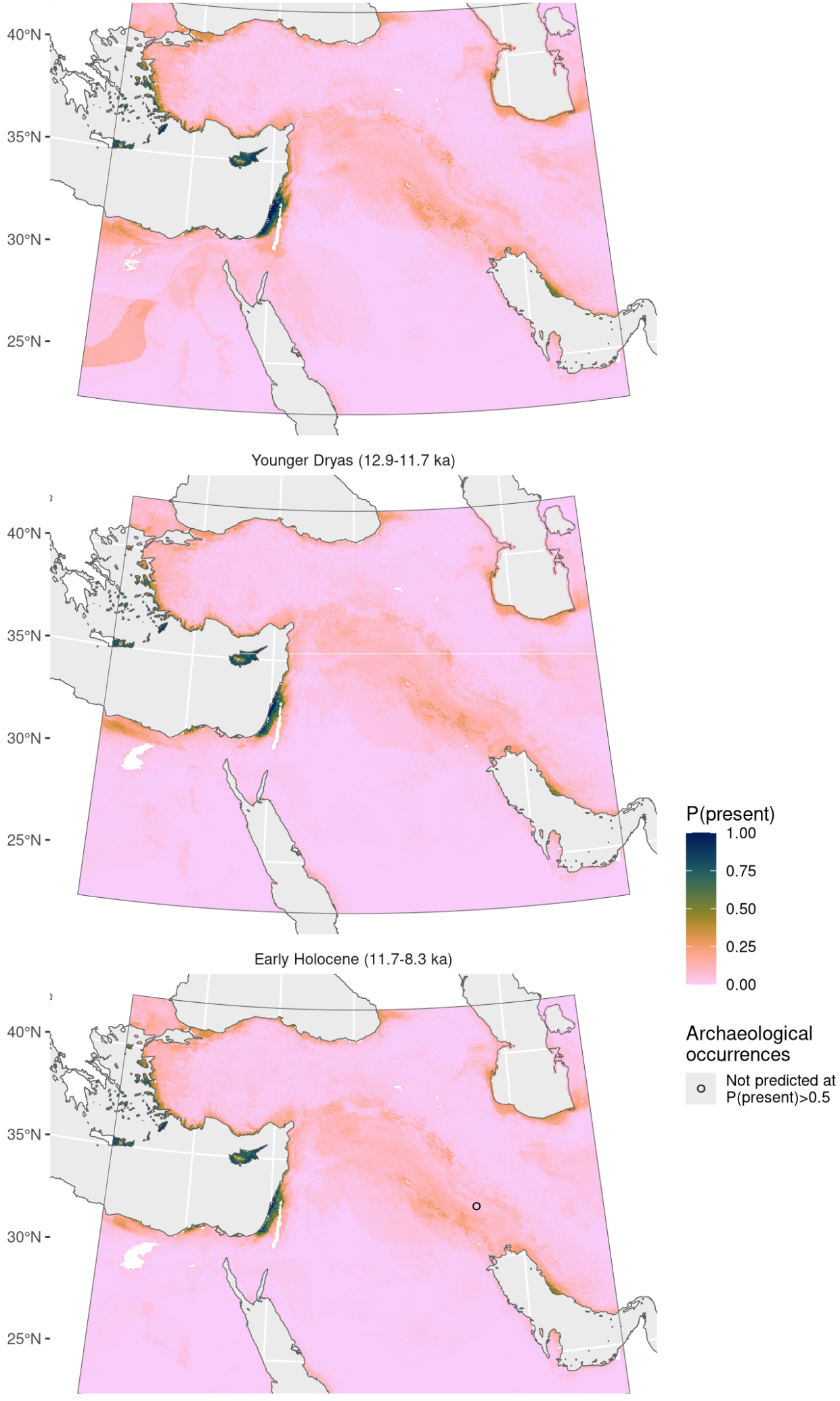
40°N
35°N
30°N
25°N
Younger Dryas (12.9-11.7 ka)
40°N
35°N
30°N
25°N
Early Holocene (11.7-8.3 ka)
40°N
35°N
30°N
25°N
P(present)
1.00
0.75
0.50
0.25
0.00
Archaeological occurrences
Not predicted at P(present)>0.5

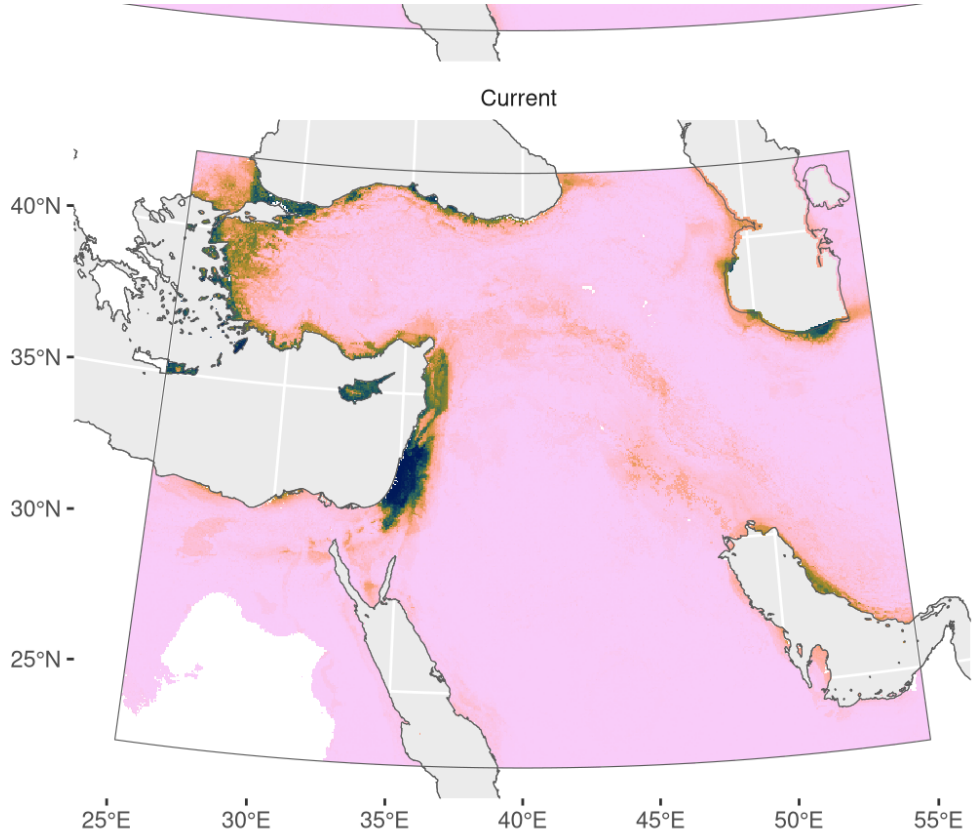


Figure 84: Predicted palaeodistributions of *Phalaris paradoxa*

Table 42: Archaeological occurrences of *Phalaris paradoxa*

Archaeological occurrences of *Phalaris paradoxa*

| Site | Age range | N assemblages | Average prop. | Source | Predicted? |
|---|---|---|---|---|---|
| Early Holocene (11.7-8.3 ka) | | | | | |
| Ali Kosh | 10.1–8.0 ka | 3 | 1.83% | ORIGINS | no |

# *Phragmites australis*

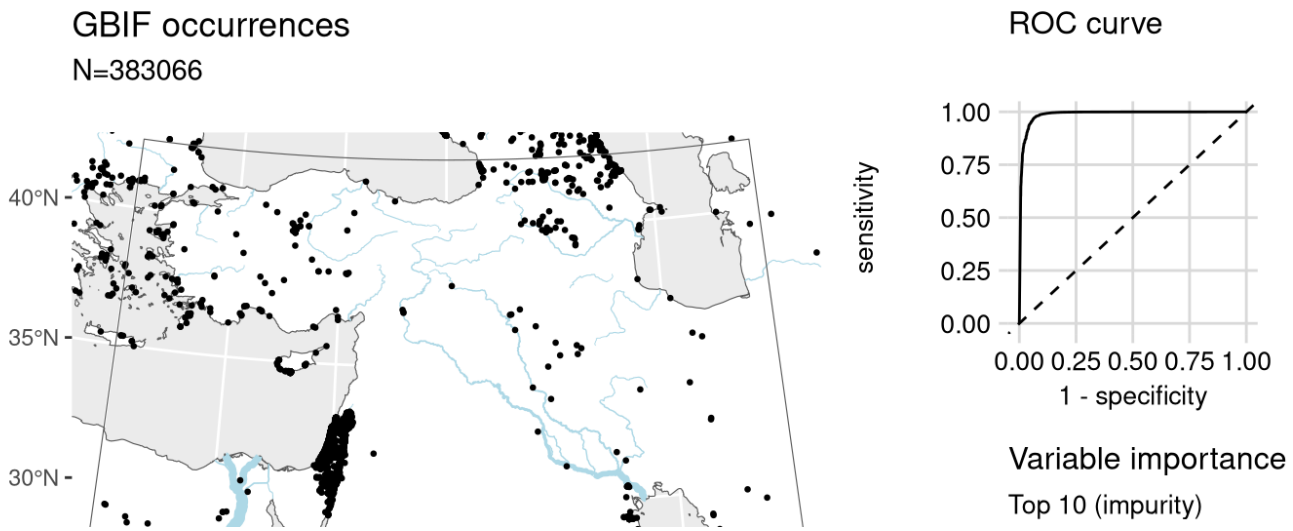

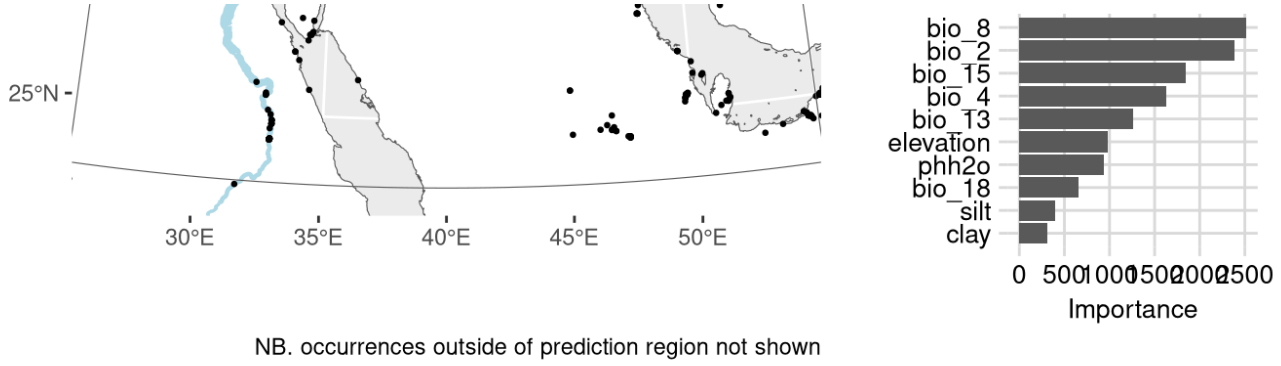


Figure 85: Fitted model summary for *Phragmites australis*

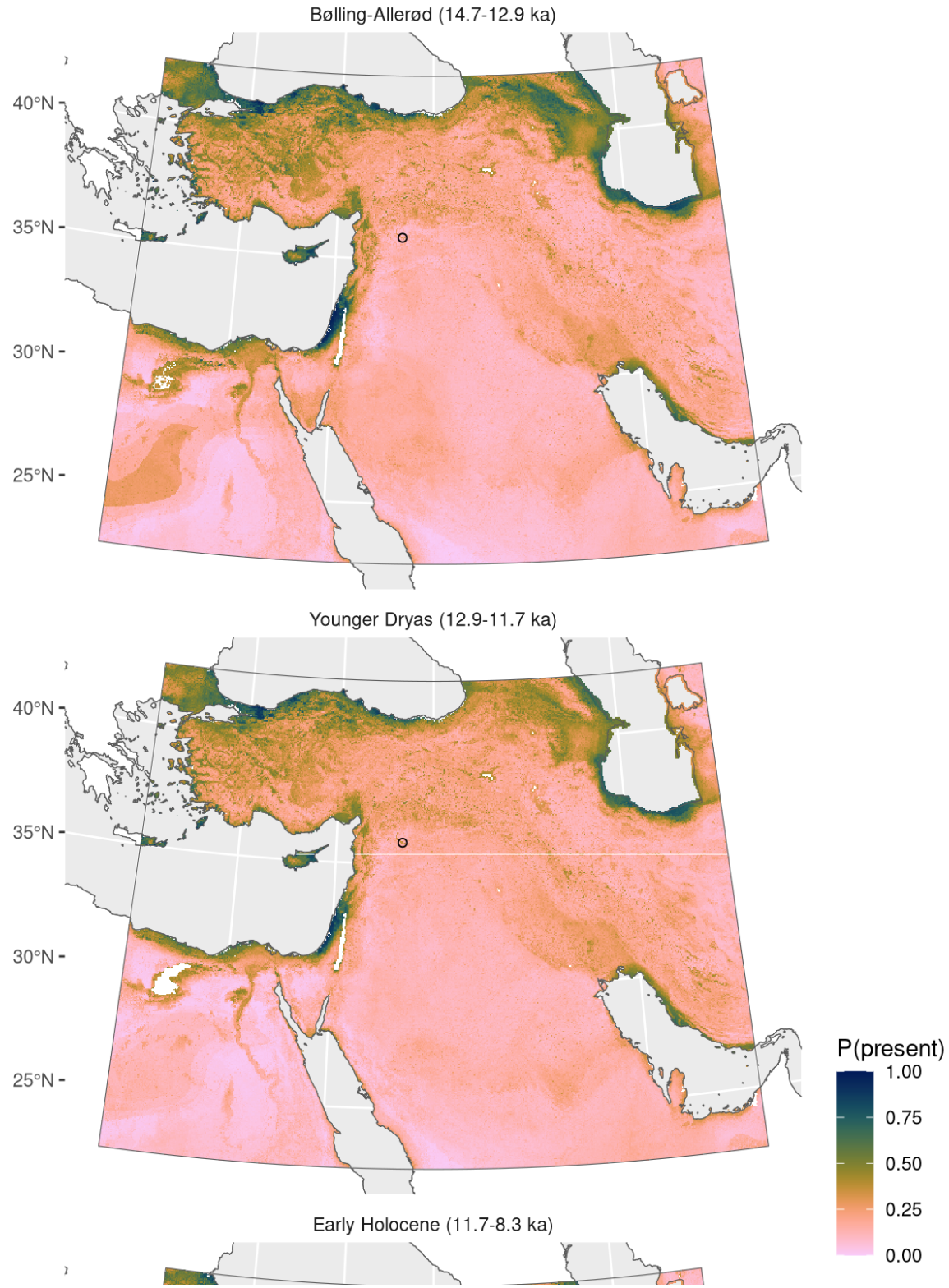

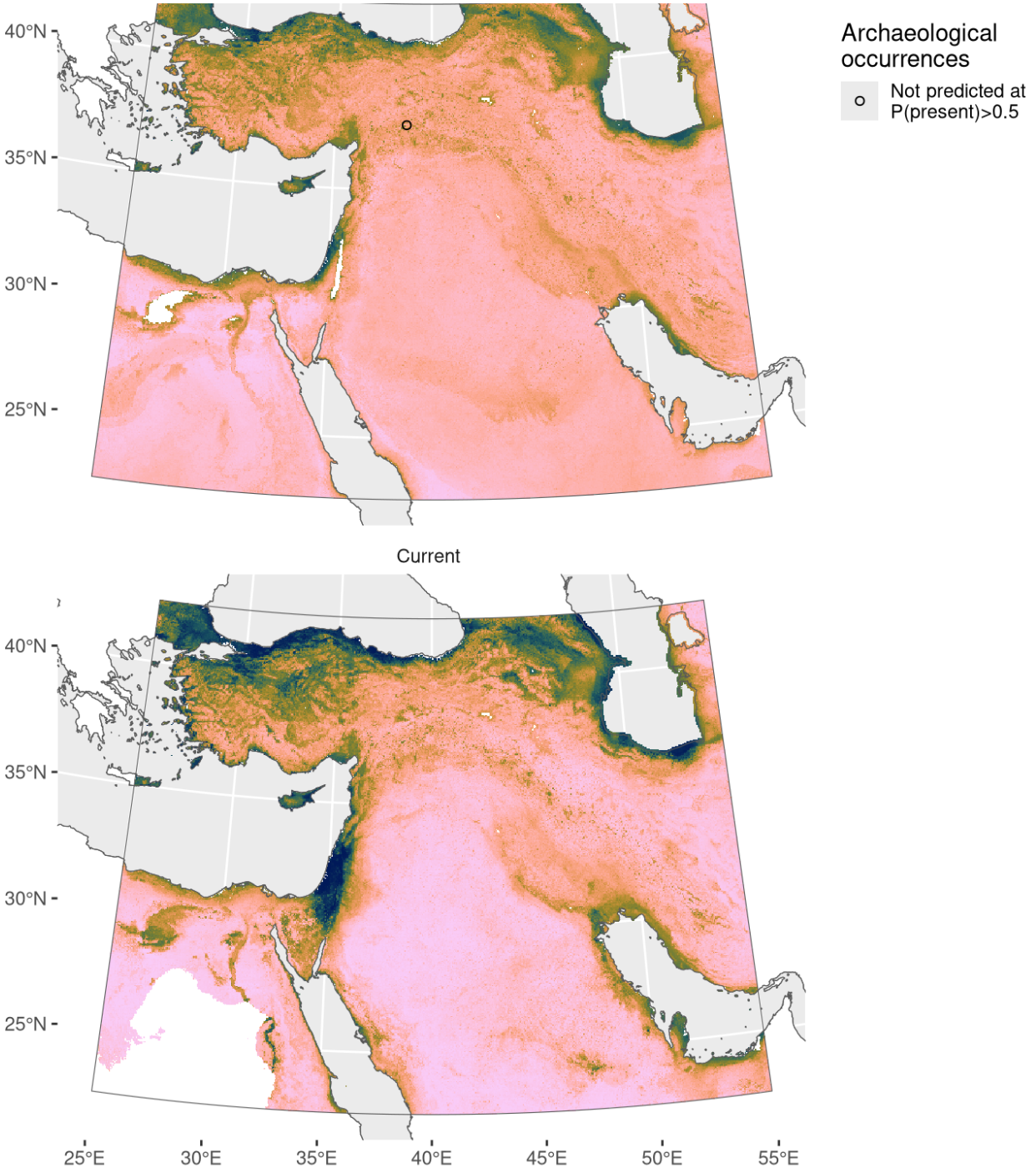


Figure 86: Predicted palaeodistributions of *Phragmites australis*

Table 43: Archaeological occurrences of *Phragmites australis*

Archaeological occurrences of *Phragmites australis*

| Site | Age range | N assemblages | Average prop. | Source | Predicted? |
|---|---|---|---|---|---|
| Bølling-Allerød (14.7-12.9 ka) | | | | | |
| Abu Hureyra | 13.1–13.0 ka | 1 | 0.16% | ORIGINS | no |
| Younger Dryas (12.9-11.7 ka) | | | | | |
| Abu Hureyra | 13.0–11.8 ka | 2 | 0.48% | ORIGINS | no |

| Early Holocene (11.7-8.3 ka) | | | | | |
|---|---|---|---|---|---|
| Nevalı Çori | 10.4–10.2 ka | 1 | 0.00% | ORIGINS | no |

# *Pistacia atlantica*

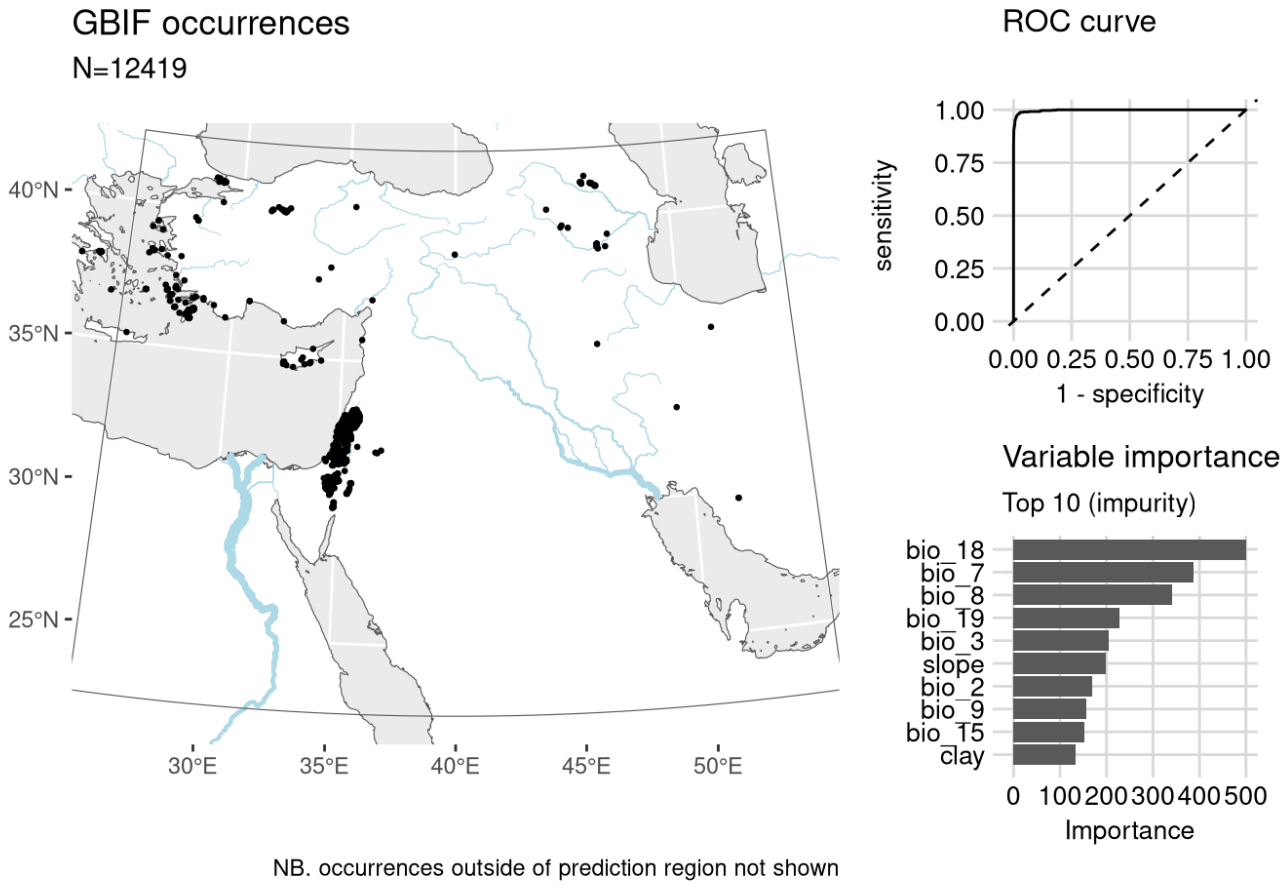


Figure 87: Fitted model summary for *Pistacia atlantica*

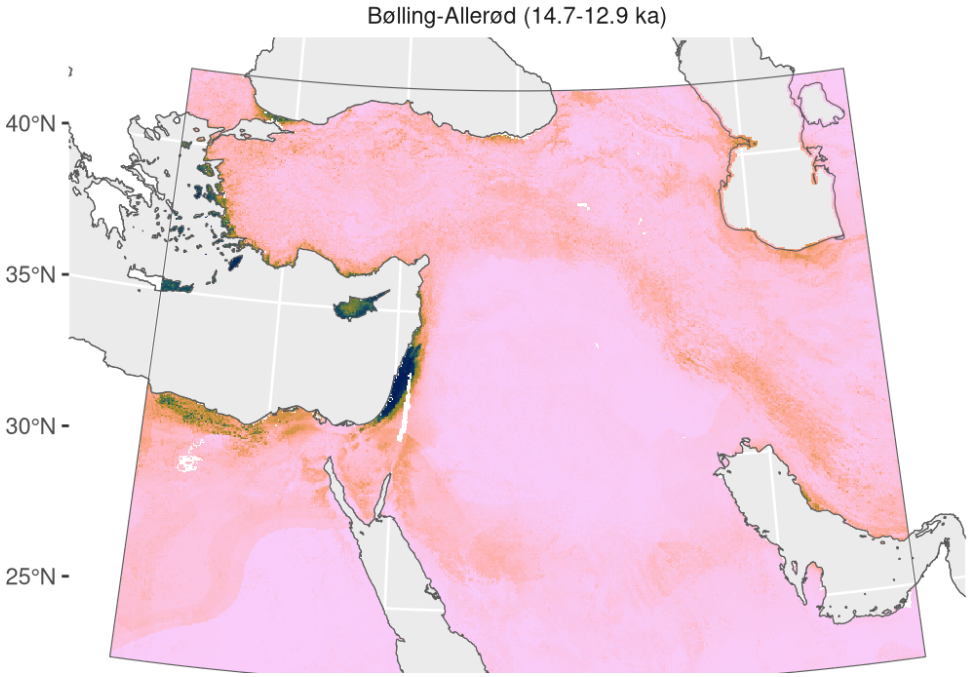

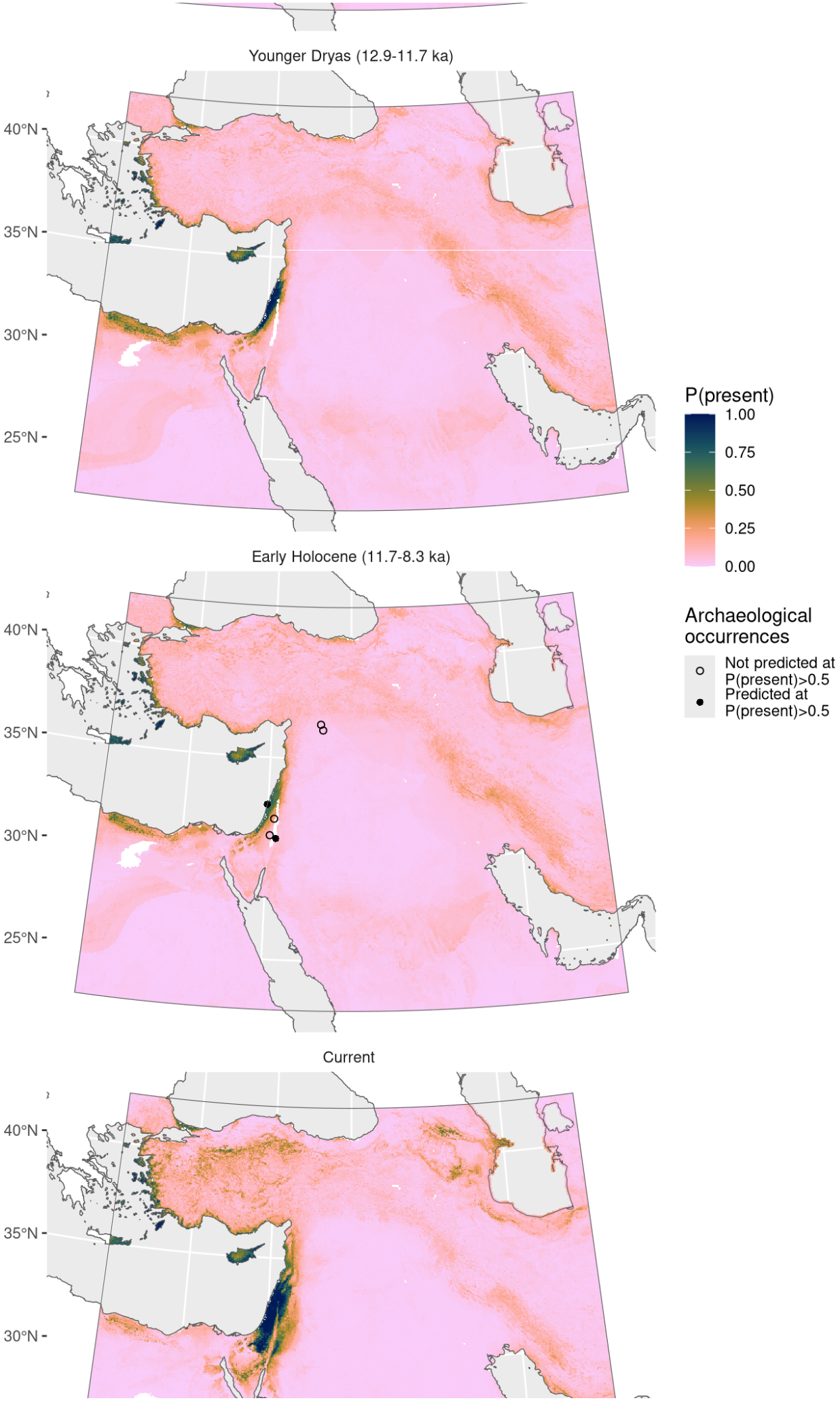
Younger Dryas (12.9-11.7 ka)
40°N
35°N
30°N
25°N
Early Holocene (11.7-8.3 ka)
40°N
35°N
30°N
25°N
Current
40°N
35°N
30°N
P(present)
1.00
0.75
0.50
0.25
0.00
Archaeological occurrences
Not predicted at P(present)>0.5
Predicted at P(present)>0.5

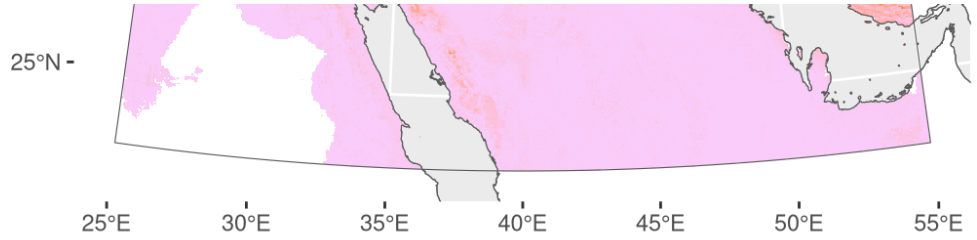


Figure 88: Predicted palaeodistributions of *Pistacia atlantica*

Table 44: Archaeological occurrences of *Pistacia atlantica*

Archaeological occurrences of *Pistacia atlantica*

| Site | Age range | N assemblages | Average prop. | Source | Predicted? |
|---|---|---|---|---|---|
| Early Holocene (11.7-8.3 ka) | | | | | |
| Netiv Hagdud | 11.6–10.6 ka | 1 | 0.25% | ORIGINS | no |
| Jerf el Ahmar | 11.4–10.7 ka | 1 | 4.59% | ORIGINS | no |
| Tell 'Abr | 11.2–10.8 ka | 1 | 0.04% | ORIGINS | no |
| El-Hemmeh | 11.1–10.5 ka | 1 | 0.13% | ORIGINS | yes |
| Nahal Hemar | 10.1–9.3 ka | 1 | 21.38% | ORIGINS | no |
| Atlit-Yam | 9.0–8.0 ka | 1 | 2.28% | ORIGINS | yes |

# *Poa bulbosa*

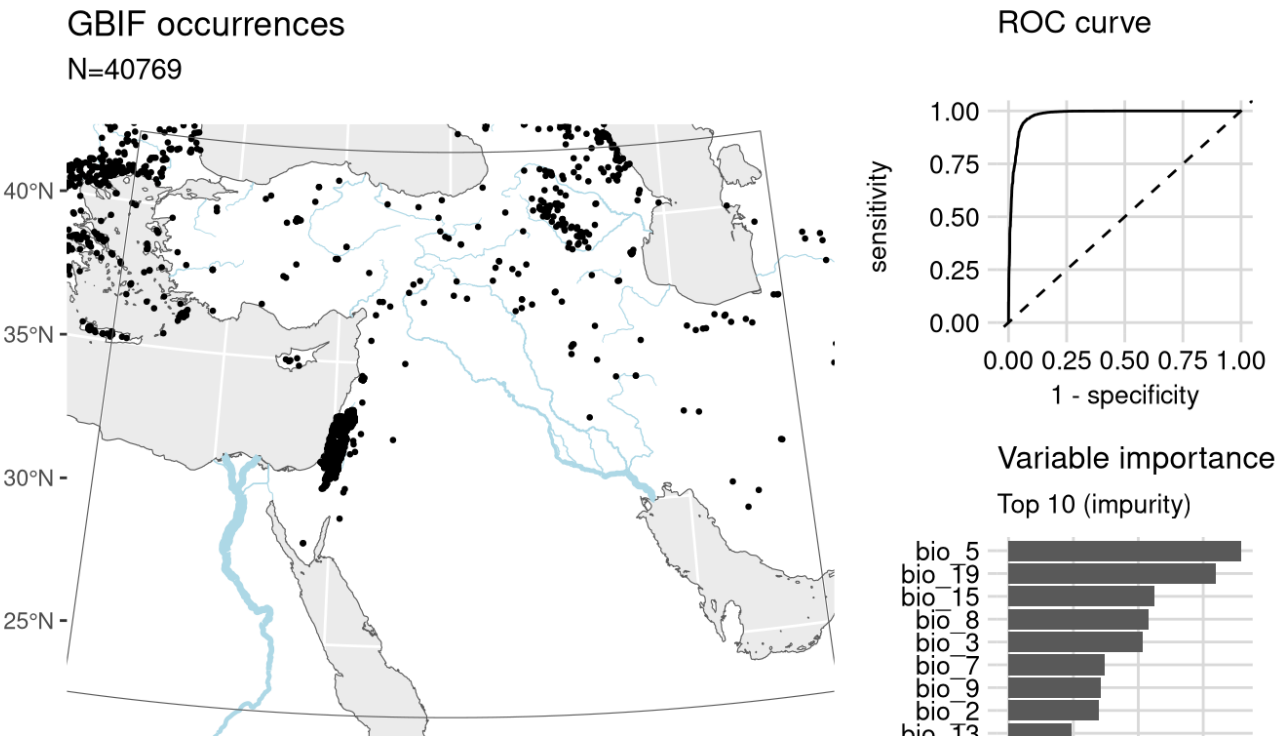

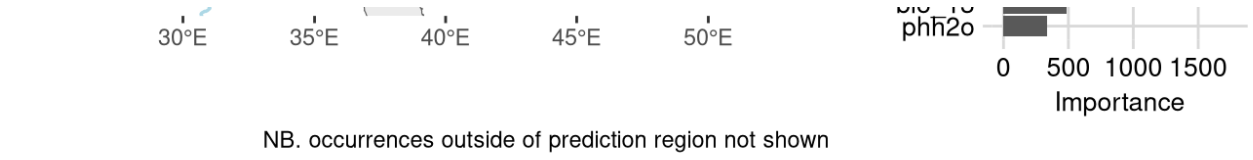


NB. occurrences outside of prediction region not shown

Figure 89: Fitted model summary for *Poa bulbosa*

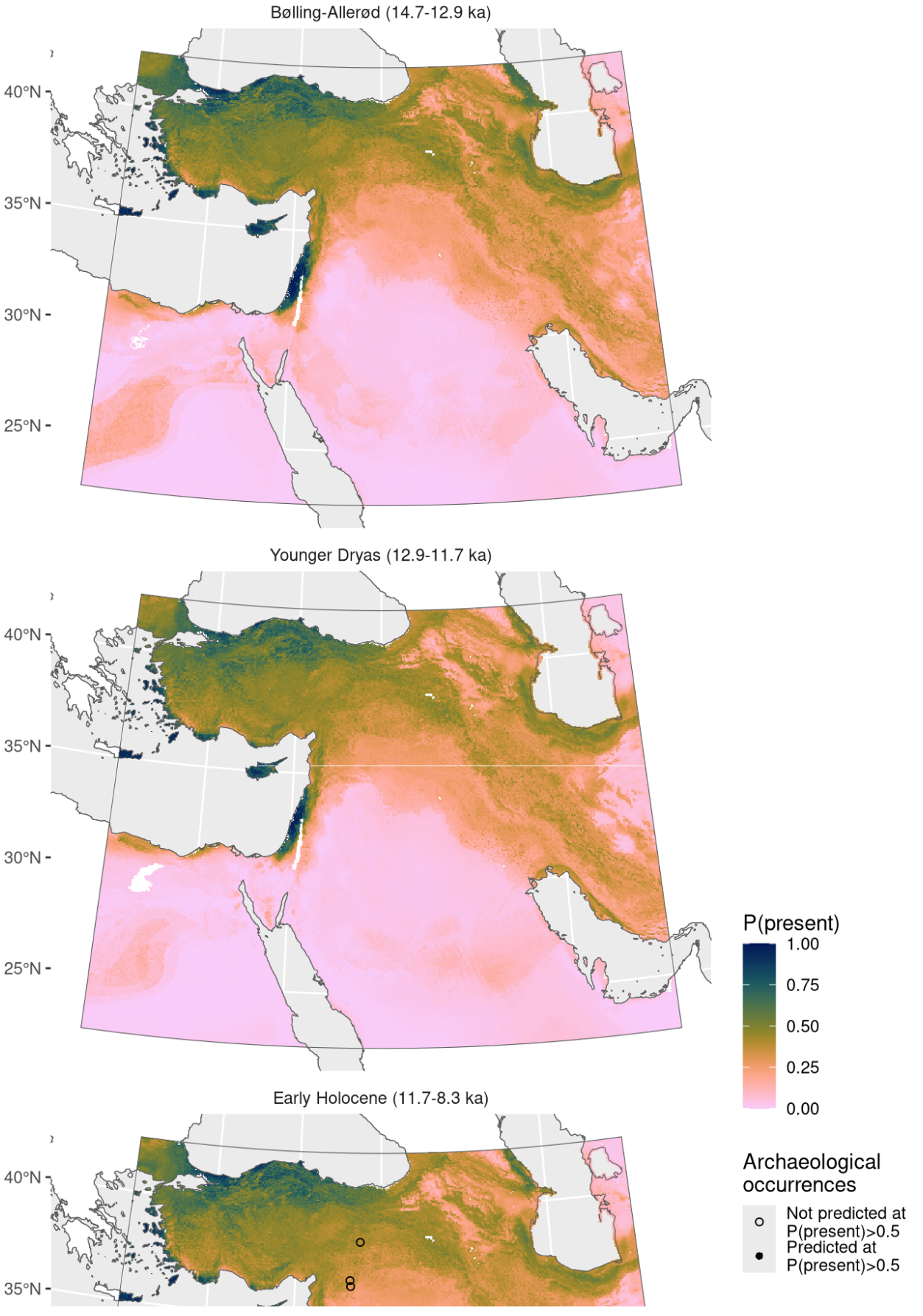

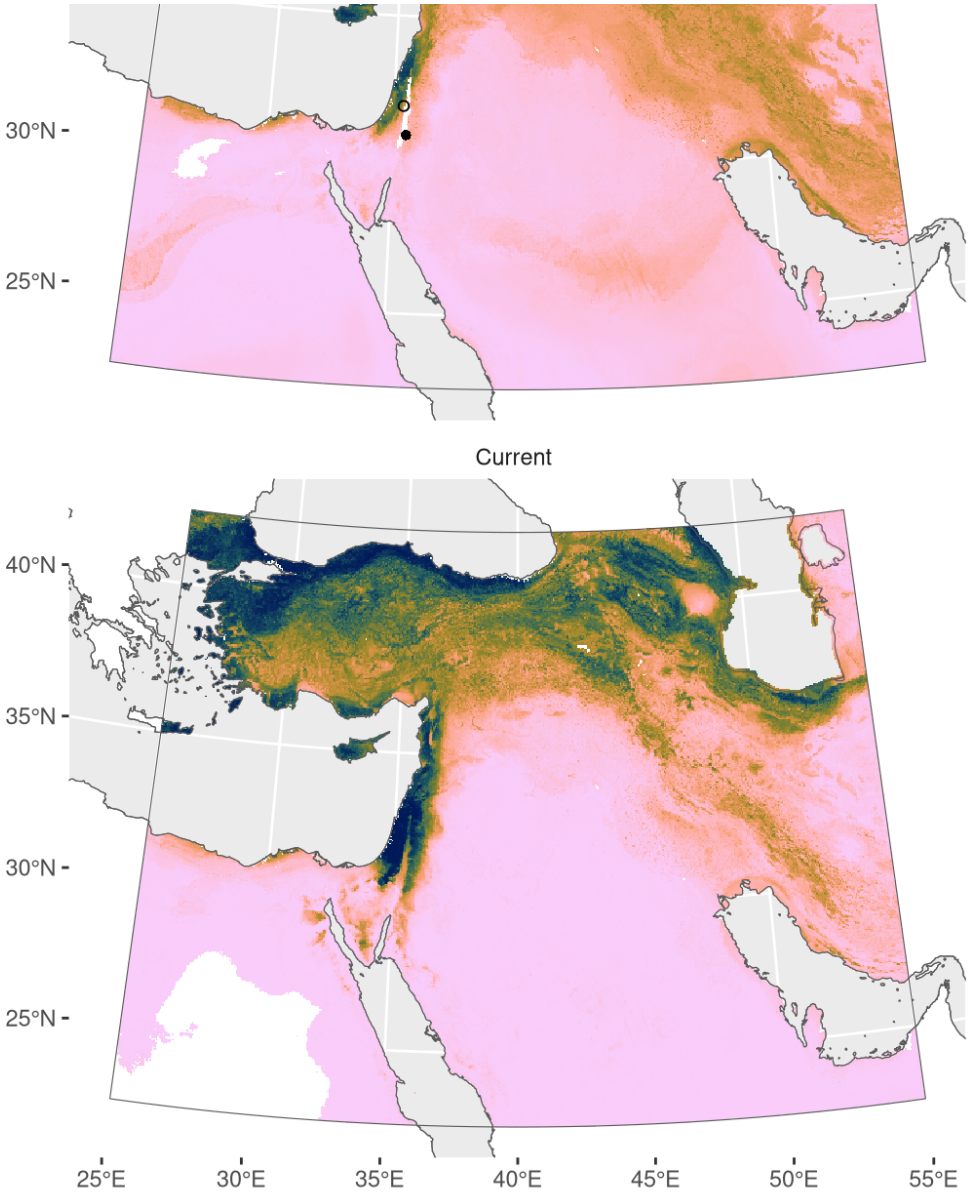


Figure 90: Predicted palaeodistributions of *Poa bulbosa*

Table 45: Archaeological occurrences of *Poa bulbosa*

Archaeological occurrences of *Poa bulbosa*

| Site | Age range | N assemblages | Average prop. | Source | Predicted? |
|---|---|---|---|---|---|
| Early Holocene (11.7-8.3 ka) | | | | | |
| Netiv Hagdud | 11.6–10.6 ka | 1 | 0.05% | ORIGINS | no |
| Jerf el Ahmar | 11.4–10.7 ka | 1 | 0.03% | ORIGINS | no |
| El-Hemmeh | 11.1–10.5 ka | 1 | 0.19% | ORIGINS | yes |
| Dja'de | 10.7–10.2 ka | 1 | 0.04% | ORIGINS | no |
| Cafer Höyük | 10.6–9.7 ka | 1 | 1.41% | ORIGINS | no |

# *Prosopis farcta*

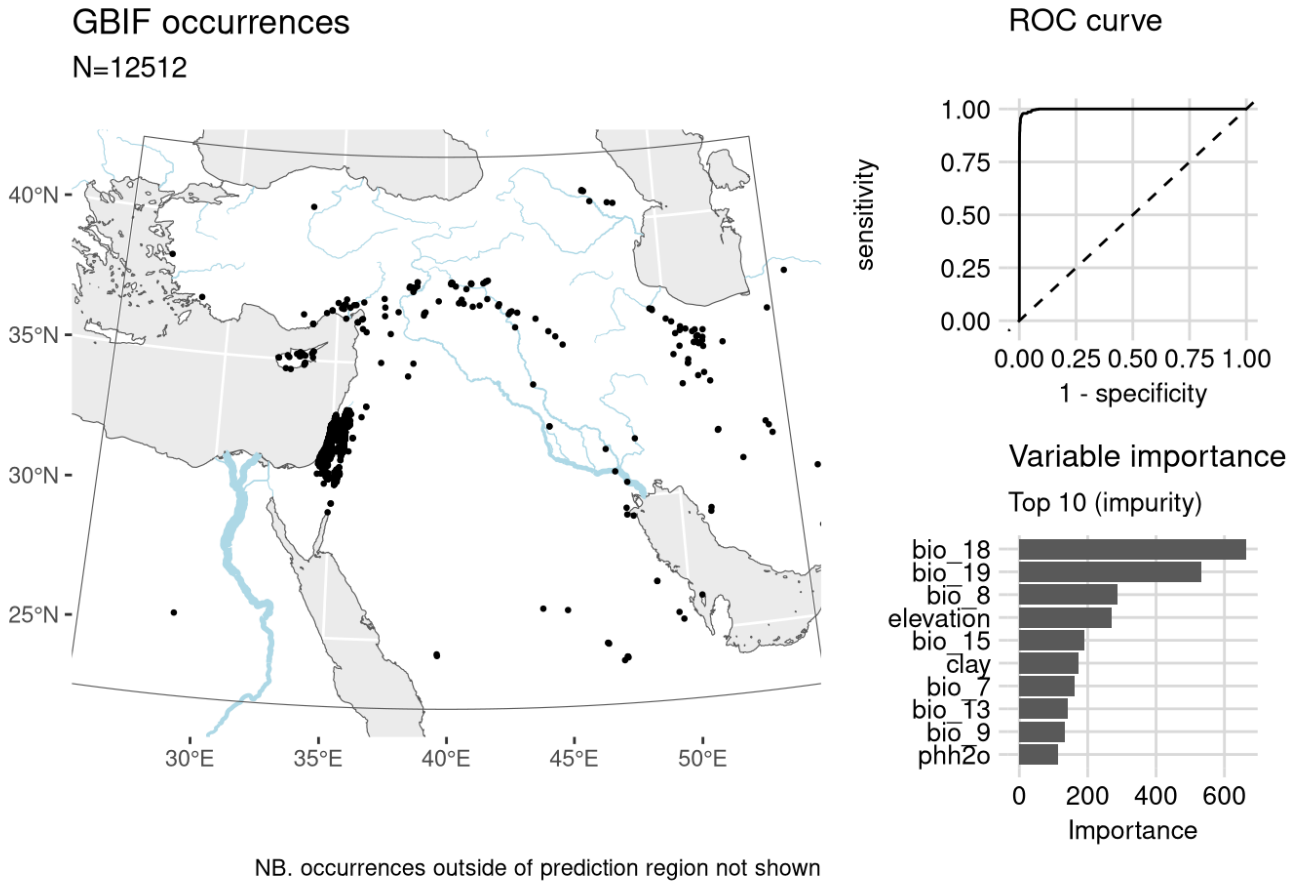


Figure 91: Fitted model summary for *Prosopis farcta*

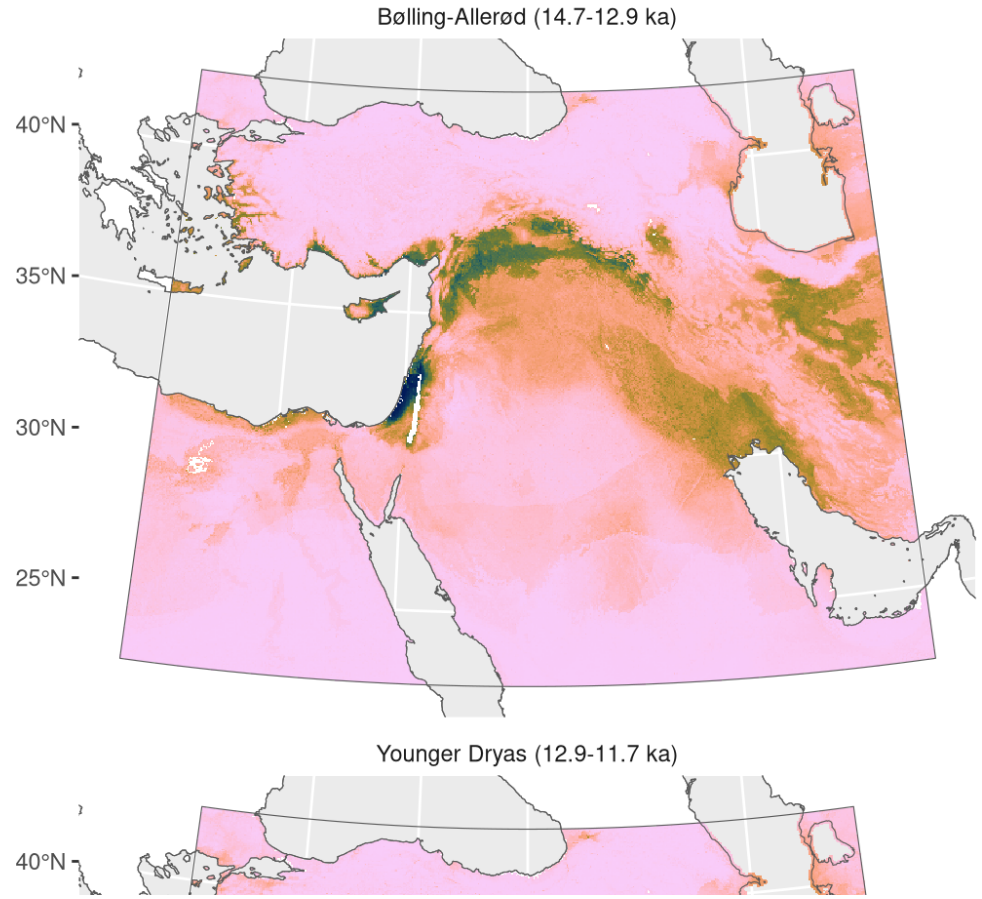

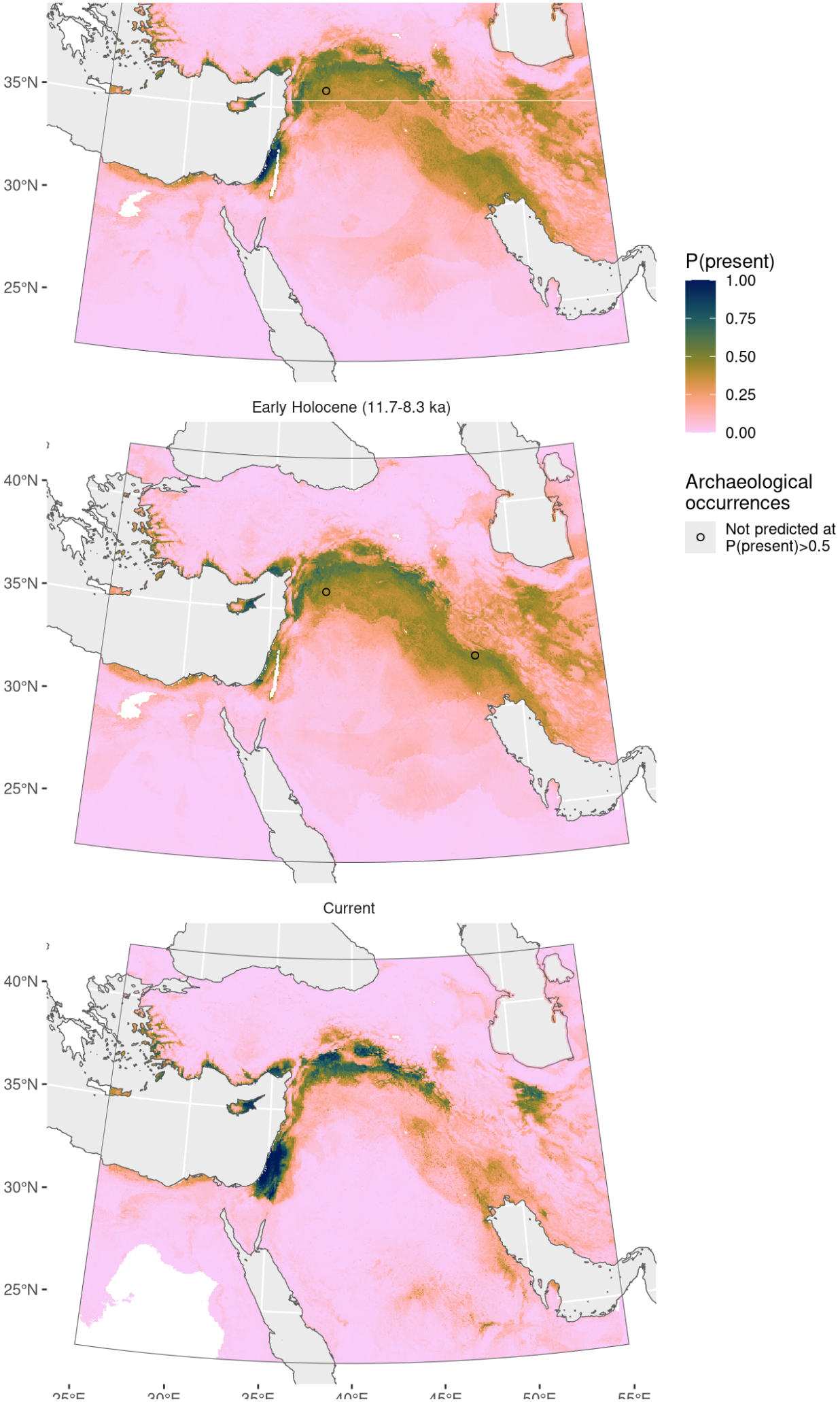
35°N
30°N
25°N
Early Holocene (11.7-8.3 ka)
40°N
35°N
30°N
25°N
Current
40°N
35°N
30°N
25°N
25°E
30°E
35°E
40°E
45°E
50°E
55°E
P(present)
1.00
0.75
0.50
0.25
0.00
Archaeological occurrences
Not predicted at P(present)>0.5

Figure 92: Predicted palaeodistributions of *Prosopis farcta*

Table 46: Archaeological occurrences of *Prosopis farcta*

Archaeological occurrences of *Prosopis farcta*

| Site | Age range | N assemblages | Average prop. | Source | Predicted? |
|---|---|---|---|---|---|
| Younger Dryas (12.9-11.7 ka) | | | | | |
| Abu Hureyra | 13.0–12.1 ka | 1 | 0.05% | ORIGINS | no |
| Early Holocene (11.7-8.3 ka) | | | | | |
| Ali Kosh | 10.1–8.0 ka | 3 | 4.83% | ORIGINS | no |
| Abu Hureyra | 9.3–8.2 ka | 1 | 0.71% | ORIGINS | no |

# *Rumex pulcher*

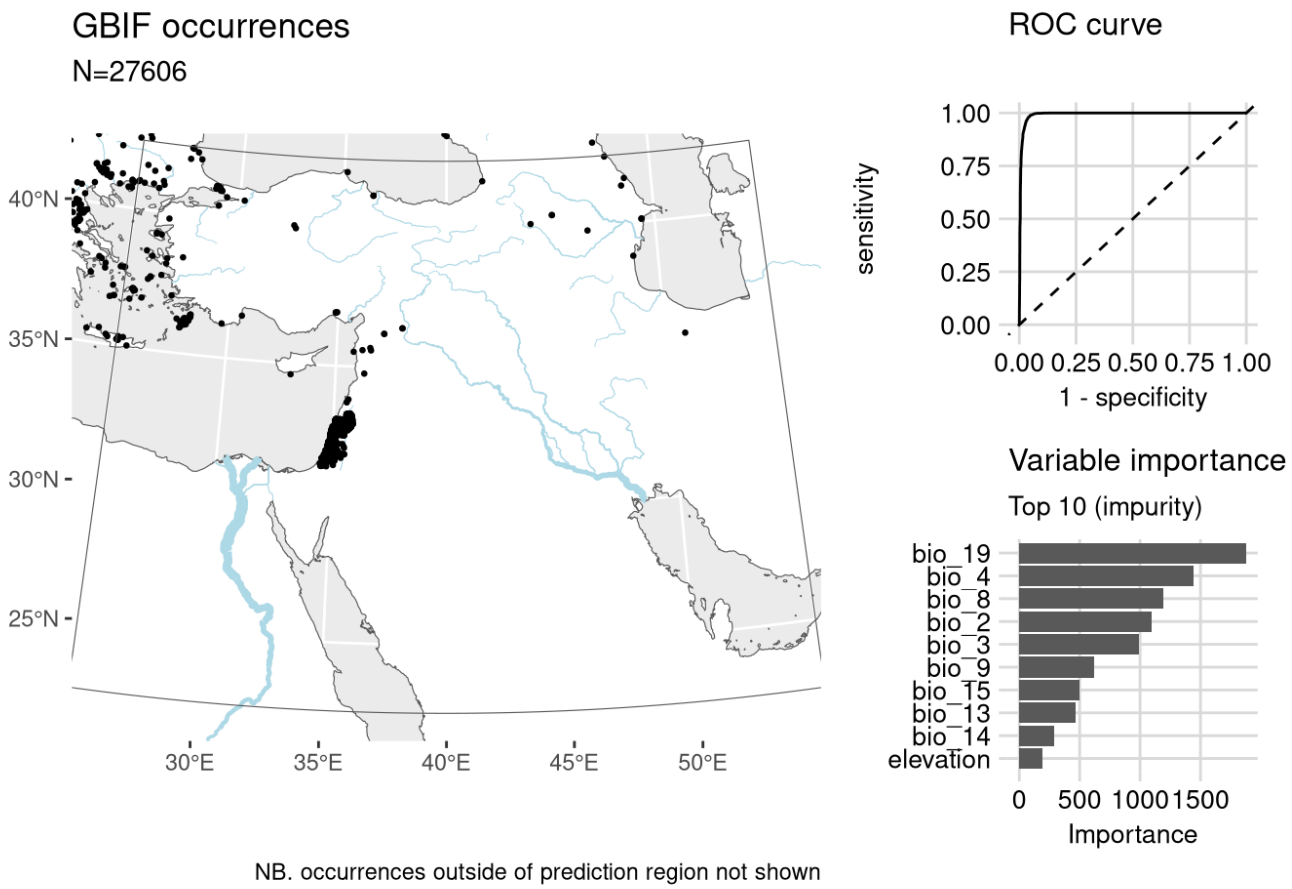


Figure 93: Fitted model summary for *Rumex pulcher*

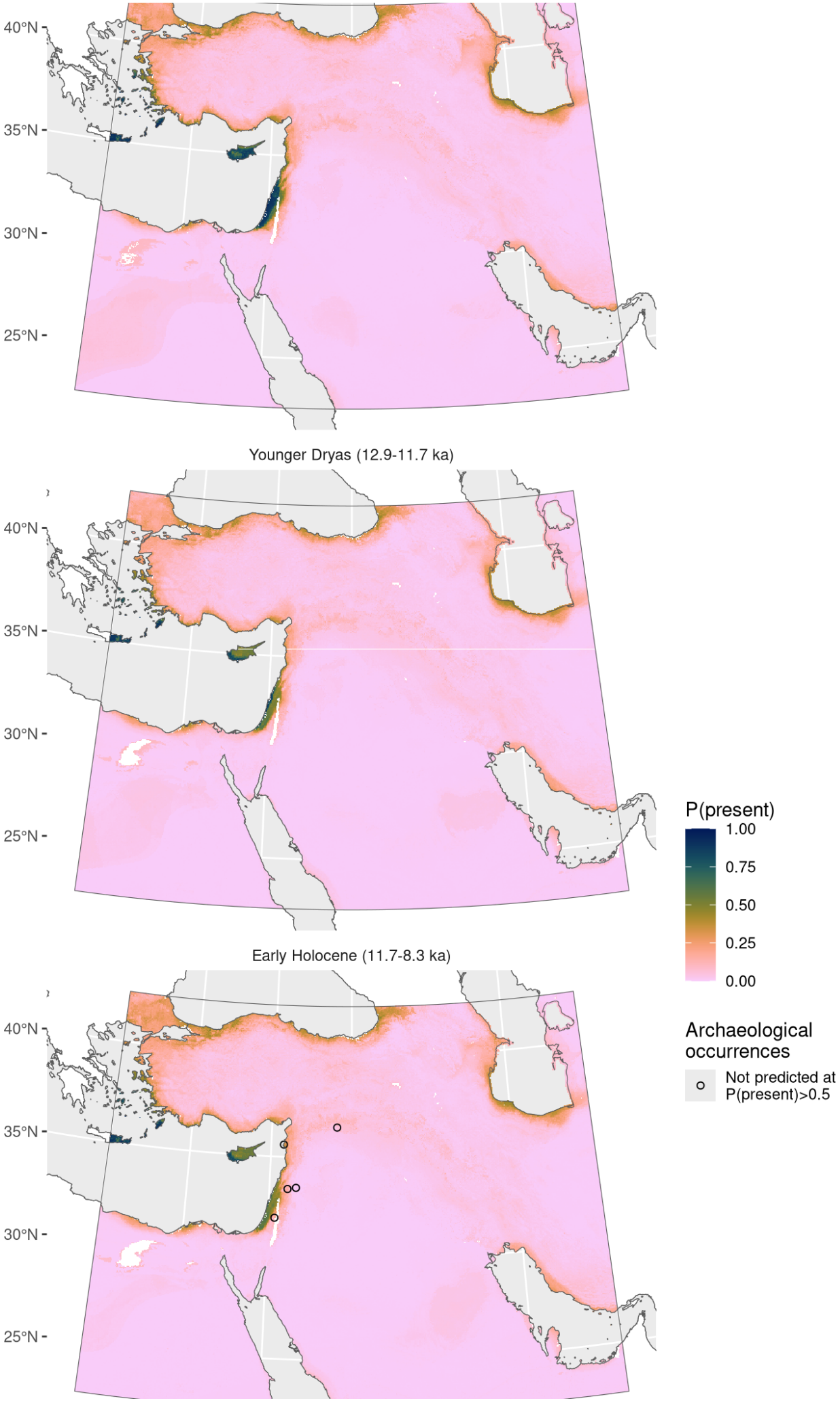
40°N
35°N
30°N
25°N
Younger Dryas (12.9-11.7 ka)
40°N
35°N
30°N
25°N
Early Holocene (11.7-8.3 ka)
40°N
35°N
30°N
25°N
P(present)
1.00
0.75
0.50
0.25
0.00
Archaeological occurrences
Not predicted at P(present)>0.5

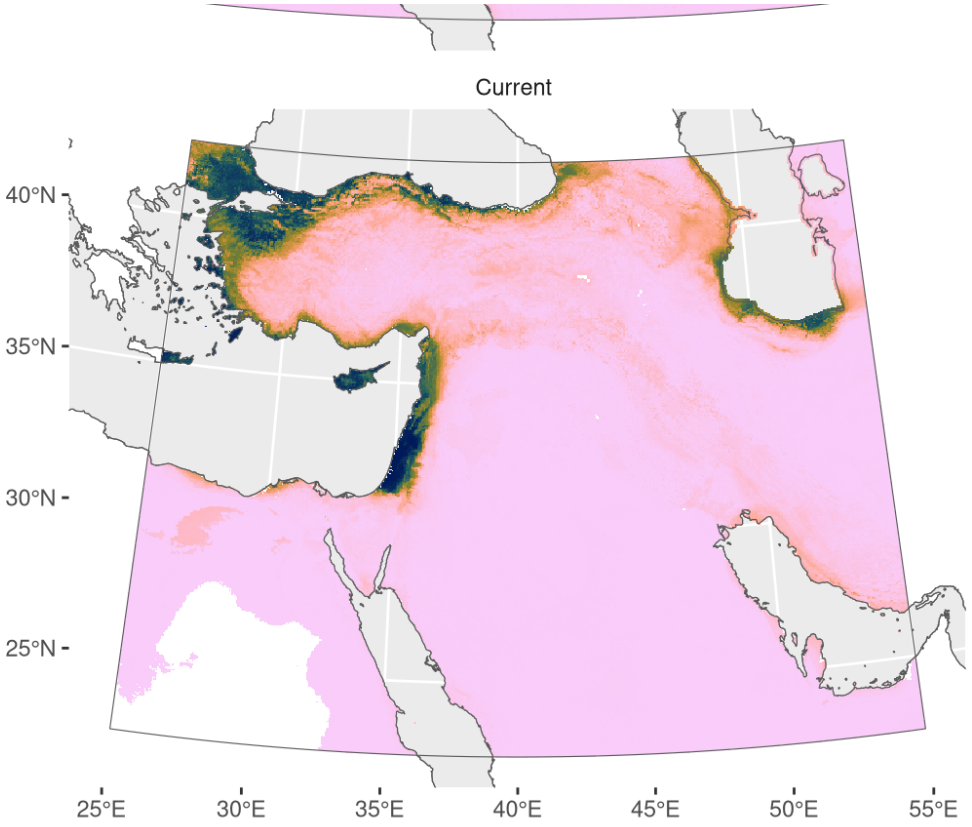


Figure 94: Predicted palaeodistributions of *Rumex pulcher*

Table 47: Archaeological occurrences of *Rumex pulcher*

Archaeological occurrences of *Rumex pulcher*

| Site | Age range | N assemblages | Average prop. | Source | Predicted? |
|---|---|---|---|---|---|
| Early Holocene (11.7-8.3 ka) | | | | | |
| Netiv Hagdud | 11.6–10.6 ka | 1 | 0.01% | ORIGINS | no |
| Tell Aswad | 10.2–9.3 ka | 1 | 0.00% | ORIGINS | no |
| Sabi Abyad II | 9.5–8.8 ka | 1 | 0.22% | ORIGINS | no |
| Ras Shamra | 9.4–8.3 ka | 2 | 0.47% | ORIGINS | no |
| Tell Ramad | 8.9–8.6 ka | 1 | 0.03% | ORIGINS | no |

# *Salsola kali*

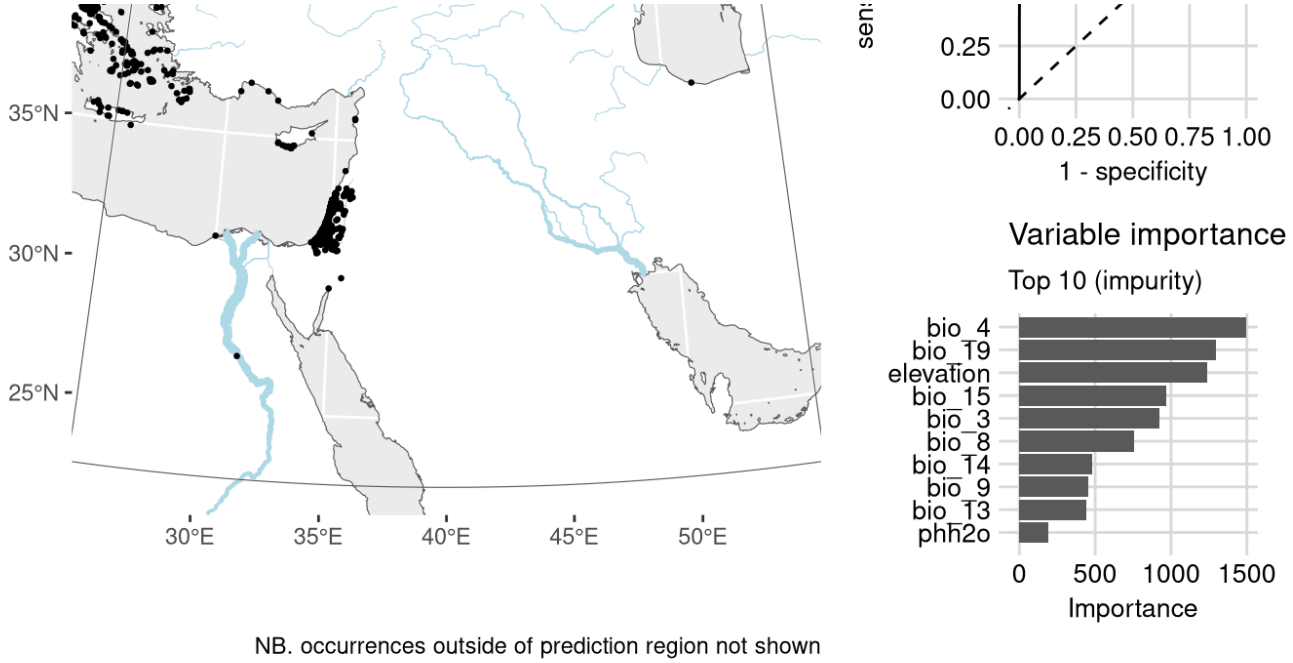


Figure 95: Fitted model summary for *Salsola kali*

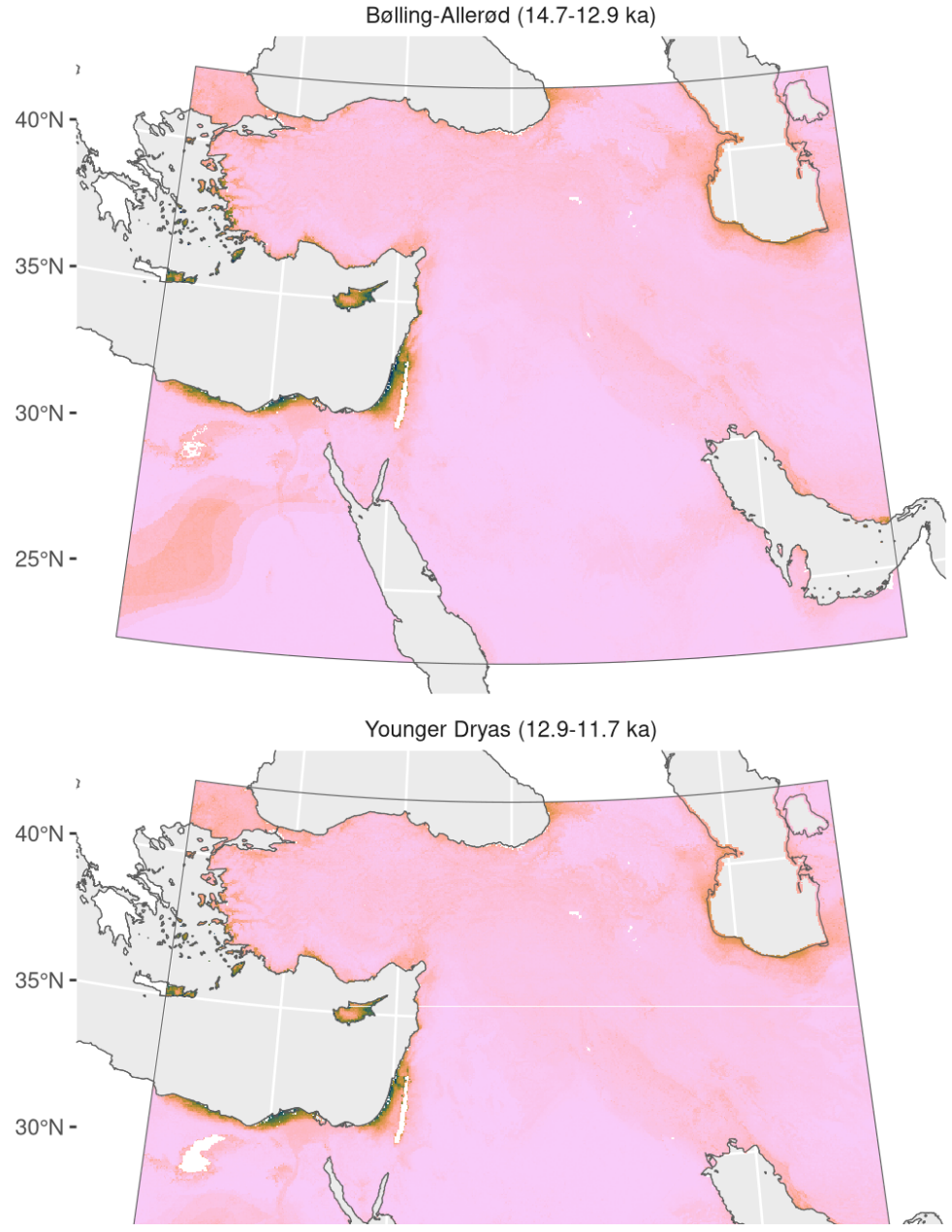

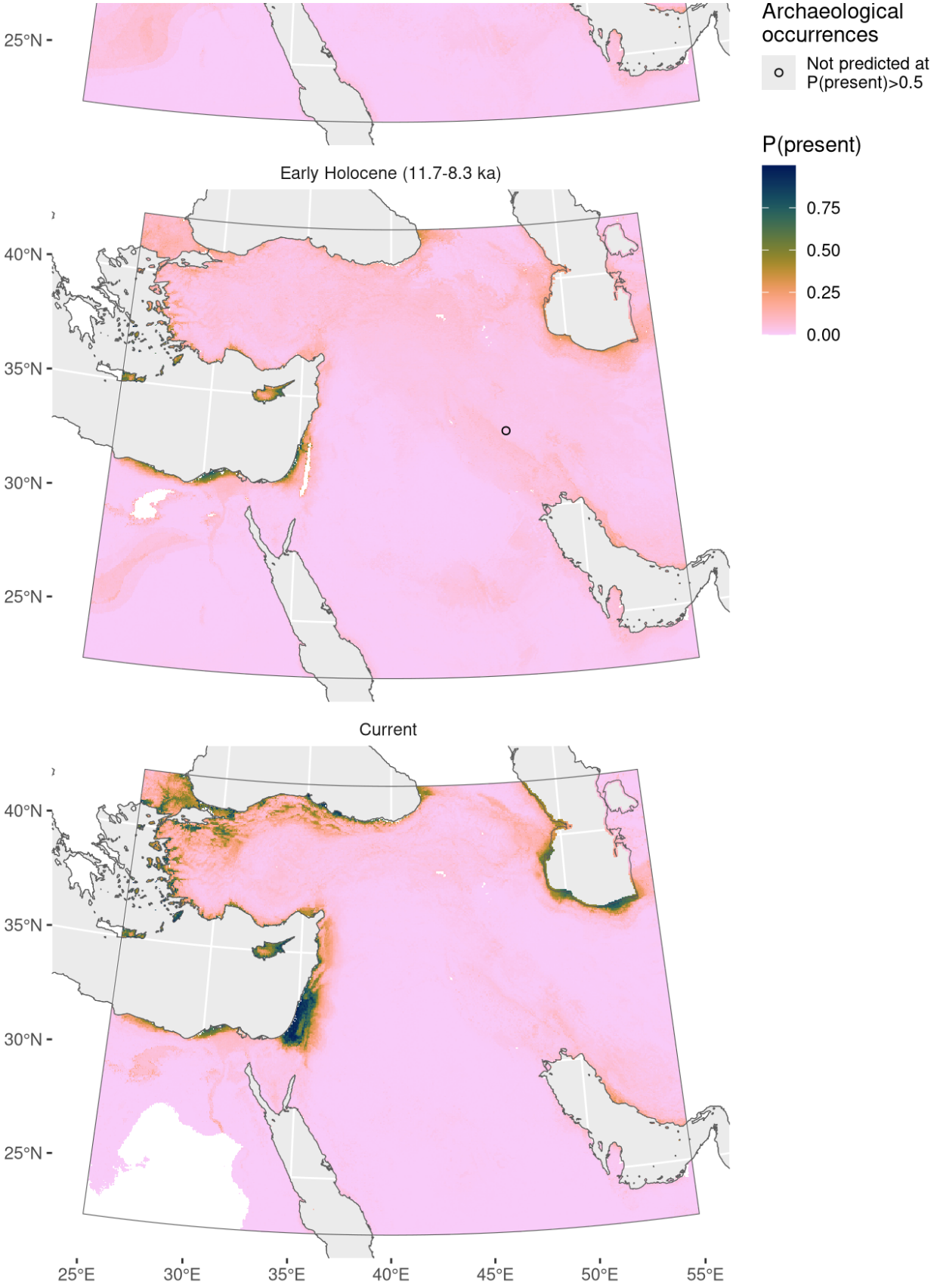


Figure 96: Predicted palaeodistributions of *Salsola kali*

Table 48: Archaeological occurrences of *Salsola kali*

Archaeological occurrences of *Salsola kali*

| Site | Age range | N assemblages | Average prop. | Source | Predicted? |
|---|---|---|---|---|---|

| | | | | | |
|---|---|---|---|---|---|
| Early Holocene (11.7-8.3 ka) | | | | | |
| Chogha Golan | 11.2–9.8 ka | 6 | 0.22% | ORIGINS | no |

# *Salvia absconditiflora*

Including Salvia cryptantha.

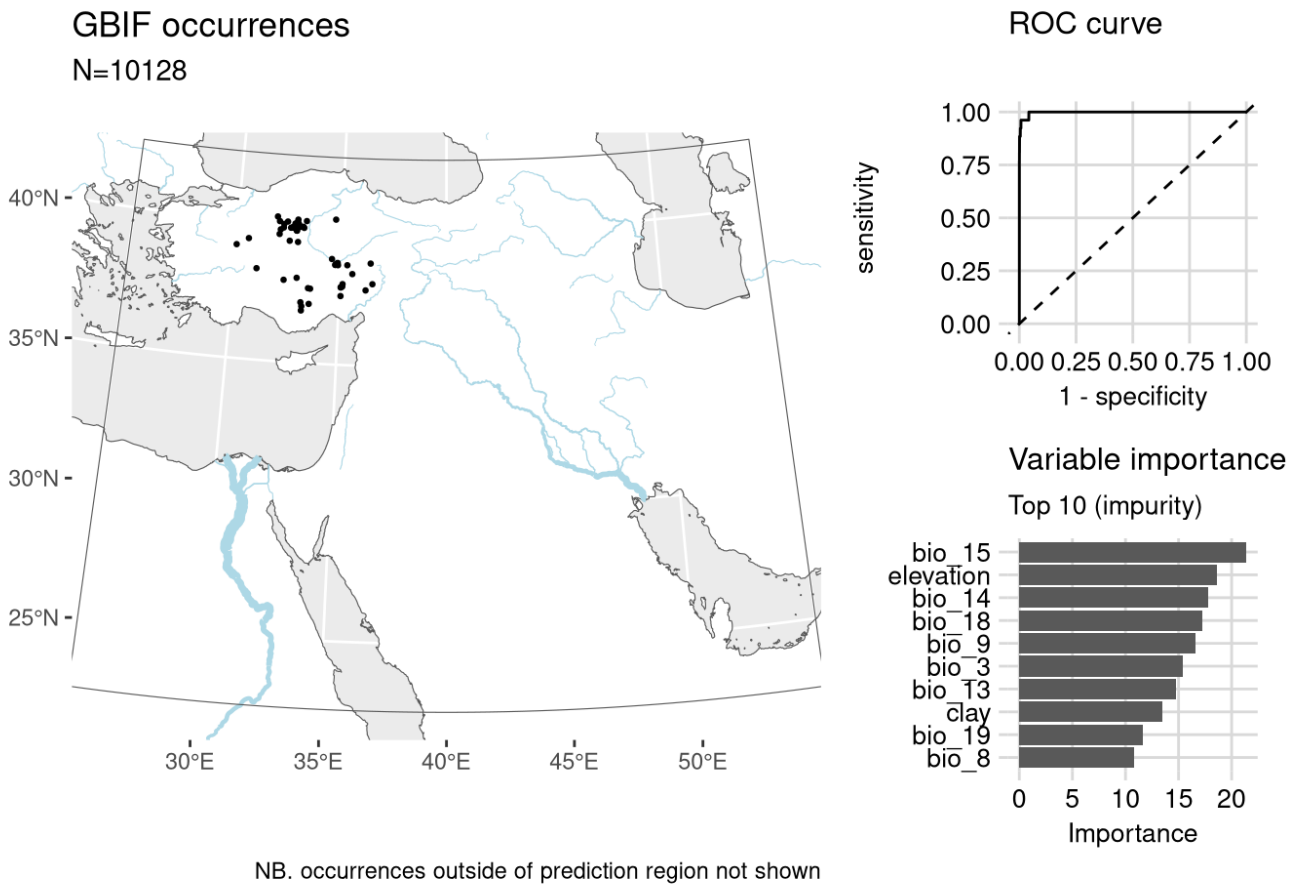


Figure 97: Fitted model summary for *Salvia absconditiflora*

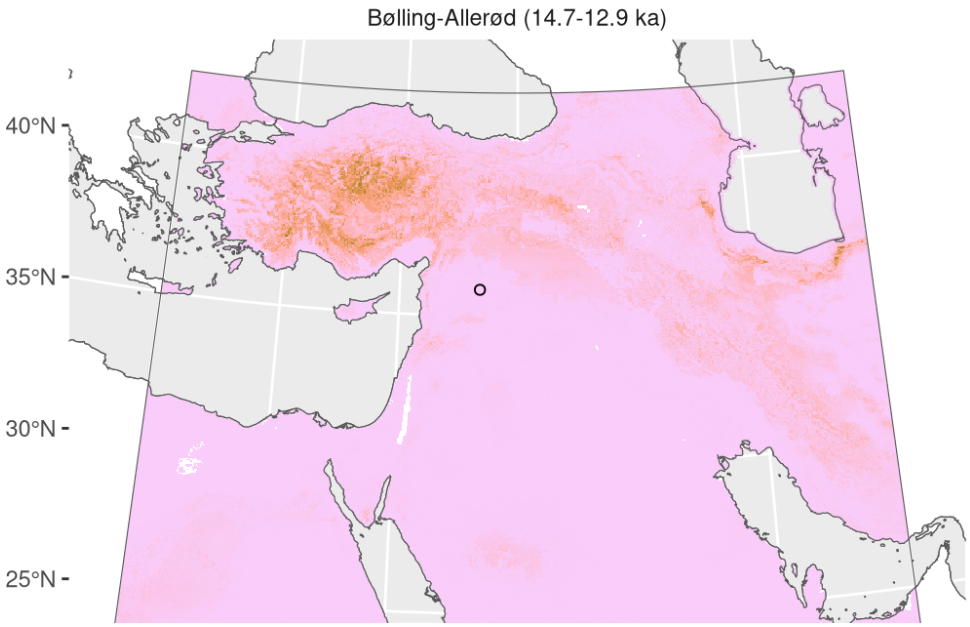

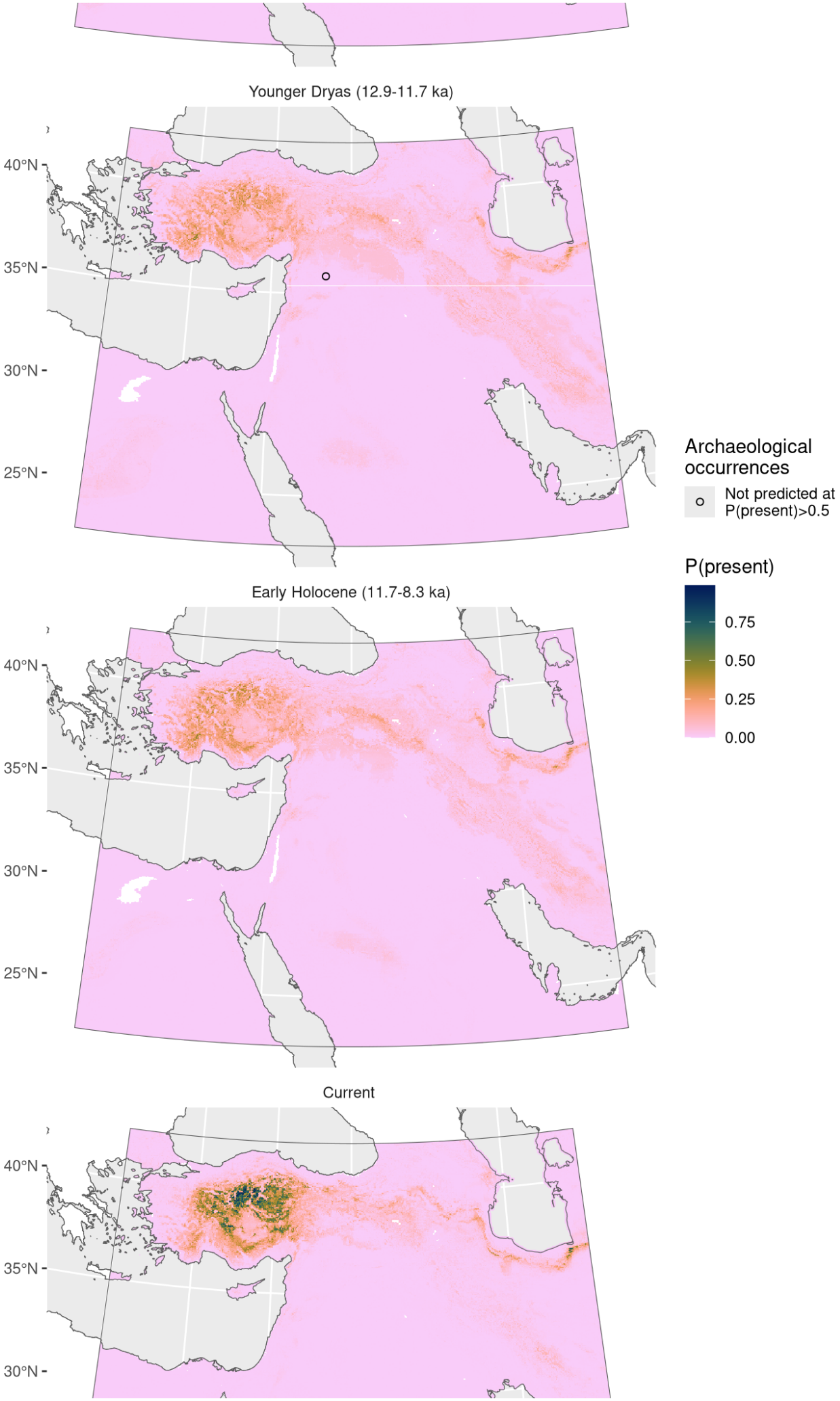
Younger Dryas (12.9-11.7 ka)
40°N
35°N
30°N
25°N
Early Holocene (11.7-8.3 ka)
40°N
35°N
30°N
25°N
Current
40°N
35°N
30°N
Archaeological occurrences
Not predicted at P(present)>0.5
P(present)
0.75
0.50
0.25
0.00

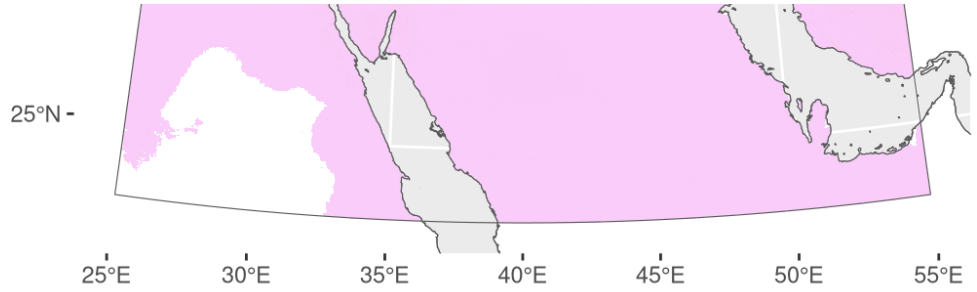


Figure 98: Predicted palaeodistributions of *Salvia absconditiflora*

Table 49: Archaeological occurrences of *Salvia absconditiflora*

Archaeological occurrences of *Salvia absconditiflora*

| Site | Age range | N assemblages | Average prop. | Source | Predicted? |
|---|---|---|---|---|---|
| Bølling-Allerød (14.7-12.9 ka) | | | | | |
| Abu Hureyra | 13.1–13.0 ka | 1 | 0.10% | ORIGINS | no |
| Younger Dryas (12.9-11.7 ka) | | | | | |
| Abu Hureyra | 13.0–11.8 ka | 2 | 0.11% | ORIGINS | no |

# *Secale cereale*

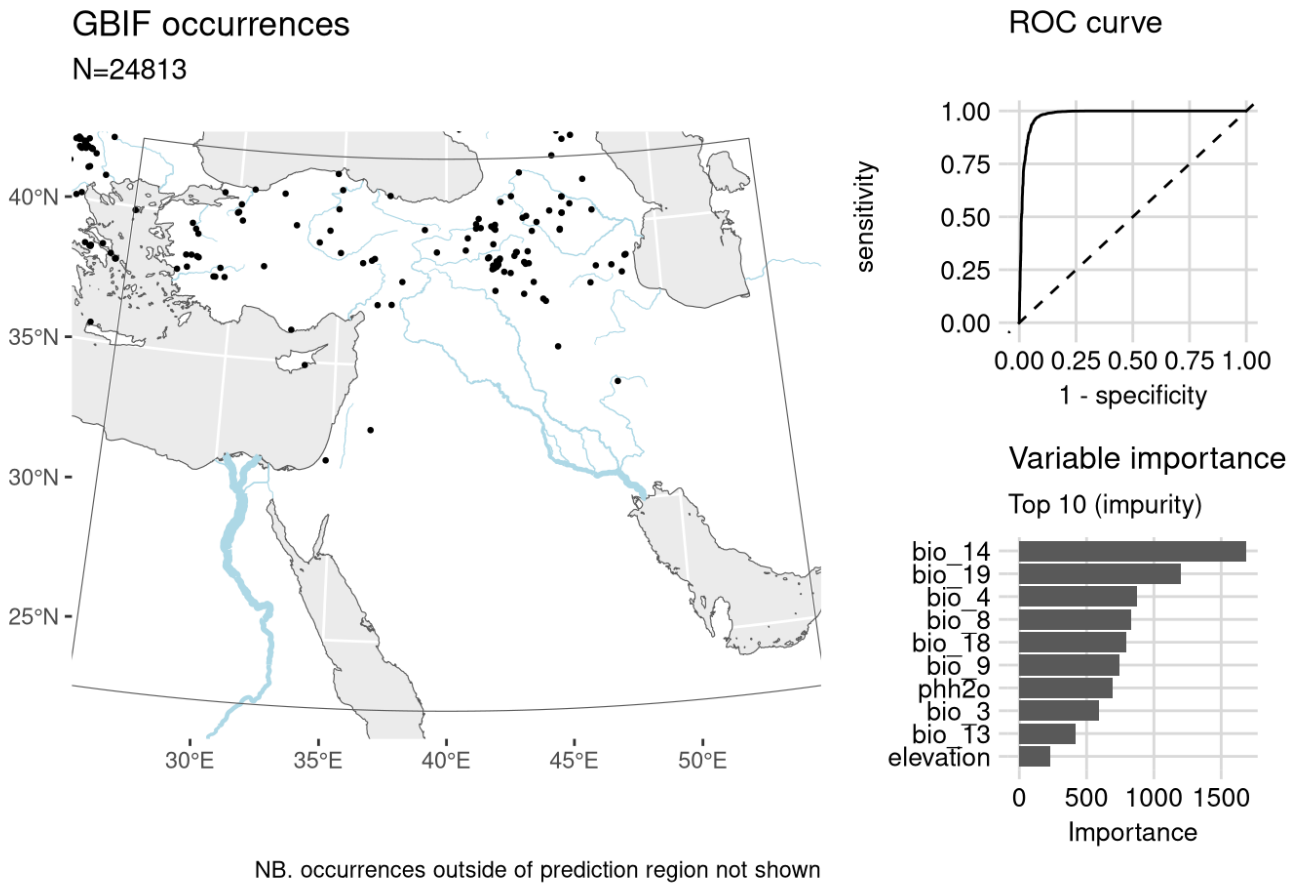


NB. occurrences outside of prediction region not shown

Figure 99: Fitted model summary for *Secale cereale*

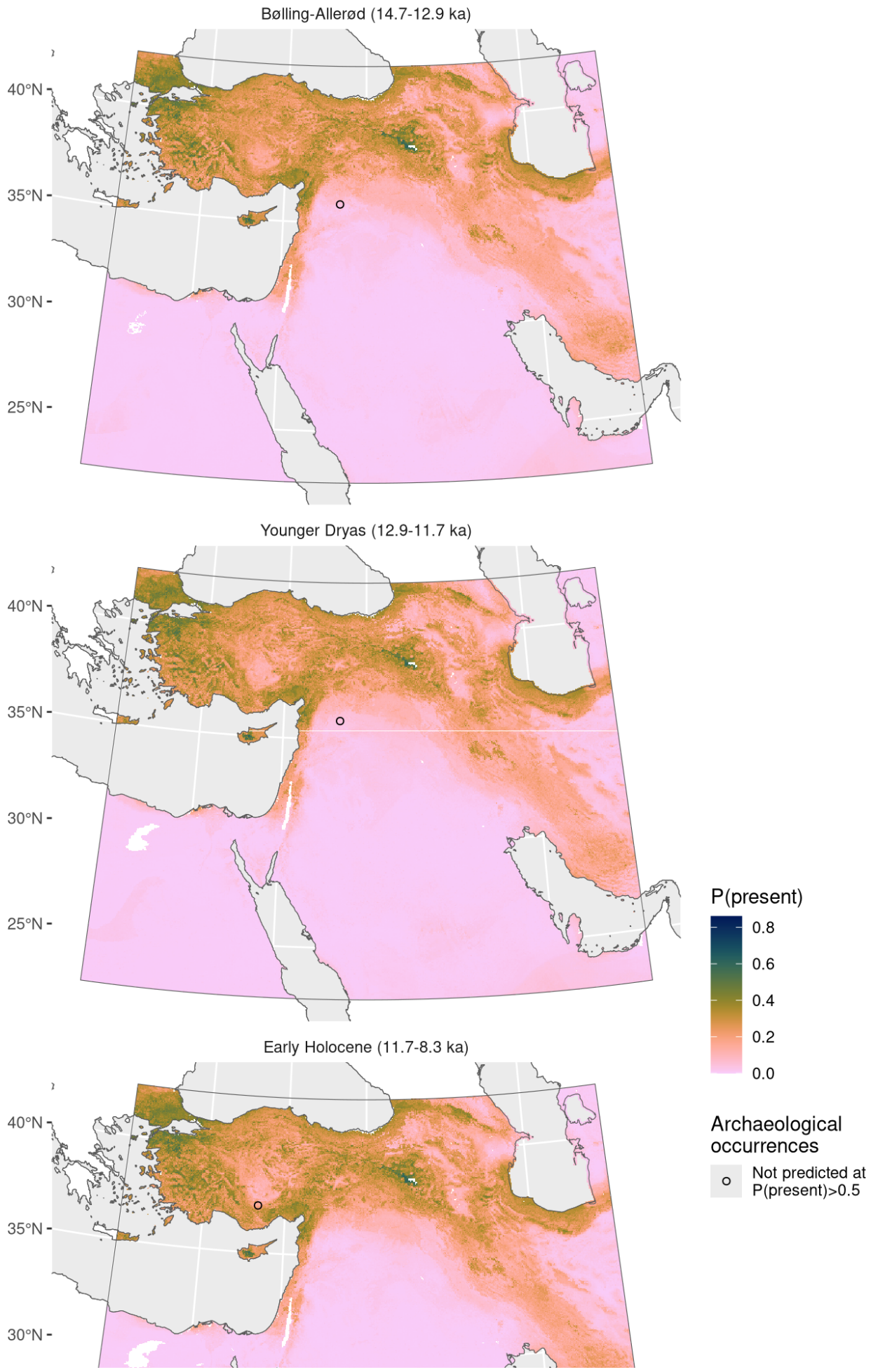

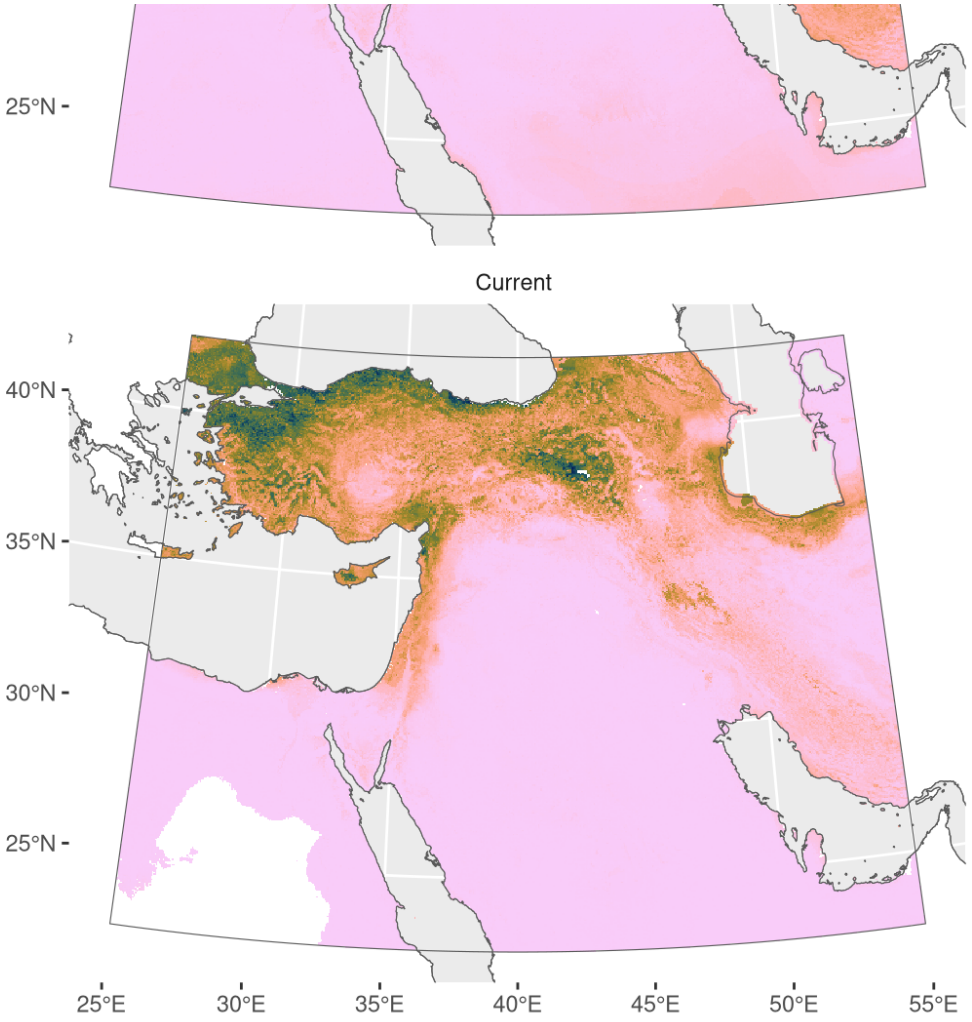


Figure 100: Predicted palaeodistributions of *Secale cereale*

Table 50: Archaeological occurrences of *Secale cereale*

Archaeological occurrences of *Secale cereale*

| Site | Age range | N assemblages | Average prop. | Source | Predicted? |
|---|---|---|---|---|---|
| Bølling-Allerød (14.7-12.9 ka) | | | | | |
| Abu Hureyra | 13.1–13.0 ka | 1 | 0.05% | ORIGINS | no |
| Younger Dryas (12.9-11.7 ka) | | | | | |
| Abu Hureyra | 13.0–11.8 ka | 2 | 0.28% | ORIGINS | no |
| Early Holocene (11.7-8.3 ka) | | | | | |
| Can Hasan III | 9.4–8.6 ka | 1 | 0.15% | ORIGINS | no |

## *Secale strictum*

Including Secale montanum.

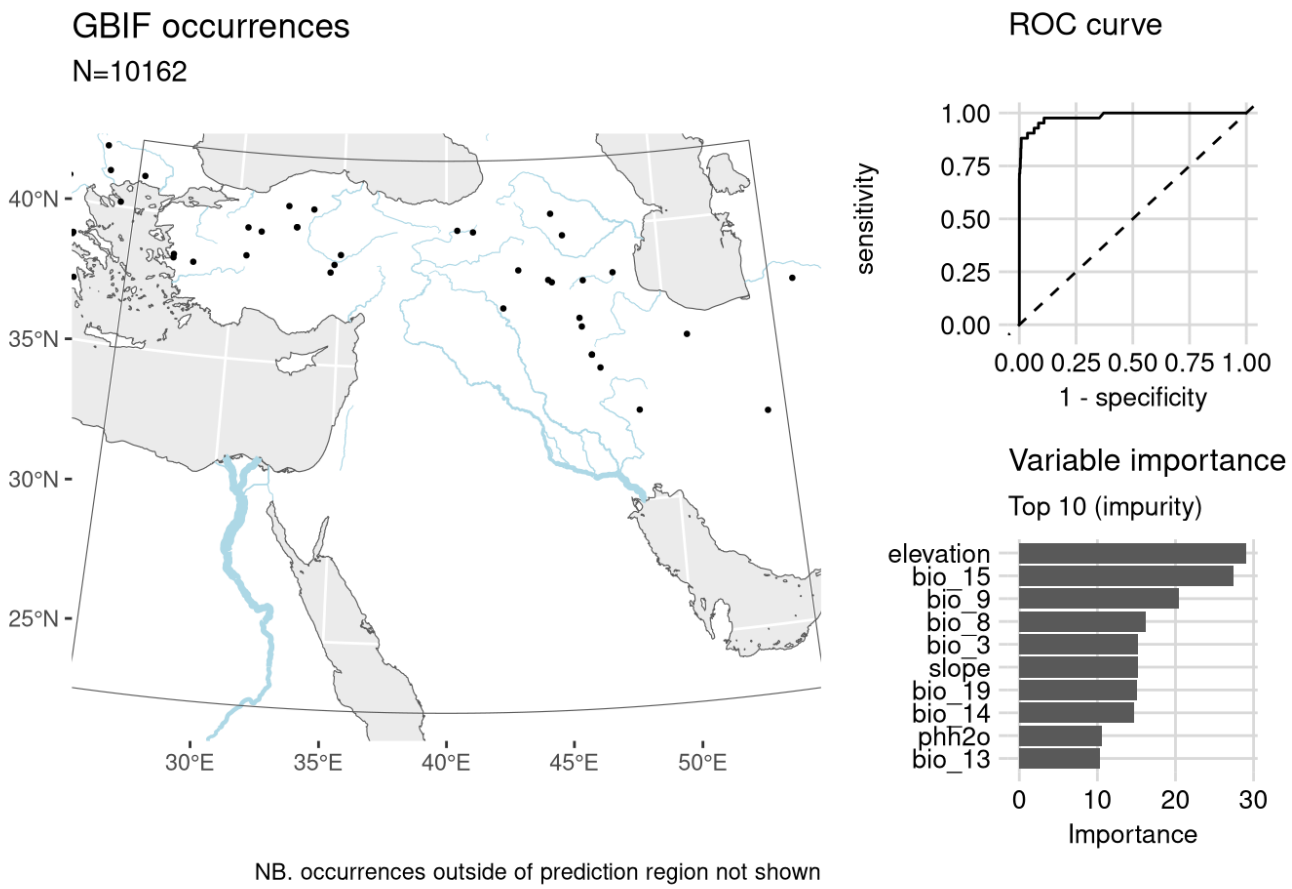


Figure 101: Fitted model summary for *Secale strictum*

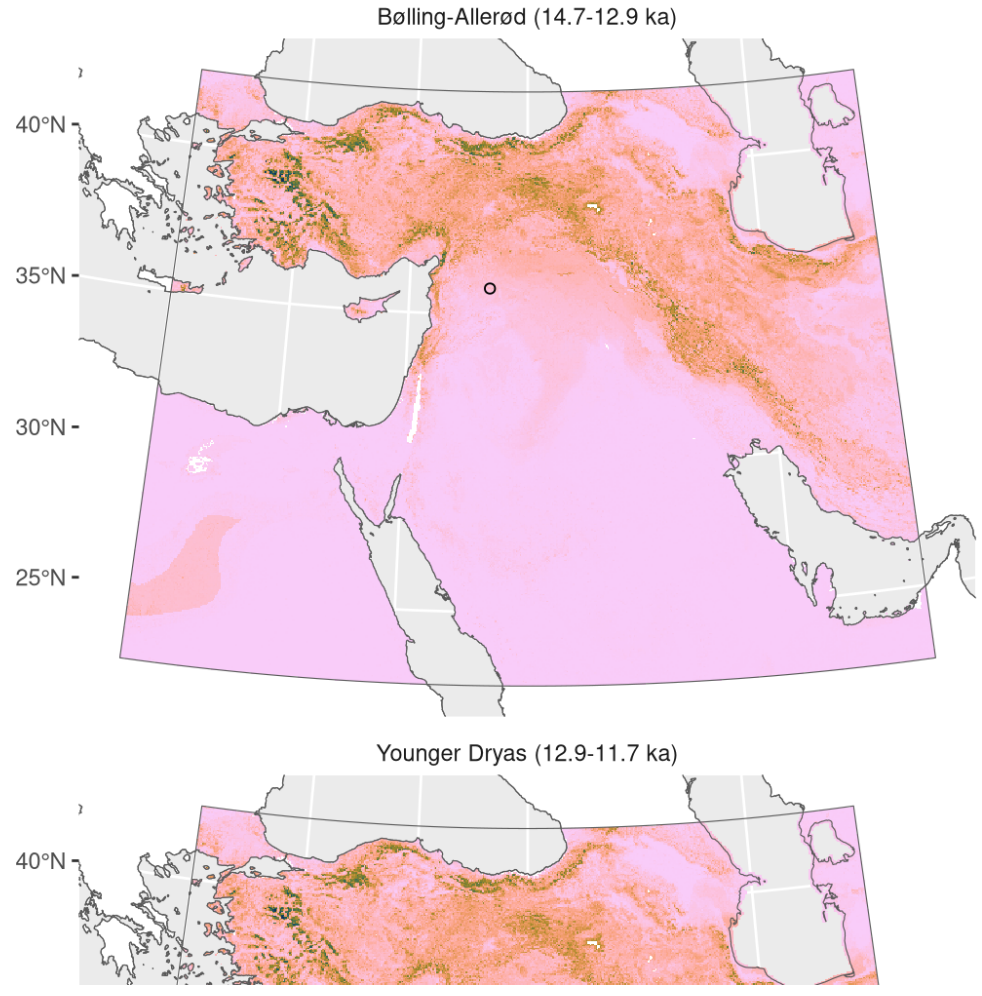

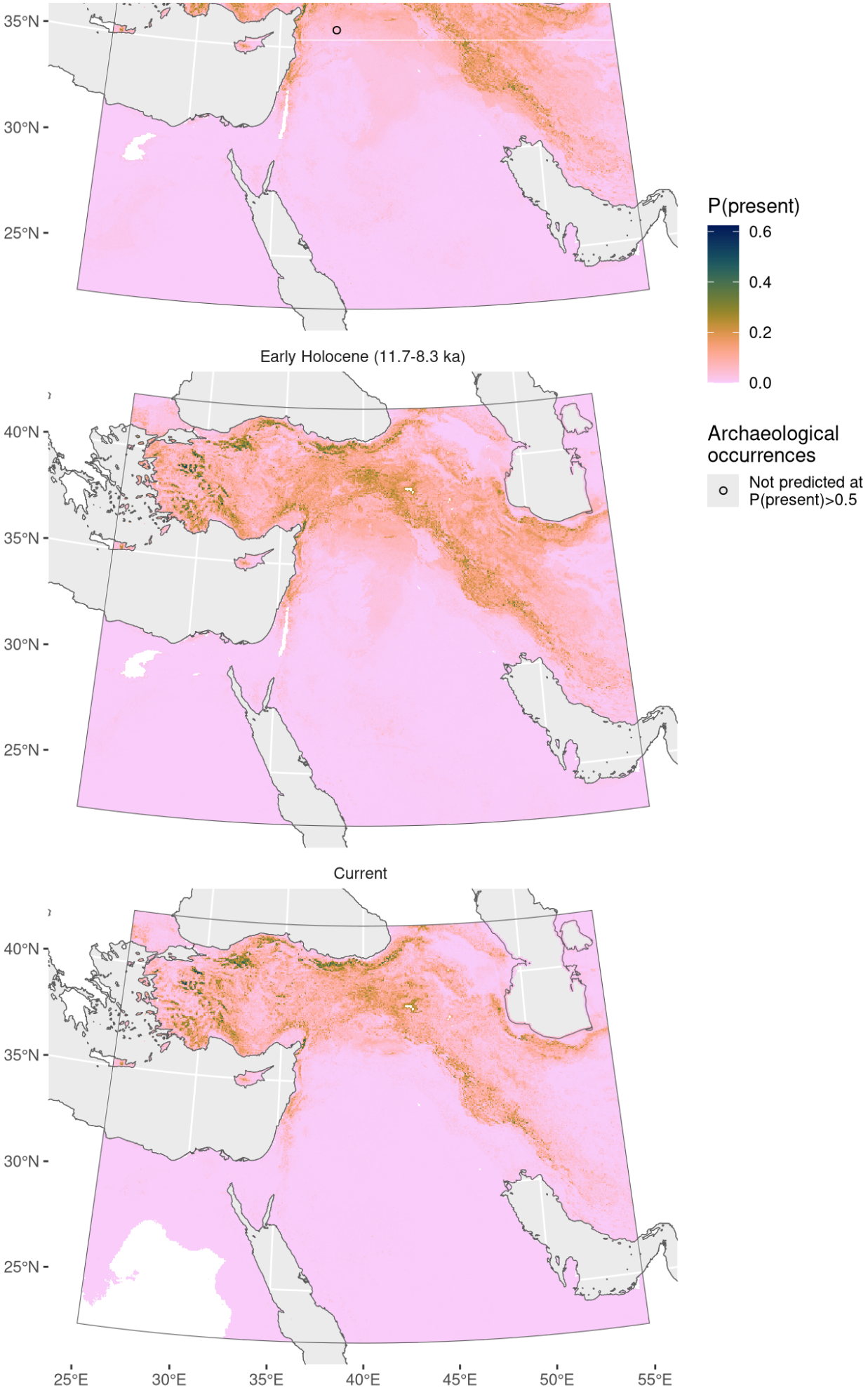


Figure 102: Predicted palaeodistributions of *Secale strictum*

Table 51: Archaeological occurrences of *Secale strictum*

Archaeological occurrences of *Secale strictum*

| Site | Age range | N assemblages | Average prop. | Source | Predicted? |
|---|---|---|---|---|---|
| Bølling-Allerød (14.7-12.9 ka) | | | | | |
| Abu Hureyra | 13.1–13.0 ka | 1 | 0.42% | ORIGINS | no |
| Younger Dryas (12.9-11.7 ka) | | | | | |
| Abu Hureyra | 13.0–11.8 ka | 2 | 0.72% | ORIGINS | no |

# *Suaeda fruticosa*

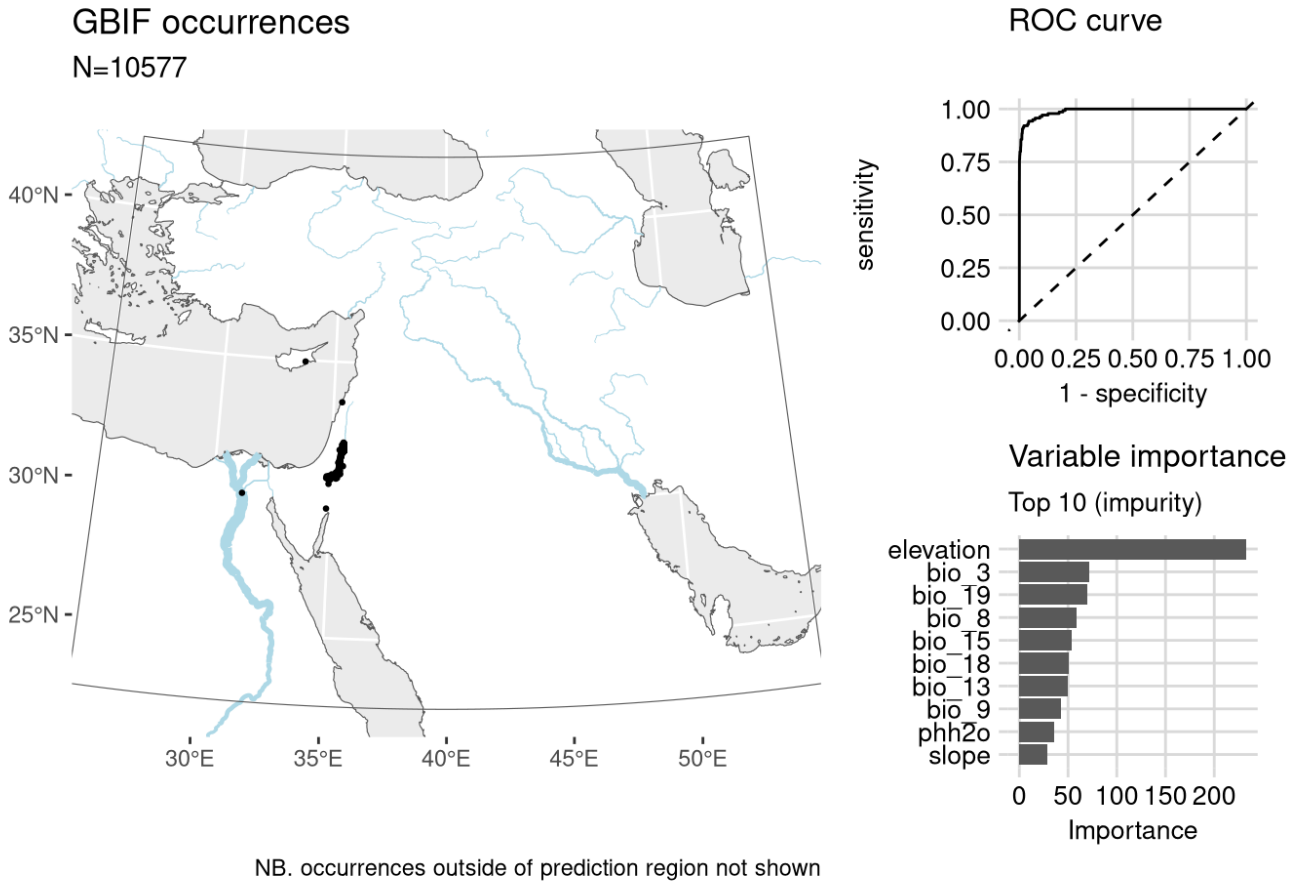


Figure 103: Fitted model summary for *Suaeda fruticosa*

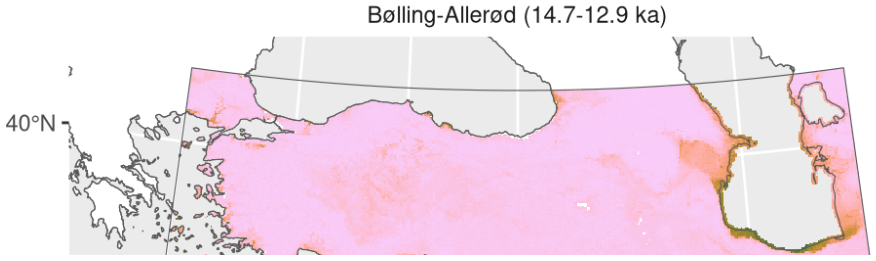

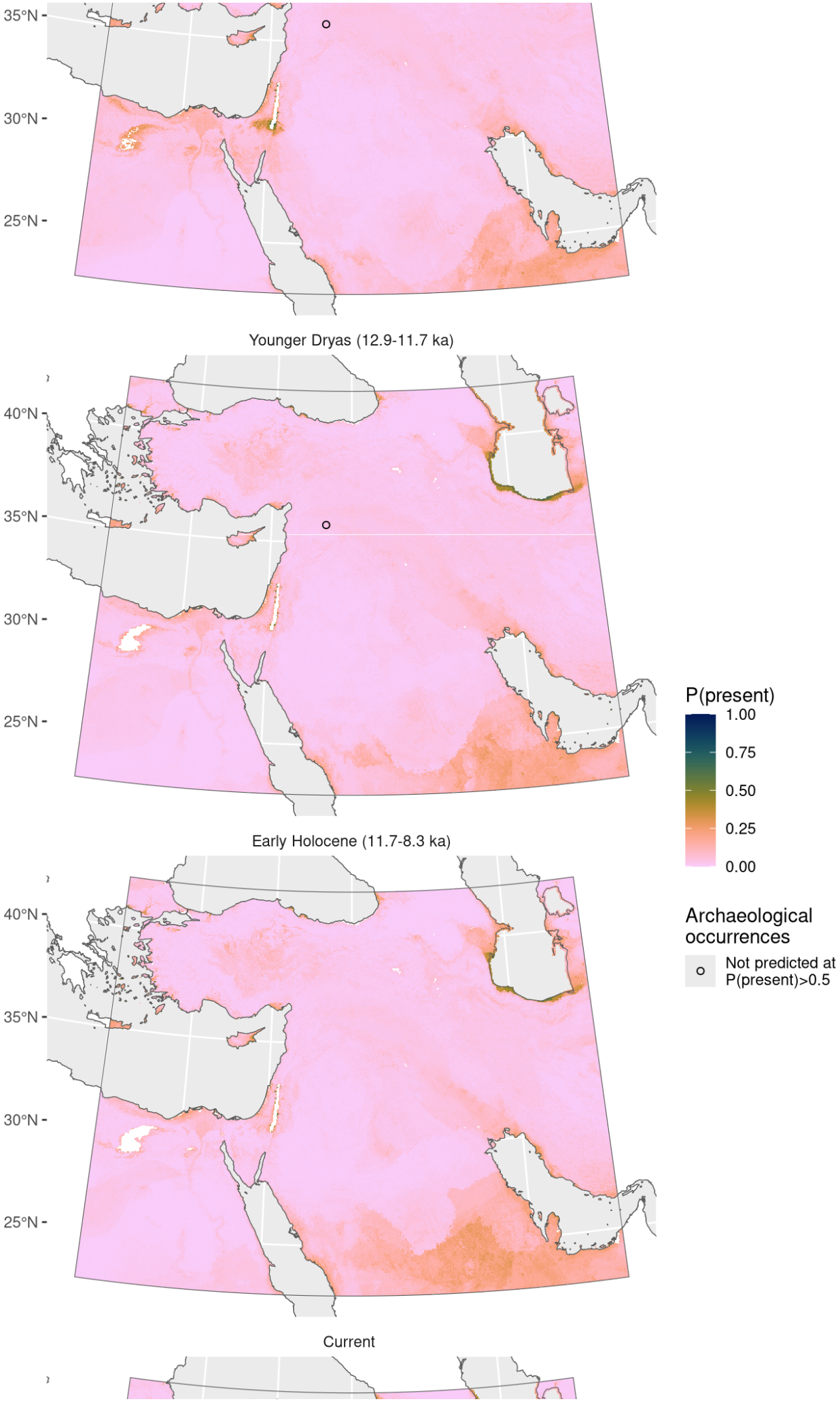
35°N
30°N
25°N
Younger Dryas (12.9-11.7 ka)
40°N
35°N
30°N
25°N
Early Holocene (11.7-8.3 ka)
40°N
35°N
30°N
25°N
Current
P(present)
1.00
0.75
0.50
0.25
0.00
Archaeological occurrences
Not predicted at P(present)>0.5

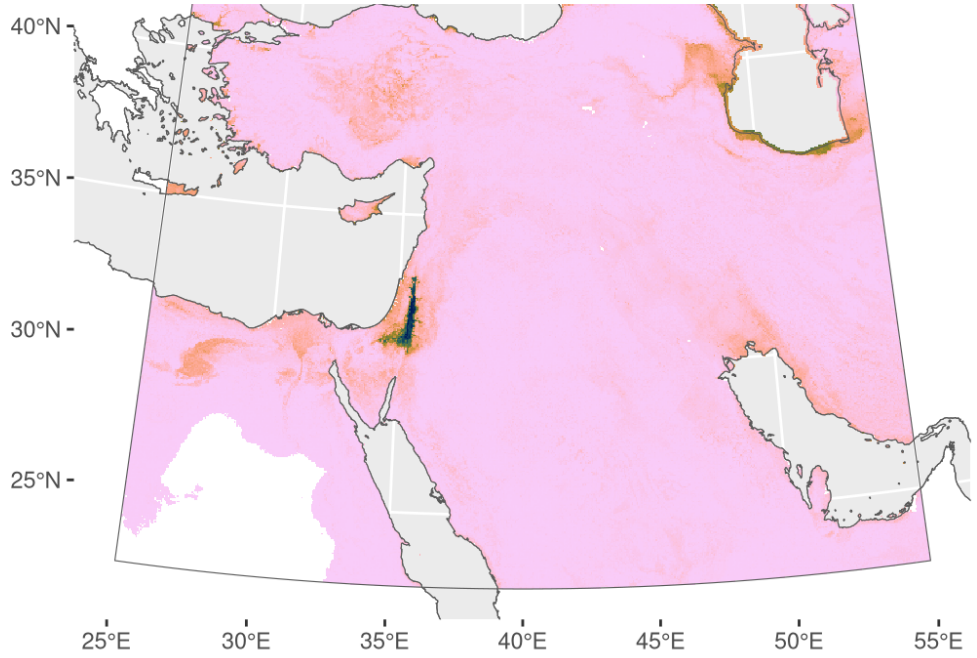


Figure 104: Predicted palaeodistributions of *Suaeda fruticosa*

Table 52: Archaeological occurrences of *Suaeda fruticosa*

Archaeological occurrences of *Suaeda fruticosa*

| Site | Age range | N assemblages | Average prop. | Source | Predicted? |
|---|---|---|---|---|---|
| Bølling-Allerød (14.7-12.9 ka) | | | | | |
| Abu Hureyra | 13.1–13.0 ka | 1 | 0.05% | ORIGINS | no |
| Younger Dryas (12.9-11.7 ka) | | | | | |
| Abu Hureyra | 13.0–11.8 ka | 2 | 0.30% | ORIGINS | no |

# *Taeniatherum caput-medusae*

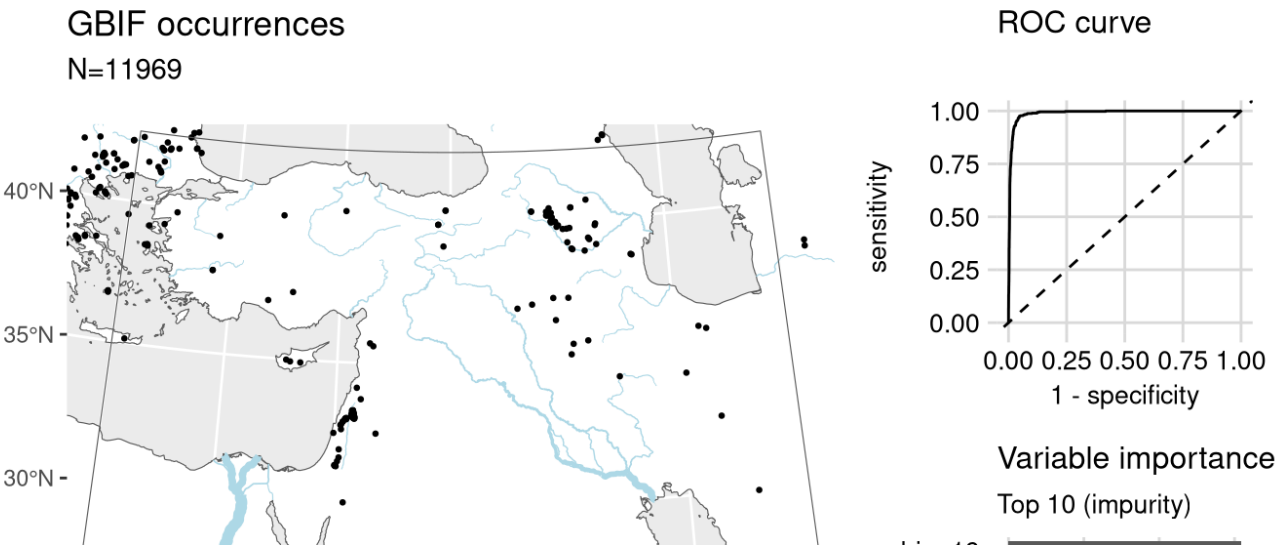

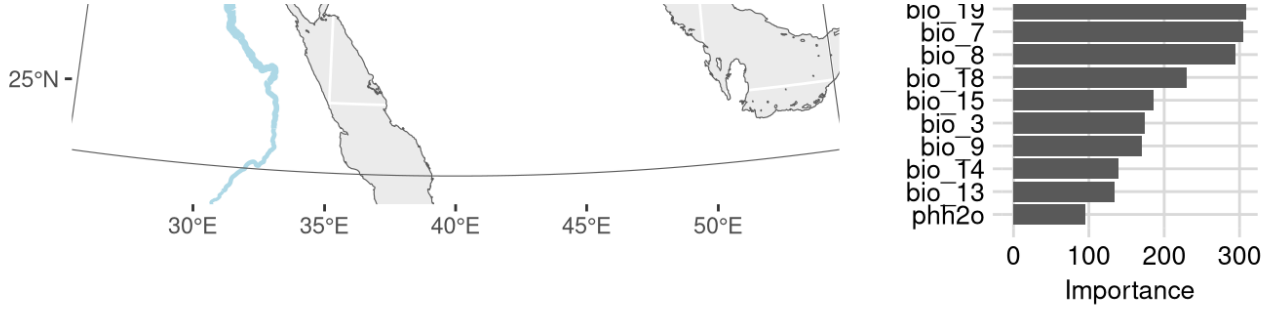


NB. occurrences outside of prediction region not shown

Figure 105: Fitted model summary for *Taeniatherum caput-medusae*

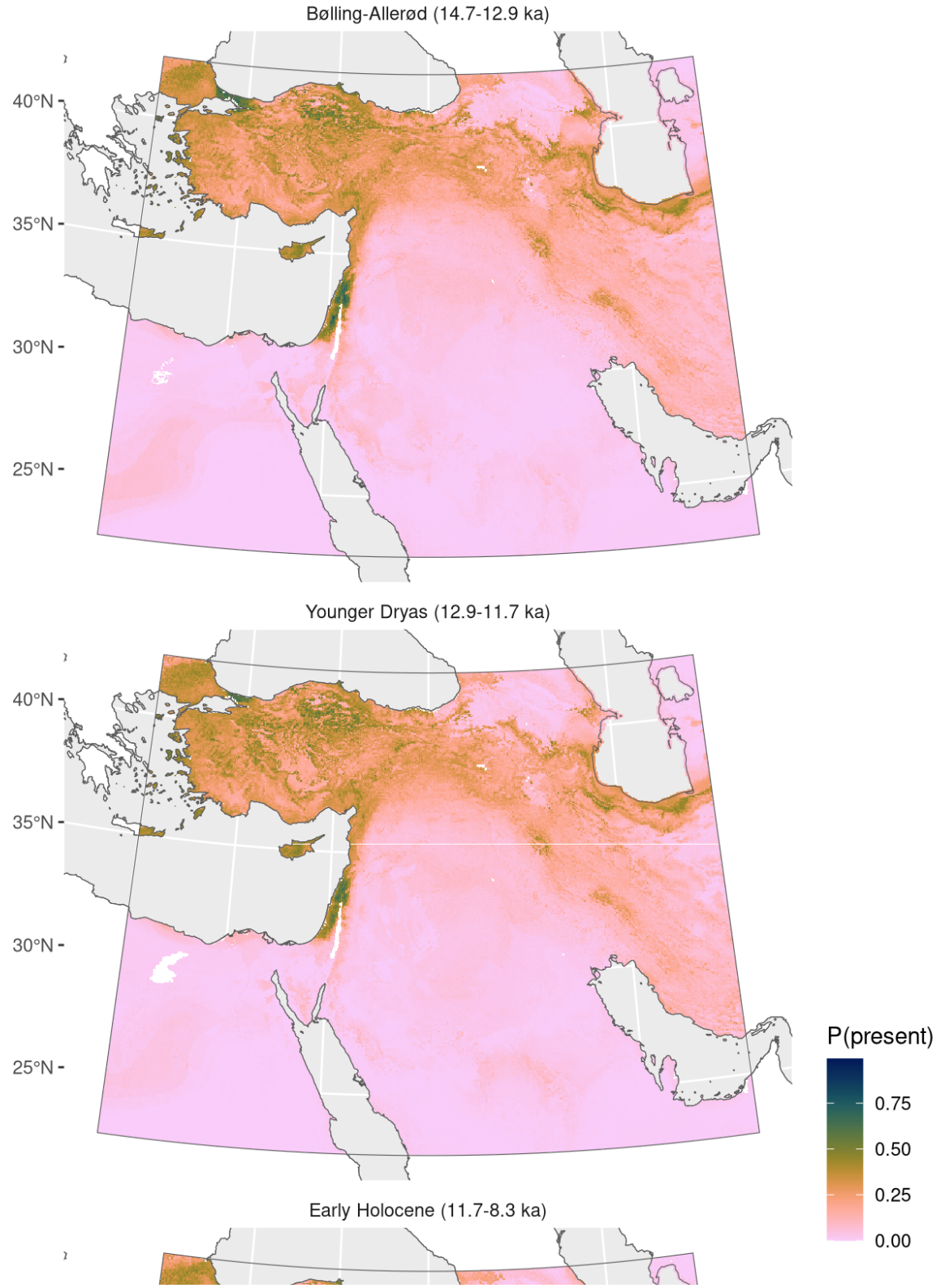

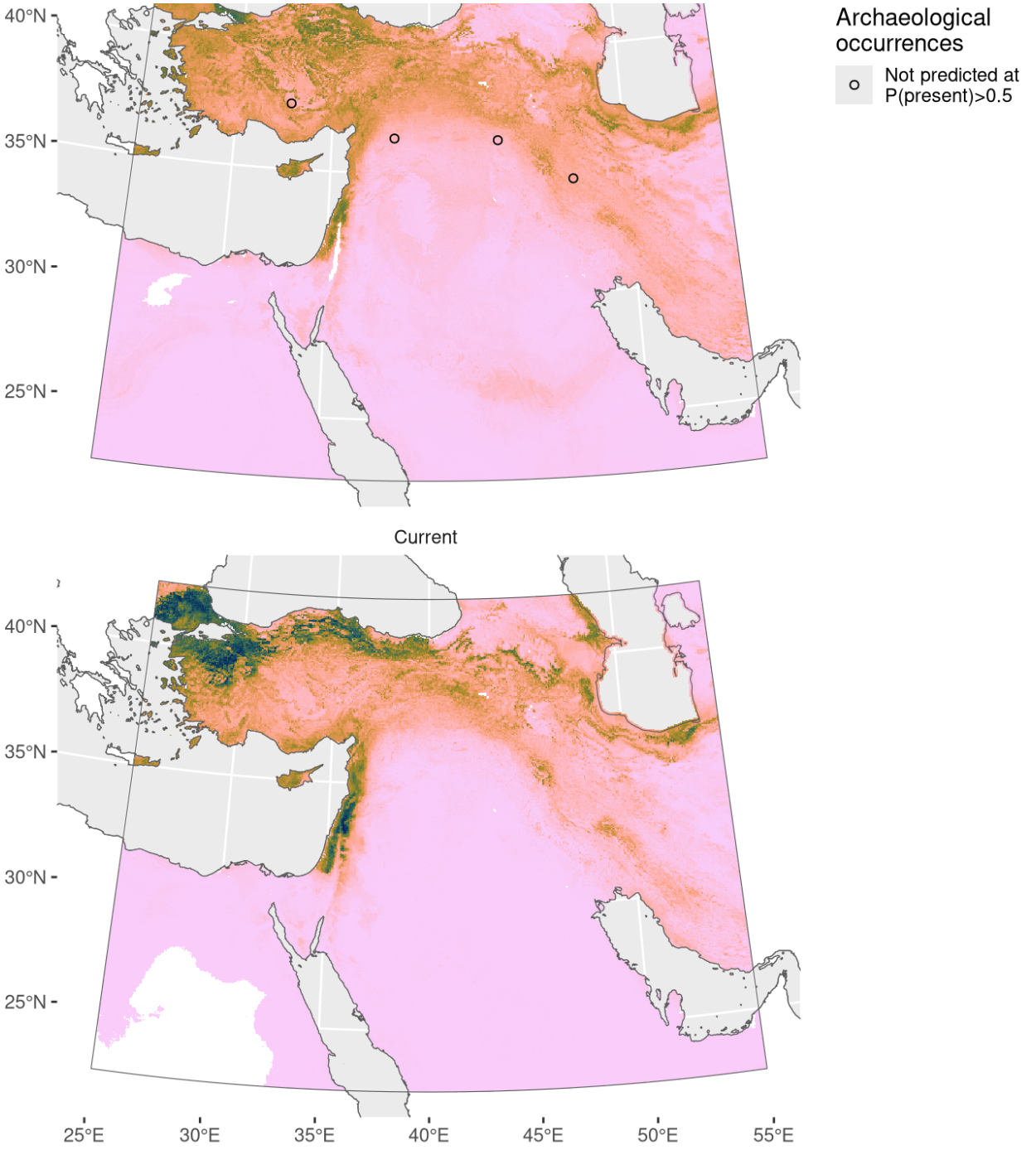


Figure 106: Predicted palaeodistributions of *Taeniatherum caput-medusae*

Table 53: Archaeological occurrences of *Taeniatherum caput-medusae*

Archaeological occurrences of *Taeniatherum caput-medusae*

| Site | Age range | N assemblages | Average prop. | Source | Predicted? |
|---|---|---|---|---|---|
| Early Holocene (11.7-8.3 ka) | | | | | |
| Jerf el Ahmar | 11.4–10.7 ka | 1 | 0.34% | ORIGINS | no |
| M'lefaat | 11.3–11.1 ka | 1 | 2.04% | ORIGINS | no |
| Sheikh-e Abad | 10.7–8.4 ka | 1 | 1.65% | ADEMNES | no |

| | | | | | |
|---|---|---|---|---|---|
| Çatalhoyuk | 9.2–8.3 ka | 1 | 0.18% | ORIGINS | no |

# *Triticum aestivum*

Including Triticum spelta and Triticum aestivocompactum.

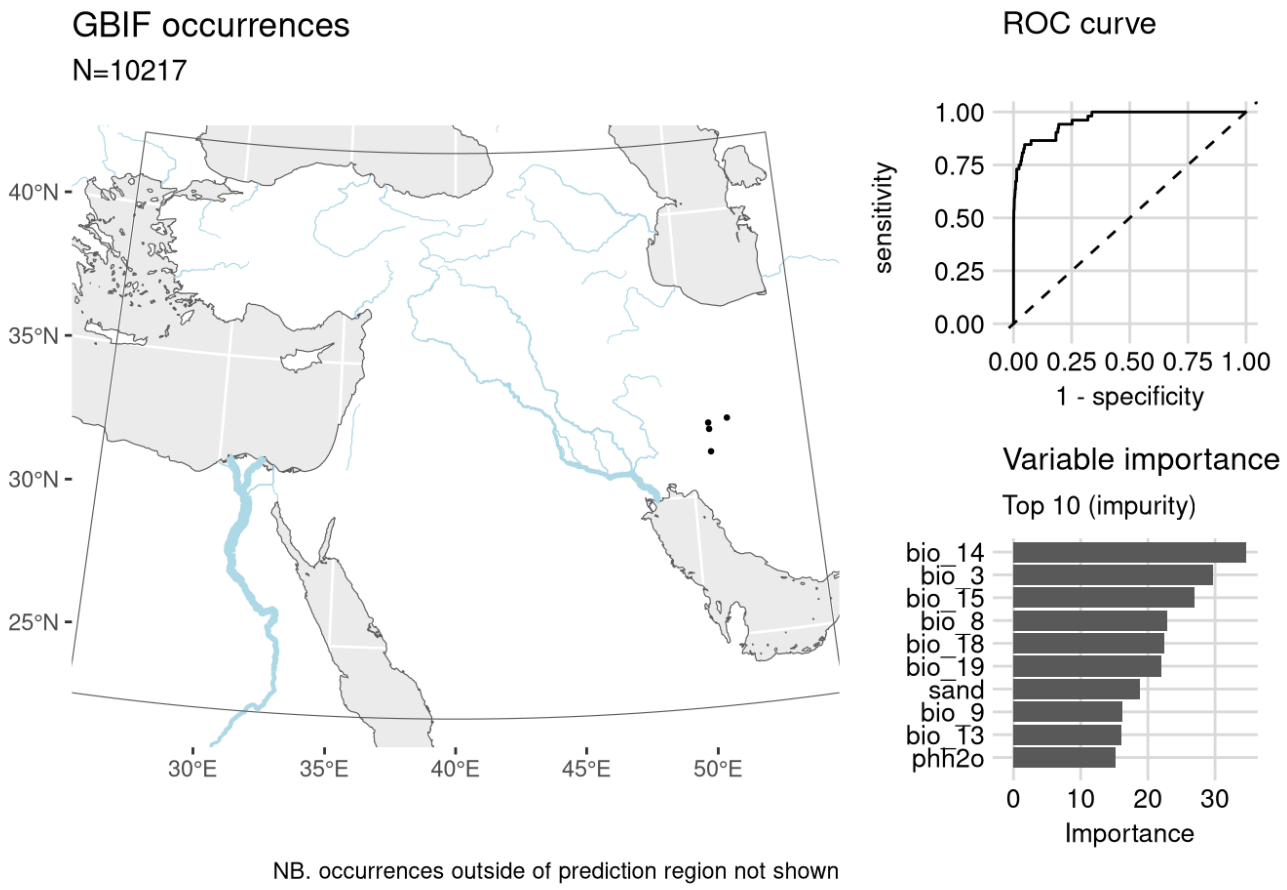


Figure 107: Fitted model summary for *Triticum aestivum*

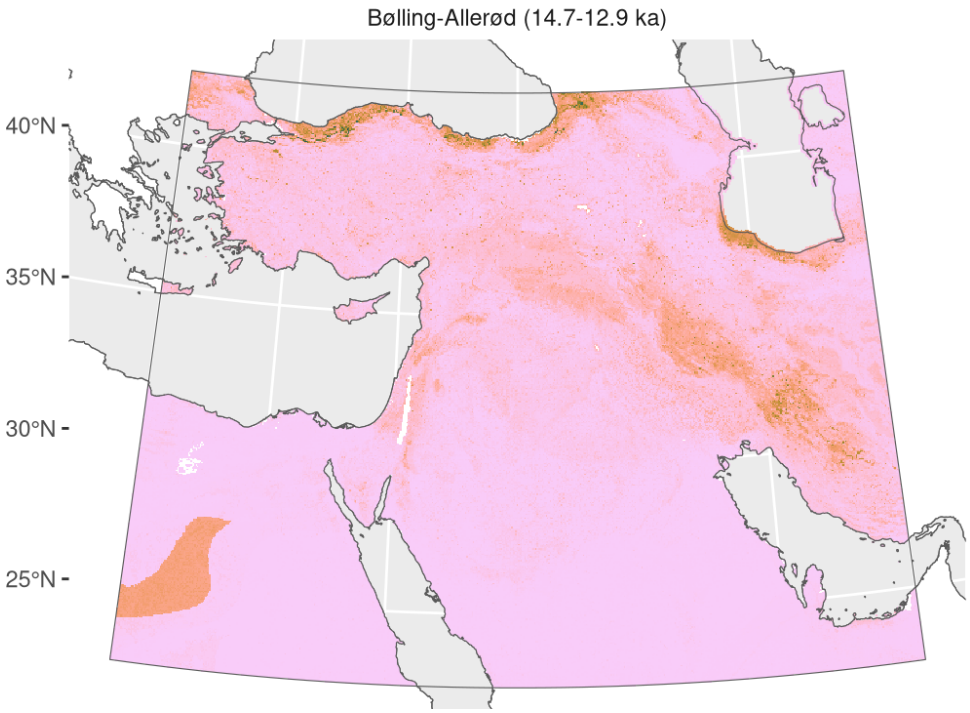

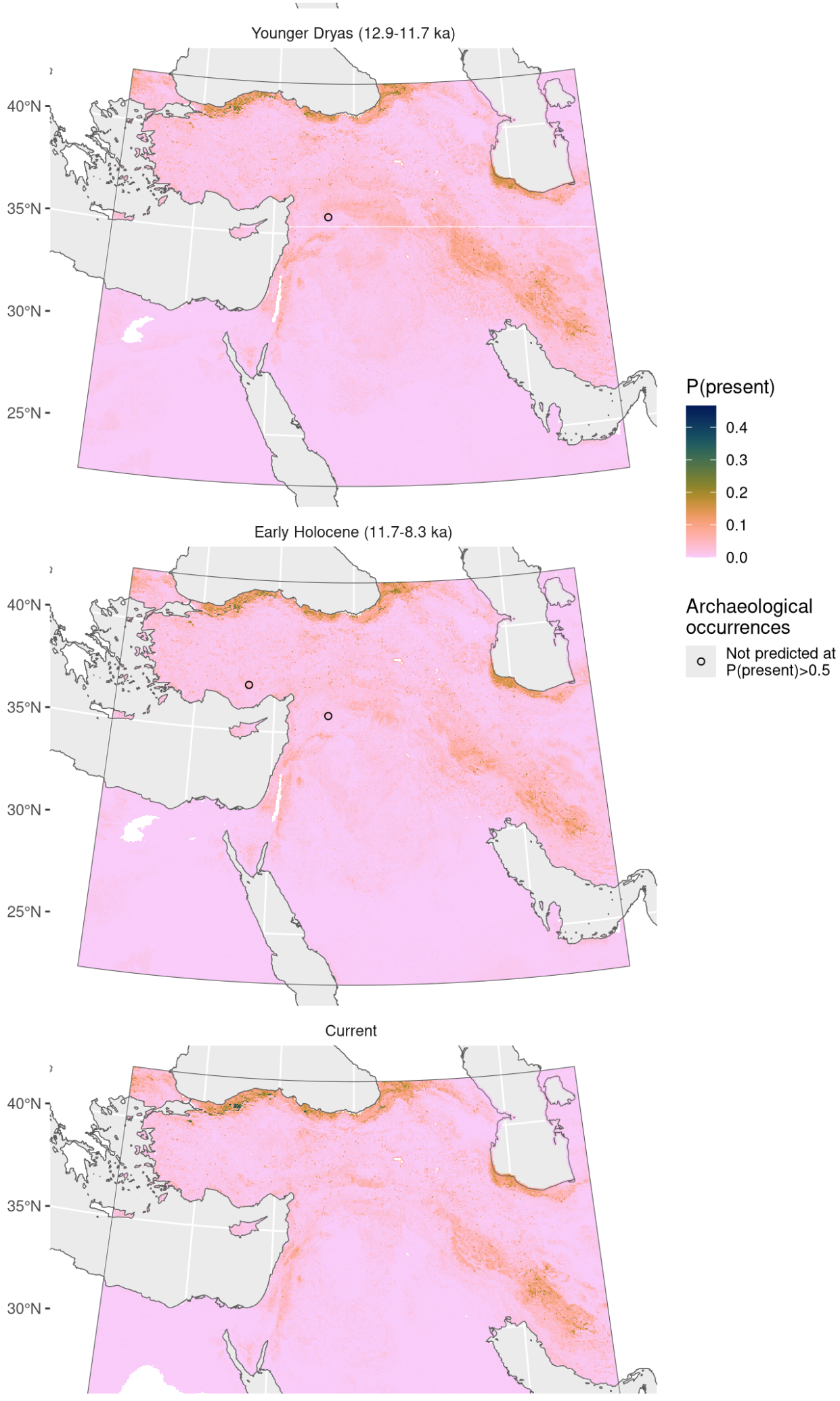
Younger Dryas (12.9-11.7 ka)
40°N
35°N
30°N
25°N
Early Holocene (11.7-8.3 ka)
40°N
35°N
30°N
25°N
Current
40°N
35°N
30°N
P(present)
0.4
0.3
0.2
0.1
0.0
Archaeological occurrences
Not predicted at P(present)>0.5

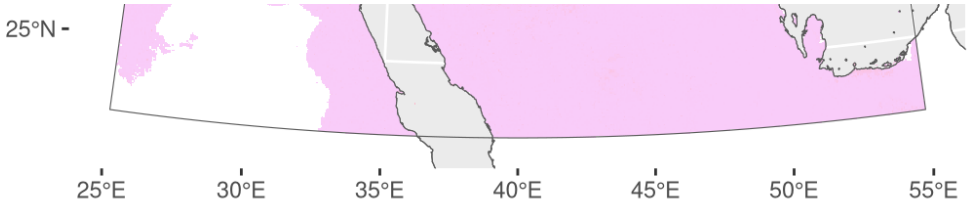


Figure 108: Predicted palaeodistributions of *Triticum aestivum*

Table 54: Archaeological occurrences of *Triticum aestivum*

Archaeological occurrences of *Triticum aestivum*

| Site | Age range | N assemblages | Average prop. | Source | Predicted? |
|---|---|---|---|---|---|
| Younger Dryas (12.9-11.7 ka) | | | | | |
| Abu Hureyra | 13.0–11.8 ka | 2 | 0.03% | ORIGINS | no |
| Early Holocene (11.7-8.3 ka) | | | | | |
| Can Hasan III | 9.4–8.6 ka | 1 | 1.44% | ORIGINS | no |
| Abu Hureyra | 9.3–8.2 ka | 1 | 0.24% | ORIGINS | no |

# *Triticum durum*

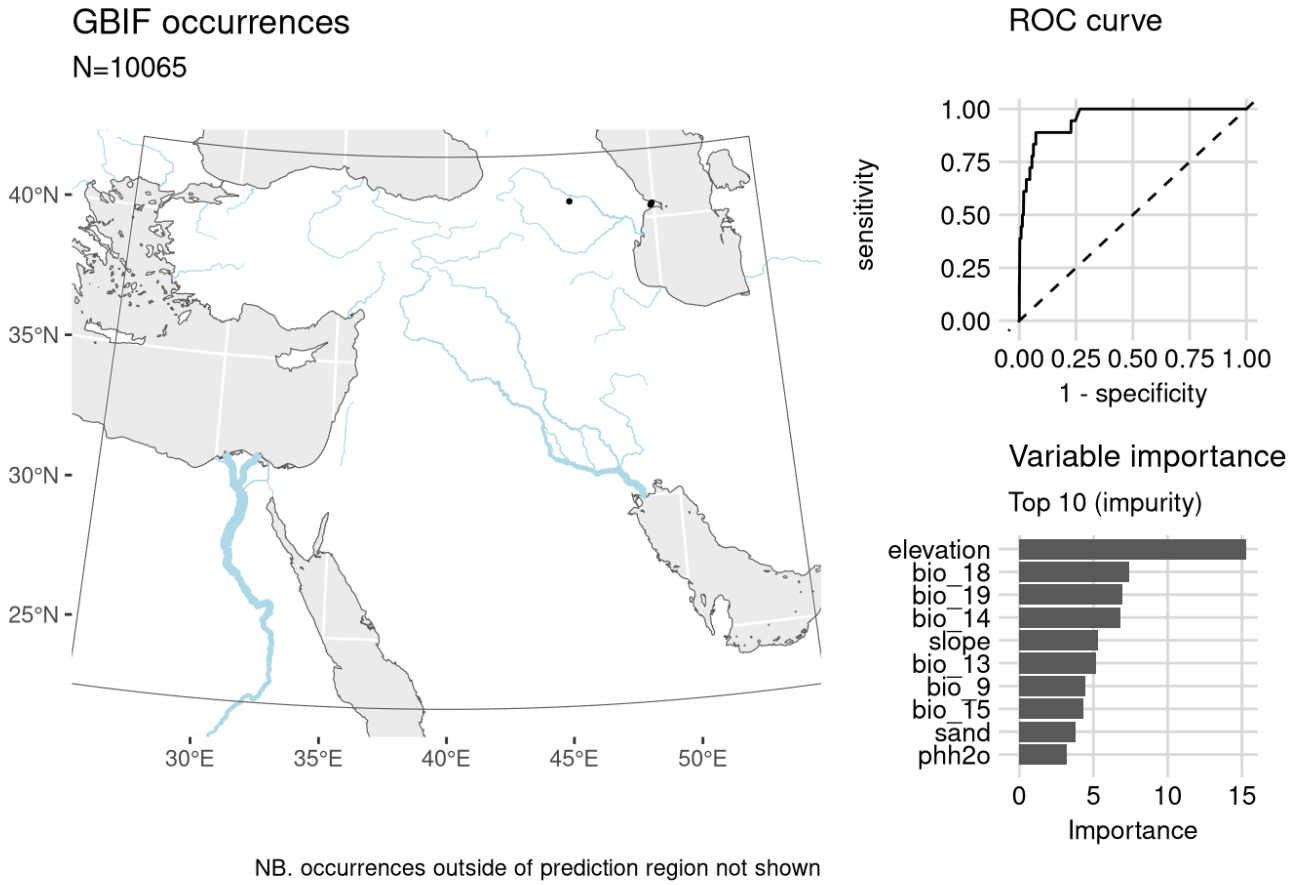

Figure 109: Fitted model summary for *Triticum durum*

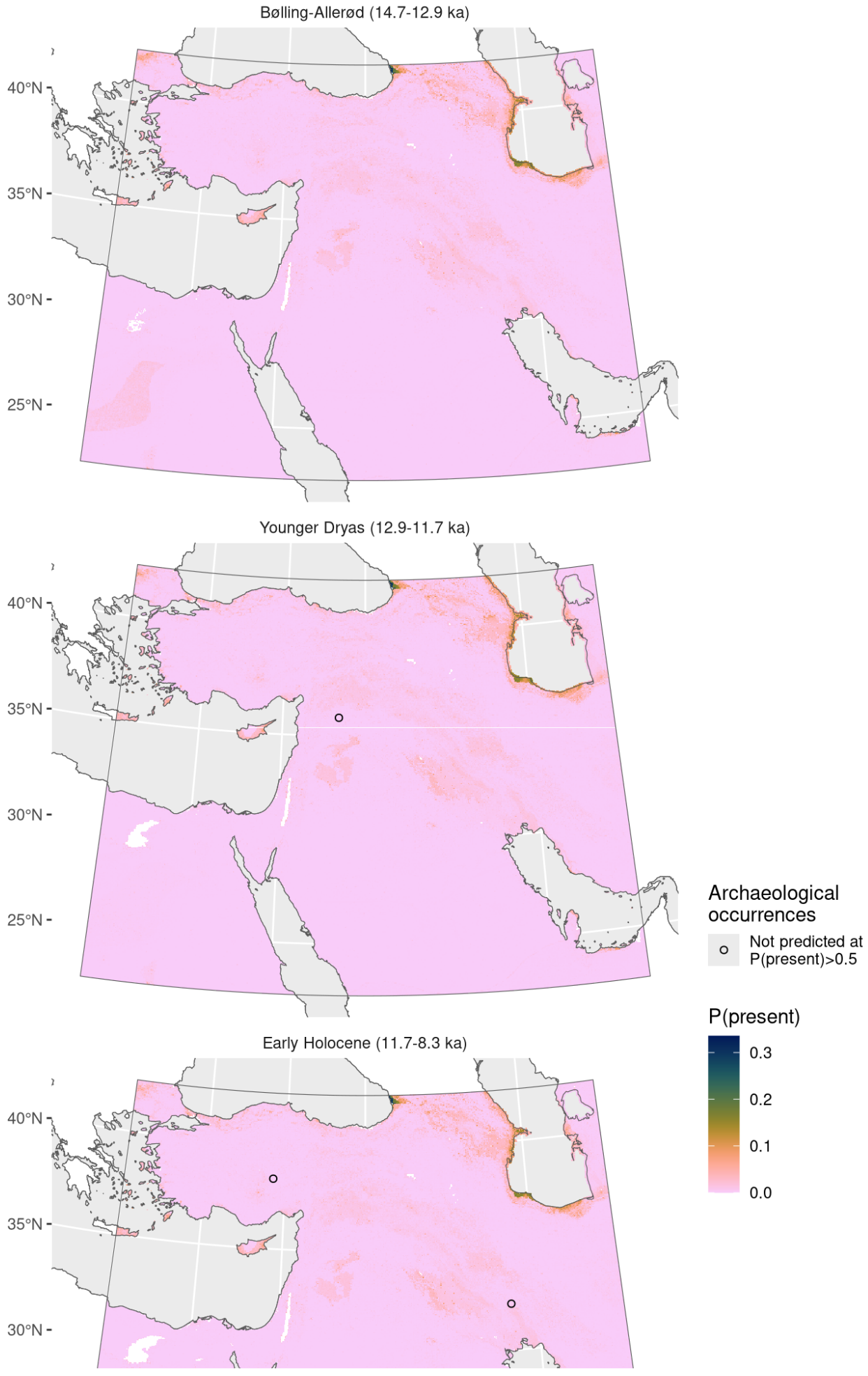

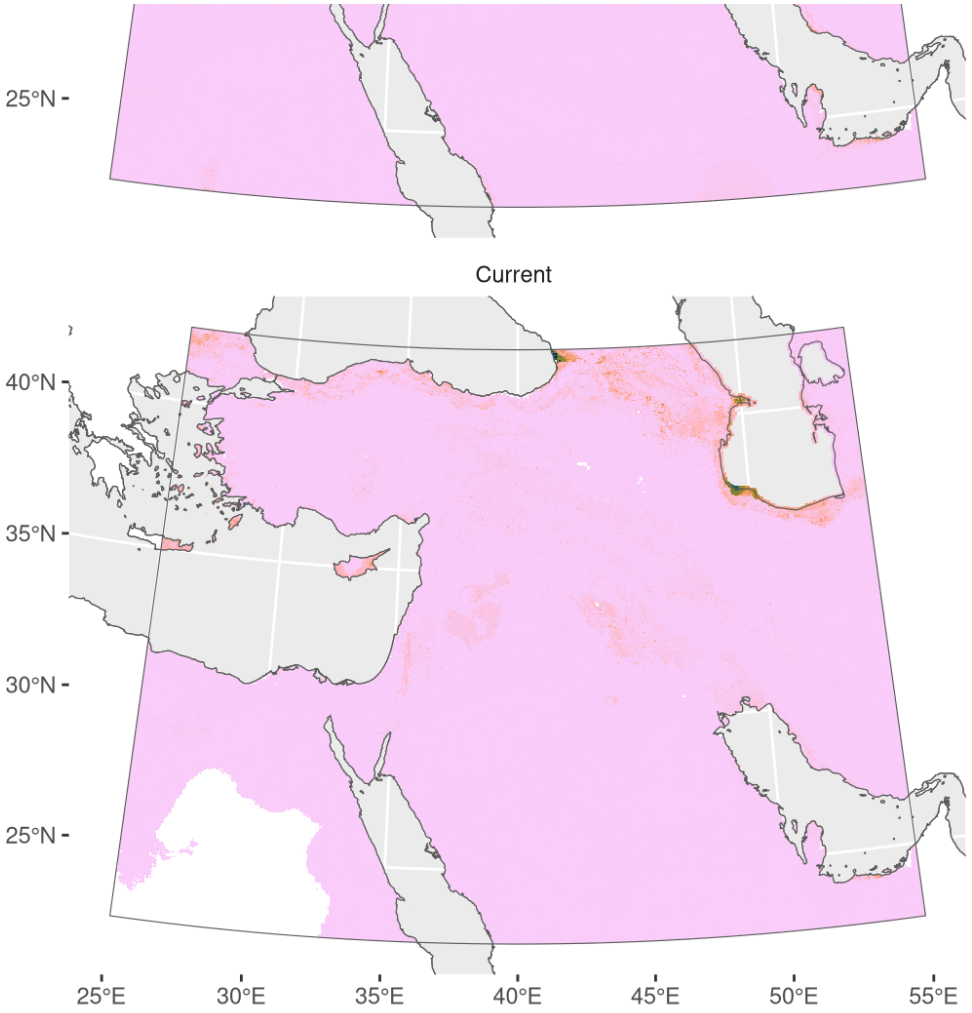


Figure 110: Predicted palaeodistributions of *Triticum durum*

Table 55: Archaeological occurrences of *Triticum durum*

Archaeological occurrences of *Triticum durum*

| Site | Age range | N assemblages | Average prop. | Source | Predicted? |
|---|---|---|---|---|---|
| Early Holocene (11.7-8.3 ka) | | | | | |
| Chogha Bonut | 12.8–8.8 ka | 1 | 0.03% | ORIGINS | no |
| Aşıklı Höyük | 9.9–9.4 ka | 1 | 0.26% | ORIGINS | no |
| Younger Dryas (12.9-11.7 ka) | | | | | |
| Abu Hureyra | 12.1–11.8 ka | 1 | 0.15% | ORIGINS | no |

# *Triticum monococcum*

Including Triticum boeoticum.

GBIF occurrences ROC curve

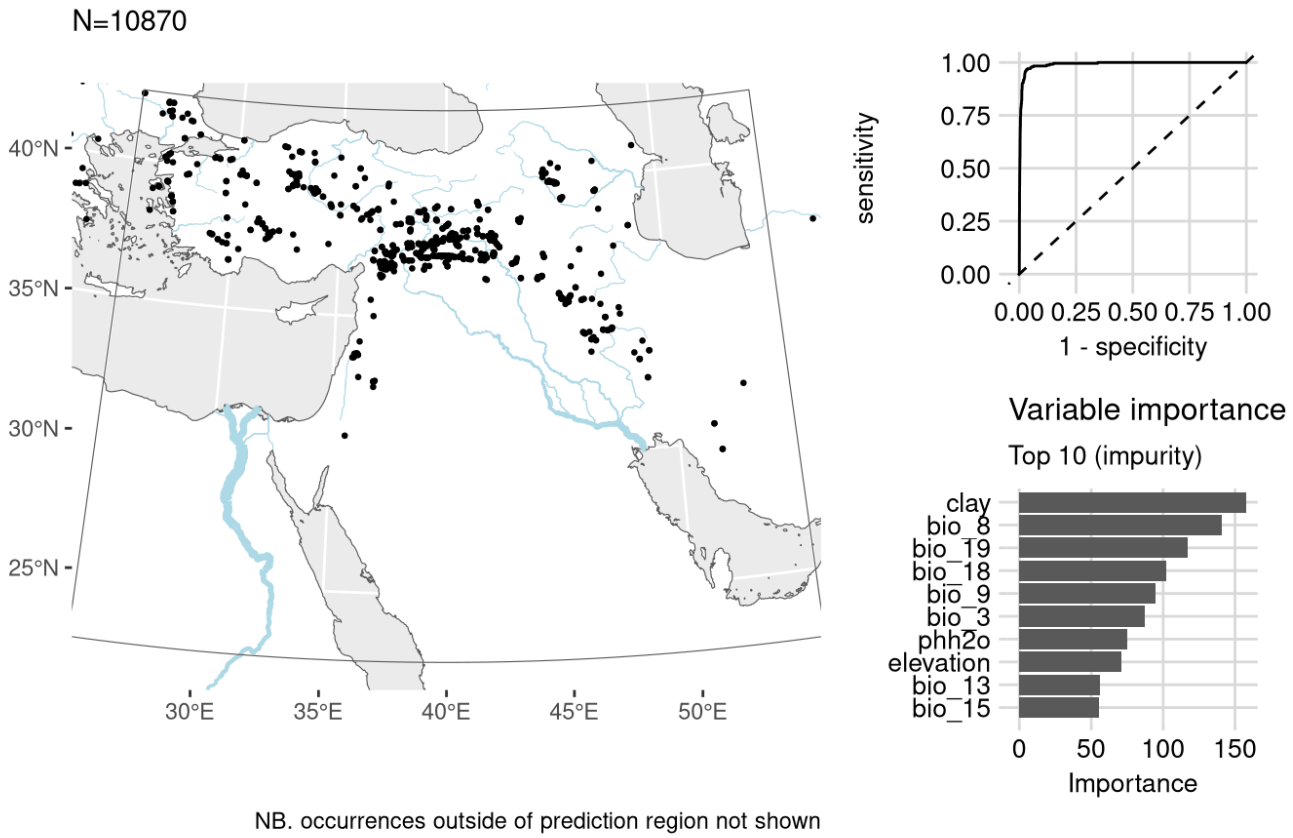


Figure 111: Fitted model summary for *Triticum monococcum*

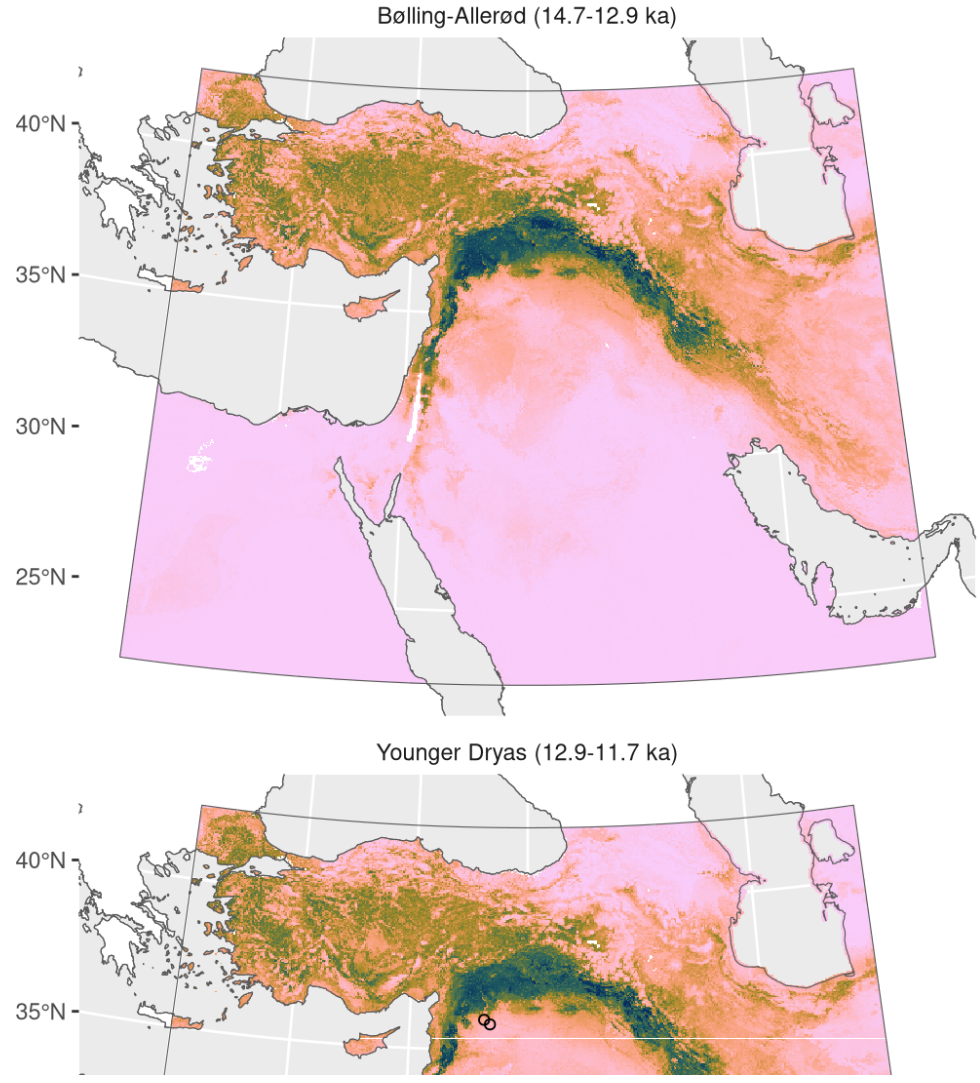

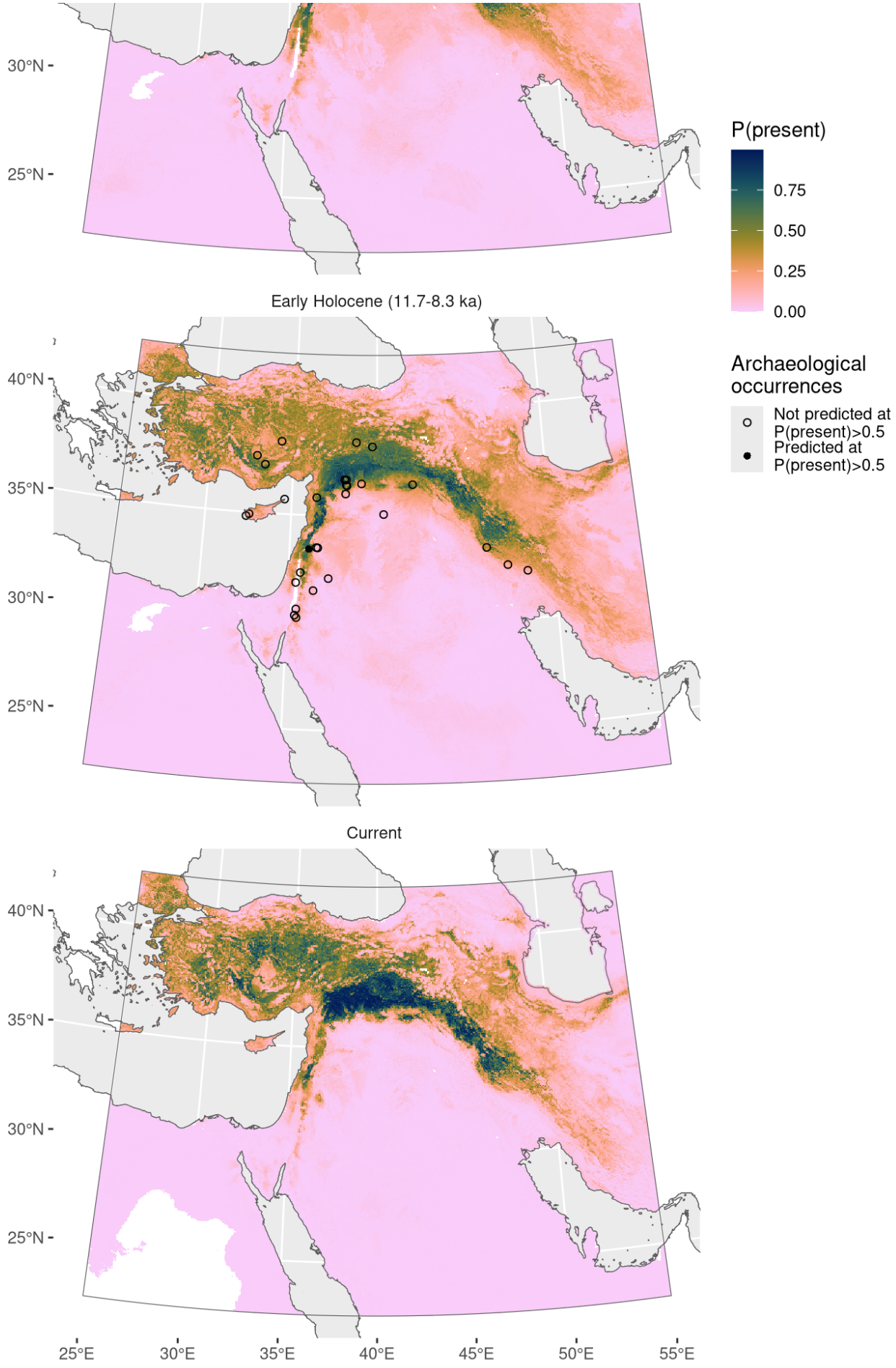


Figure 112: Predicted palaeodistributions of *Triticum monococcum*

Table 56: Archaeological occurrences of *Triticum monococcum*

Archaeological occurrences of *Triticum monococcum*

| Site | Age range | N assemblages | Average prop. | Source | Predicted? |
|---|---|---|---|---|---|
| Younger Dryas (12.9-11.7 ka) | | | | | |
| Abu Hureyra | 13.0–11.8 ka | 2 | 0.22% | ORIGINS | no |
| Mureybet | 12.1–11.9 ka | 1 | 0.44% | ORIGINS | no |
| Early Holocene (11.7-8.3 ka) | | | | | |
| Chogha Bonut | 12.8–8.8 ka | 1 | 0.00% | ORIGINS | no |
| Tell es-Sultan | 12.2–8.2 ka | 2 | 2.59% | ORIGINS | no |
| Iraq ed-Dubb | 11.7–11.2 ka | 1 | 0.09% | ORIGINS | no |
| Mureybet | 11.7–10.8 ka | 2 | 36.33% | ORIGINS | no |
| Jerf el Ahmar | 11.4–10.7 ka | 1 | 0.22% | ORIGINS | no |
| Chogha Golan | 11.2–11.1 ka | 1 | 0.20% | ORIGINS | no |
| Tell 'Abr | 11.2–10.8 ka | 1 | 1.99% | ORIGINS | no |
| Kastros | 10.8–9.9 ka | 1 | 8.28% | ORIGINS | no |
| Dja'de | 10.7–10.2 ka | 1 | 0.92% | ORIGINS | no |
| Mylouthkia | 10.6–8.8 ka | 2 | 0.27% | ORIGINS | no |
| Tell Ain el-Kerkh | 10.5–10.2 ka | 1 | 2.25% | ORIGINS | no |
| Wadi Jilat 7 | 10.2–9.3 ka | 3 | 0.95% | ORIGINS | no |
| Tell Aswad | 10.2–9.3 ka | 1 | 0.04% | ORIGINS | no |
| Ali Kosh | 10.1–8.0 ka | 2 | 0.06% | ORIGINS | no |
| Beidha | 10.1–9.5 ka | 1 | 0.00% | ORIGINS | no |
| Cafer Höyük | 10.1–9.1 ka | 2 | 6.00% | ORIGINS | no |
| Aşıklı Höyük | 9.9–9.4 ka | 1 | 0.11% | ORIGINS | no |
| Çayönü | 9.9–8.8 ka | 4 | 0.27% | ORIGINS | no |
| Halula | 9.9–9.5 ka | 1 | 0.33% | ORIGINS | no |
| Ais Giorkis | 9.6–9.4 ka | 1 | 26.12% | ORIGINS | no |

| | | | | | |
|---|---|---|---|---|---|
| Wadi Fidan A | 9.5–8.6 ka | 1 | 0.61% | ORIGINS | no |
| Sabi Abyad II | 9.5–8.8 ka | 1 | 0.07% | ORIGINS | no |
| Tell Ghoraifé | 9.5–8.6 ka | 1 | 0.54% | ORIGINS | no |
| Basta | 9.4–9.2 ka | 1 | 0.61% | ORIGINS | no |
| Dhuweila | 9.4–9.1 ka | 1 | 3.12% | ORIGINS | no |
| Can Hasan III | 9.4–8.6 ka | 1 | 0.35% | ORIGINS | no |
| Tell Ramad | 9.3–8.6 ka | 2 | 0.21% | ORIGINS | yes |
| Çatalhöyük | 9.2–8.3 ka | 1 | 0.00% | ORIGINS | no |
| Wadi Fidan C | 9.2–8.2 ka | 1 | 0.20% | ORIGINS | no |
| Bouqras | 9.2–8.6 ka | 1 | 0.02% | ORIGINS | no |
| Wadi Jilat 13 | 9.1–8.4 ka | 2 | 0.15% | ORIGINS | no |
| Tell Maghzaliyeh | 9.0–8.2 ka | 1 | 0.41% | ORIGINS | no |

## *Triticum turgidum*

Including Triticum aestivum, Triticum dicoccum, and Triticum dicoccoides.

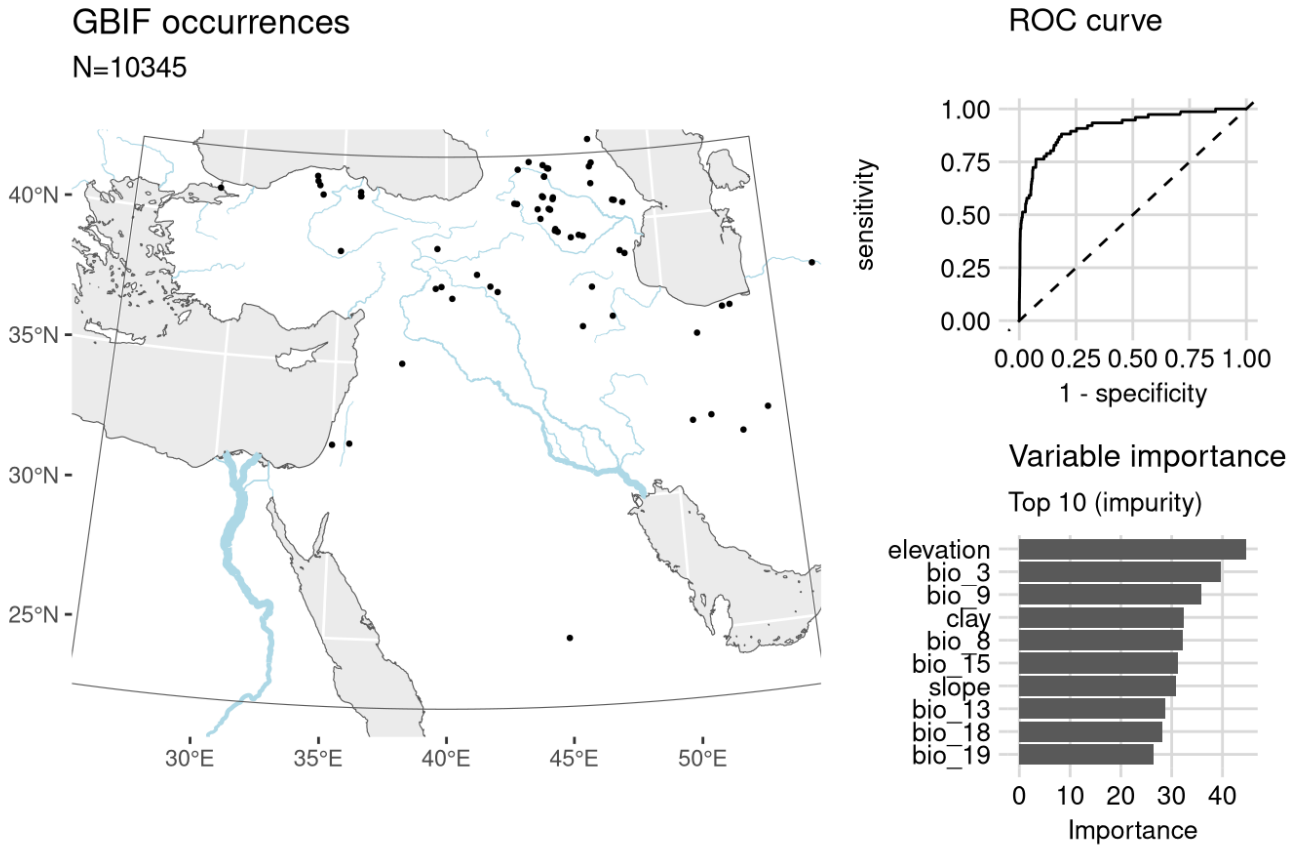


NB: occurrences outside of prediction region not shown

NB: occurrences outside of prediction region not shown

Figure 113: Fitted model summary for *Triticum turgidum*

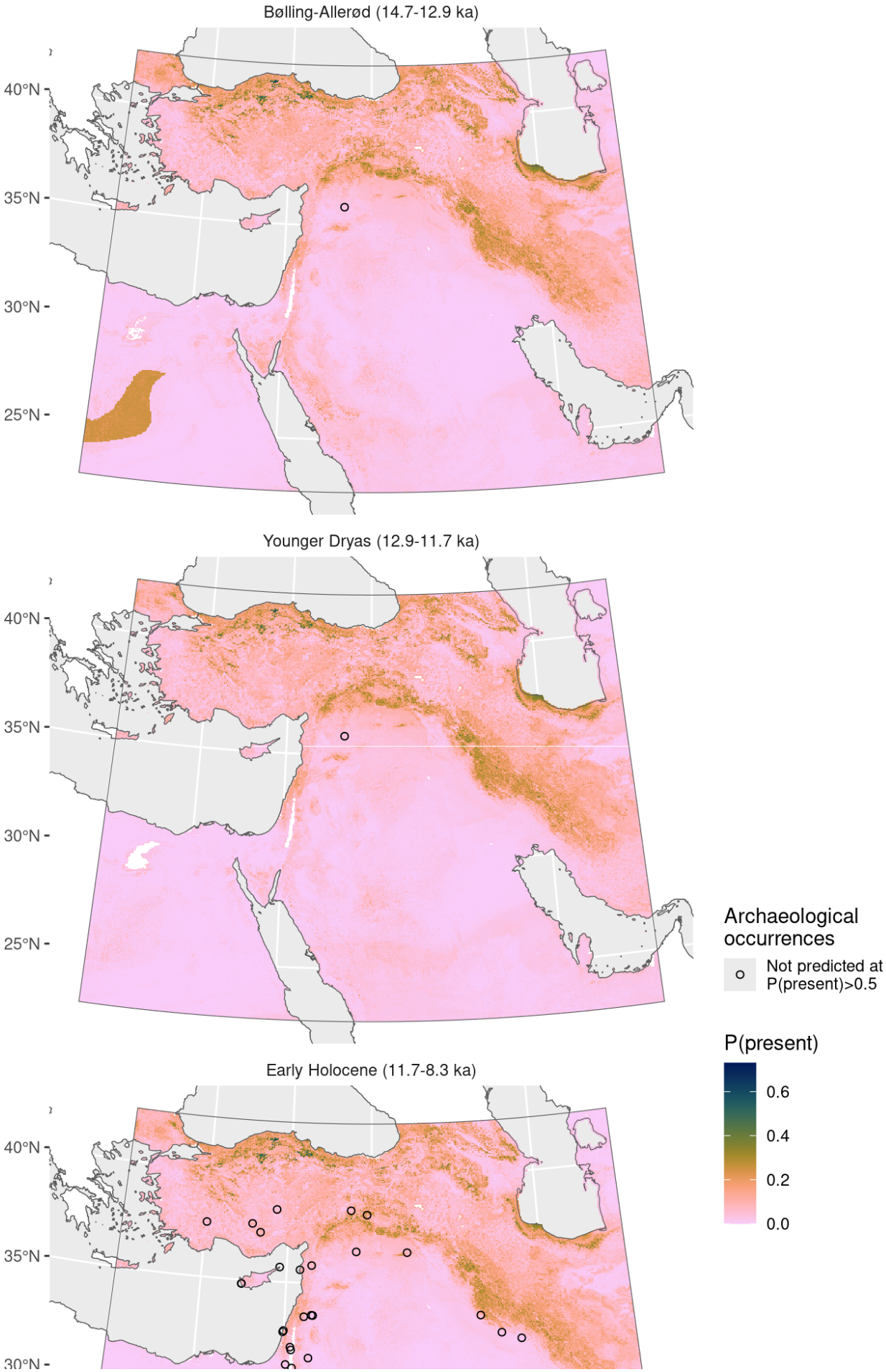

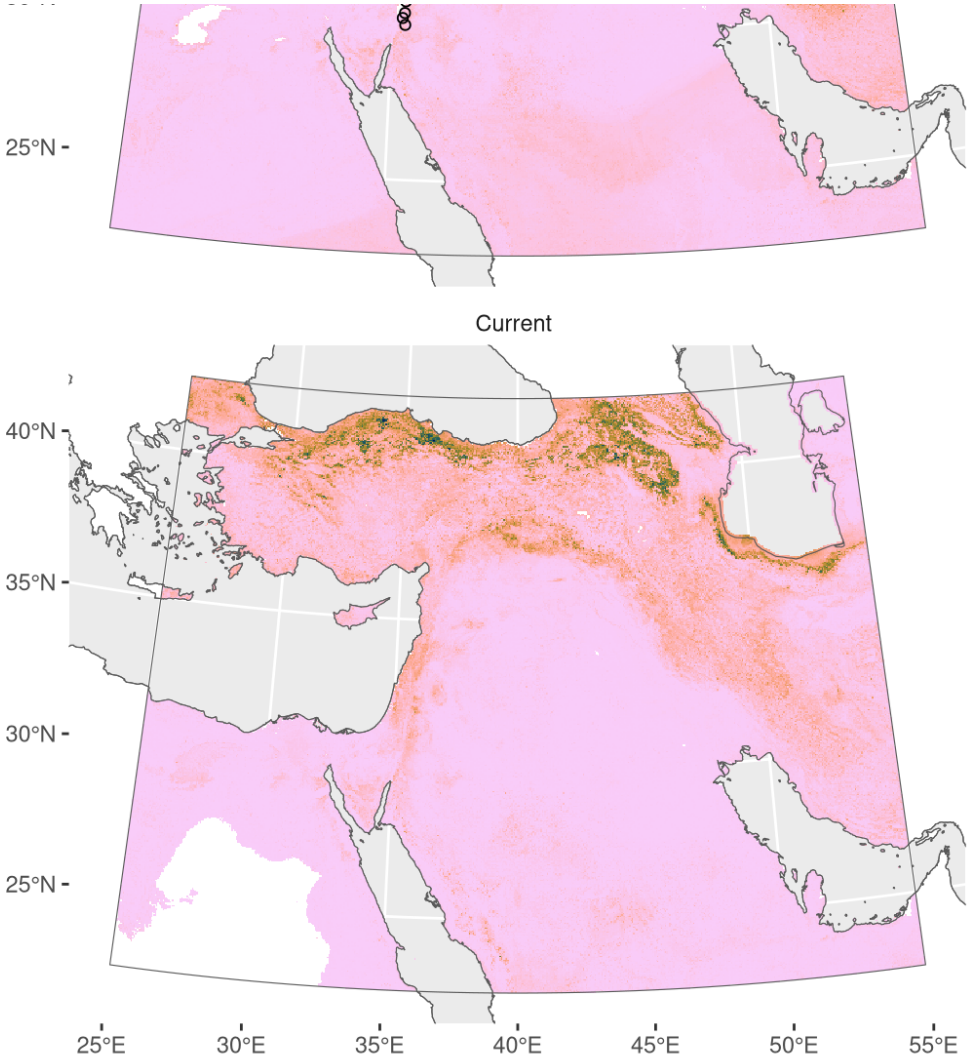


Figure 114: Predicted palaeodistributions of *Triticum turgidum*

Table 57: Archaeological occurrences of *Triticum turgidum*

Archaeological occurrences of *Triticum turgidum*

| Site | Age range | N assemblages | Average prop. | Source | Predicted? |
|---|---|---|---|---|---|
| Bølling-Allerød (14.7-12.9 ka) | | | | | |
| Abu Hureyra | 13.1–13.0 ka | 1 | 0.05% | ORIGINS | no |
| Younger Dryas (12.9-11.7 ka) | | | | | |
| Abu Hureyra | 13.0–11.8 ka | 2 | 0.07% | ORIGINS | no |
| Early Holocene (11.7-8.3 ka) | | | | | |
| Chogha Bonut | 12.8–8.8 ka | 1 | 0.17% | ORIGINS | no |
| Tell es-Sultan | 12.2–8.2 ka | 2 | 4.82% | ORIGINS | no |

| | | | | | |
|---|---|---|---|---|---|
| Nahal Oren | 12.2–9.6 ka | 2 | 10.32% | ORIGINS | no |
| Netiv Hagdud | 11.6–10.6 ka | 1 | 0.87% | ORIGINS | no |
| Tell Aswad | 11.2–9.3 ka | 3 | 2.15% | ORIGINS | no |
| Çayönü | 11.2–8.8 ka | 5 | 0.85% | ORIGINS | no |
| El-Hemmeh | 11.1–10.5 ka | 1 | 0.21% | ORIGINS | no |
| Kastros | 10.8–9.9 ka | 1 | 15.55% | ORIGINS | no |
| Kissonerga Mosphilia | 10.8–8.9 ka | 2 | 1.50% | ADEMNES | no |
| Cafer Höyük | 10.6–9.1 ka | 3 | 3.55% | ORIGINS | no |
| Mylouthkia | 10.6–8.8 ka | 2 | 1.10% | ORIGINS | no |
| Tell Ain el-Kerkh | 10.5–10.2 ka | 1 | 0.22% | ORIGINS | no |
| Shkarat Msaied | 10.2–9.9 ka | 1 | 100.00% | ORIGINS | no |
| Wadi Jilat 7 | 10.2–9.3 ka | 1 | 0.31% | ORIGINS | no |
| Hacılar | 10.2–9.4 ka | 1 | 26.37% | ORIGINS | no |
| Tell Ghoraifé | 10.1–8.6 ka | 2 | 3.08% | ORIGINS | no |
| Nahal Hemar | 10.1–9.3 ka | 1 | 1.26% | ORIGINS | no |
| Ali Kosh | 10.1–8.0 ka | 3 | 2.90% | ORIGINS | no |
| Aşıklı Höyük | 9.9–9.4 ka | 1 | 0.24% | ORIGINS | no |
| Chogha Golan | 9.8–9.6 ka | 2 | 3.26% | ORIGINS | no |
| Wadi Fidan A | 9.5–8.6 ka | 1 | 0.31% | ORIGINS | no |
| Sabi Abyad II | 9.5–8.8 ka | 1 | 1.05% | ORIGINS | no |
| Basta | 9.4–9.2 ka | 2 | 4.48% | ORIGINS | no |
| Ras Shamra | 9.4–8.3 ka | 2 | 1.11% | ORIGINS | no |
| Can Hasan III | 9.4–8.6 ka | 1 | 0.66% | ORIGINS | no |
| Tell Ramad | 9.3–8.6 ka | 2 | 4.13% | ORIGINS | no |

| | | | | | |
|---|---|---|---|---|---|
| Çatalhöyük | 9.2–8.3 ka | 1 | 0.00% | ORIGINS | no |
| Wadi Jilat 13 | 9.1–8.4 ka | 2 | 0.04% | ORIGINS | no |
| Atlit-Yam | 9.0–8.0 ka | 1 | 16.48% | ORIGINS | no |
| Tell Maghzaliyeh | 9.0–8.2 ka | 1 | 10.63% | ORIGINS | no |

# *Triticum urartu*

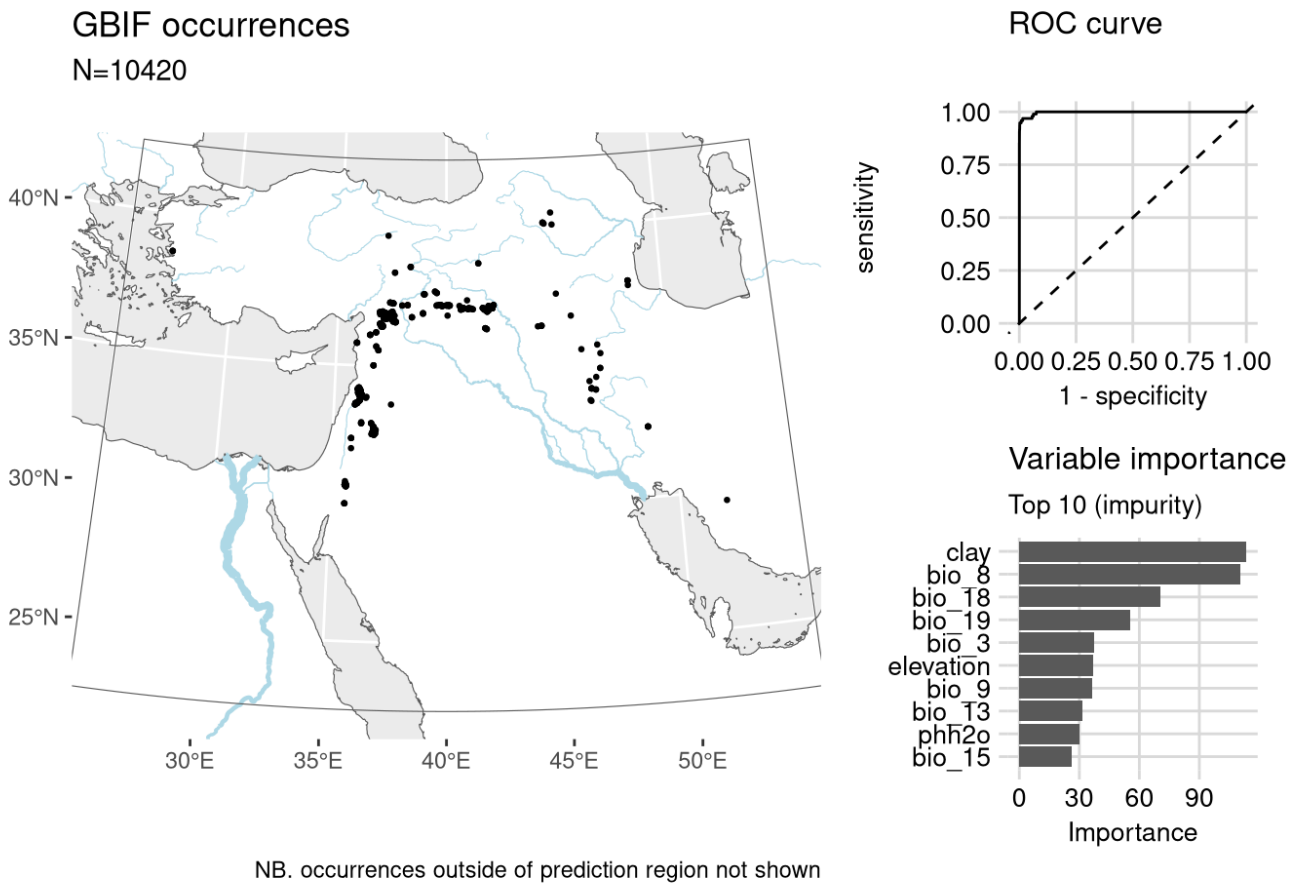


Figure 115: Fitted model summary for *Triticum urartu*

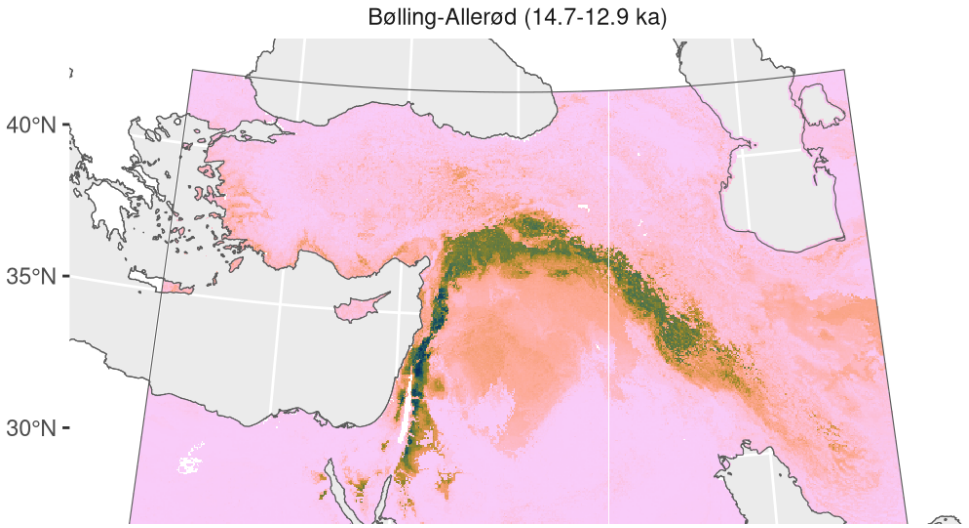

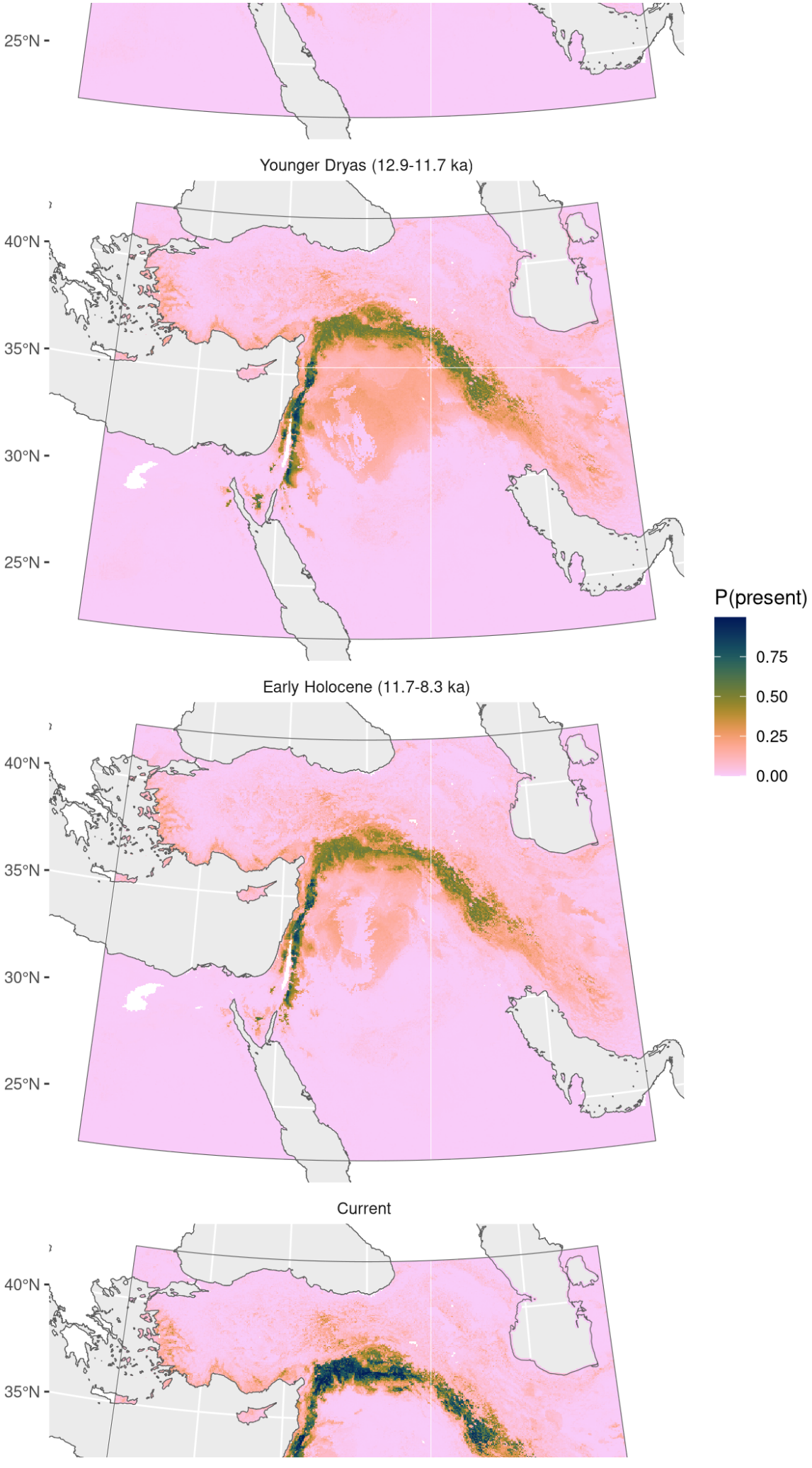
25°N
Younger Dryas (12.9-11.7 ka)
40°N
35°N
30°N
25°N
Early Holocene (11.7-8.3 ka)
40°N
35°N
30°N
25°N
Current
40°N
35°N
P(present)
0.75
0.50
0.25
0.00

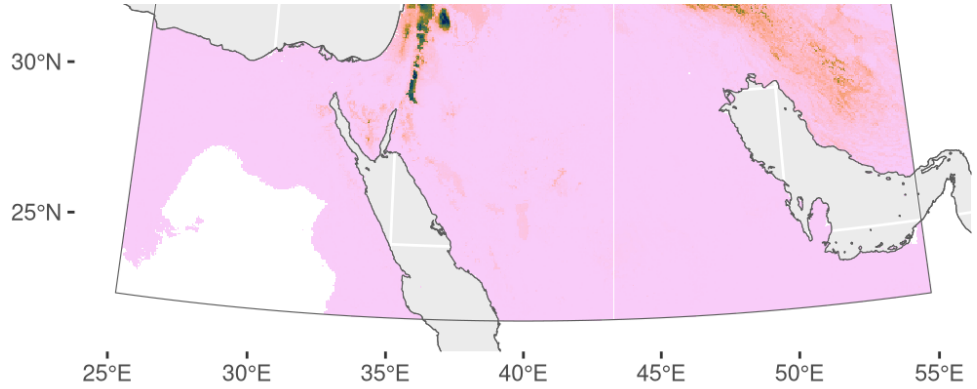


Figure 116: Predicted palaeodistributions of *Triticum urartu*

Table 58

# *Verbena officinalis*

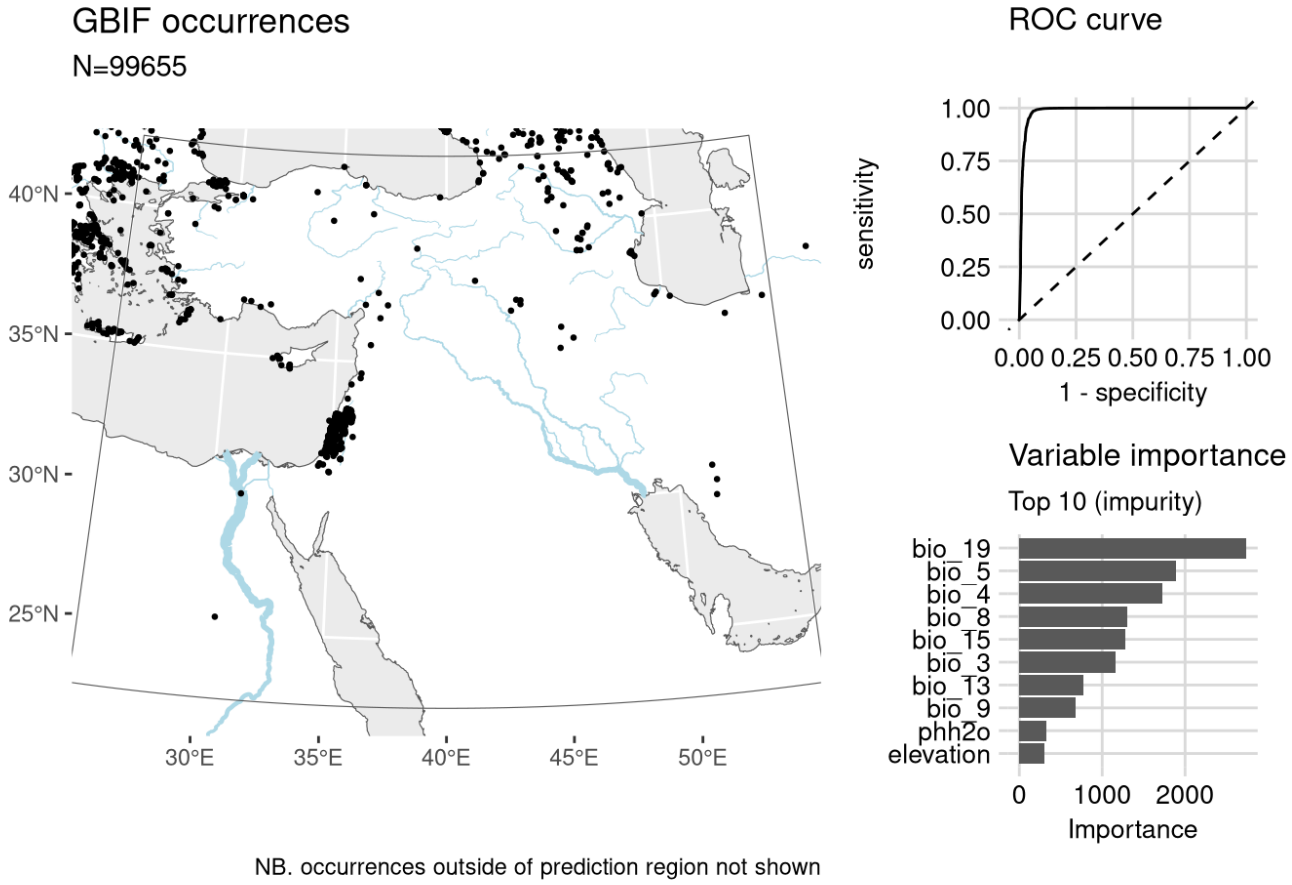


Figure 117: Fitted model summary for *Verbena officinalis*

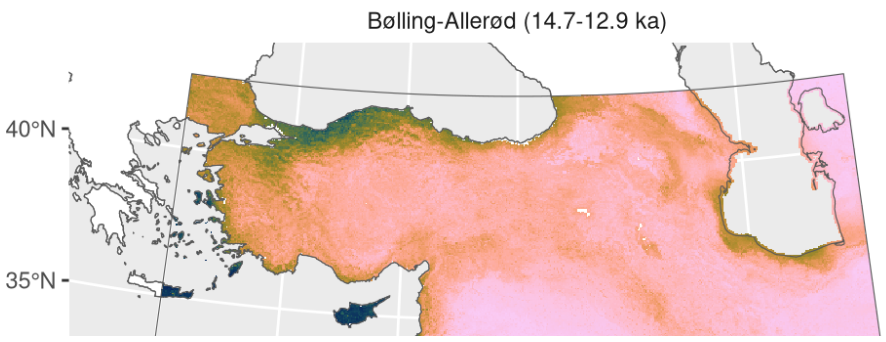

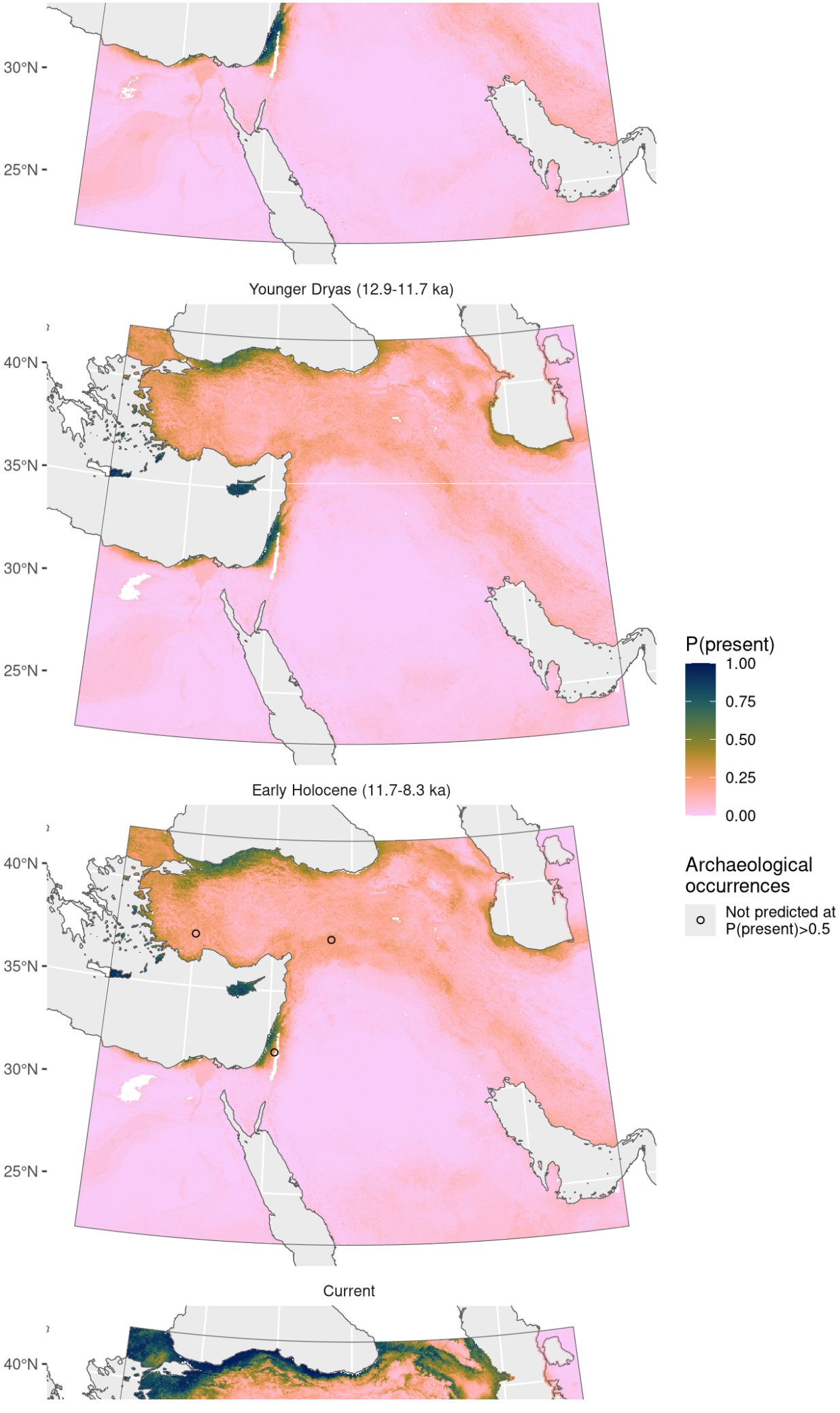
30°N
25°N
Younger Dryas (12.9-11.7 ka)
40°N
35°N
30°N
25°N
Early Holocene (11.7-8.3 ka)
40°N
35°N
30°N
25°N
Current
40°N
P(present)
1.00
0.75
0.50
0.25
0.00
Archaeological occurrences
Not predicted at P(present)>0.5

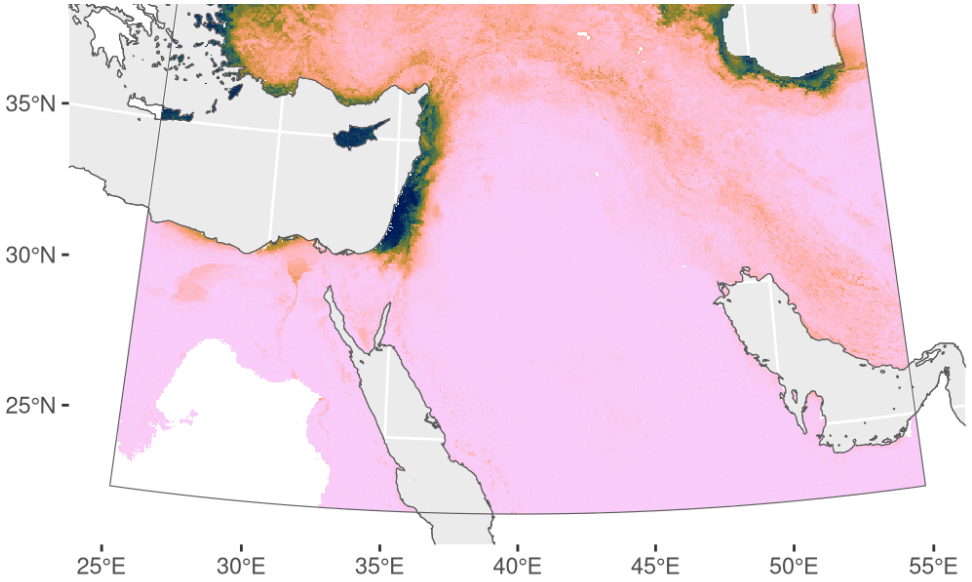


Figure 118: Predicted palaeodistributions of *Verbena officinalis*

Table 59: Archaeological occurrences of *Verbena officinalis*

Archaeological occurrences of *Verbena officinalis*

| Site | Age range | N assemblages | Average prop. | Source | Predicted? |
|---|---|---|---|---|---|
| Early Holocene (11.7-8.3 ka) | | | | | |
| Netiv Hagdud | 11.6–10.6 ka | 1 | 0.01% | ORIGINS | no |
| Nevalı Çori | 10.4–10.2 ka | 1 | 0.01% | ORIGINS | no |
| Hacılar | 10.2–9.4 ka | 1 | 1.10% | ORIGINS | no |

# *Vicia ervilia*

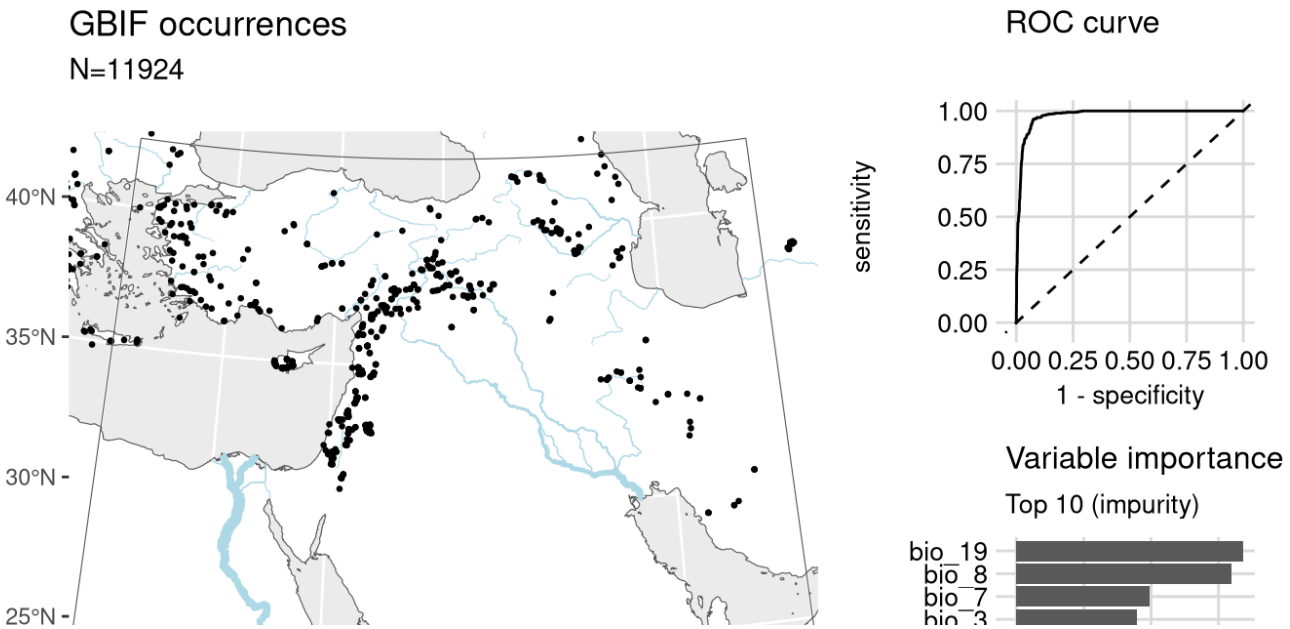

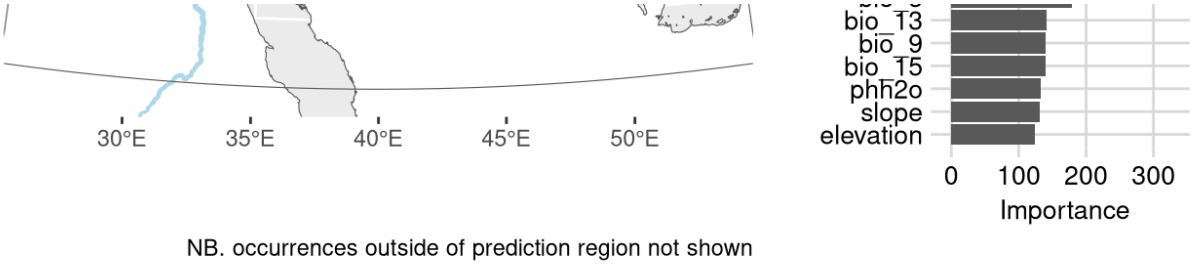


NB. occurrences outside of prediction region not shown

Figure 119: Fitted model summary for *Vicia ervilia*

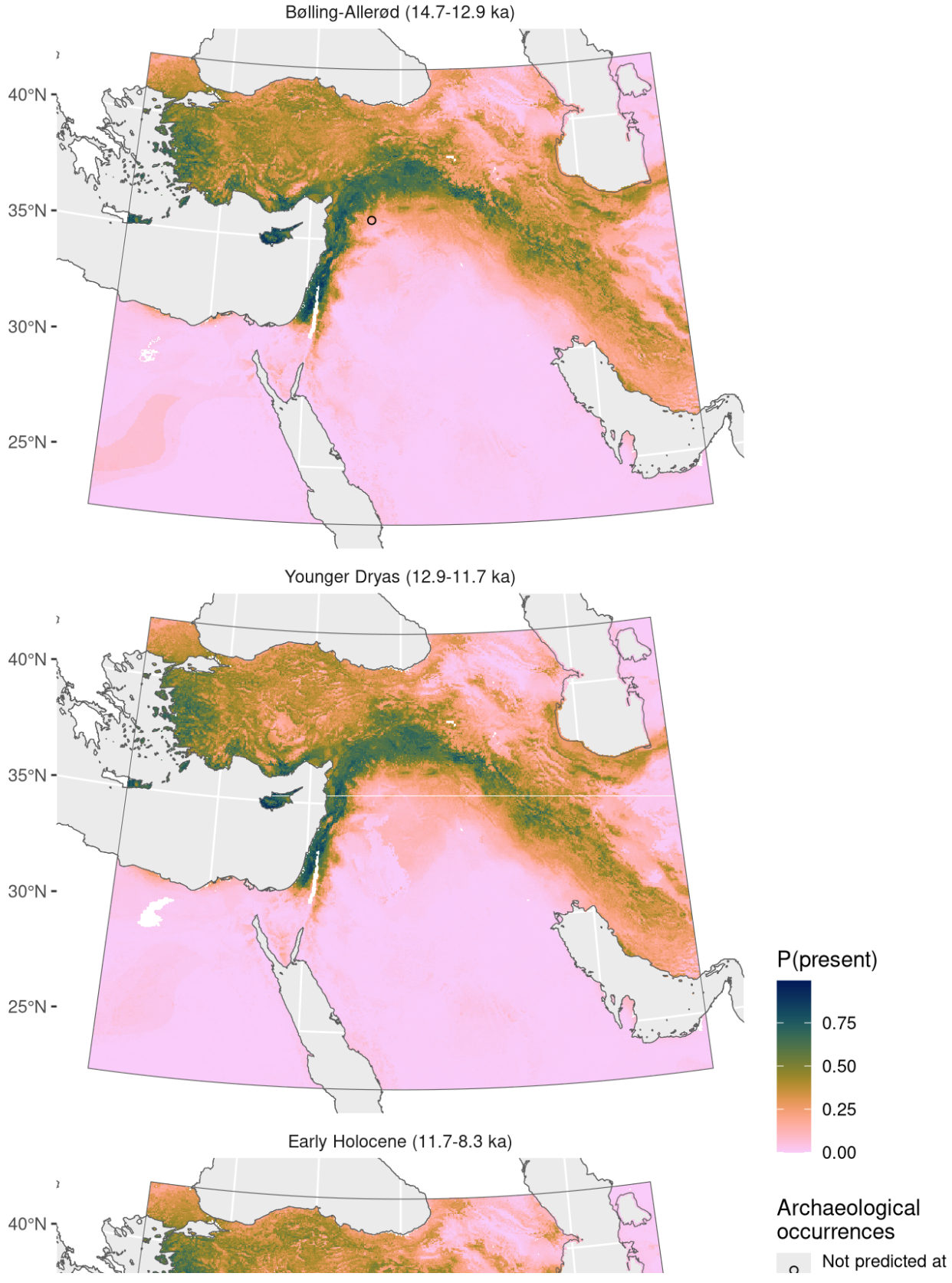

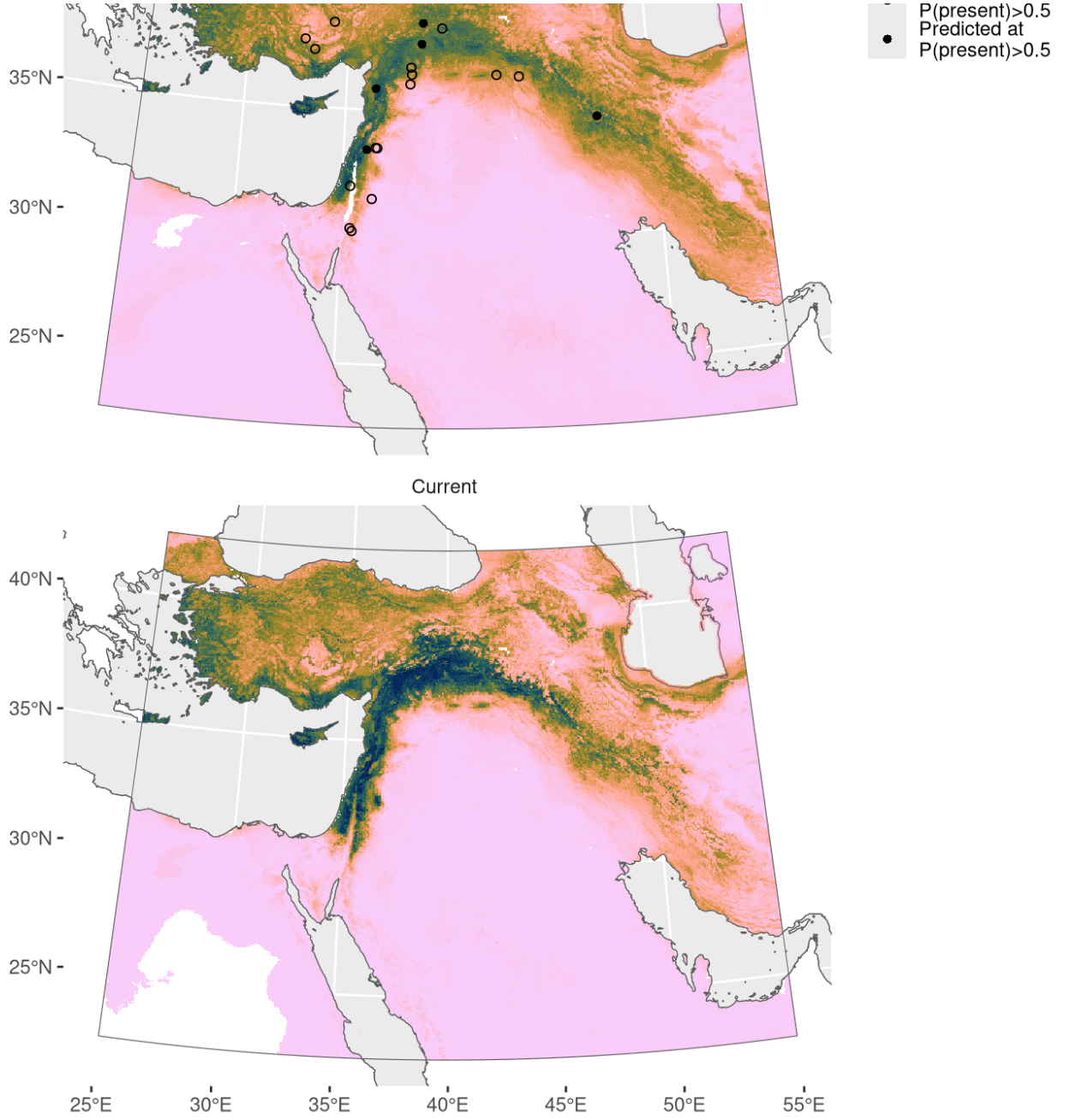


Figure 120: Predicted palaeodistributions of *Vicia ervilia*

Table 60: Archaeological occurrences of *Vicia ervilia*

Archaeological occurrences of *Vicia ervilia*

| Site | Age range | N assemblages | Average prop. | Source | Predicted? |
|---|---|---|---|---|---|
| Bølling-Allerød (14.7-12.9 ka) | | | | | |
| Abu Hureyra | 13.1–13.0 ka | 1 | 0.16% | ORIGINS | no |
| Early Holocene (11.7-8.3 ka) | | | | | |
| Qermez Dere | 11.8–9.9 ka | 1 | 0.04% | ORIGINS | no |
| Mureybet | 11.7–11.2 ka | 1 | 0.13% | ORIGINS | no |

| | | | | | |
|---|---|---|---|---|---|
| Netiv Hagdud | 11.6–10.6 ka | 1 | 0.01% | ORIGINS | no |
| Jerf el Ahmar | 11.4–10.7 ka | 1 | 0.20% | ORIGINS | no |
| M'lefaat | 11.3–11.1 ka | 1 | 6.67% | ORIGINS | no |
| Tell Aswad | 10.8–10.2 ka | 1 | 0.06% | ORIGINS | no |
| Dja'de | 10.7–10.2 ka | 1 | 0.10% | ORIGINS | no |
| Sheikh-e Abad | 10.7–8.4 ka | 2 | 2.73% | ADEMNES | yes |
| Cafer Höyük | 10.6–9.3 ka | 2 | 1.65% | ORIGINS | yes |
| Tell Ain el-Kerkh | 10.5–10.2 ka | 1 | 2.02% | ORIGINS | yes |
| Nevalı Çori | 10.4–10.2 ka | 1 | 0.26% | ORIGINS | yes |
| Wadi Jilat 7 | 10.2–9.3 ka | 1 | 0.03% | ORIGINS | no |
| Tell Ghoraifé | 10.1–9.0 ka | 1 | 0.33% | ORIGINS | no |
| Beidha | 10.1–9.5 ka | 1 | 0.00% | ORIGINS | no |
| Aşıklı Höyük | 9.9–9.4 ka | 1 | 0.55% | ORIGINS | no |
| Çayönü | 9.9–8.8 ka | 4 | 5.26% | ORIGINS | no |
| Basta | 9.4–9.2 ka | 1 | 0.61% | ORIGINS | no |
| Can Hasan III | 9.4–8.6 ka | 1 | 0.82% | ORIGINS | no |
| Tell Ramad | 9.3–8.9 ka | 1 | 0.02% | ORIGINS | yes |
| Çatalhöyük | 9.2–8.3 ka | 1 | 0.00% | ORIGINS | no |

## *Vicia faba*

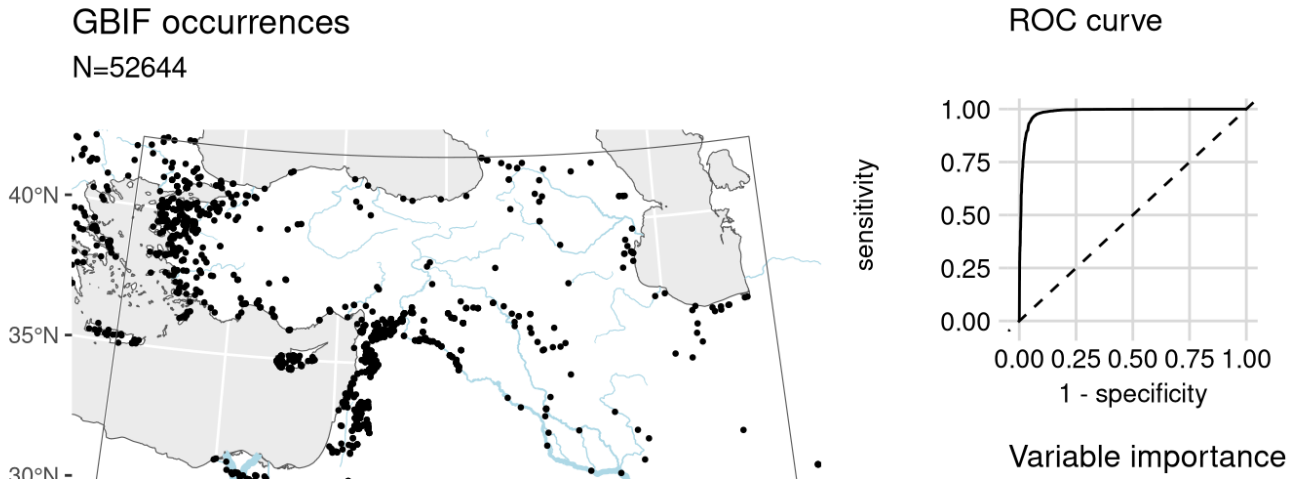

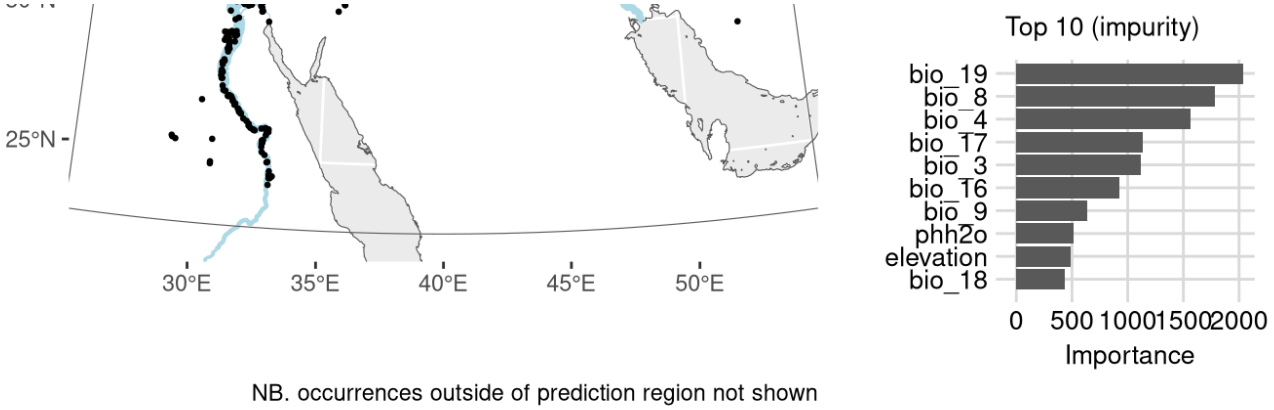


Figure 121: Fitted model summary for *Vicia faba*

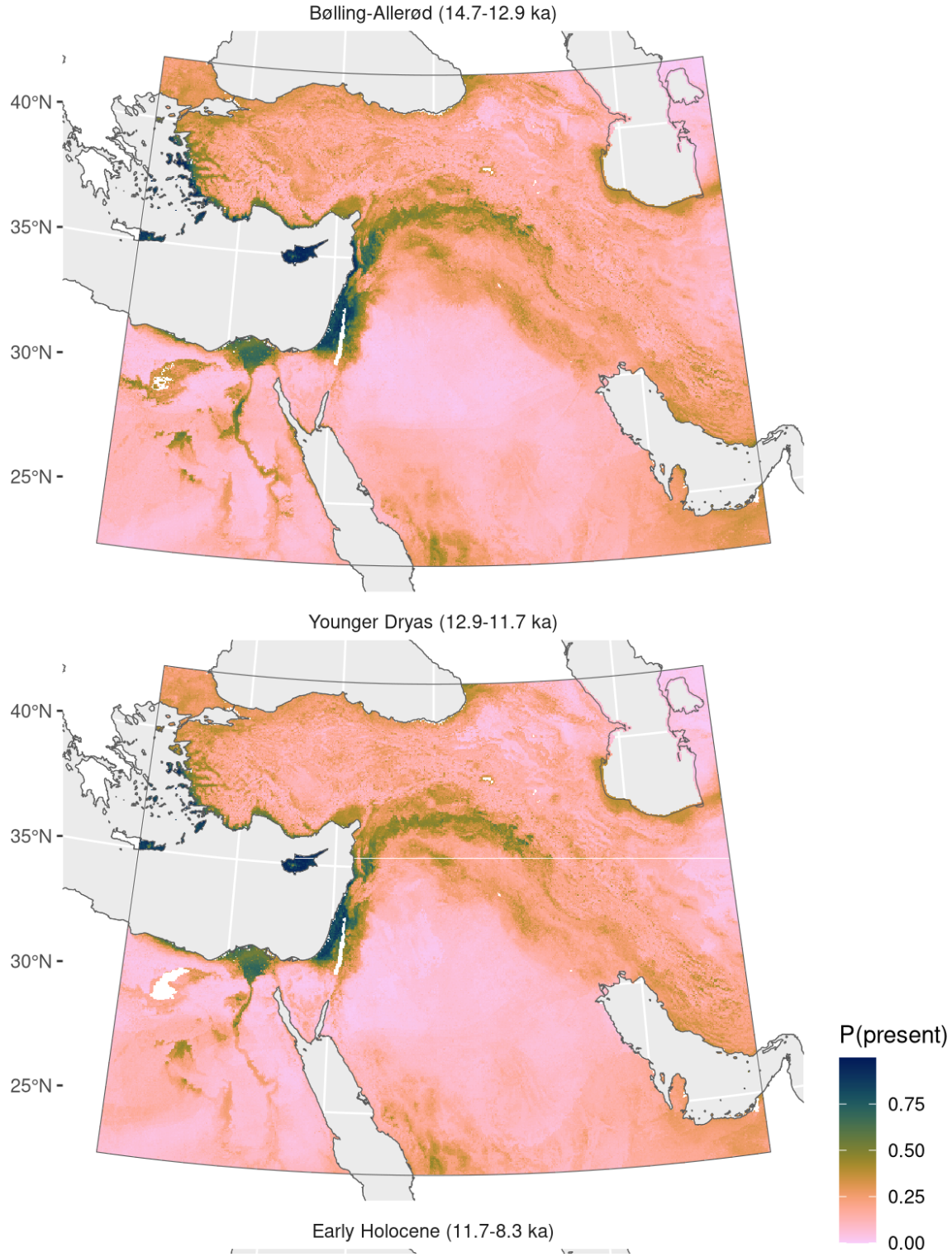

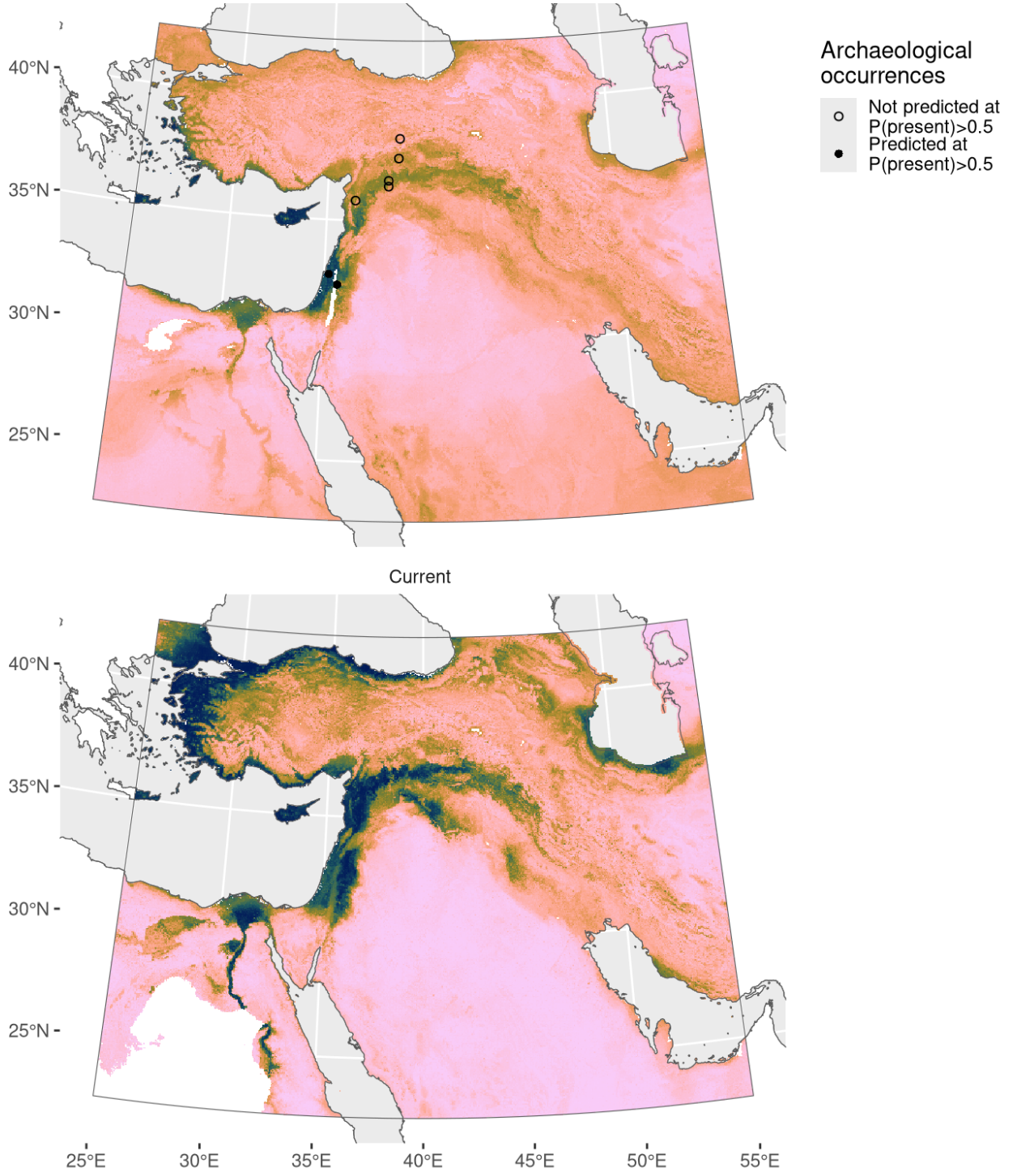


Figure 122: Predicted palaeodistributions of *Vicia faba*

Table 61: Archaeological occurrences of *Vicia faba*

Archaeological occurrences of *Vicia faba*

| Site | Age range | N assemblages | Average prop. | Source | Predicted? |
|---|---|---|---|---|---|
| Early Holocene (11.7-8.3 ka) | | | | | |
| Iraq ed-Dubb | 11.7–11.2 ka | 1 | 0.18% | ORIGINS | yes |
| Dja'de | 10.7–10.2 ka | 1 | 0.01% | ORIGINS | no |
| Cafer Höyük | 10.6–9.7 ka | 1 | 0.17% | ORIGINS | no |

| | | | | | |
|---|---|---|---|---|---|
| Çatal Höyük | 10.6–9.7 ka | 1 | 0.17% | ORIGINS | no |
| Tell Ain el-Kerkh | 10.5–10.2 ka | 1 | 19.64% | ORIGINS | no |
| Nevalı Çori | 10.4–10.2 ka | 1 | 0.04% | ORIGINS | no |
| Halula | 9.9–9.5 ka | 1 | 0.11% | ORIGINS | no |
| Yiftah'el | 8.8–8.8 ka | 1 | 0.19% | ORIGINS | yes |

## *Vicia narbonensis*

Including Vicia narbonense.

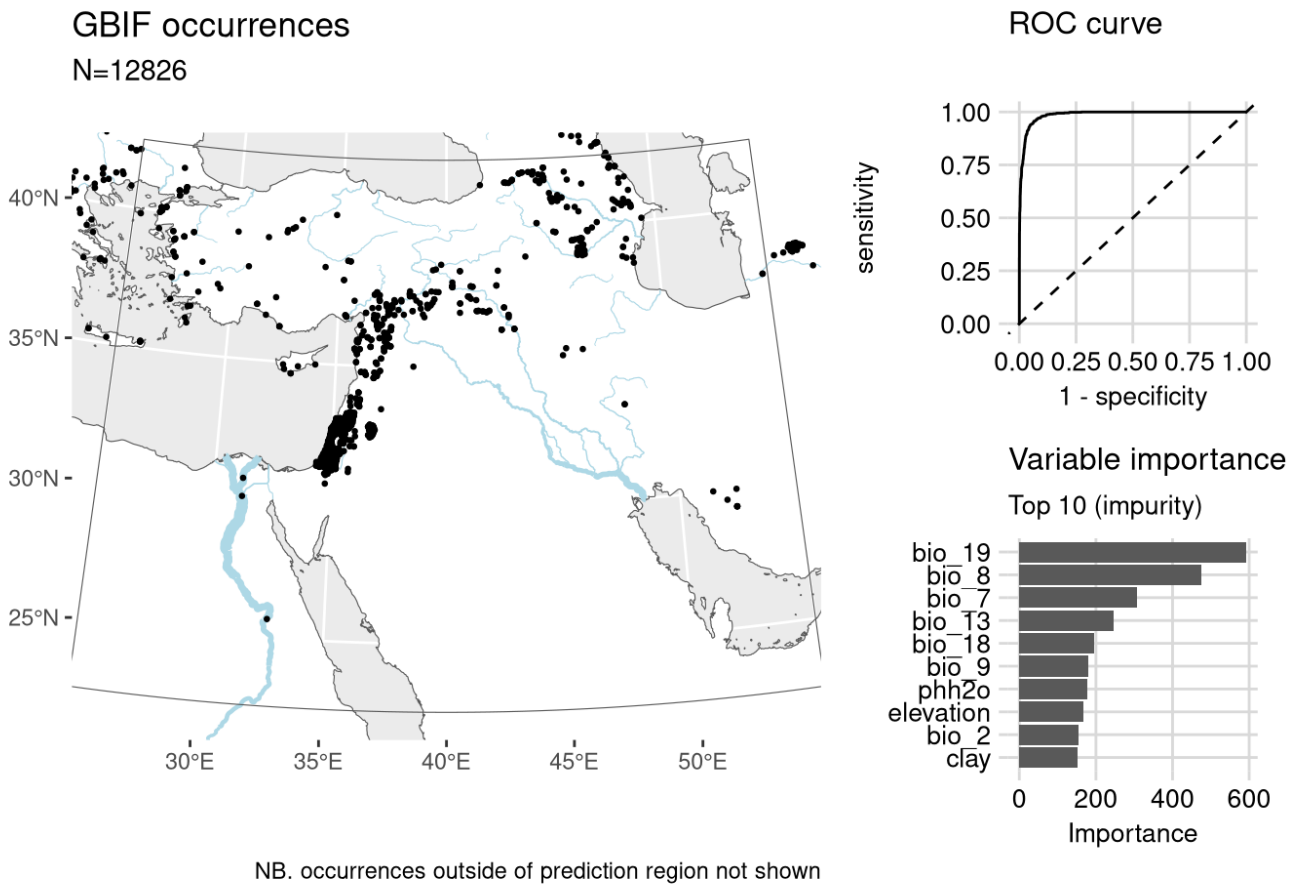


Figure 123: Fitted model summary for *Vicia narbonensis*

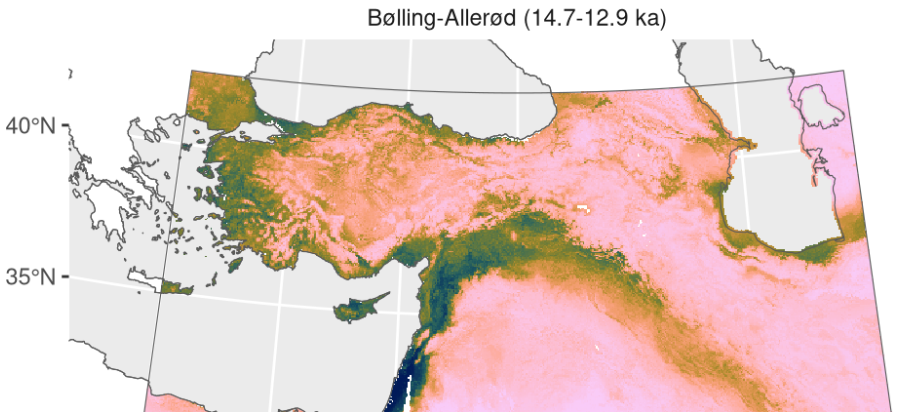

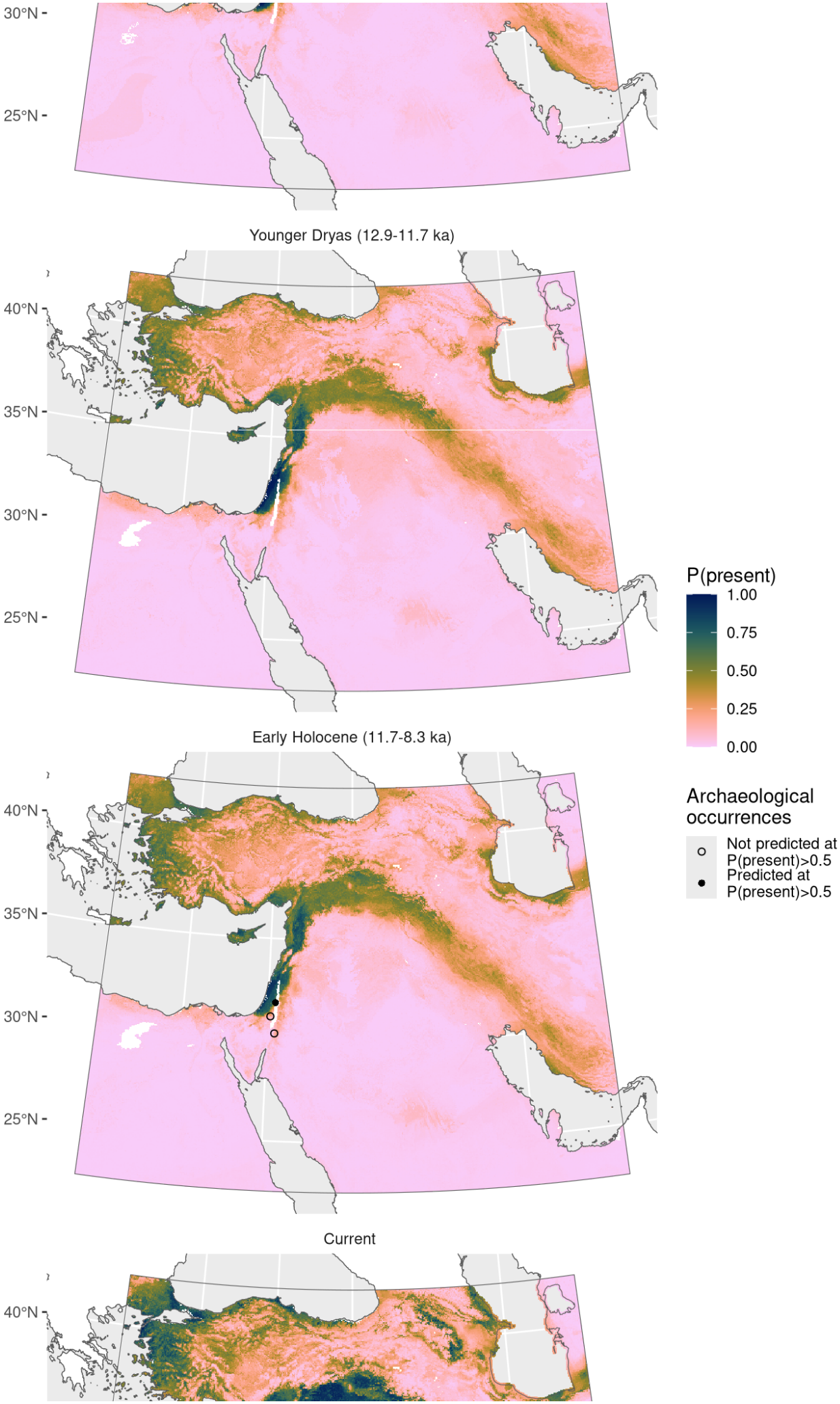
30°N
25°N
Younger Dryas (12.9-11.7 ka)
40°N
35°N
30°N
25°N
Early Holocene (11.7-8.3 ka)
40°N
35°N
30°N
25°N
Current
40°N
P(present)
1.00
0.75
0.50
0.25
0.00
Archaeological occurrences
Not predicted at P(present)>0.5
Predicted at P(present)>0.5

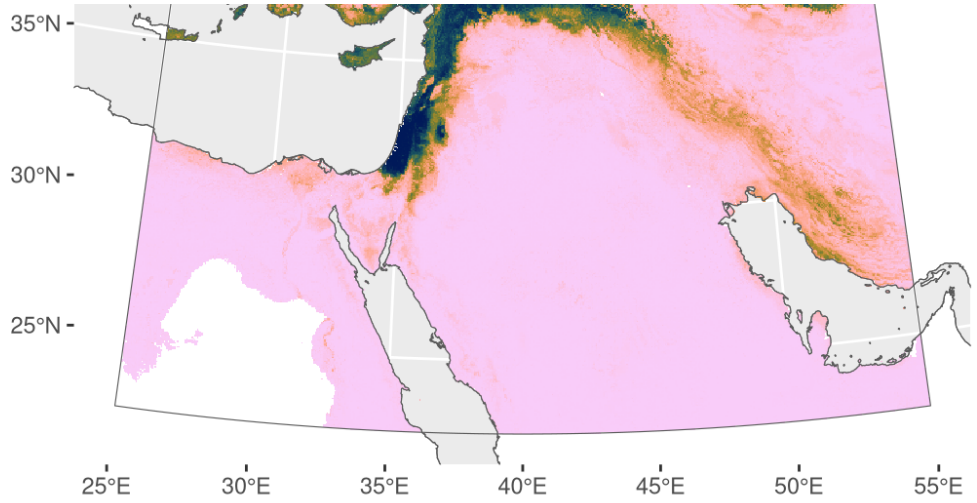


Figure 124: Predicted palaeodistributions of *Vicia narbonensis*

Table 62: Archaeological occurrences of *Vicia narbonensis*

Archaeological occurrences of *Vicia narbonensis*

| Site | Age range | N assemblages | Average prop. | Source | Predicted? |
|---|---|---|---|---|---|
| Early Holocene (11.7-8.3 ka) | | | | | |
| Nahal Hemar | 10.1–9.3 ka | 1 | 0.19% | ORIGINS | no |
| Beidha | 10.1–9.5 ka | 1 | 0.00% | ORIGINS | no |
| Tell es-Sultan | 8.9–8.2 ka | 1 | 0.39% | ORIGINS | yes |

# *Vicia orientalis*

Including Lens culinaris and Lens orientalis.

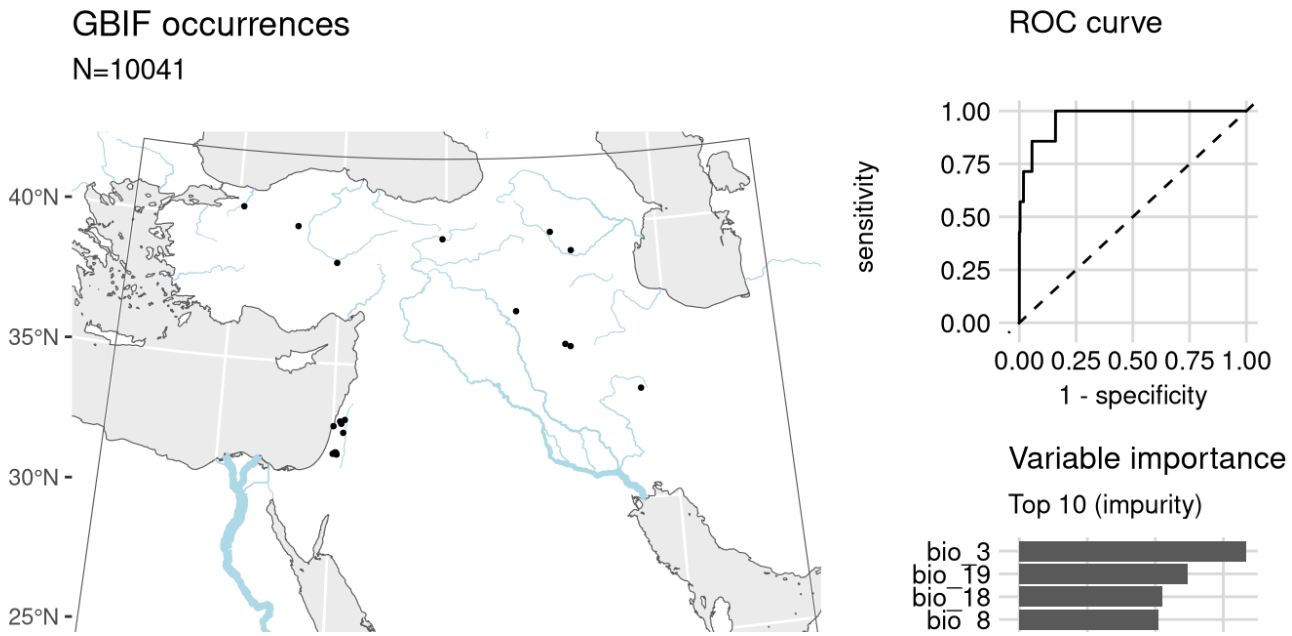

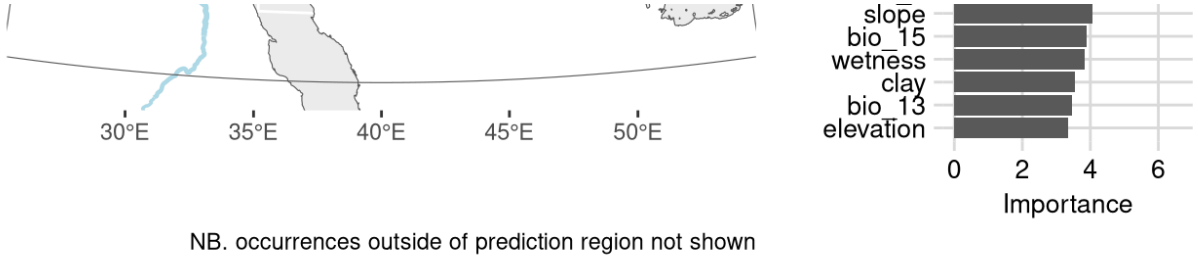


NB. occurrences outside of prediction region not shown

Figure 125: Fitted model summary for *Vicia orientalis*

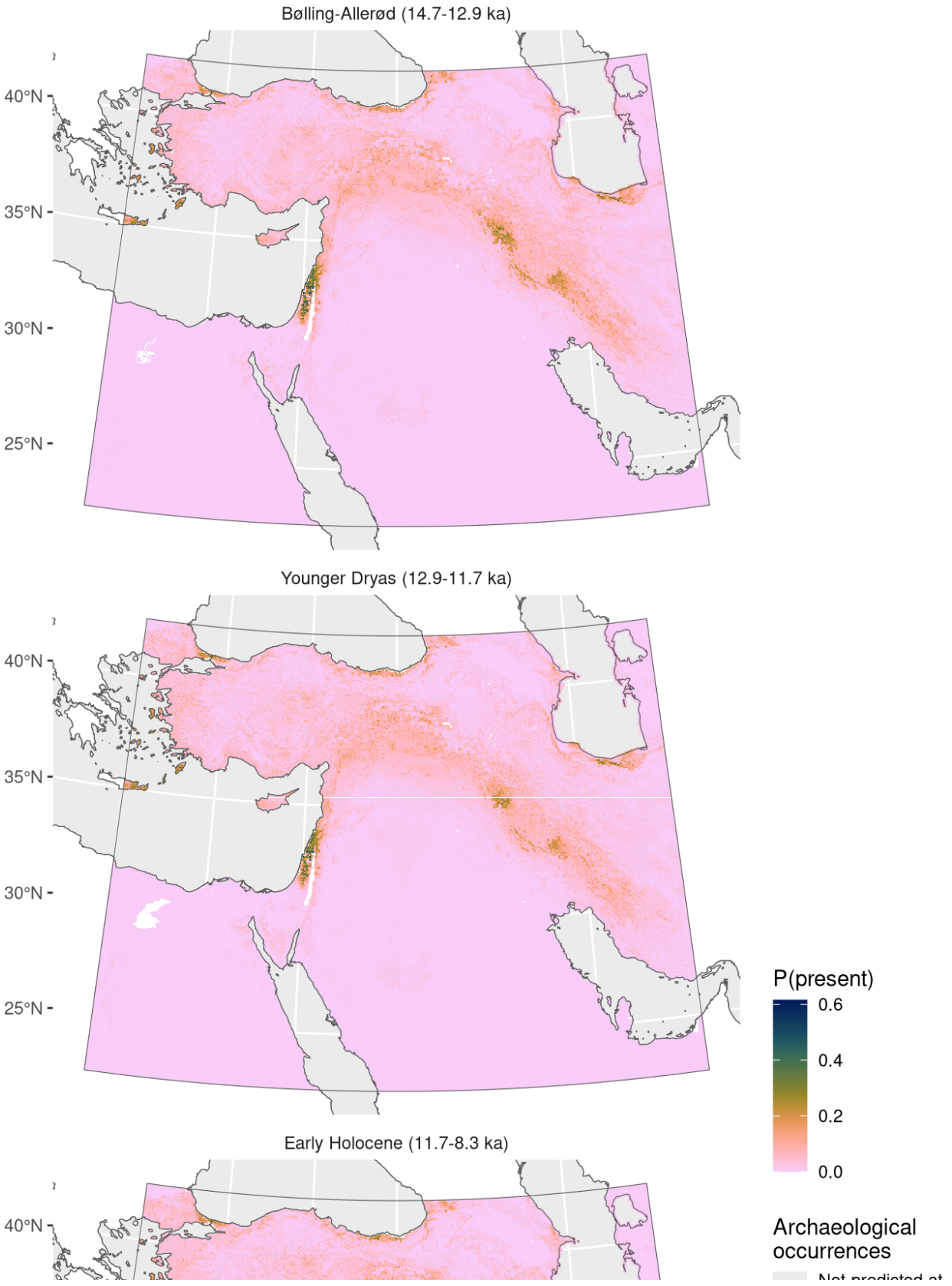

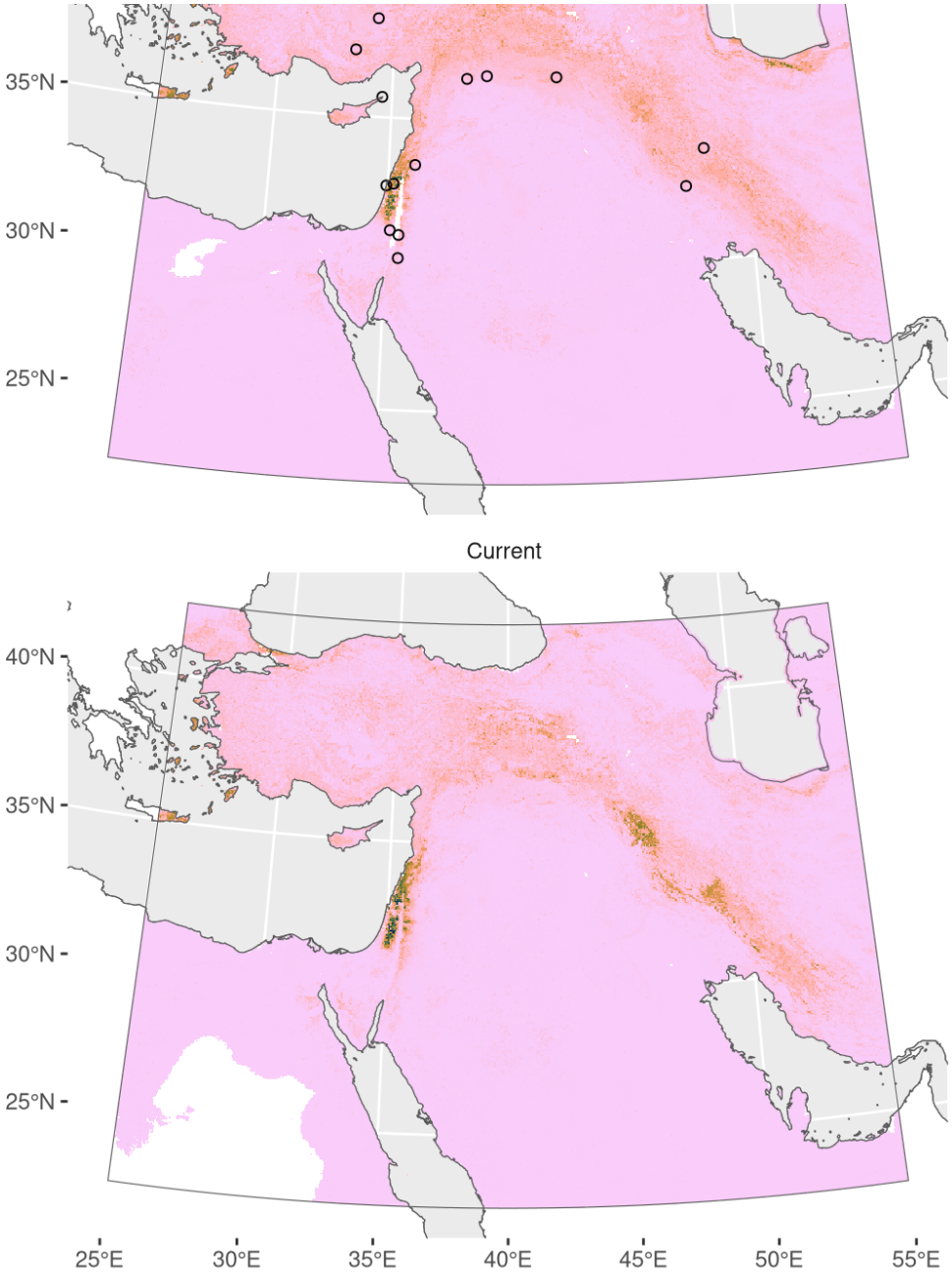


Figure 126: Predicted palaeodistributions of *Vicia orientalis*

Table 63: Archaeological occurrences of *Vicia orientalis*

Archaeological occurrences of *Vicia orientalis*

| Site | Age range | N assemblages | Average prop. | Source | Predicted? |
|---|---|---|---|---|---|
| Early Holocene (11.7-8.3 ka) | | | | | |
| Jerf el Ahmar | 11.4–10.7 ka | 1 | 0.63% | ORIGINS | no |
| El-Hemmeh | 11.1–10.5 ka | 1 | 2.58% | ORIGINS | no |
| Kastros | 10.8–9.9 ka | 1 | 13.56% | ORIGINS | no |

| | | | | | |
|---|---|---|---|---|---|
| Tepe Abdul Hosein | 10.3–9.1 ka | 1 | 33.33% | ORIGINS | no |
| Nahal Hemar | 10.1–9.3 ka | 1 | 0.33% | ORIGINS | no |
| Ali Kosh | 10.1–8.0 ka | 2 | 0.03% | ORIGINS | no |
| Aşıklı Höyük | 9.9–9.4 ka | 1 | 0.06% | ORIGINS | no |
| Sabi Abyad II | 9.5–8.8 ka | 1 | 1.34% | ORIGINS | no |
| Basta | 9.4–9.2 ka | 1 | 1.41% | ORIGINS | no |
| Can Hasan III | 9.4–8.6 ka | 1 | 0.33% | ORIGINS | no |
| Tell Ramad | 9.3–8.6 ka | 2 | 0.85% | ORIGINS | no |
| Atlit-Yam | 9.0–8.0 ka | 1 | 0.46% | ORIGINS | no |
| Tell Maghzaliyeh | 9.0–8.2 ka | 1 | 5.72% | ORIGINS | no |
| Yiftah'el | 8.8–8.8 ka | 1 | 99.81% | ORIGINS | no |

## *Vitis sylvestris*

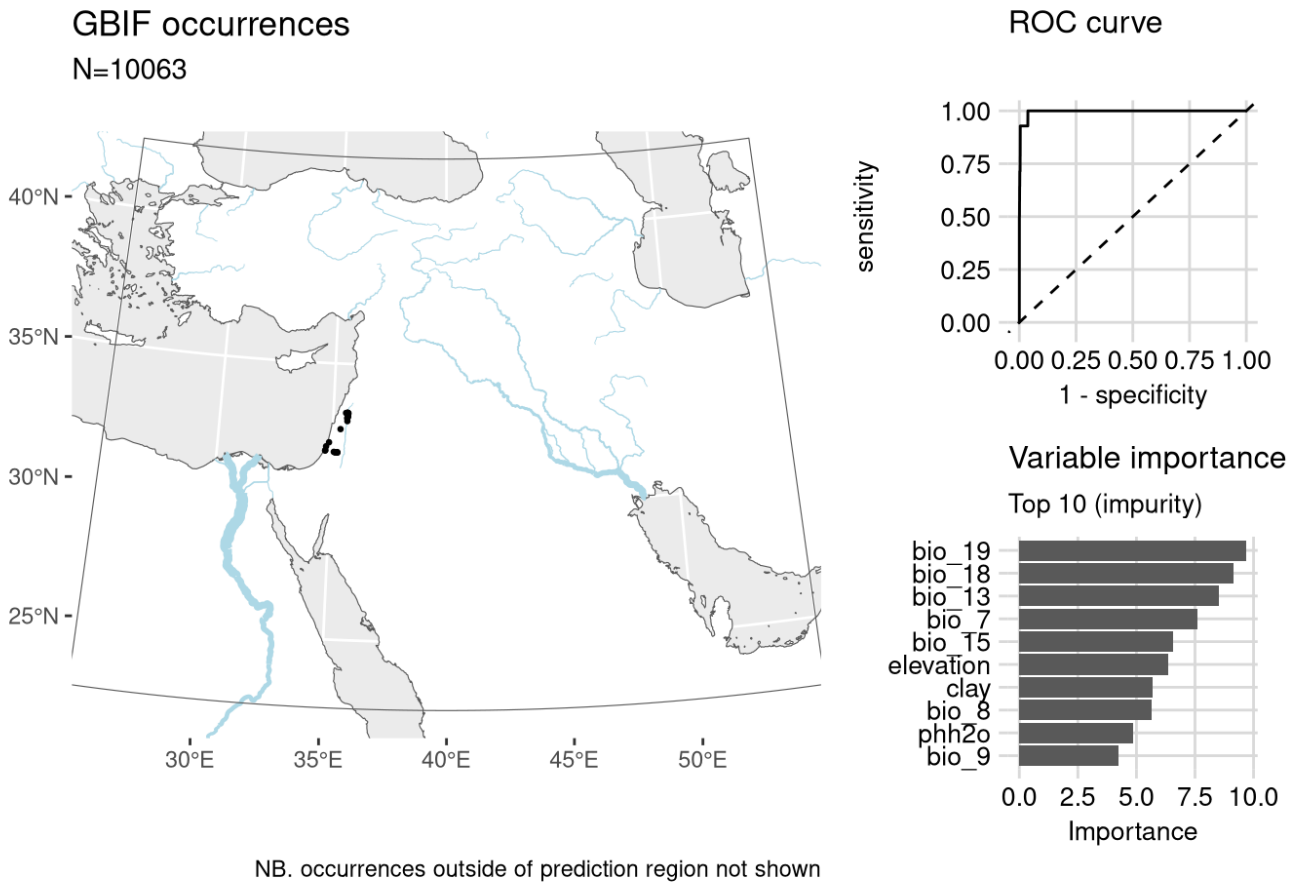


NB. occurrences outside of prediction region not shown

Figure 127: Fitted model summary for *Vitis sylvestris*

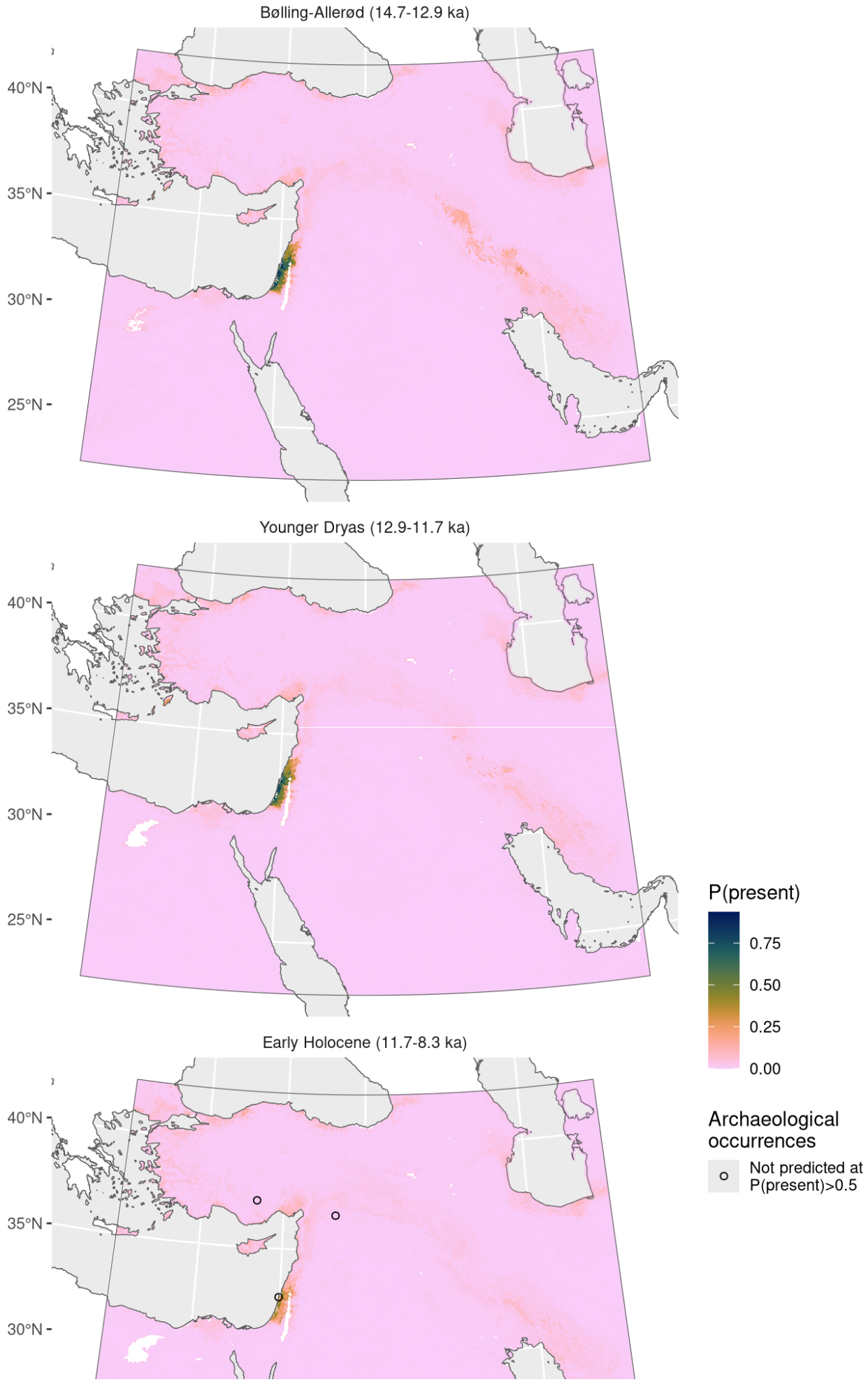

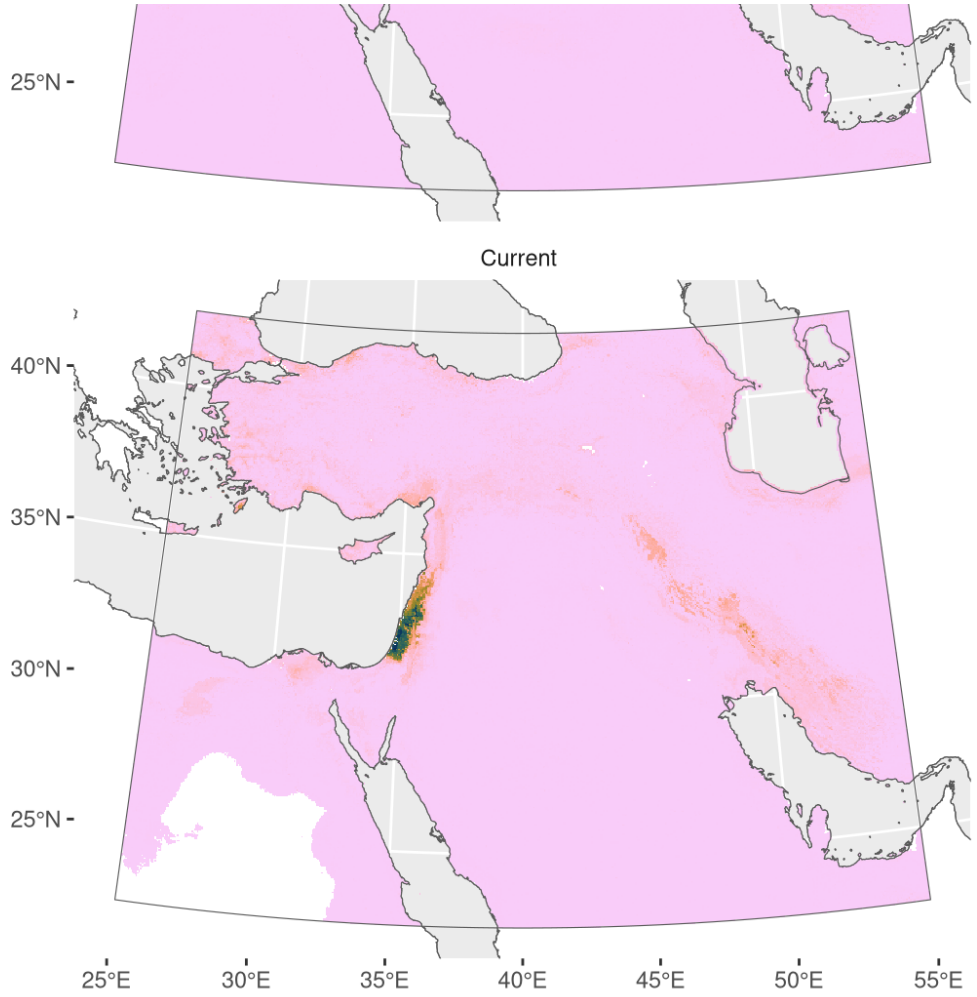


Figure 128: Predicted palaeodistributions of *Vitis sylvestris*

Table 64: Archaeological occurrences of *Vitis sylvestris*

Archaeological occurrences of *Vitis sylvestris*

| Site | Age range | N assemblages | Average prop. | Source | Predicted? |
|---|---|---|---|---|---|
| Early Holocene (11.7-8.3 ka) | | | | | |
| Dja'de | 10.7–10.2 ka | 1 | 0.01% | ORIGINS | no |
| Can Hasan III | 9.4–8.6 ka | 1 | 0.02% | ORIGINS | no |
| Atlit-Yam | 9.0–8.0 ka | 1 | 0.07% | ORIGINS | no |

# *Zygophyllum fabago*

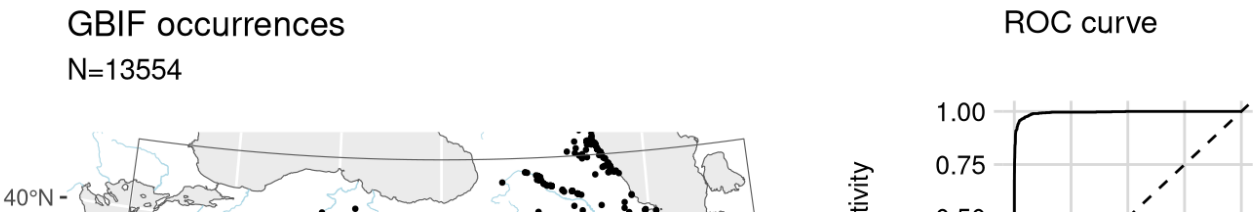

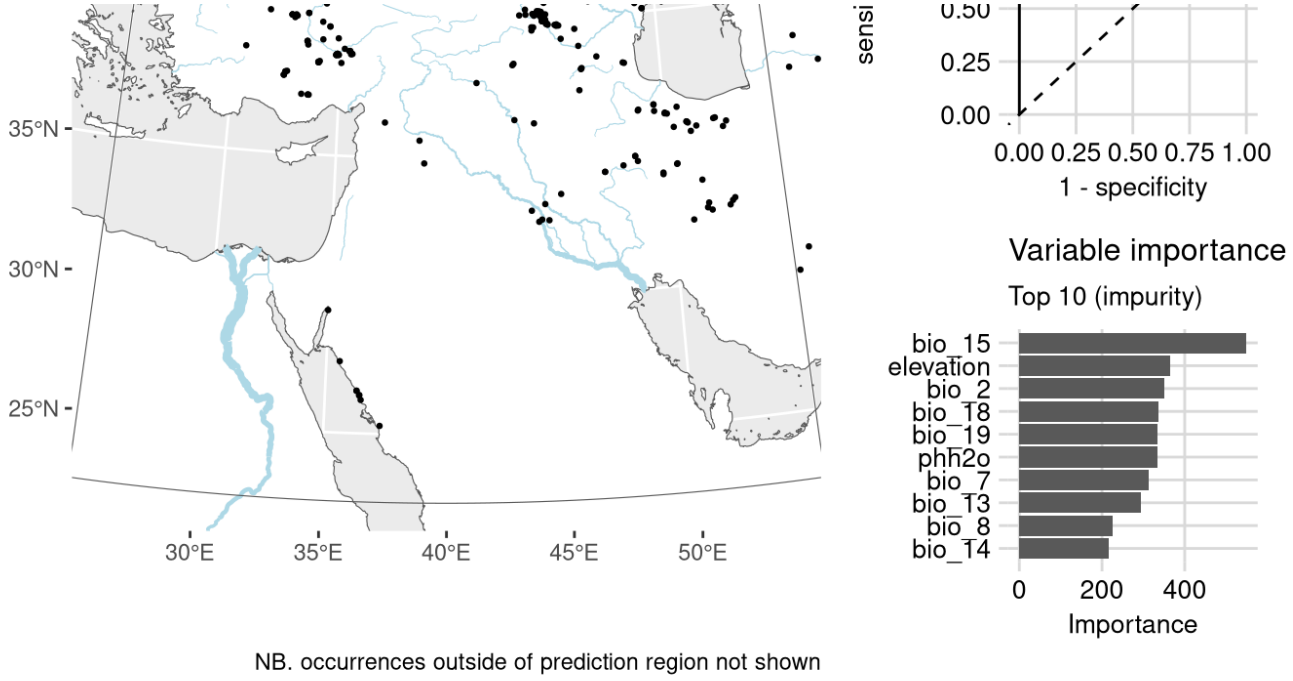


Figure 129: Fitted model summary for *Zygophyllum fabago*

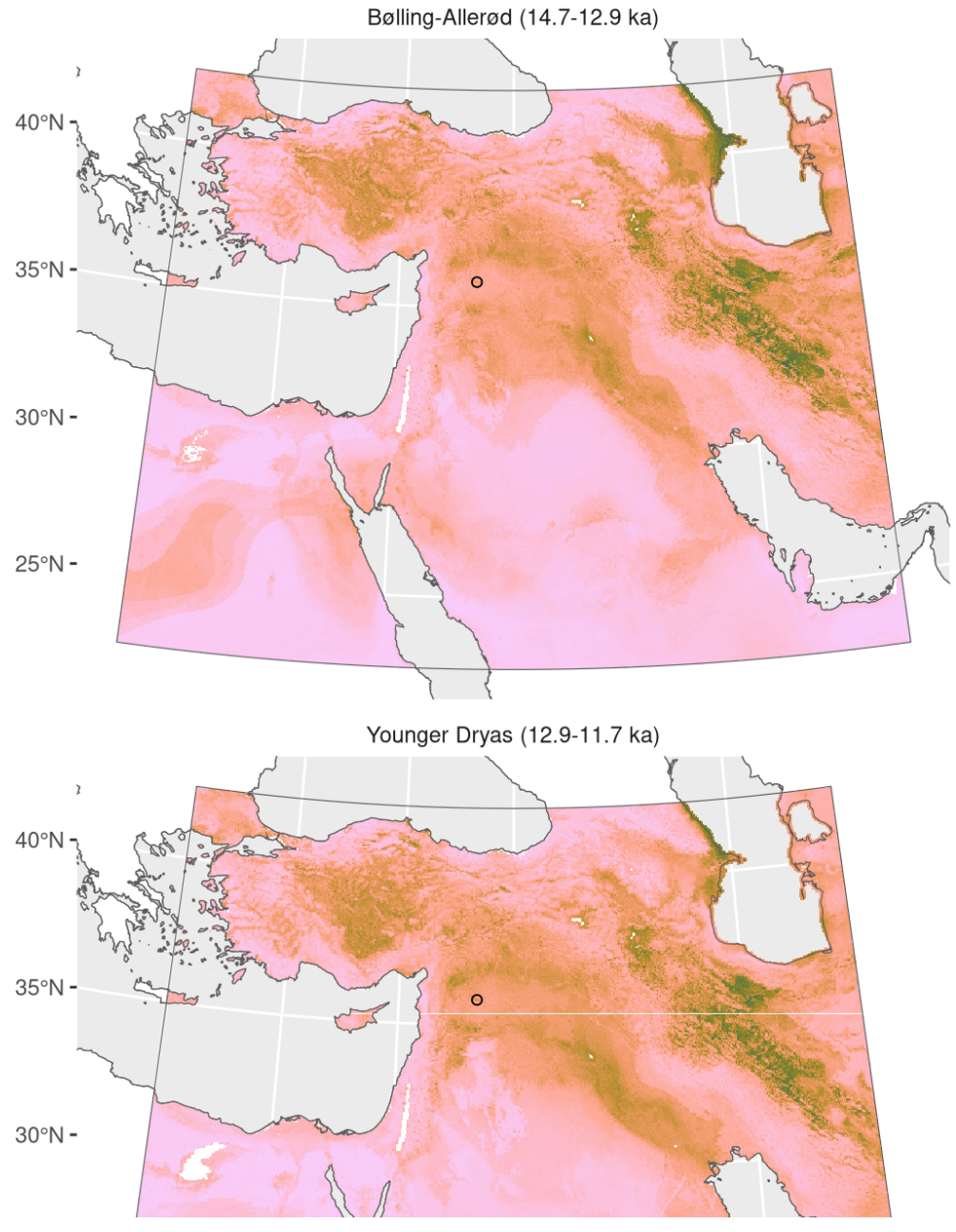

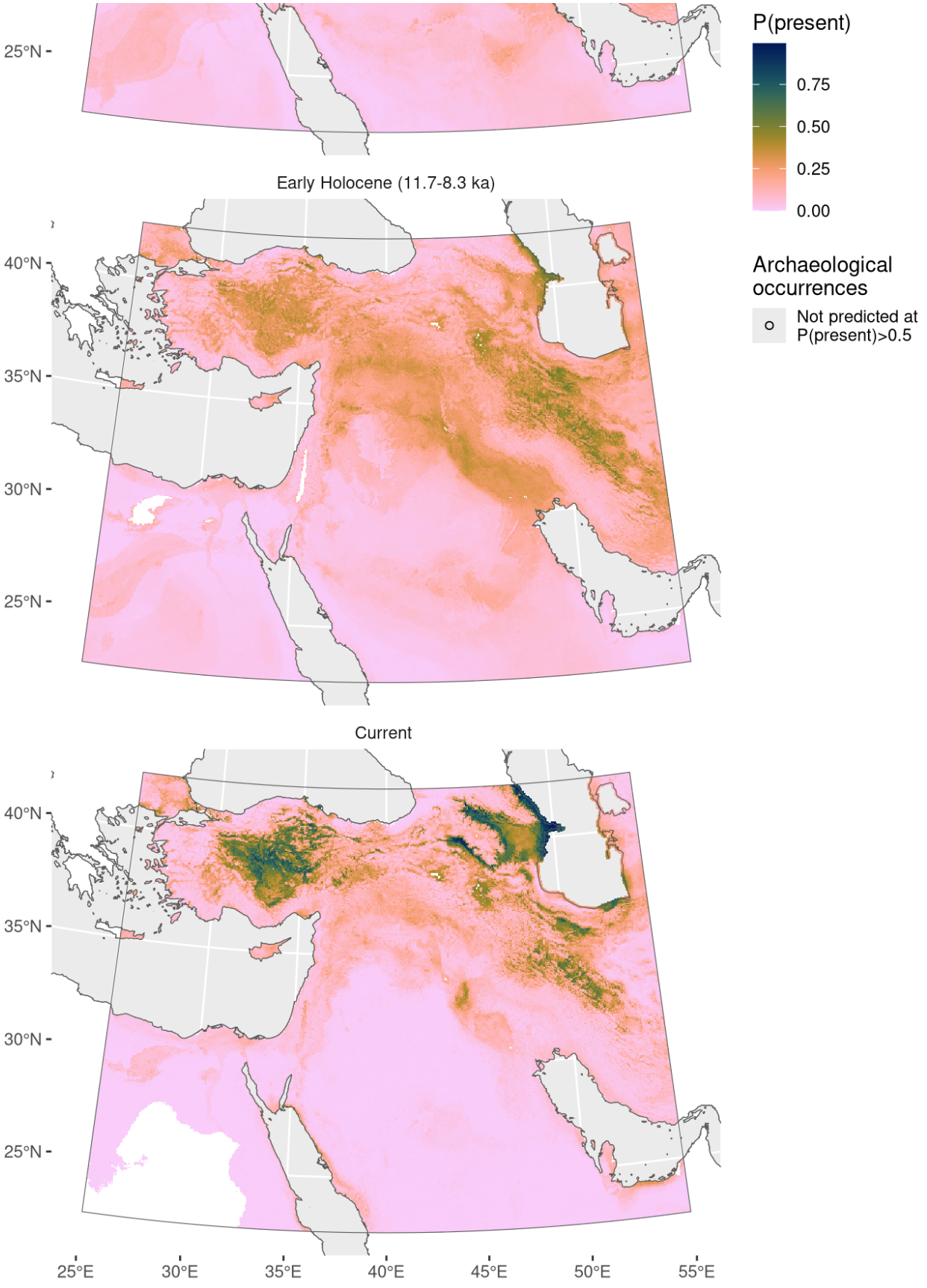


Figure 130: Predicted palaeodistributions of *Zygophyllum fabago*

Table 65: Archaeological occurrences of *Zygophyllum fabago*

Archaeological occurrences of *Zygophyllum fabago*

| Site | Age range | N assemblages | Average prop. | Source | Predicted? |
|---|---|---|---|---|---|

| | | | | | |
|---|---|---|---|---|---|
| Bølling-Allerød (14.7-12.9 ka) | | | | | |
| Abu Hureyra | 13.1–13.0 ka | 1 | 0.33% | ORIGINS | no |
| Younger Dryas (12.9-11.7 ka) | | | | | |
| Abu Hureyra | 13.0–11.8 ka | 2 | 0.43% | ORIGINS | no |